



Terms and Conditions of Use of Digitised Theses from Trinity College Library Dublin

Copyright statement

All material supplied by Trinity College Library is protected by copyright (under the Copyright and Related Rights Act, 2000 as amended) and other relevant Intellectual Property Rights. By accessing and using a Digitised Thesis from Trinity College Library you acknowledge that all Intellectual Property Rights in any Works supplied are the sole and exclusive property of the copyright and/or other IPR holder. Specific copyright holders may not be explicitly identified. Use of materials from other sources within a thesis should not be construed as a claim over them.

A non-exclusive, non-transferable licence is hereby granted to those using or reproducing, in whole or in part, the material for valid purposes, providing the copyright owners are acknowledged using the normal conventions. Where specific permission to use material is required, this is identified and such permission must be sought from the copyright holder or agency cited.

Liability statement

By using a Digitised Thesis, I accept that Trinity College Dublin bears no legal responsibility for the accuracy, legality or comprehensiveness of materials contained within the thesis, and that Trinity College Dublin accepts no liability for indirect, consequential, or incidental, damages or losses arising from use of the thesis for whatever reason. Information located in a thesis may be subject to specific use constraints, details of which may not be explicitly described. It is the responsibility of potential and actual users to be aware of such constraints and to abide by them. By making use of material from a digitised thesis, you accept these copyright and disclaimer provisions. Where it is brought to the attention of Trinity College Library that there may be a breach of copyright or other restraint, it is the policy to withdraw or take down access to a thesis while the issue is being resolved.

Access Agreement

By using a Digitised Thesis from Trinity College Library you are bound by the following Terms & Conditions. Please read them carefully.

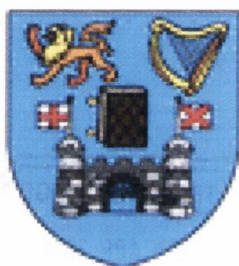
I have read and I understand the following statement: All material supplied via a Digitised Thesis from Trinity College Library is protected by copyright and other intellectual property rights, and duplication or sale of all or part of any of a thesis is not permitted, except that material may be duplicated by you for your research use or for educational purposes in electronic or print form providing the copyright owners are acknowledged using the normal conventions. You must obtain permission for any other use. Electronic or print copies may not be offered, whether for sale or otherwise to anyone. This copy has been supplied on the understanding that it is copyright material and that no quotation from the thesis may be published without proper acknowledgement.

Cyclen-based Lanthanide Complexes as Ribonuclease Mimics

By

Sinead Mulready

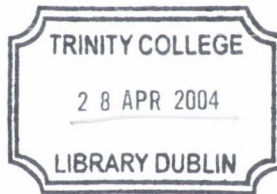
September 2003



**University of Dublin
Trinity College**

**Based on research carried out under the direction of Dr. Thorfinnur
Gunnlaugsson**

*A thesis submitted to the Department of Chemistry, University of Dublin,
Trinity College in fulfillment of the requirements for the degree of Doctor of
Philosophy.*



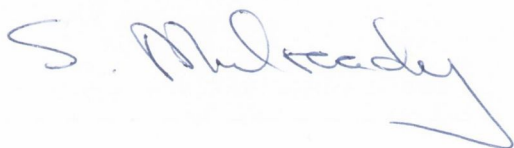
THESIS
7904
7479

DECLARATION

This thesis has not been submitted as an exercise for a degree at any other university. Except where stated, the work described therein was carried out by me alone.

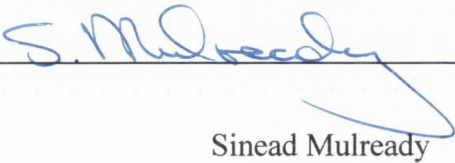
I give permission for the Library to lend or copy this thesis upon request.

Signed:

A handwritten signature in blue ink, appearing to read "S. Mulready". The signature is written in a cursive style with a long, sweeping tail on the final letter.

Declaration

This thesis is submitted for the degree of Doctor of Philosophy to the University of Dublin, Trinity College and has not been submitted for any degree or examination to this or any other University. Other than where acknowledged, all work described herein is original and carried out by the author.



A handwritten signature in blue ink, reading "S. Mulready", is written over a horizontal line. The signature is cursive and extends below the line with a long, sweeping tail.

Sinead Mulready

The shortest distance between two points is a straight line
Euclid

The shortest distance between two points is knowing the way
Anon

Abstract

This thesis, entitled "Novel Cyclen-based Lanthanide Complexes as Ribonuclease Mimics" is divided into six chapters. Chapter One introduces the field of mRNA cleavage, with emphasis on the hydrolysis of phosphodiester. First discussed are nature's methods of cleaving mRNA and phosphodiester, concentrating on the use of ribozymes and ribonucleases. The role of metal ions in these reactions is analysed. The use of metal ions to create artificial ribozyme and ribonuclease mimics is discussed, with an emphasis on the use of lanthanides and the importance of using complexed metals. A review of cyclen-based lanthanide complexes that have been used to promote the hydrolysis of phosphodiester is presented and discussion of selective mRNA cleavage is given. Chapter Two describes the synthesis and characterisation of a selection of novel cyclen-based lanthanide complexes, employing the use of amino esters as cofactors. The incorporation of glycine, alanine, valine, leucine and phenylalanine based dipeptides into the cyclen frameworks is discussed, as well as the subsequent complexation of the resulting ligands with various lanthanide ions. ^1H NMR analysis is presented for the cyclen ligands, and both solution and solid state analysis is provided for a selection of the lanthanide complexes. The X-ray crystal structures of two lanthanide complexes are discussed, and the presence of a metal-bound water molecule is noted. The crystal structures reveal the deep 'bowl-shaped' cavity of the complexes in the solid state, and the existence of a hydrophobic cavity is discussed. The presence of metal-bound water molecules in the solution state is examined by means of photophysical studies. q values of ~ 1 are found in the case of most Eu(III) and Tb(III) complexes. Chapter Three discusses the synthesis and characterisation of other cyclen-based lanthanide complexes. An attempt to introduce amino-pyridine cofactors into the cyclen framework is talked about. The synthesis of a tri-substituted cyclen system is discussed. This is synthesised by mono-protection of cyclen with *p*-methoxy sulfonyl chloride, the subsequent reaction of the free nitrogens with 2-chloro-*N*-methyl acetamide and the removal of the protecting group under Birch conditions. A number of crystal structures are discussed, including one of the Eu(III) complexed tri-substituted ligand. This clearly shows the presence of two metal-bound water molecules. Chapter Four examines the ability of these lanthanide complexes to promote the hydrolysis of a phosphodiester, namely HPNP, an mRNA model

compound. Families of compounds are discussed, beginning with **70**, which incorporates glycine methyl ester as a cofactor. Surprising activity is noted, with **La[70]** cleaving HPNP with a half-life of 1.70 h, or an increase of 3417-fold over the uncatalysed hydrolysis of HPNP. This is one of the greatest enhancements of this reaction rate in the literature. Discussion of the effect of changing the lanthanide ion within a given ligand system is presented. The effect of changing both the amino acid and the ester in the ligand system is discussed. The various trends that emerge from these studies are discussed. Binding studies are presented; the binding of various lanthanide complexes to diethyl phosphate is followed by ^{32}P NMR and their binding to diethyl phosphate, HPNP and EDTA is analysed by photophysical methods. Using the various studies described in this chapter, a discussion of the possible reaction mechanism for the hydrolysis of HPNP is presented. Chapter Five gives an account of the use of a selection of lanthanide complexes with an mRNA strand. The mRNA sequence is a 23-mer from the gag RNA of the HIV gene. Two sets of experiments are described; in the first, a selection of Eu(III) complexes are tested and the results of incubating these complexes with the mRNA are presented on a PAGE gel. A brief comparison of the activities of these compounds is provided. One compound is found to give an unexpected degree of specificity, as determined by densitometry studies carried out on the gel. A preference for cleavage at uracil bases is determined. The second set of experiments uses three different lanthanide complexes of the same ligand. These experiments confirm the results of the HPNP studies, and La(III) is found to promote hydrolysis more effectively than smaller lanthanides. Chapter Six outlines the experimental procedures used in Chapters 2, 3, 4, and 5, and presents the characterisation of the novel compounds prepared.

Acknowledgements

Thanks are due to probably hundreds of people, without whom this thing would never have been finished. Firstly, I need to give a huge thank you to every member of the Thorri Group, past and present. Claire, Caroline, Mark, Joe, Aoife, Jilly, Raman, Andrew, Anne-Marie, Flo and Lin, all of whom helped to prove that sometimes chemistry can be fun, and that the more important part of the PhD years takes place in pubs and bars, not the lab. A huge thanks to the post-docs also, who have all been so great – Fred and Celine, and especially Juile, who waded through the unenviable task that was proof-reading the early versions of my thesis! The biggest thank you goes to Thorri – having got me into this, he helped get me through it, and his overwhelming enthusiasm got me over many discouraging days.

I would like to thank John O'Brien for the enthusiastic NMR service as well as many helpful discussions, and Dr. Mark Niewenheizen in Queens for all of the X-ray crystallography in this thesis.

A huge thank you goes in the direction of the Biochemistry and Biology department in Queens, in particular Clarke Stevenson and Prof. Jerry Davies. Their welcome made Belfast a wonderful place to work in and their patience and expertise left this chemist capable of running a gel by herself.

Thanks also to all of the staff around the Chemistry department, ever helpful when I broke things and created problems for myself; John, Brendan, Paul and Martin, always to the rescue when things went wrong, and Corrine, Helen, Tess and Theresa who were always helpful when I found myself with problems, problems, problems....

Finally, to the friends and family who haven't seen too much of me in recent times – thanks for waiting! I couldn't have done this without you all. In particular, to my brother and sister who have for so long refrained from asking each and every day, 'are you not leaving home yet?' and my parents, who have for so long refrained from asking each and every day, 'Is it done yet?'

Yes it is. Thank you all.

Abbreviations

A	Adenine
Ala	Alanine
Arg	Arginine
Asn	Asparagine
Asp	Aspartic acid
BNPP	Bis(<i>p</i> -nitrophenyl)phosphate
Br	Broad
C	Cytosine
CH ₃ CN	Acetonitrile
Cpm	Cerenkov counts per minute
Cyclen	1,4,7,10-tetraazacyclododecane
Cyclam	1,4,8,11-tetraazacyclotetradecane
Cys	Cysteine
D	Doublet
DCM	Dichloromethane
DMF	Dimethyl formamide
DMSO	Dimethyl sulfoxide
DNA	Deoxyribonucleic acid
DTPA	Diethylenetriamine pentaacetic acid
EDTA	Ethylenetriamine tetraacetic acid
EPNP	Ethyl- <i>p</i> -nitrophenyl phosphate
ES	Electrospray
ES-MS	Electrospray mass spectrometry
Et	Ethyl
G	Guanine
Gln	Glutamine
Glu	Glutamic acid
Gly	Glycine
HEPES	N-2-Hydroxyethylpiperazine-n'-2-ethanesulfonic acid
His	Histidine
HIV	Human immune deficiency virus
HMQC	Hetronuclear multiple quantum correlation

HPLC	High performance liquid chromatography
HPNP	2-Hydroxy <i>p</i> -nitrophenylphosphate
IR	Infra red
Leu	Leucine
Ln	Lanthanide
Lys	Lysine
MES	4-morpholine ethane sulfonic acid monohydrate
Met	Methionine
mRNA	Messenger RNA
NMR	Nuclear magnetic resonance
NPP	4-nitrophenyl phosphate
PAGE	Polyacrilamide gel electrophoresis
Ph	Phenyl
Phe	Phenylalanine
ppm	Parts per million
Pro	Proline
RNA	Ribonucleic acid
rRNA	Ribosomal RNA
Ser	Serine
T	Thymine
THF	Tetrahydrofuran
TNP	Tris- <i>p</i> -nitrophenyl phosphate
TRIS	Tris Hydroxymethylaminoethane
Trif	Triflate (trifluorosulfonate)
tRNA	Transfer RNA
Trp	Tryptophan
Thr	Threonine
Tyr	Tyrosine
U	Uracil
UV	Ultra violet
Val	Valine

Table of Contents

Chapter One. Introduction

<i>1.1 Introduction</i>	1
<i>1.2 The role of mRNA</i>	1
<i>1.3 The Hydrolysis of Phosphodiester Bonds</i>	2
<i>1.4 Kinetics of Reactions</i>	6
1.4.1 Simple kinetics terms	6
1.4.1.1 Zero Order Reactions	6
1.4.1.2 First Order Reactions	6
1.4.1.3 Second Order Reactions	7
1.4.2 Kinetics of enzymes	8
1.4.2.1 The meaning of k_{cat}	9
1.4.2.2 The meaning of K_M	10
1.4.2.3 The meaning of k_{cat}/K_M	10
1.4.3 The pH dependence of enzymes	11
1.5 Ribonucleases	12
1.5.1 RNase A	12
1.5.2 Nuclease P1	14
1.5.3 Staphylococcal nuclease	14
<i>1.6 Ribozymes and Ribozyme Mimics</i>	15
1.6.1 Ribozyme Mimics	15
1.6.2. Requirement for Catalysis	17
<i>1.7 Phosphodiester hydrolysis by metals</i>	18
<i>1.8 Phosphodiester models</i>	20

1.9 Evaluating the Effect of Metal Ions and Salts on Phosphodiesters	23
1.10 Phosphodiester Hydrolysis using Lanthanide Complexes	28
1.11 Cyclen Derivatives	33
1.12 Towards Sequence Specific RNA Cleavage	43
1.12.1 Preferential Cleavage at Certain Base Pairs	43
1.12.2 The Antisense Approach	46
1.13 Conclusion	52
1.14 Aim of Project	53

Chapter Two. Synthesis of Amino Acid-based Complexes

2.1 Introduction	56
2.1.1 Use of Amino Acids to Promote Phosphodiester hydrolysis	58
2.2 Synthesis and Characterisation of Glycine-based Macrocycles	61
2.2.1 Synthesis of Glycine-Based Ribonuclease Mimics	62
2.2.2 Synthesis of Glycine-Based α -chloroamide Pendant Arms	63
2.2.3 Synthesis of Glycine-Based Cyclen Ligands	64
2.2.4 Complexation of Glycine-Based Cyclen Ligands	68
2.2.5 Solid State Analysis of Eu[70]	71

2.3 Synthesis of amino acid-based ribonuclease mimics incorporating alanine, valine, leucine or phenylalanine	74
2.3.1 Synthesis of chiral aminoester-based α -chloroamine pendant arms	74
2.3.2 Synthesis of aminoester -based cyclen ligands	76
2.3.3 Complexation of aminoester-based cyclen ligands	78
2.3.4 Solid State Analysis of Tb[86]	80
2.4 Lifetime Studies	83
2.6 pK_a Measurements	85
2.7 Conclusion	86

Chapter Three. Synthesis of Non Amino Acid-based Complexes

3.1 Introduction	87
3.2 Use of Amino Pyridine Moieties as Co-factors	87
3.2 Pyridine acetamide as cofactor	88
3.2.1 Synthesis of α -chloroamides incorporating amino pyridines	89
3.2.2 Synthesis of tetrasubstituted cyclen incorporating amino pyridines	90
3.2.3 Lanthanide Complexation of 103	92
3.3 Three-arm Cyclen Systems	93
3.3.1 Synthesis of tri-substituted cyclen	94
3.3.2 Mono-protection of cyclen	96
3.3.3 Tris-alkylation of cyclen	96

3.3.4 Complexation of 111	98
3.3.5 Removal of the protecting group	100
3.4 Conclusion	103

Chapter Four. Interactions with Phosphodiesteres

4.1 Introduction	104
4.1.1. Hydrolysis of HPNP	105
4.1.2 Effect of Agitation on the Reaction Mixture	106
4.2 Hydrolysis of HPNP by La[25]	107
4.3 HPNP hydrolysis by glycine derivatised complexes	107
4.3.1 Rate of HPNP hydrolysis by Ln[70] at pH 7.40	108
4.3.2 Dependence of the rate of HPNP hydrolysis by Ln[70] on pH	111
4.3.3 Effect of degassing the solution	112
4.3.4 The effect of changing the buffer	113
4.3.5 Investigation of Catalytic Turnover by La[70]	114
4.4 Changing the Co-factor: Increasing the Size of the Ester	116
4.4.1 Hydrolysis of HPNP by Ln[71]	116
4.4.2 Hydrolysis of HPNP by Ln[72]	117
4.4.2.1 Dependence of the rate of HPNP hydrolysis by Ln[72] on pH	118
4.4.3 Removing the ester completely	120
4.5 Increasing the size of the amino acid	121
4.5.1 Hydrolysis of HPNP by Ln[85]	122
4.5.1.1 Dependence of the rate of HPNP hydrolysis by La[72] on pH	125
4.5.2 Hydrolysis of HPNP by Ln[87]	126
4.5.3 Hydrolysis of HPNP by Ln[88]	126
4.5.4 Hydrolysis of HPNP by Ln[89]	127

4.5.5 Increasing the hydrophobic cavity	128
4.6. Trends of Reactivity	129
4.7 Binding of lanthanide complexes to phosphate	131
4.7.1 Evaluating binding to diethyl phosphate by ^{32}P NMR	131
4.7.2 Evaluating binding to various groups by luminescence methods	135
4.8 Towards a reaction mechanism	138
4.9 Conclusion	140

Chapter Five. Cleavage of an RNA Oligonucleotide

5.1 Introduction	142
5.2 Preparation of mRNA and Reaction Conditions and Procedures	143
5.3 Results of RNA cleavage experiments carried out with <i>Eu(III)</i> complexes	145
5.4 Results of mRNA experiments carried out with <i>Ln[70]</i> complexes	150
5.5 Conclusion	152

Chapter Six. Experimental Procedures

Chapter Seven. Future Work

References

Chapter One

Introduction

1.1 Introduction

This chapter will address many of the advances made in the field of phosphodiester hydrolysis to date, with emphasis on the cleavage of messenger RNA (mRNA). The mechanism of this reaction will be discussed initially, in particular the role played by metal ions and the methods which nature has developed, in the form of ribozymes and ribonucleases, to carry out such reactions. Some simple and non-selective ways in which science has attempted to imitate these methods and model these systems, will then be discussed, leading finally to a description of some highly efficient and selective systems that can carry out such hydrolysis in a site specific manner. Given the importance of understanding the role of mRNA, this chapter will begin with a brief outline of the central dogma of genetics.

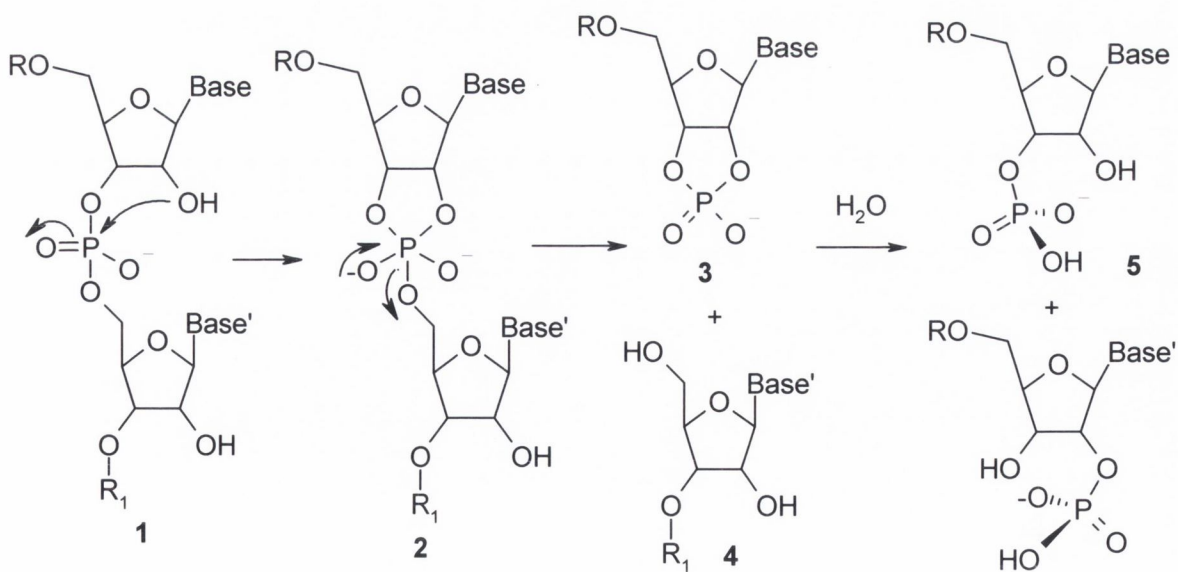
1.2 The role of mRNA^{1,2}

Genetic information is stored in every cell by DNA, however it is through RNA, more specifically mRNA that the genetic code of DNA is translated into proteins.¹ An outline of this procedure can be seen in **Figure 1.1**.¹ Initially, the DNA double helix unwinds, with one of the strands forming the template for the formation of the newly created RNA strand. The base pairs of the mRNA to be formed are complementary to those of the DNA strand, with the only difference being the replacement of T by U. Transcription begins when RNA polymerase, the transcription enzyme, locates the promoter sequence, a signal to begin transcription that is found on the DNA. As the RNA strand grows or elongates, it peels away from the DNA, allowing the two DNA strands to rejoin. Transcription ends when the RNA polymerase finds a sequence of bases in the DNA called a terminator, causing the polymerase to detach from the gene.¹

This newly created mRNA now carries the genetic information from the cell. This information must be translated from the language of the nucleic acid to the language of the protein. Specifically, the information is contained in ribonucleotide triplets, or codons, as can be seen in **Figure 1.1**. Transfer RNA (tRNA) is employed at this point. This molecule carries out two functions; it can select an amino acid and it can recognise the corresponding codon on the mRNA by means of a triplet of bases called an anticodon. Codon recognition by the anticodon operates according to normal base-pairing rules. Incorporation of the amino acids is more complex and involves the use of a family of enzymes, with each enzyme binding a specific amino acid to the correct tRNA molecule.²

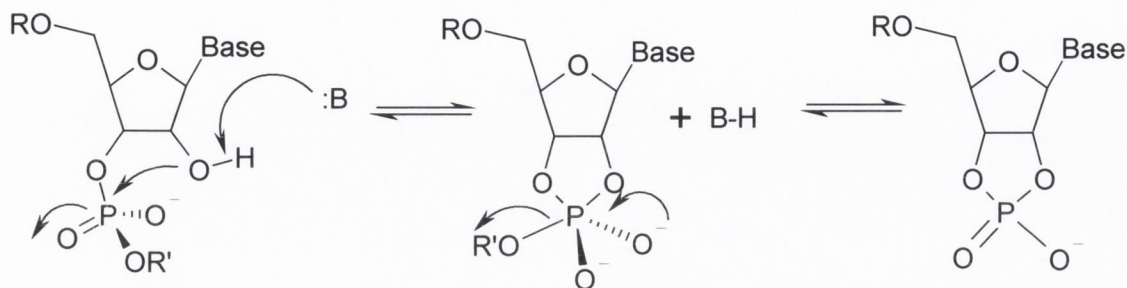
The hydrolysis of RNA phosphodiester has been investigated since the 1950s, when the instability of RNA in the presence of base was studied.⁷ The nucleotide products of the alkaline degradation were found to exist as different isomers, identical to the products of alkaline hydrolysis of 2'3'-cyclic phosphates. Therefore, it seemed probable that the hydrolysis occurred *via* such a cyclic intermediate.⁷ One of the main differences between DNA and RNA is the presence of the 2'-hydroxy group on RNA. This difference is of crucial importance to the different methods by which DNA and RNA can be cleaved; DNA tends to be cleaved by an oxidative process, which will not be discussed here, while RNA is cleaved by a hydrolytic mechanism which will be discussed below.

The alkaline cleavage of RNA has been explained by the nucleophilic attack of the deprotonated 2'-hydroxy group upon the phosphate and the subsequent displacement of the 5'-linked nucleoside.^{8,9} As shown in **Scheme 1.1**, the hydrolysis can be summarised as: a transesterification step in which an alcohol or alkoxide acts as a nucleophile, followed by a hydrolysis reaction in which a water molecule or a hydroxide ion acts as a nucleophile. Each step is pH dependant and is promoted by both general and specific acid and base catalysis.⁹ Transesterification involves attack by the 2'-hydroxy group of the ribose on the tetrahedral phosphodiester **1**, leading to a phosphorane intermediate **2** which is converted to the cyclic phosphate **3**. This cyclic intermediate is then hydrolysed, yielding the 2' or 3' monophosphates **5** and **6**.⁷



Scheme 1.1 The 2'-hydroxy group can act as a nucleophile, attacking the phosphodiester and displacing the 5'-nucleoside. The reaction is thought to go through a phosphorane intermediate (**2**), and then through the cyclic phosphate (**3**), which can be further hydrolysed to give the 2'- and 3'- monophosphates (**5, 6**).

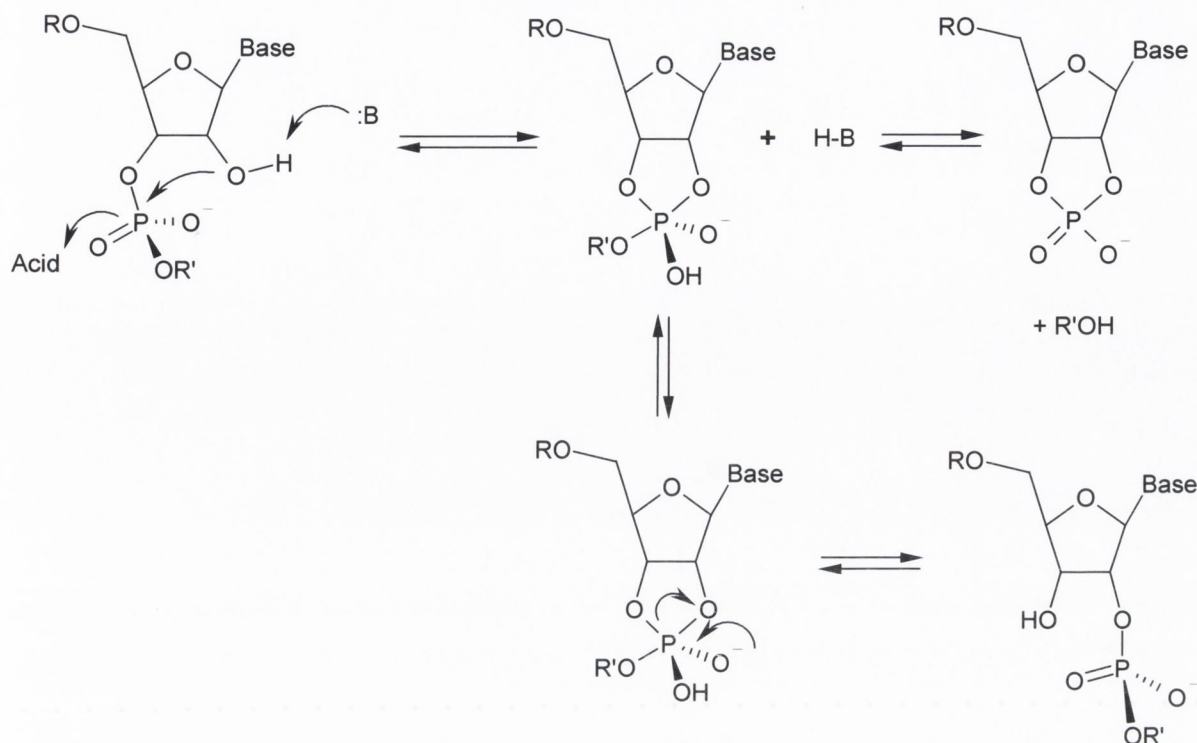
Numerous investigations have been carried out which attempt to elucidate the mechanism of this reaction, a summary of which can be found in the review by Anslyn *et al.*⁹



Scheme 1.2 Base-promoted mRNA hydrolysis, going through a dianionic phosphorane intermediate.

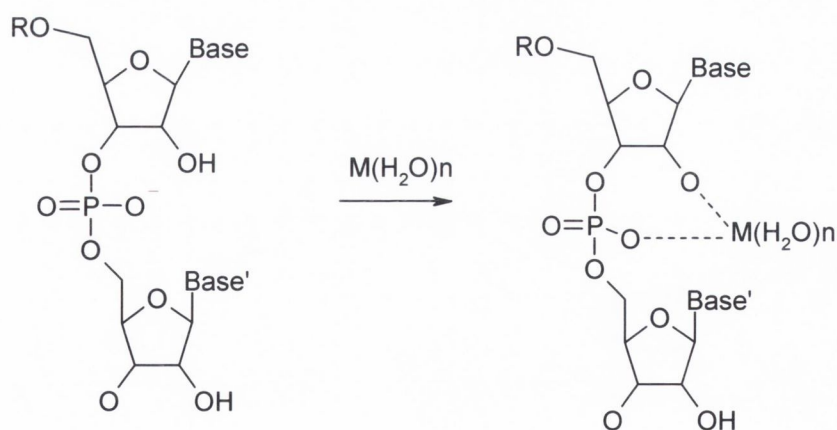
Two differing mechanisms are found which can be used to explain the results of most studies.⁹ The occurrence of one mechanism or another depends on factors such as pH, the leaving group and the presence of either acid or base. The first, shown in **Scheme 1.2**, postulates a dianionic phosphorane transition state. In this case either general or specific base catalysis is possible. The leaving group is expelled before the transition state can be protonated. This mechanism is the most suitable way of describing the cleavage of RNA models with good leaving groups. The second possibility, shown in **Scheme 1.3**, involves protonation of the phosphodiester occurring simultaneously with nucleophilic attack, thus creating a monoanionic/monoprotic phosphorane intermediate. In this case, general or specific acid catalysis is possible. It is important to note that this mechanism allows for pseudorotation to occur, thus yielding the 2' monophosphate as a product of the reaction.⁹

From the point of view of developing synthetic methods of cleaving the phosphodiester bonds of RNA, it is important to note that nucleophilic attack on an anionic phosphodiester is electronically unfavourable. In order to increase the rate of the cleavage reaction, it is necessary to be able to stabilise the negative charge, for example with a proton, metal ion or Lewis acid. This explains why RNA cleavage is catalysed by such a wide range of species, including protons,⁹ Group II metals,^{10,11,12} transition metals^{13,14,15} and lanthanide ions^{16,17,18} among others.



Scheme 1.3 Base-promoted mRNA hydrolysis via a monoanionic intermediate.

Alternatively, the reaction can be promoted by the activation of the 2'-OH. This can occur through deprotonation by means of base catalysis, by a metal hydroxide, or through coordination of the 2'-OH to a metal ion which will lower the pK_a of the hydroxyl group as is shown in **Scheme 1.4**.^{19,20} The multiple roles played by metal ions in the promotion of phosphodiester hydrolysis will be examined in more detail in Section 1.5.



Scheme 1.4 Coordination of a metal or metal hydroxide to the 2'-OH lowers the pK_a of the hydroxyl group.

In summary, while the base promoted hydrolysis of mRNA has been investigated for many years, there is much that remains unknown. If science is to efficiently and

selectively cleave the phosphodiester bonds of RNA, it is necessary to investigate how this task is carried out by nature. First, it is important to understand how the activity of such enzymes, and indeed, enzyme mimics, is described and quantified, therefore Section 1.4 will provide a brief outline of kinetics.

1.4 Kinetics of Reactions

Throughout this chapter, the hydrolytic activity of various compounds will be described in terms of their rates of reaction. This section offers a brief revision of kinetic terminology, with particular attention to that relevant to the study of enzymes and catalysts.

1.4.1 Simple kinetics terms^{21,22}

Kinetics is the study of the rates of chemical reactions and the factors that can affect these rates, such as temperature, concentration and solvent. The rate of a reaction is defined as the change in concentration of one of the reactants or products of a reaction per unit time.²¹

1.4.1.1 Zero Order Reactions

A simple zero order rate law has the form:

$$-\Delta[A]/\Delta t = k[A]^0 = k \quad (i)$$

This can be converted to give the relationship between concentration and time:

$$[A] = [A]_0 - kt \quad (ii)$$

Where $[A]$ is the concentration of A measured at time t and $[A]_0$ is the initial concentration of A at time $t = 0$. If a reaction is zero order, a plot of $[A]$ against t should be linear; conversely, if a plot of $[A]$ against t is not linear, the reaction is not zero order.

1.4.1.2 First Order Reactions

A first order law has the form:

$$-\Delta[A]/\Delta t = k[A]^1 \quad (iii)$$

And the corresponding integrated rate law is:

$$\ln[A] = \ln[A]_0 - kt \quad (iv) \quad \text{or} \quad [A] = [A]_0 e^{-kt} \quad (v)$$

Therefore a plot of $\ln[A]$ against t will give a straight line if the reaction is first order.

1.4.1.3 Second Order Reactions

A second order rate law has the form:

$$-\Delta[A]/\Delta t = k[A]^2 \quad (vi)$$

The corresponding integrated rate law becomes:

$$1/[A] = 1/[A]_0 + kt \quad (vii) \quad \text{or} \quad [A]^{-1} = [A]_0^{-1} + kt \quad (viii)$$

Thus a plot of the inverse of the concentration against time t gives a straight line in the case of a second order equation.

Using rate law, the concentration at a desired time or the time taken to reduce the concentration by a given amount can be calculated. Similarly, the half-life ($t_{1/2}$) of a reaction can be calculated; this is the time taken for a given concentration of a reactant to be reduced to half its initial value. Depending on the order of the reaction, this may or may not be dependant on the initial concentration. In the case of a first order rate law:

$$\ln([A]/[A]_0) = -kt \quad (ix)$$

At a time equal to one half-life ($t_{1/2}$): $[A] = \frac{1}{2} [A]_0 \quad (x)$

$$\ln(\frac{1}{2} [A]_0/[A]_0) = -kt_{1/2} \quad (xi)$$

Solving for $t_{1/2}$ gives: $t_{1/2} = -\ln(\frac{1}{2})/k \quad (xii)$

Therefore, the half-life of a first order reaction depends only upon the rate constant of the reaction. The half-life of second order reaction can be derived similarly.

Other terms that will be mentioned when describing simple kinetics are k_{obs} , the observed rate constant, or the measured rate constant. This is to be distinguished k_{rel} , or the relative rate constant, which is the increase in the rate of a reaction over that of the uncatalysed reaction.

1.4.2 Kinetics of enzymes²²

The brief outline above concerns mainly reactions that do not involve catalysis. However, the distinguishing kinetic feature of reactions that are catalysed by enzymes is that they exhibit saturation, and the kinetics that pertain to this will be described here. Enzymes are found to exhibit saturation kinetics, meaning that, the rate shows first-order dependence on the concentration of the substrate at low concentration, however at higher concentrations, the rate becomes independent of concentration (zero order with respect to concentration of substrate) as it approaches a limit. This behaviour is defined by the Michaelis Menten equation.^{21,22}

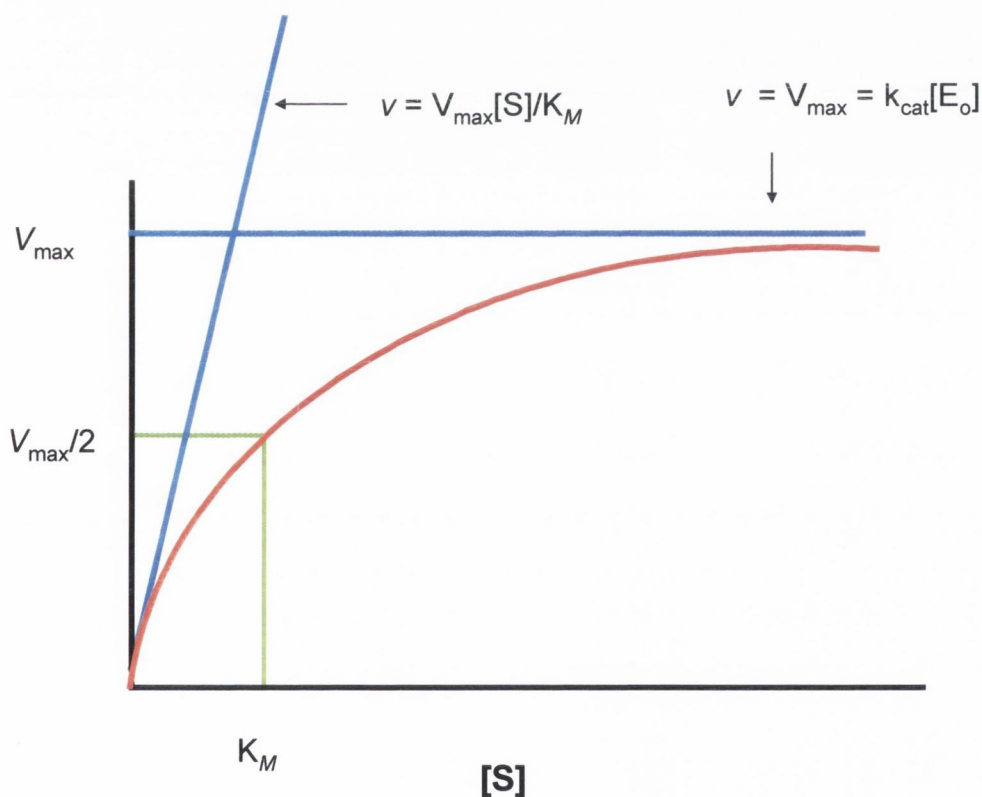


Figure 1.2 Reaction rate v plotted against substrate concentration $[s]$ for a reaction obeying Michealis Menten kinetics

The Michaelis-Menten equation is derived by assuming that the concentration of the enzyme is negligible compared to that of the substrate, which is true in the case of catalytic reactions. It is also assumed that what is measured is the initial rate v of

formation of products, *ie*, that the newly formed product has not accumulated considerably and the substrate has not been considerably depleted. Thus, changes in reagent concentration are linear with time.

Experimentally, it is found that v is proportional to the concentration of the enzyme $[E]_0$. v follows saturation kinetics with respect to the concentration of the substrate, $[S]$, meaning that at low $[S]$, v increases linearly with $[S]$ but as $[S]$ increases v increases more slowly until at a high value of $[S]$, v tends towards a limiting value, V_{\max} . This is expressed by the Michaelis –Menten equation:

$$v = \frac{[E]_0[S]k_{cat}}{K_M + [S]} \quad (xiii)$$

$$\text{Where } k_{cat}[E]_0 = V_{\max} \quad (xiv)$$

The concentration of substrate at which $v = \frac{1}{2} V_{\max}$ is called K_M , or the Michaelis constant. At very low $[S]$, where $[S] \ll K_M$, the equation takes the form:

$$v = [E_0][S] \frac{k_{cat}}{K_M} \quad (xv)$$

Having presented the background and equations pertaining to catalytic behaviour, the following section will discuss the physical meaning of these terms.

1.4.2.1 The meaning of k_{cat} ²²

k_{cat} is a first order rate constant that refers to the properties of enzyme-substrate, enzyme-intermediate and enzyme-product complexes. In a simple mechanism in which there is only one enzyme –substrate complex and all of the binding steps are fast, k_{cat} is the first order rate constant for the conversion of ES (enzyme-substrate) to EP (enzyme-product). In more complicated reactions, where additional intermediates occur during the reaction, k_{cat} is a function of all of the first order rate constants for the reaction. k_{cat} is known as the turnover number of an enzyme as it represents the maximum number of substrate molecules converted to products by the enzyme per unit time.

1.4.2.2 The meaning of K_M ²²

K_M is the substrate concentration at which $v = V_{\max}/2$. It can also be viewed as an apparent dissociation constant in cases where the simple Michaelis-Menten mechanism is in place. Thus the concentration of the free enzyme in solution may be calculated from:

$$\frac{[E][S]}{\Sigma [ES]} = K_M \quad (xvi)$$

where $\Sigma [ES]$ is the sum of all bound enzyme species.

1.4.2.3 The meaning of k_{cat}/K_M ²²

The reaction rate for low substrate concentrations is given by:

$$v = (k_{\text{cat}}/K_M)[E]_o[S] \quad (xvii)$$

Thus k_{cat}/K_M is an apparent second-order rate constant. k_{cat}/K_M relates the reaction rate to the concentration of free enzyme. At low concentrations of substrate, $[E]$ (free enzyme concentration) $\sim [E]_o$ (total enzyme concentration) and the reaction rate is given by:

$$v = [E][S] \frac{k_{\text{cat}}}{K_M} \quad (xviii)$$

The Michaelis-Menten equation is often transformed into a linear form in order to analyse data. The Lineweaver-Burk plot is a double-reciprocal method that is often used. This inverts both sides of equation to give:

$$1/v = 1/V_{\max} + K_M/V_{\max}[S] \quad (xiv)$$

Plotting $1/v$ against $1/[S]$ gives an intercept of $1/V_{\max}$ on the y-axis as $1/[S]$ tends towards zero, and of $1/[S] = -1/K_M$ on the x-axis, as shown in **Figure 1.3**. The slope of the line is K_M/V_{\max} .

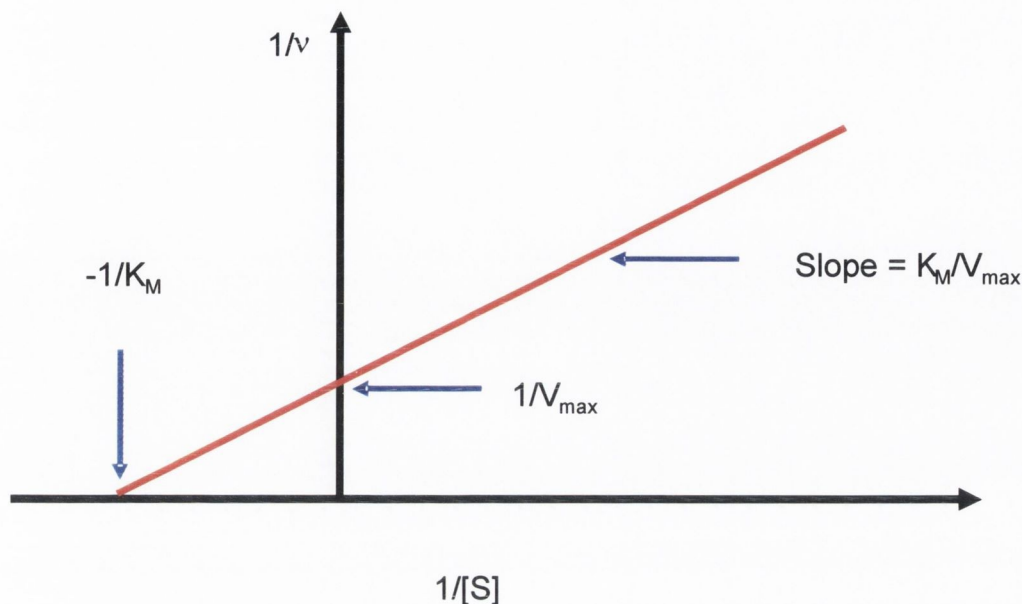


Figure 1.3 The Lineweaver-Burk plot

1.4.3 The pH dependence of enzymes²²

The pH dependence of enzyme catalysed reactions can reveal important information about the mechanism of the enzyme catalysis. If the catalytic activity of a given enzyme is pH-dependent, the enzyme must have 'catalytic' groups that are capable of ionizing within the pH range in question. Therefore the pK_a values of these groups could in theory be determined by the pH-rate dependence exhibited.

It is widely reported that the catalytic activity of enzymes generally shows a bell-shaped dependence on pH. This is indicative of the presence of at least two ionising groups which change their protonation state as the pH is raised from a value at which the enzyme is inactive. Catalytic activity often requires that one such group be deprotonated while the second remains protonated. Essentially, the activity of the catalyst requires the presence of both the acid and the base.

The activity of such a catalyst can be modelled in the way depicted in **Figure 1.4**.²² In this scheme, **E** is an enzyme which initially possessed two protons, **EH₂**. When one proton has been lost (**EH**), the enzyme can bind the substrate **A**, giving **EHA⁻** and catalysing its reaction to product **P**. The product can only be formed when the catalyst has lost one, and only one, of its protons. However, the substrate **A** can be bound by any form of the enzyme; with one proton, two protons or no protons.

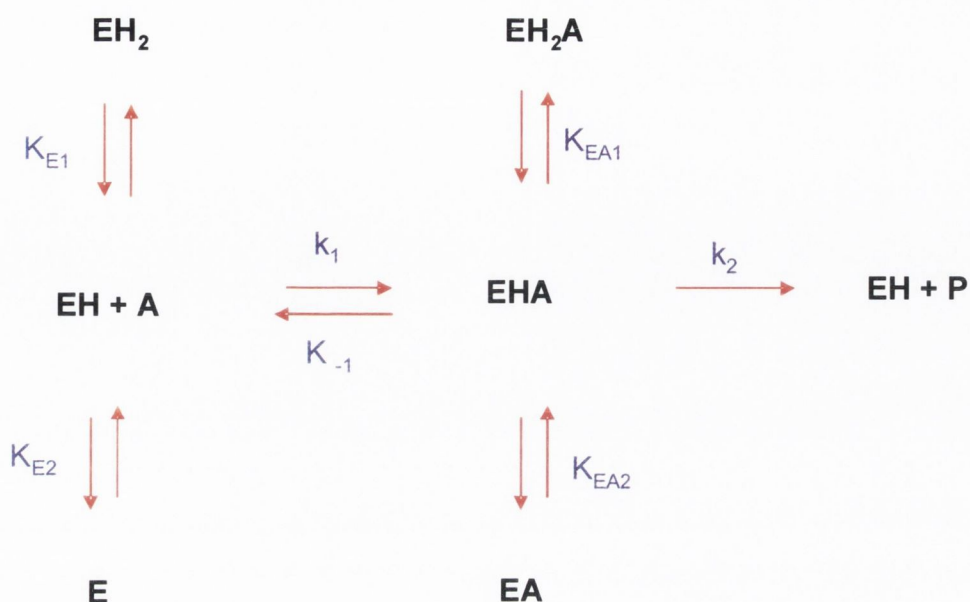


Figure 1.4 Scheme outlining the behaviour of a catalyst with two ionisable protons and its interaction with substrate A to produce product P .²²

1.5 Ribonucleases

Nature has provided enzymes that efficiently and selectively catalyse the hydrolysis of RNA in the form of ribonucleases and ribozymes.²³⁻

²⁷ Outlined in this section are some examples of ribonucleases, illustrating their salient features.²¹

1.5.1 RNase A²¹

Bovine pancreatic ribonuclease A (RNase A), is one of the most carefully studied nucleases that can hydrolyse mRNA. It consists of a polypeptide chain of 124 amino acid residues, and was one of the first enzymes to be sequenced. The crystal structure of RNase has also been resolved, giving a great deal of information about the active site of this enzyme and the possible mechanism of its action. RNase A is thought to catalyse the cleavage of RNA in a two step reaction, in which a cyclic phosphate is formed and then immediately hydrolysed. The nuclease is specific for RNA over DNA and is selective for pyrimidine bases (U and C) over purines.

The mechanism of the catalyst was illuminated by the pH-rate profile which is bell shaped, peaking at neutral pH. Within the active site of RNase A, two histidine residues,

His-12 and His-119, are thought to act in concert to provide general acid – general base catalysis. In **Scheme 1.5**, it can be seen that His-12 initially behaves as a general base by deprotonating the 2'-hydroxy group, while His-119 acts as a general acid in the cyclisation of the phosphate by providing a proton for the phosphate intermediate. This cyclic phosphate is then hydrolysed in a reaction in which His-119 is the general base and His-12 the general acid as can be seen in **Scheme 1.5a**. The pK_{as} of the two histidine residues have been determined to be 5.8 and 6.2 at 40 °C, implying that a considerable amount is ionised at physiological pH.

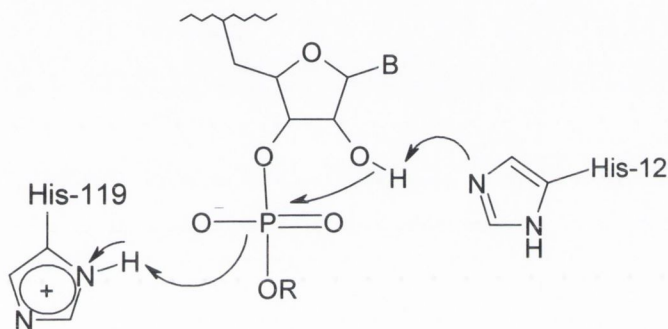


Figure 1.5a

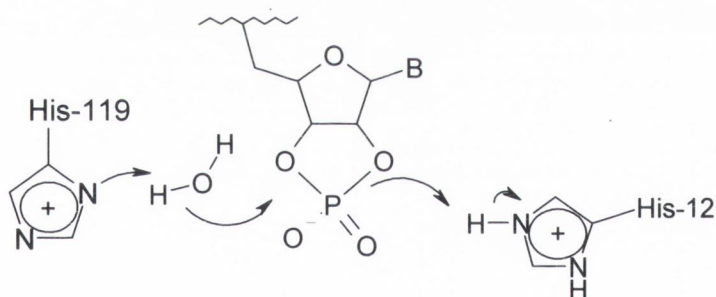


Figure 1.5b

Figure 1.5 *Phosphodiester hydrolysis by Ribonuclease 1. These schemes demonstrate how the reaction is catalysed by general-acid (1.5a) and general-base (1.5b) catalysis by two histidine residues, His-12 and His-119*

Many studies have been carried out to investigate the importance of these two imidazole residues in catalysis.²⁸ A 1994 study of mutant ribonucleases in which either the His12 or His119 was substituted for an alanine were investigated and these were found to have significantly reduced affinity (in the order of 10^{-4}) for the transition state during the cleavage for either polycytidylic acid or UpA.²⁹ In contrast, it was reported that the replacement of the histidine residues had no effect on the model compound uridine 3' (p-nitrophenyl phosphate). This illustrates the point, which will be shown again later, that a model compound may not accurately mimic the reactions of a natural system.

1.5.2 Nuclease P1³⁰

In another example, P1 nuclease was found to possess three zinc ions in its active site, as shown in **Figure 1.6**. This figure is taken from the review by Wilcox.³⁰ This nuclease was found to hydrolyse single stranded DNA and RNA. The crystal structure of the active site showed that two Zn(II) ions are bridged by Asp and a water molecule while the third Zn(II) is ligated by solvent molecules. Other protein ligands, including histidine residues, provide a 5-coordinate trigonal-bipyramidal geometry for each ion.³⁰ These three features, metal ions, metal-bound water molecules and amino acid residues, will be seen to play a vital role in RNA hydrolysis.

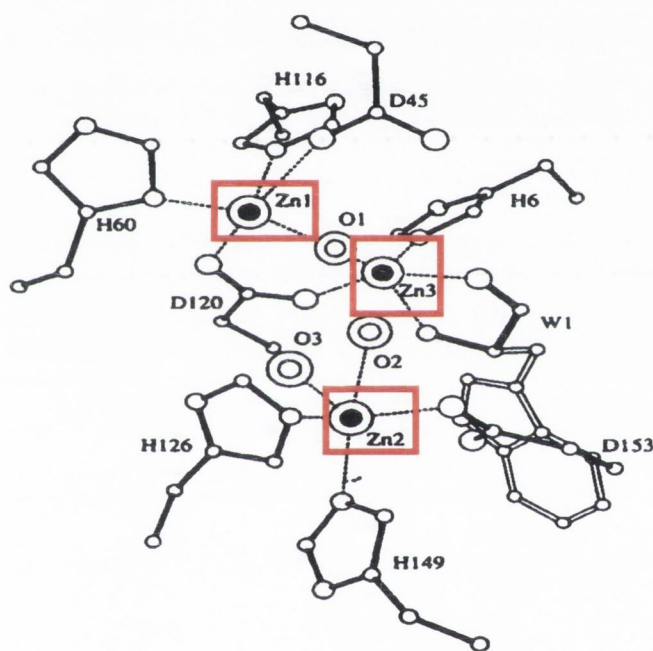


Figure 1.6³⁰ The active site of Nuclease P1, highlighting the three zinc ions and the bridging water molecules.

1.5.3 Staphylococcal nuclease²¹

Staphylococcal nuclease is known to cleave DNA and RNA, however, despite knowledge of its structure, the mechanism of the hydrolysis is not fully understood.²¹ The active site of the enzyme was found to possess arginine residues (Arg-35 and Arg-87) which are thought to hydrogen bond to the phosphate, activating it to nucleophilic attack, as shown in **Figure 1.7**. The Glu-43 residue can then act as a general-base catalyst for the attack of H₂O. It was also found that calcium ions are necessary for hydrolysis of the phosphate to occur, but their role is not understood.²¹

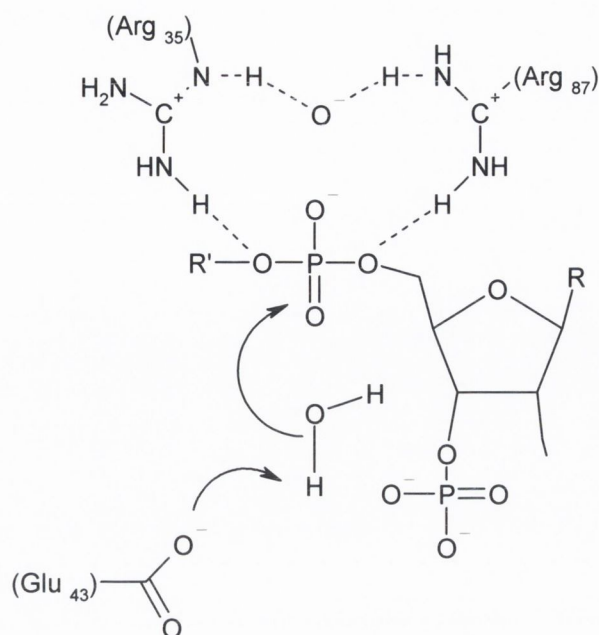


Figure 1.7²¹ *Phosphodiester hydrolysis by Staphylococcal nuclease. The phosphodiester is stabilized by hydrogen-bonding with two Arg centres in the enzyme, while a Glu residue acts as a general-base catalyst for the attack of H₂O.*

1.6 Ribozymes and Ribozyme Mimics

A ribozyme is a molecule that can act as an enzyme, catalyzing the cleavage of other ribonucleotide strands.^{1,2} In 1983 Altman *et al.* reported that Ribonuclease P, an enzyme known to contain both protein and RNA components and which is responsible for cleaving tRNA, in fact relied upon the RNA component alone to carry out the cleavage reaction.³¹ While it was discovered that the protein increased the activity, the RNA by itself was a very efficient catalyst, exhibiting Michaelis Menten kinetics. Of importance to us is the fact that once more a metal ion was found to be involved in the hydrolytic process, with a requirement for catalysis being either a high concentration of magnesium or a low concentration of magnesium in combination with spermidine as a base.³¹

1.6.1 Ribozyme Mimics^{3,7,32}

It is of little surprise that the methods and mechanisms employed by nature to cleave phosphodiester linkages have been used by science as templates, with the selectivity offered by ribozymes seeming particularly attractive. A ribozyme mimic is defined as “*a synthetic molecule that cleaves RNA in a sequence directed manner, using biomimetic chemical reactions such as transesterification and hydrolysis*”.⁷ Ribozyme mimics are constructed by covalently attaching a nucleophilically active RNA cleavage catalyst into a DNA oligonucleotide. These ribozyme mimics are selective due to the Watson-Crick

hydrogen bonding of the DNA strand to its complementary RNA sequence. They are chemoselective because RNA is cleaved nucleophilically with far greater ease than DNA, since DNA has no 2'-OH functionality on its sugar unit. This method is modeled on the 'antisense method,' as shown in **Figure 1.8**.³³

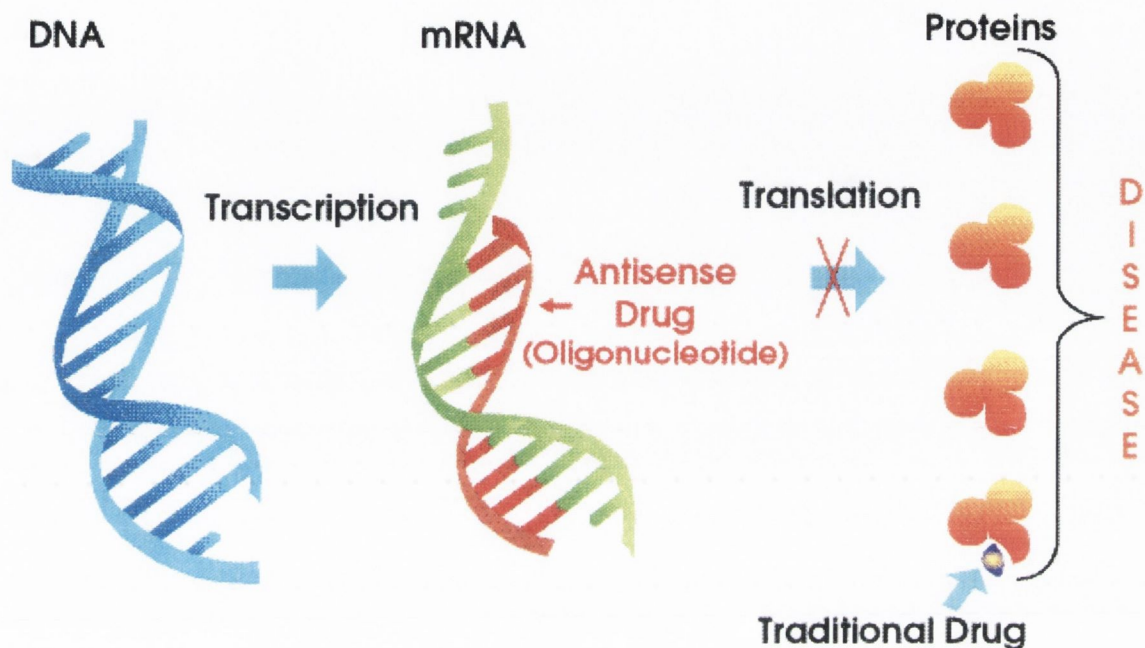
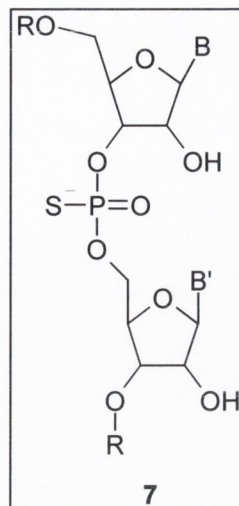


Figure 1.8.³³ A schematic illustrating the antisense approach. Protein synthesis is inhibited when an oligonucleotide that Watson-Crick binds to the complementary mRNA, thus preventing translation.

This presents the possibility of a powerful method of drug design. If the nucleotide sequence of the target molecule is known, the inhibitor is known to be the complementary oligonucleotide, thus paving the way for rational drug design.^{3, 32}

In 1997, Santaro and Joyce reported the development of a DNA enzyme that could cleave RNA under physiological conditions.³⁴ It was composed of a 15-mer catalytic domain within two substrate-recognition domains of seven to eight deoxynucleotides each. By changing the sequence of the recognition domains, different RNA substrates could be targeted. The activity of the enzyme depended on the presence of Mg^{2+} ions. It showed very high catalytic efficiency ($k_{cat}/K_M = 10^9 M^{-1}min^{-1}$) under multiple turnover conditions.³⁴ The mechanism by which artificial oligodeoxyribonucleotides (ODNs) inhibit translation differs from that involved in the natural antisense method. DNA drugs utilize the natural nuclease RNase-H, which specifically degrades the RNA species in a DNA-RNA duplex. Therefore this method would seem to offer a selective and catalytic

method of RNA cleavage. However, difficulties such as trans-membrane delivery and degradation of the ODNs by intra- or extracellular enzymes have inhibited progress.³ Attempts have been made to improve stability and delivery properties by modifying the ODNs, by for example incorporating a phosphorothioate linkage **7**, which reduces cleavage by nucleases.³ This approach has had some success and has led to the first antisense drugs in clinical trial and one, Vitravene, on the market.³⁵ However, it has been found that altering the DNA backbone can result in loss of RNase-H activity as the cleavage by the RNase enzyme is specific to the RNA in a RNA-DNA duplex and will not work if DNA analogues are used instead.³



In summary, synthetic ribozyme mimics have many advantages over natural ribozymes;⁷ for example they have lower molecular weights and so have an advantage in drug delivery. They also have separate recognition and cleavage domains so these can be optimised separately. Natural ribozymes have complex tertiary structures that rely on incorporation into natural RNA residues, whereas when using ribozyme mimics stability can be optimised. Most importantly, they allow selectivity in the RNA sequence to be cleaved, by the choice of a complementary oligonucleotide.^{3,7,32}

1.6.2. Requirement for Catalysis

One of the most important requirements for catalytic turnover is 'cleavage within the DNA-RNA duplex'.^{7,36,37,38} The reason for this is that the strength of DNA-RNA binding is length dependent. Thus cleavage within the duplex region reduces the binding constant between the ribozyme mimic and the RNA allowing the cleavage products to be released, freeing the catalyst. Therefore internal cleavage is greatly favoured over external cleavage, as in the four-step reaction mechanism in **Figure 1.9**.

In **A**, the complex-bearing DNA probe (in blue) comes into contact with the complementary RNA target strand (in yellow). In **B**, the two strands Watson-Crick bind, putting the complex in position to cleave the RNA at an internal position. In **C**, this cleavage has been carried out but the DNA and the fragmented RNA (in yellow and green) are still bound together. In **D**, the ribozyme mimic is released intact, leaving the cleaved mRNA and this completes one catalytic cycle. The alternative to this is external

cleavage which occurs when the complex or hydrolysis agent is incorporated at one end of the DNA strand. This leads to cleavage at the end of the duplex region. This external cleavage can result in product inhibition, as the DNA-RNA binding constant will be much higher, preventing the release of the cleavage agent.

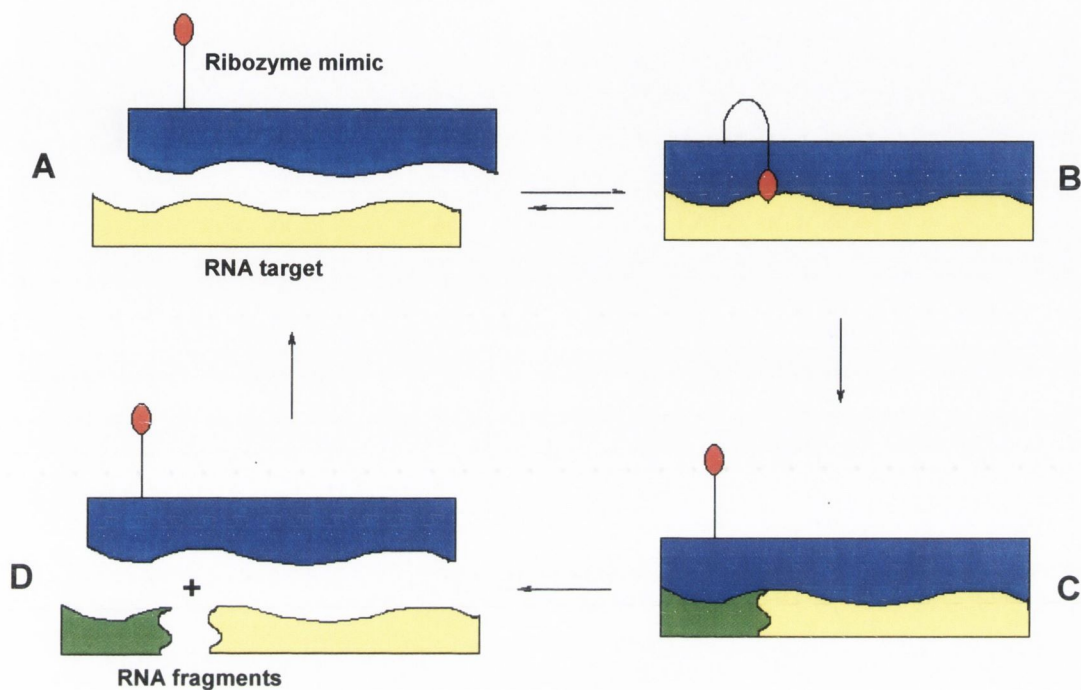


Figure 1.9 A catalyst incorporated into a DNA oligonucleotide (blue) binds to a complementary RNA strand (yellow), cleaving it within the duplex and then releasing the product fragments (yellow and green). This scheme allows for catalytic turnover.

1.7 Phosphodiester hydrolysis by metals

As was mentioned in Section 1.2, the hydrolysis of phosphodiester linkages can be promoted by the presence of metal ions. Equally, it was seen in Section 1.5 the metal ions are often found in the active sites of both ribozymes and ribonucleases and are known to play a crucial role in promoting hydrolysis of phosphodiester linkages, although the mechanisms of such behaviour are not always fully understood. The remainder of this thesis will deal with the use of various metal ions in the field of phosphodiester hydrolysis, and the efforts that have been made to emulate the actions of ribozymes and ribonucleases. First, however, it is important to understand more clearly the function of these metal ions in the hydrolytic process.

Some of the proposed ways in which metal ions can promote phosphodiester hydrolysis have been discussed in reviews by Chin *et al.*,³⁹ Burstyn *et al.*,⁴⁰ and Kraemer.⁴¹ The modes of activation can be loosely divided into two categories:³⁹

- 1 *Inner sphere methods*, in which hydrolysis is promoted by the metal ion itself, or a water molecule that is directly bound to the metal ion.
- 2 *Outer sphere methods*, in which the hydrolysis is promoted by a water molecule or hydroxide ion that is hydrogen bonded to the metal-bound water molecule.

From the point of view of the work that will be discussed in this thesis, the first category, inner sphere methods, is of greater importance, and these methods will be discussed in greater detail.

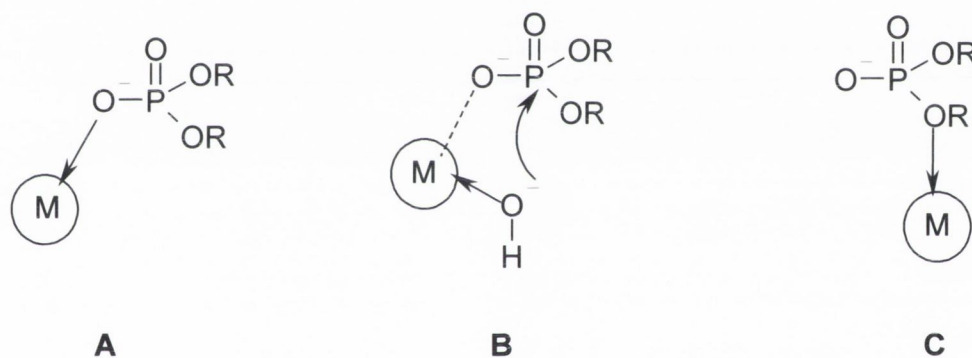


Figure 1.10. Three inner-sphere methods of metal promoted hydrolysis of a phosphodiester. **A:** Lewis acid activation of the phosphoryl oxygen. **B:** Nucleophilic attack of the phosphodiester by a metal-bound hydroxide. **C:** Leaving group activation.

The general methods can be further broken down as illustrated in **Figure 1.10**.³⁹ Firstly, Lewis acid activation can occur, in which the metal coordinates to the phosphoryl oxygen, stabilizing the negative charge and permitting the 2'-hydroxy group of RNA to cleave the phosphodiester, as shown in **[A]**. This is one of the most important roles played by metal ions in the promotion of phosphodiester hydrolysis, and it will be referred to again in Chapters 2, 3, 4 and 5. A second, an equally important role played by metal ions involves nucleophilic activation of the hydrolysis reaction by a nucleophile such as an hydroxide ion, derived from a deprotonated water molecule, which is coordinated to the metal. This can now attack the phosphodiester nucleophilically, as

shown in [B]. The use of a metal-bound water is also of great importance in the work which will be described in later chapters. A final inner-sphere method of activation involves leaving group activation, in which the metal ion coordinates to the leaving group [C].

As well as the methods outlined above, which are direct, or inner sphere methods, there are two outer sphere activation methods, shown in **Figure 1.11**. These methods are of less importance to the work that will be discussed throughout the rest of this thesis. A water molecule that is hydrogen bonded to the metal-bound water can behave as a nucleophile (intermolecular general base catalysis) [D] or promote general acid catalysis [E].

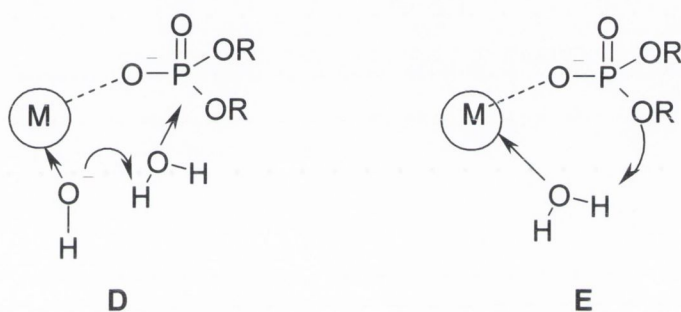


Figure 1.11. Two outer-sphere methods of metal promoted hydrolysis of a phosphodiester. **D:** A metal-bound hydroxide ion acting as a nucleophile. **E:** A metal-bound water molecule promoting general acid catalysis.

1.8 Phosphodiester models

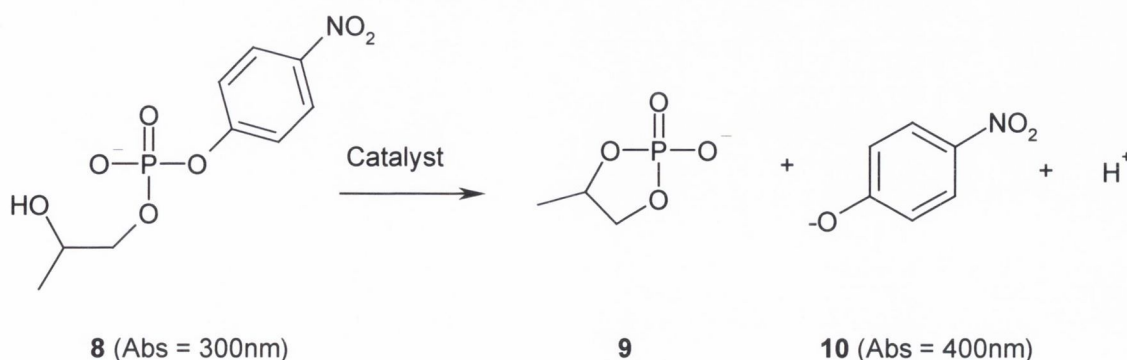
Phosphodiester hydrolysis has been found to be accelerated by a wide range of metal species and the effect of numerous metals on both RNA and RNA model compounds has been investigated. Before discussing any of these results, it is pertinent to consider the types of phosphodiesters that have been investigated. A number of different methods are available to investigate metals or complexes which may potentially cleave phosphodiester bonds.⁷ Many of the results discussed in the next chapters are obtained from work carried out using model compounds that model the behaviour of RNA, rather than on RNA itself. This is mainly for convenience, and to avoid the complications found with handling RNA. Such model compounds usually contain a phosphodiester bond with a good leaving group.⁷

One of the most commonly used RNA model compounds, and the one that will be most commonly mentioned in this thesis, is **HPNP** (hydroxypropyl *p*-nitrophenylphosphate)

8.⁴² There are a number of advantages to using **HPNP** as an RNA model compound for hydrolysis studies:

- * it contains a phosphodiester
- * it possesses a good leaving group, making the hydrolysis quicker to follow
- * it contains a hydroxy group which can act as an internal nucleophile, essentially mimicking the behaviour of the 2'-hydroxy group of mRNA

As well as these structural features, **HPNP** is a popular model compound for this work because of the ease of study of its hydrolysis. The hydrolysis of this compound can be monitored by UV/vis spectroscopy as it absorbs at 300nm and one product of the hydrolysis, *p*-nitrophenolate **10**, absorbs at 400nm, as can be seen in **Scheme 1.7**.⁴³ This provides an easy way to evaluate the rate and degree of phosphodiester hydrolysis, as the decrease in absorbance at 300 nm or and increase in absorbance at 400 nm can be followed and plotted against time to evaluate the kinetics of the reaction. In the absence of a catalyst, **HPNP** degrades, due to internal nucleophilic attack by the hydroxy group. The rate constant for the hydrolysis of **HPNP** at 37 °C and pH 7.40 using 10 mM HEPES buffer was evaluated by Breslow *et al.*, and reported as $1.2 \times 10^{-4} \text{ h}^{-1}$.⁴³ Therefore, rate of hydrolysis of **HPNP** by a particular agent is generally reported as both the rate constant of the reaction (k) and the relative rate constant (k_{rel}), which is the difference between the rate obtained the presence of the agent and that obtained without any catalyst.



Scheme 1.7. The hydrolysis of 2-hydroxy-*p*-nitrophenylphosphate (**HPNP**) to give a cyclic phosphate and *p*-nitrophenolate which can be monitored by UV/vis spectroscopy.

Some other phosphodiester model compounds that will be mentioned throughout this chapter are **BNPP**, **NPP**, **TNP** and **EPNP**, the full names and structures of which are shown in **Table 1.1**. These also release *p*-nitrophenolate upon hydrolysis but do not possess a hydroxy group and so are viewed primarily as models for the phosphodiester bonds of DNA.

Table 1.1 Phosphodiester Model Compounds

A selection of popular RNA and DNA model compounds, possessing good leaving groups.

Abbreviation	Full name	Structure
BNPP 11	Bis(<i>p</i> -nitrophenyl) phosphate	
NPP 12	4-Nitrophenyl phosphate	
EPNP 13	Ethyl- <i>p</i> -nitrophenyl phosphate	
TNP 14	Tris- <i>p</i> -nitrophenyl phosphate	

It is important to remember that although these model compounds possess phosphodiester groups, they are not an accurate representation of the true nature of RNA; their hydrolysis is often faster due to the presence of a good leaving group.⁷ Apart from these model compounds, many groups have worked with dinucleotides, as shown in **Figure 1.12**, which resemble RNA phosphodiester bonds more closely than activated model complexes.⁷

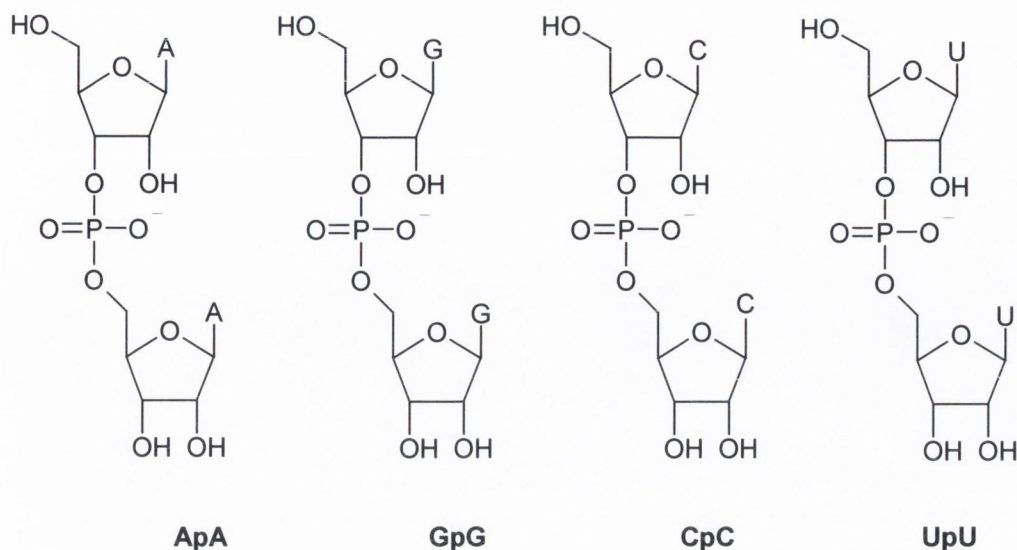


Figure 1.12. The four simple dinucleotides that use RNA bases, where A = adenine, G = guanine, C = cytosine and U = uracil.

In **Figure 1.12**, the four dinucleotides using the bases of RNA are shown. Mixed dinucleotides are also used, as in **ApG** or **CpU**. These substrates have the advantage over RNA that there is only one possible site of cleavage and that the cleavage products can be separated and analysed by HPLC.^{44,45} A great advantage of using dinucleotides to investigate hydrolysis is that any selectivity of a particular catalyst for one base over another may be determined.^{46,47} Ultimately, to examine the effect of a potential ribonuclease or ribozyme mimic upon RNA, it is necessary to work with RNA itself. It will be seen that such studies can produce quite different results to those given by model compounds due to various factors, such as the complex, polymeric, polyanionic nature of the longer mRNA strands.⁷

1.9 Evaluating the Effect of Metal Ions and Salts on Phosphodiester

The previous section examined the way in which metal ions can promote phosphodiester hydrolysis, and some of the phosphodiester that can be used to evaluate the rate of such hydrolysis. This section will look at the results of attempting to hydrolyse simple phosphodiester with salts or complexes of divalent metal ions.

In 1993, Breslow *et al.* reported the promotion of **HPNP** hydrolysis by some simple metal chlorides,⁴³ the results of which can be seen in **Table 1.2**.

Table 1.2 Hydrolysis of HPNP by Metal Chlorides⁴³

Metal chloride	$k \times 10^2 \text{ h}^{-1}$	k_{rel}
CaCl ₂	0.032	3
MgCl ₂	0.53	46
ZnCl ₂	1.7	150
PbCl ₂	32	2800
EuCl ₂	88.9	7700
TbCl ₂	110	9500
YbCl ₂	109	9500

These measurements were carried out at 37 °C and pH 7.0 in 10 mM HEPES buffer and used a 2.7-fold molar excess of metal salt relative to **HPNP**. It can be seen from these results that the trivalent lanthanide chlorides were more effective promoters of hydrolysis than the divalent transition metal chloride salts tested.⁴³

Similar studies were carried out by Morrow *et al* who tested a variety of nitrate salts for their ability to cleave **HPNP**, **Table 1.3**.⁴⁸ As was found by Breslow *et al.*,⁴³ a wide range of metals were capable of promoting the rate of hydrolysis, with lanthanides generally found to be far more effective than transition metal ions or Group II salts. These studies were carried out at pH 6.85, 37 °C and using 10mM HEPES buffer. The rate was found to be affected by the buffer type and concentration. When 15 mM HEPES buffer was used, the rate of **HPNP** hydrolysis by Cu(II), Zn(II), Co(II), Mn(II) and Ni(II) were found to double, while in the case of Pb(II) and La(III) the rate of hydrolysis remained unchanged.⁴⁸ When TRIS buffer was used, the rates for Pb(II) and La(III) again remained consistent, whereas that of Zn(II) was reduced by a factor of five and many of the transition metals were completely inactive. Kinetic experiments without buffer were not possible due to the sensitivity of the reaction to pH. It was suggested by the authors that a possible reason that was suggested for this difference in activity due to buffer was complexation of the metal ions by the buffers. This would affect catalytic transesterification by reducing coordination sites on the metal ions. As TRIS contains a primary amine, it could act as a reasonably good ligand for transition metal ions.⁴⁸

Table 1.3 Hydrolysis of HPNP by Metal Nitrates⁴⁸

Metal nitrate	Rate ($M^{-1}s^{-1}$)	Metal	Rate ($M^{-1}s^{-1}$)
La(III)	0.13	Pb(II)	0.20
Nd(III)	0.26	Cu(II)	0.040
Eu(III)	0.32	Zn(II)	0.018
Gd(III)	0.54	Co(II)	0.0026
Tb(III)	0.57	Mn(II)	0.0024
Yb(III)	0.40	Ni(II)	0.0016
Lu(III)	0.17	Mg(II)	0.0074
		Ca(II)	0.0048

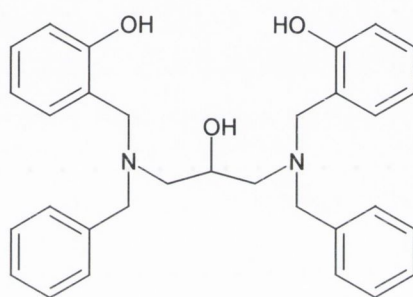
Simple aqueous solutions of zirconium and hafnium chloride cleaved **HPNP** and **BNPP** faster than other transition metal salts, and in the case of Zr^{4+} , faster than lanthanide cations.⁴⁹ Kinetic studies were carried out at 37 °C in unbuffered aqueous solution, adjusted at 25 °C to pH 3.5 with HCl. Reactions were monitored over eight half-lives. The activity of Hf^{4+} and Zr^{4+} may be explained by the fact that these species carry a 4⁺ charge as opposed to the 3⁺ charge of the lanthanides.⁴⁹ The greater Lewis acidity is better able to stabilise the negative charge on the phosphodiester, promoting internal nucleophilic attack.

1.8.1 Use of multiple metal charges to cleave phosphodiesters

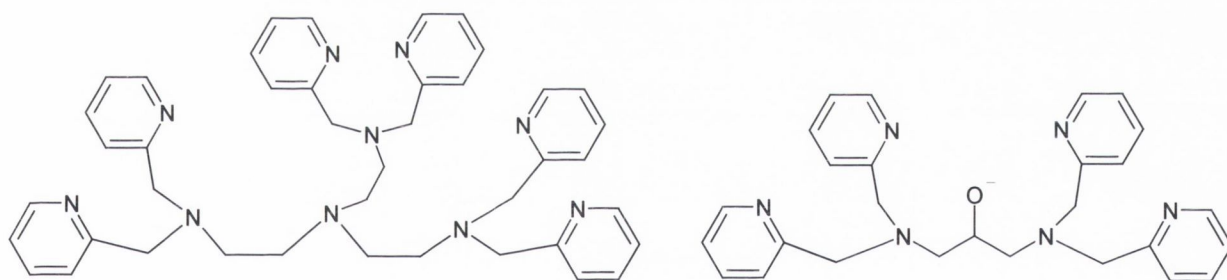
As well as testing single metal ions, many groups have worked with combinations of metal ions, sometimes using two molar equivalents of the same metal ion, or in some cases, two different metal ions in combination which have been tested using a variety of phosphodiester substrates.⁵⁰⁻⁵³ The results of some of these measurements will be presented here. It is important to note that while metal salts have been used successfully to cleave phosphodiesters, as shown in the previous section, it is generally desirable to work with complexed metal ions. There are a number of reasons for this; many metal ions are toxic to the human body, in particular the lanthanides, (which will be discussed in Section 1.9), so when considering the therapeutic applications of this research, the kinetic and thermodynamic stability of complexes with respect to metal dissociation is important. The use of ligands can also allow for two or more metal ions to be used synergistically. Some metal complexes that have had success in promoting phosphodiester cleavage will be discussed in this section. It should be noted that the

measurements discussed throughout this chapter were carried out using various substrates, including **HPNP**, **BNPP** and different dinucleotides, and that reaction conditions such as temperature, pH and solvents also vary from experiment to experiment. These factors make direct comparison of results impossible.

Hetero-dinuclear complexes have been reported by Komiyama *et al.* using the dinucleating ligand **15**.⁵⁴ Using this ligand, Fe(III)/Zn(II) and Fe(III)/Cd(II) systems were prepared in situ and ApA was added. The rate of ApA cleavage was pH dependent with the fastest rate achieved at pH 5. A rate constant of $3.0 \times 10^{-3} \text{ h}^{-1}$ was obtained with the Fe(III)/Cd(II) system at pH 5.6 and 50 °C.⁵⁴



15



16

17

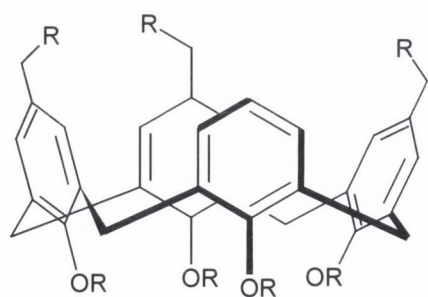
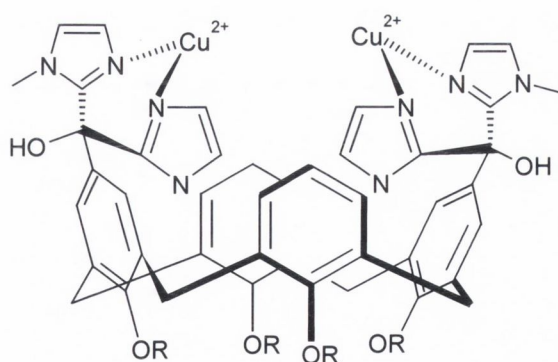
The use of multiple metal ions was again shown by Komiyama *et al.* who reported a series of ligands, such as **16** and **17**, that incorporated pyridine moieties.^{55,56} These were complexed with Zn(II) to give the corresponding mononuclear, dinuclear and trinuclear compounds. The hydrolytic activity of the complexes towards ApA at pH 6.9 and 50 °C was found to increase significantly with increasing number of metal ions; no hydrolysis was found with an analogous mononuclear complex, significant hydrolysis occurred in the presence of **Zn₂[17]** and even greater hydrolysis occurred in the presence of **Zn₃[16]**.⁵⁶ These kinetics obtained from these measurements are summarized in **Table 1.4**.

Table 1.4 Hydrolysis of diribonucleotides by polynuclear Zn(II) complexes

 $Zn_3[15]$ and $Zn_2[14]$ ⁵⁶

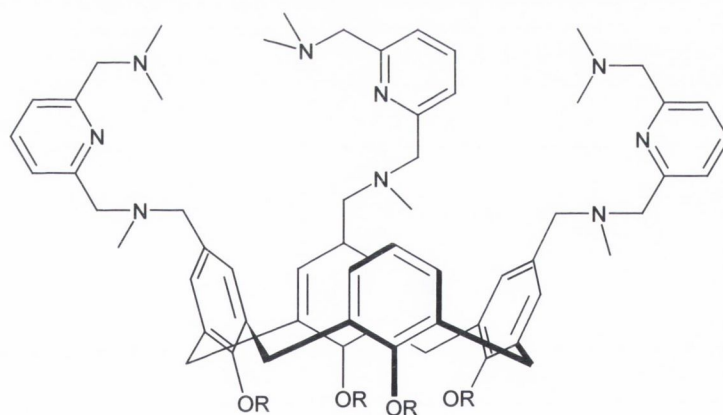
Substrate	10^5 k/s^{-1}	$T_{1/2}$
Using $Zn_3[16]$		
CpA	72	960
ApA	46	1400
GpA	26	2700
UpA	16	4500
ApG	17	4100
GpC	8	8500
Using $Zn_2[17]$		
CpA	6	11000
ApA	5	15000
GpA	5	15000
UpA	6	12000

Reinhoudt *et al.* have worked on phosphodiester cleavage using calixarene-based di- and trinuclear catalysts, incorporating either Zn(II) or Cu(II) ions.⁵⁷⁻⁶² The calixarene framework, **18**, provides a molecular “scaffold” which gives the binuclear complexes a rigid spatial orientation.

**18****19**

Early work involved the use of a calix[4]arene functionalised with two Zn(II) centres, which was found to bind strongly to **HPNP** and, at pH 7.0, 25 °C, increased the rate of hydrolysis by a factor of 23,000 compared to the uncatalysed reaction.⁶² These measurements were carried out in 1:1 acetonitrile/20 mM HEPES buffer solution. The

pH-rate curve was found to be bell shaped, with a maximum rate at pH 7.5. It was hypothesised that this pH may have been optimal as a balance was struck between the rate of binding (which involves displacement of a nucleophilic water or hydroxide molecule) and the rate of cleavage (which is promoted by such a water or hydroxide molecule). Using a 4-fold excess of **HPNP**, it was shown that the complex exhibited turnover without loss of activity. A similar system using two Cu(II) centres was found to increase the rate of **HPNP** hydrolysis even further, as well as exhibiting turnover,⁵⁸ while a mononuclear reference compound lacking the calixarene backbone was reported to have lower activity. This set of experiments was carried out in 35 % EtOH/20 mM HEPES buffer solution, at 25 °C and at various pHs. A Cu(II) bound hydroxide ion was found to act as a base in the intramolecular transesterification of the compound.⁵⁸ This dinuclear catalyst was also found to promote cleavage of the DNA model compound **EPNP**. Another di-Cu(II) system, this time incorporating bis-imidazole cofactors, **19**, was tested for activity at 25 °C using 35 % EtOH/20 mM HEPES buffer.⁵⁷ Activity was optimal at pH 7.4, and it was postulated that this was due to the presence of at least one protonated amine at this pH, which can therefore assist the hydrolysis reaction as a general acid.



20

1.10 Phosphodiester Hydrolysis using Lanthanide Complexes

Lanthanide ions are powerful Lewis acids and have been found to promote phosphodiester transesterification, hydrolysis and RNA cleavage under mild conditions.^{7,40,41} It can be seen from the work of Breslow⁴³ and Morrow,⁴⁸ presented in **Table 1.2** and **Table 1.3**, that lanthanides salts cleave **HPNP** far more efficiently than do the corresponding divalent metal salts. Promotion of both DNA and RNA cleavage has been reported for different lanthanide ions.⁶³ Ce(IV) has been shown to promote the cleavage of DNA under physiological conditions, while trivalent lanthanides have shown

activity for RNA cleavage.⁶³ It should be noted that the cleavage of DNA by lanthanide ions occurs through an oxidative pathway as opposed to the hydrolytic mechanism that has been discussed for RNA cleavage.

Opinions on which lanthanide ions are most effective in the cleavage of phosphodiester are divergent; an insight into this divergence is detailed in the remainder of this chapter. Studies at pH 7.0 have shown that the catalytic activity of the lanthanide ions increase with atomic number.⁶³ All of the lanthanide ions were reported to show similar pH-rate constant profiles, consisting of a steep slope in the lower pH range followed by a plateau at higher pH. This can be explained by the formation of the active $[\text{Ln}_2(\text{OH})_2]$. The relative activity of a given ion can then be explained by the concentration of the active species at a given pH (which increases with atomic number).⁶³

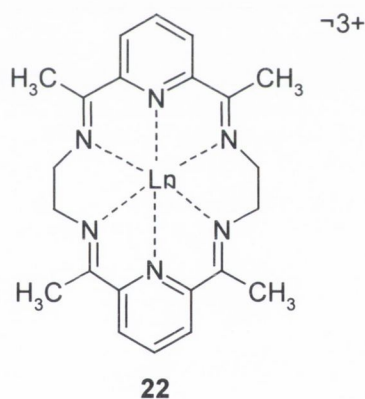
A more recent investigation⁶⁴ by Schneider *et al.* using **BNPP** as a phosphodiester, reported a 66-fold increase in the rate of hydrolysis between La(III) and Er(III) but a drop in activity for Yb(III) and Lu(III). This unexpected behaviour of the later lanthanide ions may be due to cation clustering which leads to decreased activity. However, Komiyama *et al.* has reported *accelerated* hydrolysis of cyclic adenosine monophosphate by a Ce(III) cluster.⁶⁵ In the case of CeCl_3 , the rate for the hydrolysis was 1.2 min^{-1} , representing a 10^{10} - 10^{11} fold increase over the uncatalysed reaction while the half life of the cyclic phosphate was reduced from half a million years to 35 s. From the steep slope of the pH-rate constant profile between pH 6.5 and 8, it was suggested that the formation of a $[\text{Ce}_3(\text{OH})_5]$ cluster was responsible for the enhancement in the hydrolysis.⁶⁵ Similarly, a La(III) dimer formed from LaCl_3 was shown by Chin *et al.* to cleave ApA very rapidly.⁶⁶ The studies were carried out at 25°C between pH 8.4 and pH 9.9 and followed by HPLC. In this case the active species was thought to be $[\text{La}_2(\text{OH})_5^+]$.⁶⁶

Free lanthanides, although they promote RNA cleavage, cannot be used directly in the human body due to their toxicity and the fact that they can form insoluble hydroxides which will precipitate out of solution.⁶⁷ Therefore if we are to think in terms of medical applications, it is important that they are complexed, and that these complexes are stable and inert to metal loss. The coordination of lanthanide ions occurs through ionic bonding interactions and thus ligands possessing negatively charged donor groups, or donor groups with large dipole moments such as carboxylic acid or carboxyl amides are

preferred. In solution, lanthanides tend to have high coordination requirements, with coordination numbers of 9-10 commonly found. However many ligands normally used to bind lanthanides (*eg.* EDTA), form complexes which do not cleave RNA.⁶⁸ It is therefore necessary to design ligands that bind lanthanides strongly but do not inhibit catalysis.

As previously mentioned in Section 1.1.3, it would be hoped to ultimately incorporate an active, stable complex into an oligonucleotide and therefore the presence of a functional group that will allow this is an advantage. The following section will review some of the most successful attempts at complexing lanthanides with a view to hydrolysing phosphodiester, with particular emphasis on the use of cyclen.

A number of different ligand systems will be discussed in this section, with emphasis on both the stability and the hydrolytic activity of the corresponding lanthanide complexes. The Schiff-base ligand **22** was investigated by Morrow *et al.* as a promoter of phosphodiester hydrolysis.⁶⁹



La(III) and Eu(III) complexes of **22** were prepared and tested with **HPNP** at 37 °C and pH 7.4, using 10 mM HEPES buffer.⁷⁰ The La(III) complex cleaved **HPNP** with a rate constant of 0.046 M⁻¹s⁻¹ while the Eu(III) complex gave a rate constant of 0.12 M⁻¹s⁻¹. It was proposed that the Eu(III) complex was more effective than the La(III) complex as it was more inert to metal dissociation. This Eu(III) complex was also shown to cleave ApU, and indeed, showed catalytic turnover.⁷⁰ Further studies in 1993 showed that the Eu(III) complex did not cleave RNA in a duplex.⁷¹ This complex, which had cleaved single stranded RNA as well as RNA model compounds, was shown to be unable to cleave a strand of RNA that was part of a DNA-RNA hybrid. As discussed in Section

1.5.2, a cleavage within the duplex is a condition for catalytic hydrolysis, so this result meant that **Eu[22]** was unsuitable for further biological investigation.

The effect of the choice of lanthanide ion on the stability of complexes was investigated in more detail using a series of lanthanide complexes of the same Schiff-base **22**.⁷² The rate of decomposition was found to depend heavily on the lanthanide ion, as can be seen in **Table 1.5**. From this it can be seen that the rates of decomposition did not vary linearly with the size of the lanthanide ions; the Gd(III) complex showed the fastest dissociation, followed by the La(III) complex, while the Tb(III) complex was found to be the most stable.⁷² These measurements were carried out at 37 °C and pH 7.3, using 10 mM HEPES buffer. The presence of competing ligands such as EDTA (ethylenediaminetetraacetic acid) or DTPA (diethylenetriaminepentaacetic acid) was shown to have a significant effect on the stability of the complexes. The rate constants for the decomposition of **La[22]** in the presence of such competing ligands are presented in **Table 1.6**.⁷²

Table 1.5 First order rate constants for the decomposition of lanthanide complexes of [22]⁷²

Complex	$k_{\text{obs}}(\text{s}^{-1})$
La(III)	$5.1 (\pm 0.1) \times 10^{-6}$
Eu(III)	$3.7 (\pm 0.3) \times 10^{-6}$
Gd(III)	$6.7 (\pm 0.5) \times 10^{-6}$
Tb(III)	$1.4 (\pm 0.3) \times 10^{-6}$

Table 1.6 First order rate constants for the decomposition of La[22] in the presence of competing ligands⁷²

Competing Ligand	$k_{\text{obs}}(\text{s}^{-1})$
EDTA	$4.0 (\pm 0.2) \times 10^{-4}$
DTPA	$5.5 (\pm 0.4) \times 10^{-5}$
Sodium phosphate	$3.2 (\pm 0.1) \times 10^{-5}$
Sodium citrate	$6.4 (\pm 0.3) \times 10^{-6}$

The use of cryptate-based lanthanide complexes to cleave phosphodiester has also been investigated. Lanthanide complexes of cryptate (2.2.1), **23**, were reported by Oh *et al.*⁷³⁻

Lanthanide complexes of tris(carbamoylmethyl)-triazacyclononane, **24**, have been prepared which incorporate either Y(III) or Eu(III).⁷⁶ This ligand provides six coordination sites for the encapsulated lanthanide ions, leaving it coordinatively unsaturated. Thus, it was expected that the additional binding site would be available for the binding of small molecules, for example, a water molecule or a phosphate diester. A crystal structure of the Y(III) complex showed that the metal was nonacoordinate with a metal-bound water molecule and two bound triflate counterions. However, it was found that these complexes dissociate rapidly in aqueous solution (25 minutes at pH 6 and 37 °C, with Cu(II) as a trapping agent).⁷⁶

A recently reported Ce(IV) complex of the same triazacyclononane system **24** has shown rapid hydrolysis of **HPNP**, giving a rate acceleration of 7400-fold.⁷⁷ This is an impressive result and represents one of the largest increases in the rate of **HPNP** hydrolysis to date. An important point to note about this result is that the measurements were carried out in degassed solution. This removed the possibility of metal-bound water molecules binding to carbonates present in the aqueous solution.⁷⁷ This precaution has not been previously documented by other groups, as biological conditions (37 °C and pH 7.4) are normally used, and therefore direct comparison of results is not possible. The hydrolytic activity was further tested by incubating the complex with a tRNA strand.⁷⁷ This resulted in complete degradation of the strand within 6 hours. While the efficiency of the complex is impressive, it is important to note that Ce(IV) can also cleave DNA oxidatively, making such a compound inappropriate for incorporation into oligonucleotide conjugates.⁶³

1.11 Cyclen Derivatives

One particular macrocyclic system that has come under investigation by many groups is 1,4,7,10-tetraazacyclododecane (cyclen), which, upon functionalisation, has been found to form stable lanthanide complexes.^{66,78} Cyclen-based lanthanide complexes have been investigated extensively in MRI contrast agent research^{79,80} as a result of their kinetic and thermodynamic stability. There are many advantages to the use of cyclen as a ligand for lanthanide ions including:

- * good kinetic and thermodynamic stability of the resulting complexes
- * the ease of modification through altering of pendant arms
- * the possibility of modification for attachment to biomolecules (eg, oligonucleotides)

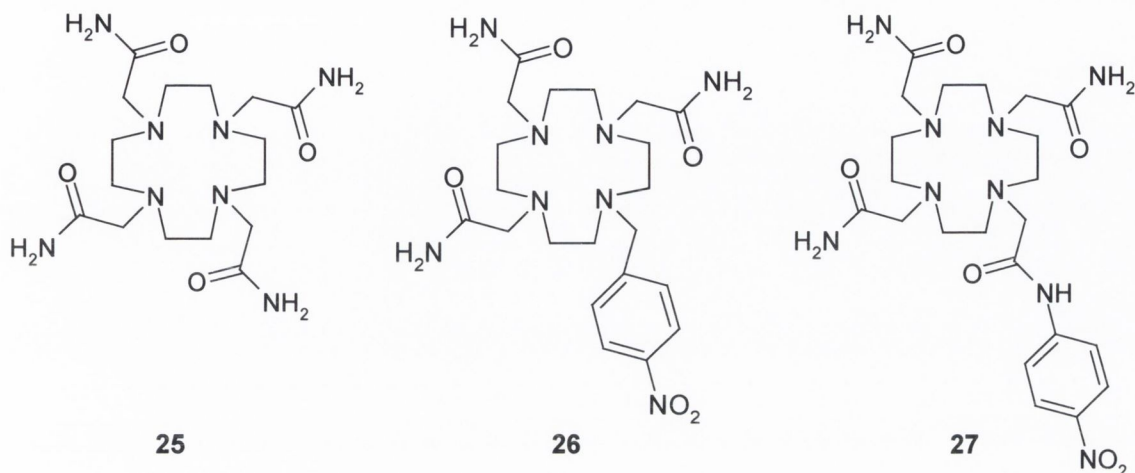
These features will be examined in more detail in the following section. While a variety of such cyclen-based systems have been developed for both MRI research^{81,82} and photophysical work,⁸³⁻⁸⁵ this section will concentrate on those that have been used to promote the cleavage of phosphodiester.

The first cyclen-based system discussed in this section is **25**, a tetraamide macrocycle.⁶⁸ This was designed as a neutral ligand, which would bind lanthanides while maintaining an overall positive charge on the resulting complex. La(III), Eu(III) and Dy(III) complexes were formed; these were found to be inert to metal loss in water at 37 °C and pH 6.0 in the presence of an excess of Cu(II), with half-lives of 6.7 days, 1.8 days and six weeks respectively.⁷¹

The hydrolytic activity of these complexes were tested with **HPNP** and oligomers of adenylic acid (A₁₂-A₁₈). The La(III) complex was found to be active in both cases, while the Eu(III) and Dy(III) did not promote hydrolysis, at 37 °C and pH 7.4. The La(III) complex cleaved **HPNP** with a rate of $5.8 \times 10^{-2} \text{ h}^{-1}$ and the oligomers of adenylic acid with a pseudo-first order rate constant of 0.57 h^{-1} .⁶⁸ Therefore, it can be seen that hydrolytic activity depends heavily on the choice of lanthanide ion.^{68,71}

This differences in activity between the La(III) complex and those of the smaller lanthanides were postulated to be due to the smaller number of coordination sites available for small molecule binding. The crystal structure of the La complex showed a ten-coordinate La(III) ion with eight coordination sites being provided by the ligand, while the ninth and tenth coordination sites were a metal-bound ethanol molecule and a metal-bound triflate molecule. **Eu[25]** was nine-coordinate with the ninth site being occupied by a water molecule. Binding studies were carried out using diethyl phosphate, and were followed by ³¹P NMR. Experimental conditions were not provided. Binding was not found to occur between the Eu(III) complex and diethyl phosphate, while the La(III) complex was found to bind to diethyl phosphate with a binding constant of $47.5 \pm 0.5 \text{ M}^{-1}$. This was of significance as the first step of ester hydrolysis most likely involves

the binding of the catalyst to the substrate. Therefore the effectiveness of a possible catalyst is highly dependent upon free coordination site availability for phosphate binding.⁷¹



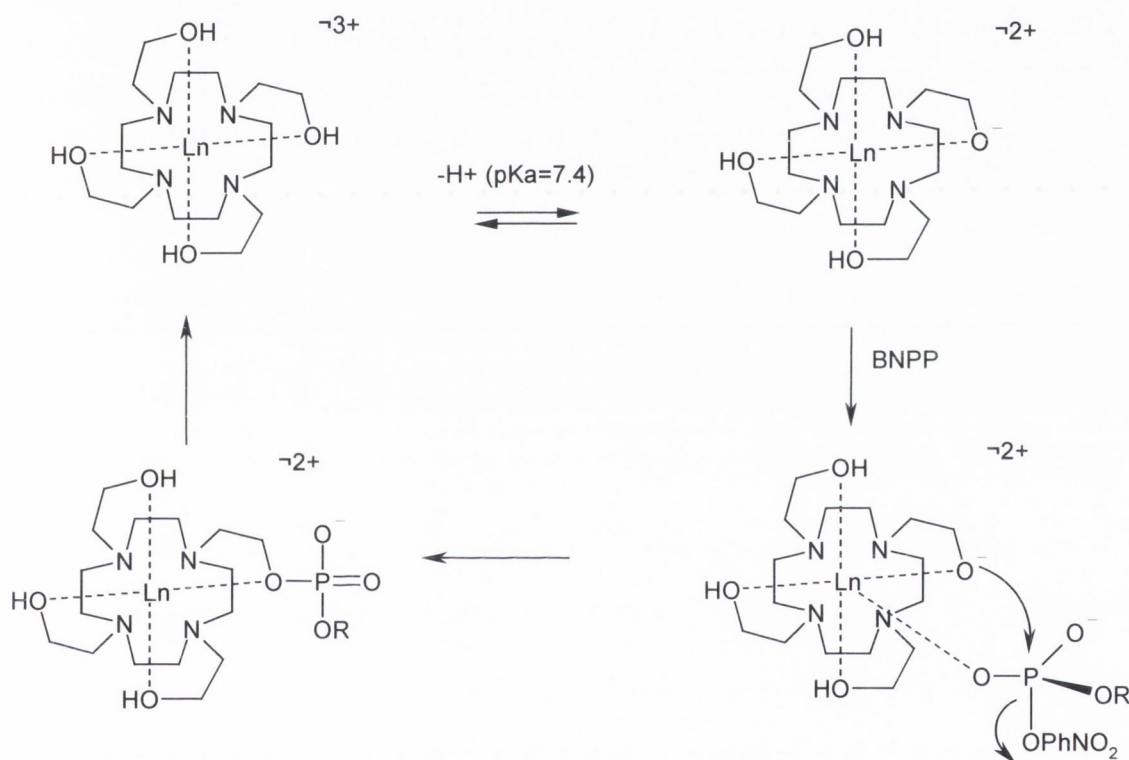
A recent paper by Morrow *et al.* reported that a thorium complex of **25** was found to promote transesterification of **HPNP**, showing that the activity of tetravalent cations can also be harnessed or even increased by complexation with a suitable ligand.⁸⁶ This system was shown to be extremely resistant to dissociation in metal exchange experiments with copper.⁸⁶

To investigate whether RNA cleavage ability was related to the number of coordination sites available, **25** was modified by Morrow *et al.* to give the heptadentate system **26**, prepared by replacing one amide group on **25** with a non-coordinating group.⁶⁹ A Eu(III) complex of this modified macrocycle was shown to promote transesterification of **HPNP** at pH 7.40 and 37 °C. The reaction was first order in complex over the concentration range 0.3-0.9 mM and a plot of k_{obs} against the concentration of **Eu[26]** gave a second order rate constant of $3.7 \text{ M}^{-1} \text{ s}^{-1}$.⁶⁸ The catalytic activity of this complex was in contrast to the inactivity of **Eu[25]**⁶⁸ and it was postulated that this activity could be due to the greater number of coordination sites available for small-molecule binding in **Eu[26]** compared to in **Eu[25]**.⁶⁹ This work suggested that two free coordination sites were necessary for the promotion of phosphodiester hydrolysis by these systems.

The cyclen system **25** was also modified by Akkaya *et al.*,⁸⁷ this time a ligand was formed, **27**, which retained the eight donor atoms of the original system but which was found to have increased RNA cleavage ability. **La[27]** was prepared and tested with **HPNP** at 25 °C and pH 7.4 using 50 mM HEPES buffer.⁸⁷ The reaction was followed

Table 1.7 BNPP Hydrolysis by Ln[28] complexes⁸⁸

Complex	Rate (h ⁻¹)	Temp
None	1.3x10 ⁻¹¹	25°C
Eu[28]	0.9x10 ⁻⁵	25°C
Eu[28]	2.0x10 ⁻⁴	37°C
La[28]	2.7x10 ⁻⁵	37°C

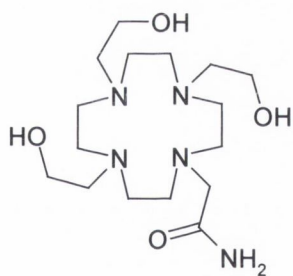
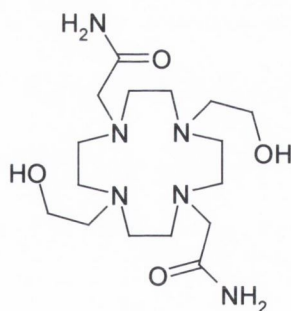
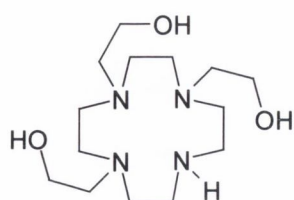
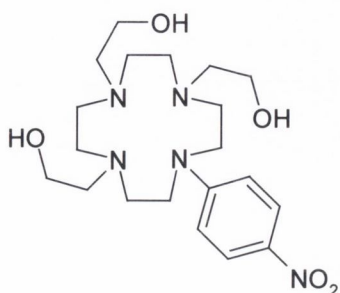
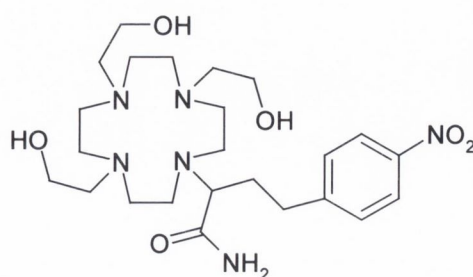
Scheme 1.9.⁸⁸ The proposed mechanism for the catalytic hydrolysis of BNPP by Ln[28]

Further to this, a ligand incorporating 2-hydroxypropyl cofactors was reported **29**.⁸⁹ This introduced a chiral centre into the complex. The system was prepared from racemic propylene oxide and a mixture of stereoisomers was formed. This mixture was complexed with La(III), Eu(III) and Lu(III).⁸⁹ Upon crystallisation of the Eu(III) complex from ethanol it was found that the unit cell consisted of two [Eu(THP)(H₂O)]³⁺ cations with 6 triflates, two ethanol molecules and one uncoordinated water molecule of

solvation. The two cations within the unit cell were diastereoisomers of each other; one being (*RRRS*) and the other being (*SSSR*). The ligand was also synthesised with all of the chiral centres in the *S*-configuration, by using *S*-propylene oxide. The complexes of this were found to be more stable than those of the mixed isomers, with half-lives in water for the La(III), Eu(III) and Lu(III) complexes of 73, 100 and 53 days respectively; this ligand formed stable complexes with early, middle and late lanthanide ions.⁸⁹ When complexes of **29** were treated with HPNP, the hydrolysis was found to be initially first order in lanthanide complex concentration in the 0.400-1.00 mM concentration range and then independent of complex concentration at higher concentrations of complex (>1.00 mM). The results obtained from these measurements are presented in **Table 1.8**.⁸⁹

Table 1.8 Kinetic data for the transesterification of HPNP by various lanthanide complexes at 37 °C⁸⁹

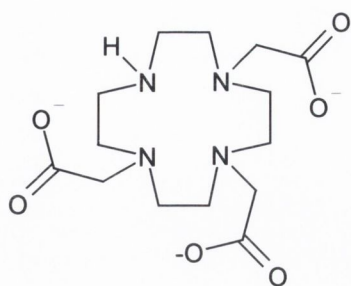
Complex	$10^2 k_2$ ($M^{-1} s^{-1}$)	$10^4 k_{cat}$ (s^{-1})	K (M^{-1})
Eu[28]	7.2	9.5	62
La(S-THP)	6.3	6.6	130
Eu(S-THP)	1.4	1.8	68
Lu(S-THP)	0.088		

**30****31****32****33****34**

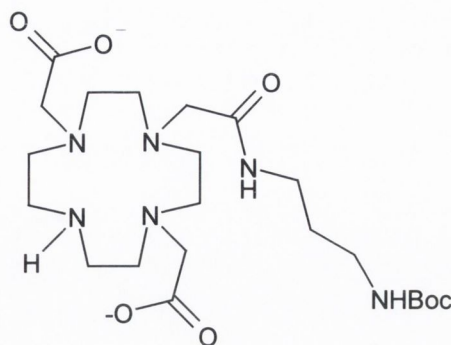
A series of mixed-pendant arm macrocycles was prepared by Morrow *et al.*,⁹⁰ in order to investigate the relative effects of the amide and hydroxyethyl arms on the ability of such complexes to promote the hydrolysis of phosphodiester. It was known from the respective four-arm systems (**26** and **27**) that the amide arm promoted stability of the lanthanide complex while the hydroxyethyl arm increased the rate of cleavage, as it can act as a nucleophile. **28** was modified to give **30**, by incorporating one amide arm in the place of a hydroxyethyl arm. A system was also made with mixed hydroxyethyl and two amide arms **31** by protecting two nitrogens with nitro benzyl groups before adding the hydroxyethyl arms, deprotecting and then adding the amide arms. Finally, a choice of alternative groups were used in conjunction with three hydroxyethyl arms; **32** consisted of only the three hydroxyethyl arms with the fourth nitrogen left unsubstituted, **33** incorporated a nitrophenyl group in the fourth position, yielding a heptadentate ligand and **34** was a mixed aromatic amide and hydroxyethyl system. It was found that dissociation of Eu(III) complexes was reduced in the presence of an amide arm compared to that without an amide arm. However this result was not as significant as expected for either of the mixed arm ligands.⁹⁰ The kinetics of metal ion dissociation were measured by UV/vis in the presence of a ten-fold excess of Cu²⁺ salt at 37 °C and at pH 6.0. The half lives for Eu(III) complexes of **30** and **31** were found to be 13 and 14 days respectively, while complete dissociation of **Eu[32]** was found after 20 hours under identical conditions.⁹⁰ Alternatively, dissociation was measured in the presence of an excess of competing ligands such as EDTA. Under these conditions, **Eu[34]** proved the most stable, with 41 % dissociation after three days. **Eu[32]** and **Eu[33]**, the two complexes without amide groups, were shown to be the least stable, dissociating rapidly in the absence of EDTA and within minutes in the presence of such competition. The kinetics for the hydrolysis of **HPNP** and **BNPP** by **Eu[30]**, **Eu[31]** and **Eu[34]** at pH 7.3 were also examined, at pH 7.3 and 37 °C, and the results are presented in **Table 1.9**. It was seen that the rate of cleavage of **HPNP** was reduced by a factor of ten when a hydroxyethyl group was replaced with an amide group, *eg*, **30** compared to **28**.⁹⁰

Table 1.9 Hydrolysis of phosphodiester by mixed-arm cyclen systems⁹⁰

Complex	Rate of cleavage of HPNP(s ⁻¹)	Rate of cleavage of BNPP(s ⁻¹)
Eu[30]	0.93x10 ⁻⁵	3.5x10 ⁻⁶
Eu[31]	0.10x10 ⁻⁵	None observed
Eu[34]	1.4x10 ⁻⁵	1.5x10 ⁻⁴



34



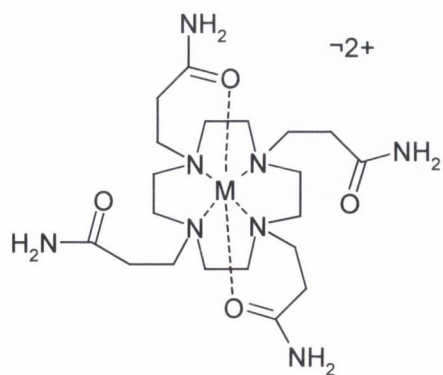
35

In 1996, the hydrolysis of **HPNP** by a neutral lanthanide-cyclen complex was reported by Kalesse *et al.*⁹¹ It should be noted that the previous cyclen-based ligands described in this chapter have been neutral, resulting in an overall positive charge to the corresponding lanthanide complex. Eu(III), Y(III) and La(III) complexes of **34** were prepared and the **Eu[34]** was found to cleave **HPNP** most rapidly. This was in contrast to the results of Morrow *et al.*, who reported that complexes of the larger Ln(III) ions were more effective.^{68,71} The charged species **35** was synthesised for the purpose of comparison and this was found to give no improvement in rate of hydrolysis over the neutral complex.⁹¹ It must be noted that although the rate of hydrolysis reported was high, these readings were obtained at 50 °C while most of the corresponding results from the literature have been carried out at 37 °C. Therefore, although the rates of cleavage appear high, the rate enhancements relative to the uncatalysed reaction were in the range of 300-500-fold. The rate was found to increase sharply between pH 7.3 and 8.3, an effect observed for both the neutral and the positively charged complexes.⁹¹ The full pH-rate dependence was not reported. A summary of the kinetic data for the cleavage of **HPNP** is given in **Table 1.10**.

Table 1.10 Kinetic data for the transesterification of HPNP by neutral lanthanide complexes⁹¹

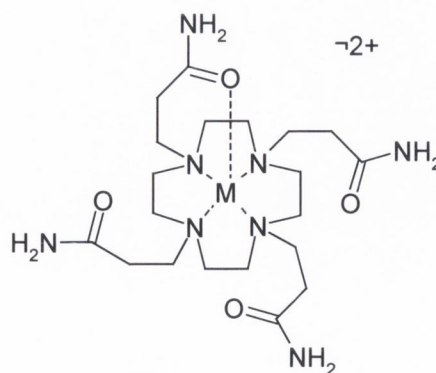
pH	$k_{\text{background}}$	$k_{\text{obs}}(\text{s}^{-1})$	$k_{\text{obs}}(\text{s}^{-1})$	$k_{\text{obs}}(\text{s}^{-1})$	$k_{\text{obs}}(\text{s}^{-1})$
		Eu[34]	Y[34]	La[34]	Eu[35]
7.3	2.3×10^{-6}	1.5×10^{-4}	1.0×10^{-4}	1.0×10^{-4}	1.0×10^{-4}
8.0	2.4×10^{-6}	2.3×10^{-4}	1.1×10^{-4}	1.3×10^{-4}	3.0×10^{-4}
8.25	2.9×10^{-6}	3.1×10^{-4}	1.3×10^{-4}	3.0×10^{-4}	3.3×10^{-4}
8.31	4.5×10^{-6}	4.5×10^{-4}	2.0×10^{-4}	4.5×10^{-4}	4.0×10^{-4}

Another variation of the cyclen based systems involved changing the distance between the metal ion and the donor atoms on the pendant arm, as seen in **36** and **37**.⁹² X-ray crystallography showed that in the Co(II) and Ni(II) complexes, the metal ion was bound to the four cyclen nitrogens and two acylato oxygens, **36**, with two water molecules completing the coordination sphere. Due to the smaller size of Cu(II) and Zn(II), these were found to bind to only one of the acylato-oxygens, as shown in **37**. These complexes were found to have poor stability and could be seen to degrade by mass spectrometry, with loss of pendant arms.⁹² The Co(II) complex was shown to promote cleavage of supercoiled DNA.⁹²



M = Co(II), Ni(II)

36

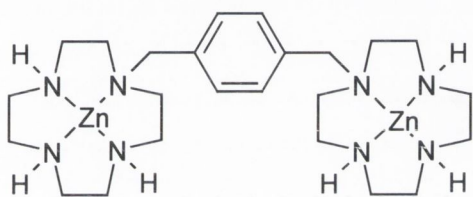
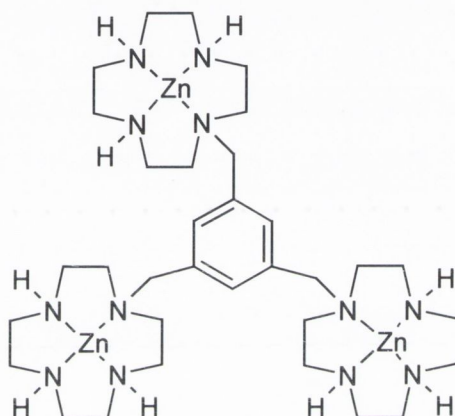


M = Cu(II), Zn(II)

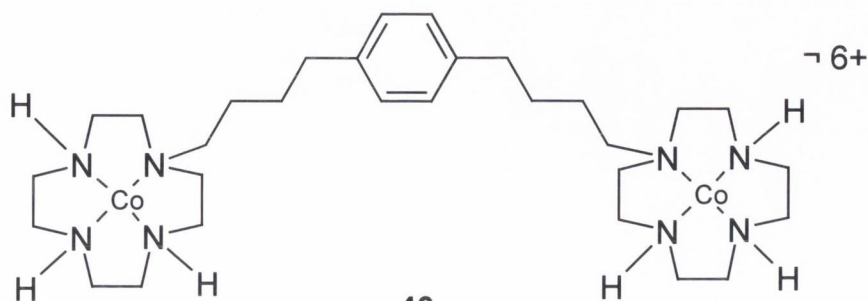
37

One advantage of the cyclen system is the ease with which it can be modified to yield a bis or tris system. A number of authors have reported the linking of cyclen moieties *via* a spacer, thus creating a bi- or tri-nucleating ligand.⁹³⁻⁹⁵

As has been mentioned previously, catalytic systems with two or three metal ions have been shown to efficiently cleave phosphodiesteres. Kimura *et al.* reported the linking together of two and three cyclen systems *via* a benzene linker as in **38** and **39**.^{93,94} However, the subsequent synthesis of the Zn(II) complexes was designed for DNA cleavage *via* a redox pathway rather than for RNA hydrolysis so these will not be discussed further.

**38****39**

A similar bis-cyclen system, **40**, incorporating two Co(III) ions, was reported to cleave **BNPP** by Czarnik *et al.*⁹⁵ This bis complex was found to cleave **BNPP** at 25 °C and pH 7.0 with a rate of $2.2 \times 10^{-5} \text{ s}^{-1}$, corresponding to a 10^7 -fold increase in rate over the uncatalysed reaction. This rate of cleavage was found to be 3.2 times faster than that obtained by the corresponding single cyclen-Co(III) complex, with the increase in rate being attributed to cooperation between the two metal centres.⁹⁵

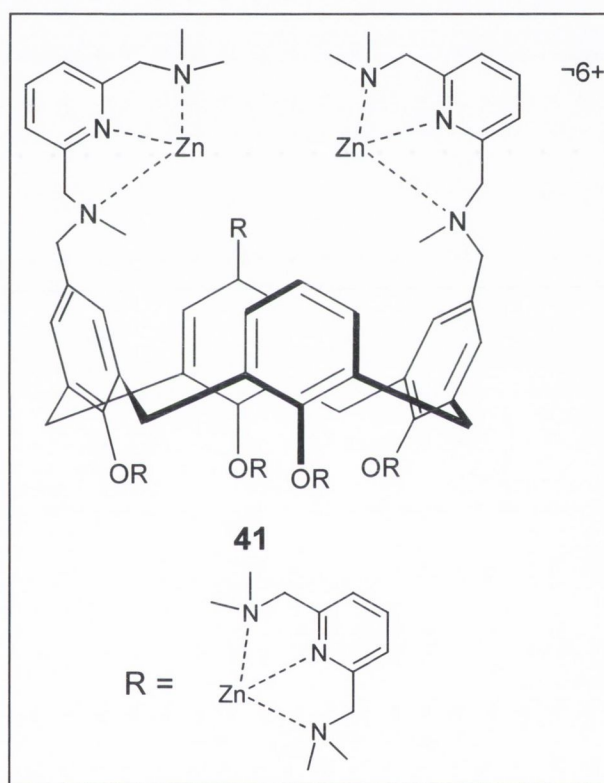
**40**

1.12 Towards Sequence Specific RNA Cleavage

This section will give an overview of some of the metal based compounds that have been used to promote the cleavage of dinucleotides and mRNA in a site-specific manner. First, some complexes that have been shown to cleave one base, or type of base, over others will be discussed. Then the covalent incorporation of metal complexes into oligonucleotides will be discussed; this employs the antisense method that was previously discussed in Section 1.3, and some of the results obtained by such an approach will be presented.

1.12.1 Preferential Cleavage at Certain Base Pairs

A tri-Zn(II) complex, using the same type of calixarene scaffold as shown previously in **18** and incorporating pyridine moieties was reported by Reinhoudt *et al.*⁴⁷ The activity of $\text{Zn}_3[\mathbf{41}]$ was investigated with a selection of dinucleotides, at 50 °C in 35 % EtOH/20 mM aqueous HEPES buffer. The results of these experiments are presented in **Table 1.11**. The reaction was monitored by HPLC. A rate maximum was found at pH 8.0. Turnover was exhibited by this complex, with three equivalents of UpU being completely hydrolysed. It was found that GpG and UpU were hydrolysed more rapidly than



other dinucleotides and this was explained by their possession of an acidic amide group which could be deprotonated by a Zn(II) bound hydroxy group. It was postulated that the anionic nitrogen could then coordinate to the Zn(II) complex, thus orientating the dinucleotide within the catalytic site, to be hydrolysed by the other two Zn(II) centres.⁴⁷ **Figure 1.14** shows a molecular modelling diagram, taken from Reinhoudt *et al.*, which illustrates this theory. With differences in rate of hydrolysis for GpG compared to UpU, these results suggested the possibility for selectivity in the cleavage of RNA.⁴⁷

Table 1.11 Rate of hydrolysis of dinucleotides by $Zn_3[41]$ ⁴⁷

Substrate	$k_{obs}/10^5 s^{-1}$
GpG	72
UpU	8.5
CpC	6.1
GpA	4.6
ApG	2.7
ApA	0.44

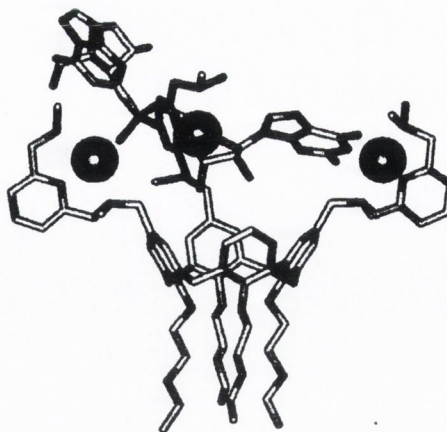
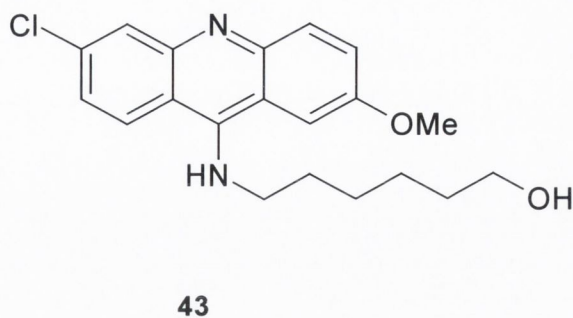
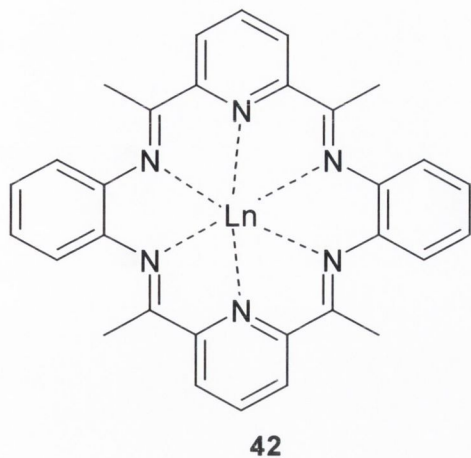


Figure 1.14⁴⁷ Molecular modelling study by Reinhoudt *et al.* of the interaction between $Zn_3[41]$ and the substrate GpG.

It has been reported that lanthanide complexes of some bulky ligands can give rise to selective cleavage of an RNA strand. Komiyama *et al.* reported that La(III) and Ce(III) complexes of **42** showed selective cleavage of a 76-mer tRNA when incubated at 30 °C and pH 7.5.⁹⁶ The level of selectivity was greater when the complexes were used than when the measurements were carried out with the free metal ions, suggesting that the conformation or size of the ligand played a role in the level of selectivity. This selectivity was explained by the tertiary structure of the tRNA; the catalyst preferentially attacked at “bulges” in the RNA.⁹⁶ These are exposed areas of RNA caused by hairpinning. The hydrolysis was evident after a short period of time, with evidence of strand cleavage after as little as 20 minutes. The extent or rate of this cleavage was not quantified. The same strand without tertiary structure was hydrolysed less effectively; with no measurable hydrolysis found after 21 hours. However, no selectivity was found when free metal ions or iminodiacetate complexes were used, again suggesting that the structure of the macrocyclic ligand played a role in determining the selectivity of the cleavage.⁹⁶



The vulnerability of “hairpinned” RNA has recently been further exploited by the same authors, with a number of systems designed to create an artificial hairpin in an RNA strand which can then be preferentially targeted by lanthanide ions.⁹⁷ The method involved a combination of free lanthanide ions and two DNA strands, each of which was complementary to a portion of the RNA to be cleaved. When hybridisation occurred, a “bulge” was created in the RNA and this point alone was vulnerable to attack by the lanthanide ions. By choosing the two DNA strands with care, highly site specific cleavage was obtained. To further improve the targeting of the desired RNA site, one of the DNA strands was attached to acridine **43** which activates the hydrolysis of the RNA linkage.⁹⁷ Using this system, with LuCl_3 , 90 % of a 39-mer was selectively hydrolysed in 48 hours at pH 8.0 and 37 °C.

Kalesse *et al.* reported the targeting TAR RNA of HIV-1 with a cyclen moiety attached to the Tat protein.⁹⁸ It is known that the Tat protein binds to the TAR RNA with the arginine residues of the protein making specific contact and that this is important in relation to the transcription of viral DNA. Therefore uncomplexed, unfunctionalised cyclen was attached to the arginine-rich region of the Tat protein.⁹⁸ It was attached at one position to a nonapeptide using solid-phase synthesis. Prior to the cleavage experiments, samples were incubated with either Eu(III) or Zn(II) salts for a 15 minute period. It was found that the uncomplexed cyclen conjugate gave selective and efficient cleavage of the RNA strand.⁹⁸ This result was surprising, as generally metal ions are necessary to promote phosphodiester hydrolysis. This result was repeated at pH 6.0 and 7.4, with little hydrolysis occurring at pH 8.0, indicating a pH dependent reaction. The only reaction site observed was located between a uridine and a guanidine. Addition of

Eu(III) or Zn(II) were shown to inhibit the reaction. The uncomplexed-cyclen reaction was retested in the presence of EDTA and found to give the same result.⁹⁸

Kalesse *et al.* recently reported the synthesis of tyrosine-cyclen conjugates, and the selectivity that they exhibit for uridines.⁹⁹ A cyclen moiety conjugated to a polypeptide gave selective cleavage at one site (between bases U31 and G32) of the TAR RNA of HIV. In order to further investigate this selectivity, the bases involved were changed; U31 was changed to A31 in one example, C30 and G32 were changed to uridines in another model (this example therefore contained an extra base pairing, giving a loop of 4 bases instead of 6). When U was changed to A, no cleavage occurred. In the case where three uridines were located together, no cleavage was observed, despite the presence of the originally cleaved U31. It was proposed that the 9-mer peptide bound to the RNA while cyclen interacted with uracil. Therefore the interaction could be prevented by unfavourable positioning of cyclen.⁹⁹

Conjugates such as these were prepared in the hope of obtaining unspecific binding to RNA and interaction between cyclen and uridine. Tyrosine was chosen as its side chain could increase binding while a nucleophilic group could promote hydrolysis. Various derivatives were synthesised, with an amino group converted to a guanidinium in some cases. It was found that only one derivative successfully cleaved the target and it cleaved not only the U31 but also the loop. The rate or extent of reaction was not quantified.⁹⁹

1.12.2 The Antisense Approach

In section 1.5, the preparation of ribozyme mimics was discussed. This involves the covalent incorporation of a hydrolytically active species into an oligonucleotide. This section will deal with some recent attempts to prepare fully artificial, selective ribozyme mimics.

An early example of a synthetic sequence-selective ribonuclease was reported by Komiyama *et al.*¹⁰⁰ Iminodiacetate was attached to a 15-mer DNA strand which was complementary to a targeted section of the 39-mer RNA strand shown in **Figure 1.15**. A 1:1 mixture of **44** and Lu(III) was found to selectively hydrolyse RNA at 37 °C, and pH 8. 7.3 % hydrolysis was reported after 4 hours, increasing to 17% after 8 hours.¹⁰⁰

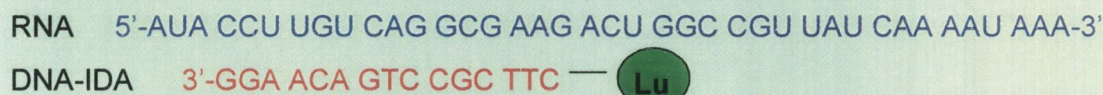
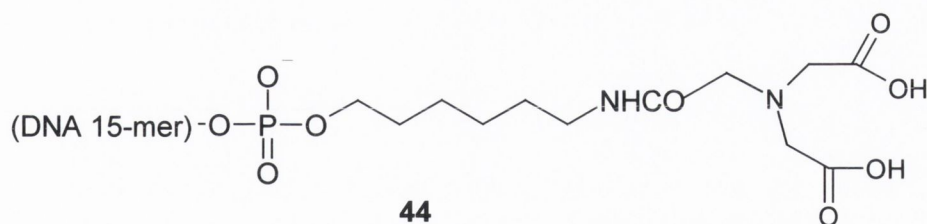
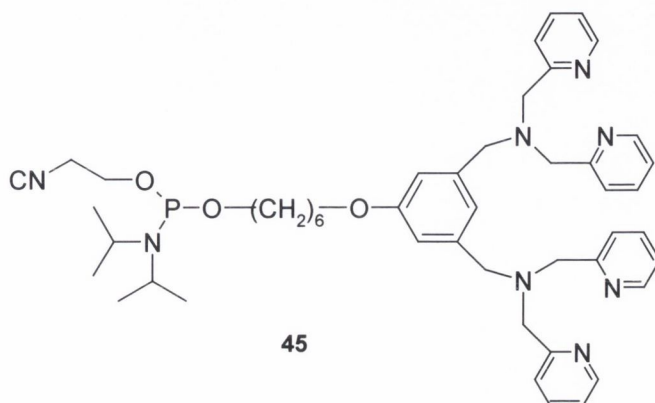


Figure 1.15¹⁰⁰ The 39-mer target RNA strand and the DNA-IDA complex (represented schematically) designed to cleave it. The scission sites are marked with arrows

From these results it seems that for cleavage to occur the lanthanide ion must be complexed to the iminodiacetate, since without the DNA-IDA, Lu(III) shows no ability to cleave RNA. It was estimated that 95 % of the Lu(III) ions were complexing to the iminodiacetate under the reaction conditions. In this study it was also found that Tl(III) and Eu(III) ions show selectivity for RNA cleavage. When La(III) was used, it was found to be only half as efficient. Regardless of the lanthanide used, the scission sites were the same.¹⁰⁰

The same group reported the preparation of **45**, which was then tethered to the 5' end of DNA oligonucleotides.¹⁰¹ This dinucleating species is based on similar ligands discussed previously.^{55,56} The 36-mer RNA shown in **Figure 1.16** was successfully hydrolysed by a combination of the modified DNA and a two-fold excess of Zn(II) ions at pH 7.0 and 37 °C. The selectivity was very high, with cleavage at only one point, as indicated by the arrow in **Figure 1.16**, even in the presence of an excess of metal ions. The degree of hydrolysis was not quantified.¹⁰¹



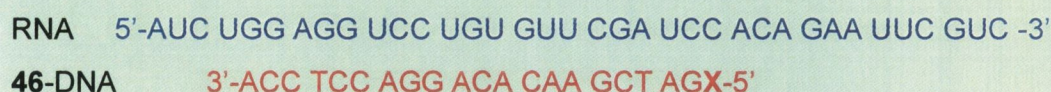
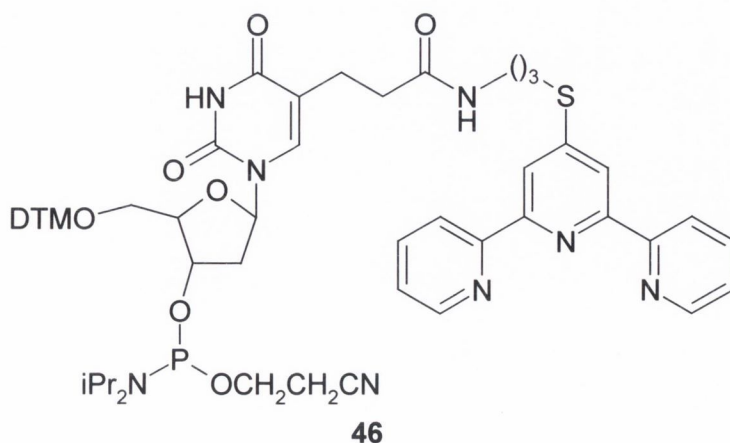


Figure 1.16.¹⁰¹ The sequences of The 36-mer RNA strand to be cleaved and the modified oligonucleotide in which 'X' is a residue carrying compound **45**

One of the most promising approaches in recent years has been the incorporation of stable lanthanide complexes into oligonucleotides, to form a ribozyme mimic. Unlike the situation in many of the cases discussed above, this method allows for the characterisation of the metal complex prior to measurements and prevents the possibility of free metal ions being responsible for RNA cleavage.

In 1994, an example of such work was reported by Bashkin *et al.*, who described the first example of a 'wholly synthetic, functional mimic of a ribozyme.'¹⁰² This design emphasized the need for the separation of recognition (the ODN) and activity (the metal complex) functions. Knowing that (terpyridyl)Cu^{II}OH⁺ could promote the hydrolysis of RNA,^{103,104} a derivative of such a complex, **46**, was incorporated into a DNA probe that was complementary to a 159-mer sequence from the gag RNA from the HIV gene, shown in **Figure 1.17**. Reactions were carried out for 72 h at 45 °C and analysed by polyacrilamide gel electrophoresis. In the presence of Cu(II), the ribozyme mimic successfully cleaved the target strand between two bases only.¹⁰²



5'-¹(775)GGAGAAAUUUAUAAAGAUGGAUAAUCCUGGGAUUAAAUAAA
 AUAGUAAGAAUGUAUAGCCCUACCCAGCAUUCUAGACAUAAGACAAGGAC
 CAAAGAACCCUUUAGAGACUAUGUAGACCGGUUCUAUAAAACUCUAAGAG
 CCGAGCAAGUUCAGAG (933)-3'

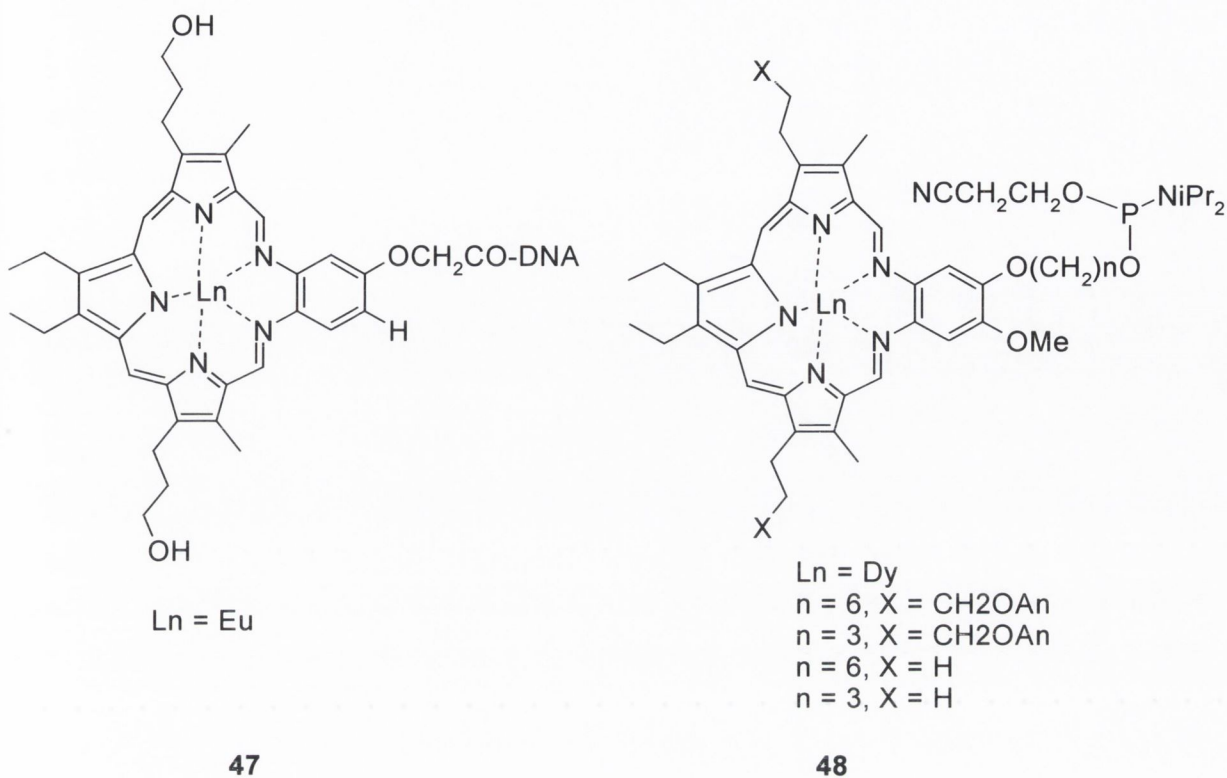
Figure 1.17. Sequence of the 159-mer RNA target. The ribozyme mimic uses a sequence complementary to the underlined region.

The 159-mer RNA strand was incubated with the ribozyme mimic at 45 °C in 20 mM HEPES buffer at pH 7.5 over 72 hours. The results were analysed by PAGE. No cleavage was observed in the absence of the ribozyme mimic. When the ribozyme mimic was used in the absence of Cu(II) ions, no hydrolysis was found to occur over the 72 hour period. However, in the presence of both the ribozyme mimic and Cu(II) ions, 18-25 % cleavage was found. The cleavage was seen to occur at only sites, both within the duplex region.¹⁰²



Figure 1.18. Sites of cleavage observed when the 159-mer of Figure 1.17 was incubated with Bashkin *et al.*'s ribozyme mimic.¹⁰²

Sessler *et al.* have worked with texaphyrin complexes such as **47**, containing various lanthanides.¹⁰⁵⁻¹⁰⁷ In 1994, this group reported that **Eu[48]**, when attached to an oligonucleotide, (CTC GGC CAT AGC GAA TGT TC) cleaved a 30-mer RNA strand at only one site.¹⁰⁵ The RNA strand was radiolabelled at the 3'-end using ³²P and incubated with complex-containing oligonucleotide for 24 h at 37 °C in an aqueous solution containing 50 mM HEPES at pH 7.5, 100 mM NaCl and 25 μM EDTA. 30 % cleavage was observed by PAGE after this time.¹¹² Cleavage was not observed when a non-complimentary oligonucleotide was used or when on oligonucleotide without a metal complex was tested. Control reactions indicated that ambient light, type of buffer (TRIS acetate or HEPES, EDTA, pH 6.0-8.0) and presence or absence of oxygen did not effect the reaction.¹⁰⁵ Use of different spacers connecting the complex with the DNA oligonucleotide was not examined.



In 1997, the same group reported the preparation of phosphoramidite derivatives of dysprosium(III) texaphyrin, **Dy[48]** and their introduction into DNA using differing lengths of spacer group, as shown in **Figure 1.19**.¹⁰⁷ In these studies it was found that the rate of RNA cleavage was related to the length of the linking section joining the metal complex to the DNA oligonucleotide. A shorter link resulted in an increased rate of RNA cleavage. Studies have also been carried out to investigate the effect of attaching the complex at an internal position within the oligonucleotide instead of at the 5'-end.²³ This formation allows the release of RNA fragments after cleavage. Cleavage of RNA strand 3 by 2 and 1 was studied.¹⁰⁷

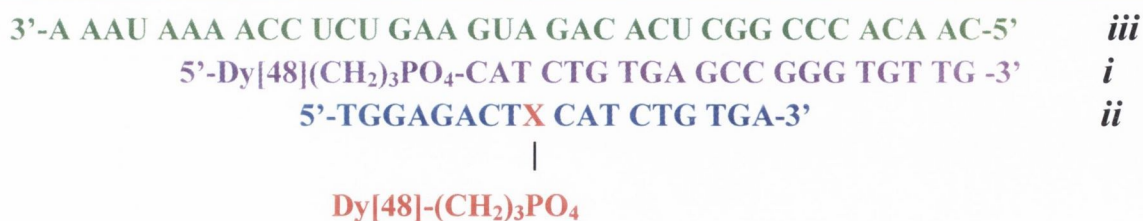
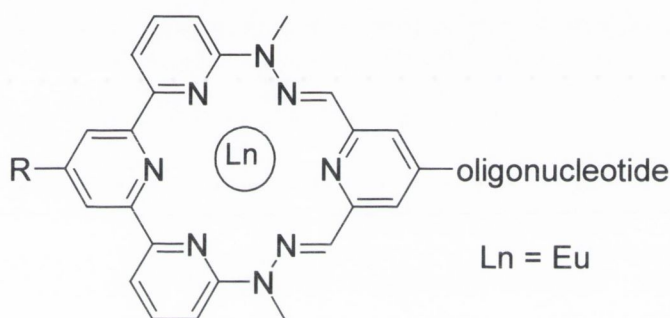


Figure 1.19¹⁰⁷ RNA strand 3 was cleaved by the two ribozyme mimics **i** and **ii**. **i** incorporates the active agent at the end of the oligonucleotide and **ii** incorporates it within the oligo.

These two systems showed a similar ability to cleave RNA but one system was found to be catalytic and the other was not. When a ten-fold excess of RNA was used 5 % of RNA was cleaved in 24 hours by **1**, while 67 % was cleaved by **2**. This showed that **2** exhibited catalytic turnover while **1** did not.¹⁰⁷

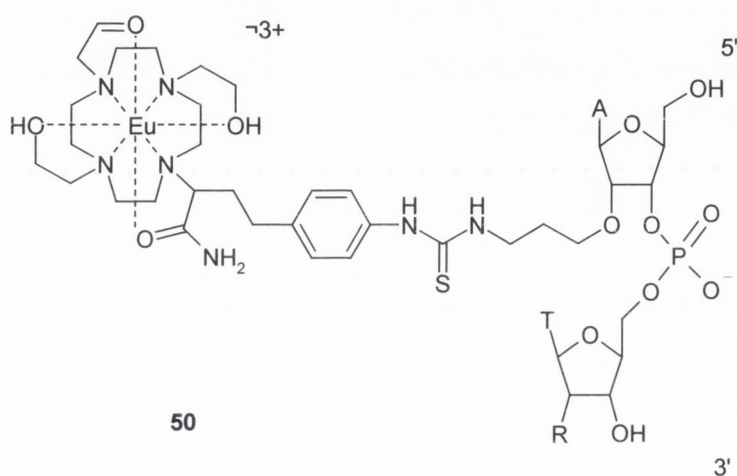
Similarly, Haner *et al.* have worked on systems such as **49** which consisted of lanthanide based macrocyclics incorporated into oligonucleotides.^{108,109,110} This group has worked on creating bulged RNA which is more easily cleaved than duplexed RNA. Hence, a reaction with a fully complementary 29-mer RNA strand was compared to that with a 31-mer which was identical except for two extra nucleotides in the centre of the strand which, upon hybridisation, were designed to bulge out.



49

After incubation for 16 hours the fully matched RNA was found to have only slight cleavage while the 31-mer had been cleaved almost quantitatively. The cleavage was not confined to the bulge, but also occurred at the adjacent bases. The best reported result was 90 % cleavage of the target at 37 °C in 16 hours.¹⁰⁹ Significant differences were found in the extent of cleavage depending on factors such as the position of the catalyst within the oligonucleotide and minor structural differences in the catalyst. Further experiments suggested that bulged RNA is cleaved preferentially to single stranded RNA. The crystal structure of one of these complexes, prior to incorporation within the oligonucleotide, has been reported and it was noted that two coordination sites of the Eu(III) were occupied by water molecules, suggesting that the complex has a tendency to bind to O- ligands such as phosphate groups.¹⁰⁹ Turnover has been achieved by using 2'-methoxyethoxy-modified conjugates which cleave RNA with the same efficiency as unmodified conjugates but bind RNA more strongly.

More recently an analogue of **28** was prepared by attaching the Eu(III) complex to an oligonucleotide.¹¹¹ The resulting ribozyme mimic, **50**, was shown to cleave a target RNA strand. However, cleavage was slower than had been expected from the results of the untethered complex **28**, and some metal dissociation was found by mass spec analysis after 24 hours.¹¹¹ Specificity was not as great as had been anticipated by the authors and it was suggested that this might be due to the choice of linker arm. Adducts of **28** and nucleotides were identified among the products of cleavage and this added to the evidence that the mechanism involves a nucleophilic displacement reaction, with the metal activated hydroxyethyl group as the nucleophile.¹¹¹



1.13 Conclusion

This chapter has provided an overview of many of the advancements in the field of mRNA cleavage in recent years. It can be seen that nature has developed efficient, and more importantly, selective methods to hydrolyse the phosphodiester linkages that join the bases of mRNA, in the form of ribozymes and ribonucleases. The cleavage of phosphodiesters has been shown to be readily promoted by the use of various metal ions; Ca(II), Zn(II) and Mg(II) ions are found in nature to serve this purpose.

The synthesis of artificial cleavage agents has taken advantage of these facts, and many groups have investigated the effects of various metals and combinations of metal pairs on both mRNA and RNA model compounds. This chapter has highlighted the use of lanthanide ions in this role; these have been found to be particularly effective, both when used as free ions and when complexed in ligands. Cyclen-based complexes of lanthanide ions have been studied by many groups, for their photophysical properties and as MRI contrast agents as well as in the field of RNA cleavage. Such complexes have been seen to be very active when tested with **HPNP** and other phosphodiesters. An important

feature of such complexes is the presence of lanthanide-bound water molecules, as these can promote the hydrolysis of a phosphodiester through nucleophilic activation. There is also the potential to covalently incorporate an active complex into an oligonucleotide of choice, forming in effect a ribozyme mimic, with the choice of oligonucleotide determined by the sequence of mRNA strand to be cleaved and the position at which cleavage is required. This presents the possibility of fully artificial, selective mRNA hydrolysis, and is the ultimate aim of this field of research. Sequence-specific RNA cleavage could be used in the treatment of any disease that involves the production of harmful proteins, including bacterial, viral and fungal infections. As has been shown in this chapter, a wide variety of ribozyme mimics have been prepared over the last ten years and, again, many of the most successful examples have been based on lanthanide complexes. One of the most important areas of research in this field now is to develop the best possible ligand systems to bind lanthanide ions without inhibiting the catalysis of mRNA.

1.14 Aim of Project

It has been clearly shown that metal ions, in particular, lanthanide ions, are useful agents for the promotion of hydrolysis of the phosphodiester bonds of mRNA and RNA model groups. The work described in this thesis will concentrate on the hydrolytic activity of complexed lanthanide ions. Complexation of metal ions provides many advantages in this area of research; it is necessary, first of all, when working with ions that may be toxic, however it provides a platform into which various cofactors can be built, which may aid the promotion of hydrolysis.

One of the most interesting developments in the field is the recent work involving modification of the cyclen framework, which provides a wide variety of options in terms of the possibility to experiment with different pendant arms. Of interest in the work to be described here is how the incorporation of different pendant arms can affect the behaviour of the corresponding lanthanide complexes in relation to their ability to cleave RNA and RNA model compounds.

There are a number of factors which influence the activity of a complex in cleaving RNA (or **HPNP**):

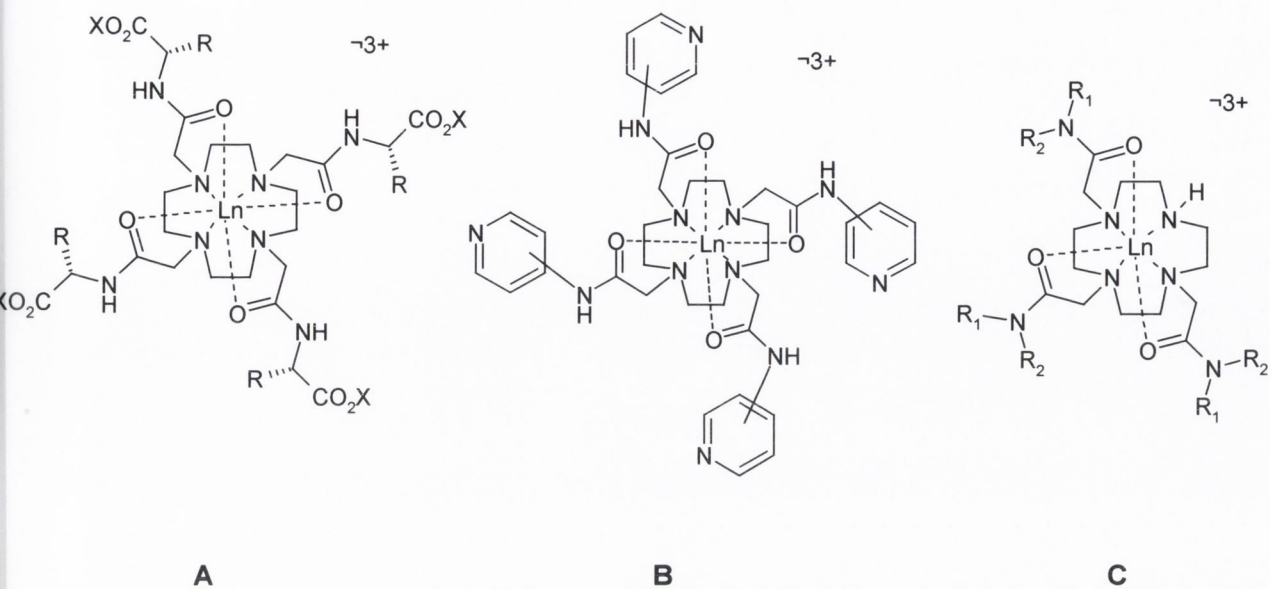
- The choice of lanthanide ion. In many cases, the larger lanthanides are reported as being more active than the smaller ions, however this is not always the case
- The number of metal-bound water molecules. It has been suggested that the activity of a complex is greater when two metal-bound water molecules are present in a complex
- The pK_a of the metal-bound water molecules. Since it is the metal-bound hydroxide that aids nucleophilic attack upon the phosphodiester, the pK_a of the metal-bound water is of great importance

It must be assumed that all of these features are effected by the choice of ligand within which a given lanthanide is complexed; indeed it might be possible to ‘fine-tune’ such features by altering the nature of the cofactors attached to the ligand. Of particular interest was the idea of how the size of the cofactor would influence the geometry and activity of the complexes. Three general types of cyclen ligands will be discussed in this thesis and these are illustrated below:

A: Incorporating pseudo-dipeptide moieties. In light of their role in the active sites of ribonucleases, the idea of incorporating amino acid-based cofactors into a cyclen framework was considered, work which will be discussed in detail in Chapter Two.

B: Incorporating aminopyridine moieties. A notable feature of ribonucleases is their ability to promote phosphodiester cleavage through acid base catalysis. It is possible that the presence of aminopyridine groups could provide such a function. This work will be described in Chapter Three

C: Functionalising only three of the cyclen nitrogens. Such a compound has the advantage that it can later be incorporated into an oligonucleotide for use as a ribozyme mimic. This work will be described in Chapter Three.



The synthesis and characterization of these complexes will be discussed, along with the efforts made to evaluate their activity as potential ribozyme and ribonuclease mimics.

Chapter Two

Synthesis of Amino Acid
Based Complexes

2.1 Introduction

In Chapter One, the use of complexed lanthanide ions as ribozyme and ribonuclease mimics was discussed in detail. As discussed in section 1.13, the aim of this project is to prepare a series of ribonuclease mimics, based on the use of complexed lanthanide ions. This chapter will deal with the preparation and characterisation of such compounds. The ligand that we used to complex the lanthanide ions is cyclen; the principal reasons for this have been discussed previously (section 1.8), and can be briefly summarised as follows:

- * it is relatively easily modified^{68,90,112,113,114}
- * when modified, it is known to form kinetically and thermodynamically stable lanthanide complexes^{78,89}
- * it has the potential to be incorporated into a biological device (eg, into a DNA oligonucleotide)^{87,115}
- * when embedded in such a cyclen ligand, the Lewis acidity of the lanthanide ion is maintained^{69,71}
- * when embedded in such a system, the lanthanide ion is coordinatively unsaturated; additional binding sites are available for small molecule binding.^{68,69,71}

There are a number of ways in which the cyclen system can be modified, some of which were seen in section 1.10. **Figure 2.1** shows a selection of cyclen systems with four pendant arms, each of which can coordinate a lanthanide through the four carbonyl oxygens of the pendant arms as well as the four amides of the macrocyclic ring itself.⁷¹ Thus, it is known that such tetrasubstituted cyclen ligands provide eight coordination sites for an encompassed metal ion. **A** is commonly known as DOTA, and is one of the first cyclen based MRI contrast agents.⁷⁸ It is a tetraalkylated cyclen system which incorporates acetic acid based moieties. **B** was reported by Parker *et al.* in 1997, and incorporated four phosphinate moieties.¹¹⁶ **C** was reported by Gunlaugsson in 2001 as a luminescent chemosensor that could determine pH in an acidic environment.¹¹⁷ This system incorporates four quinoline moieties. These systems show the versatility of cyclen as a macrocyclic base, upon which larger structures can be built. Therefore, we can alter the size, the shape, and the properties of such complexes by choosing the pendant arms with care.

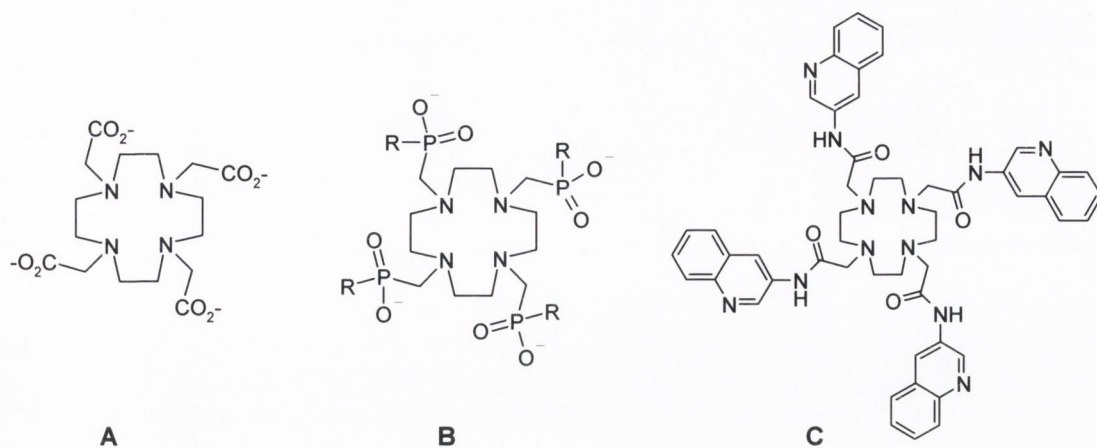


Figure 2.1 Previously reported cyclen-based ligands with four pendant arms, capable of coordinating a lanthanide ion. **A** is DOTA, one of the first MRI contrast agents,⁷⁸ **B** was reported by Parker et al. as an MRI contrast agent,¹¹⁶ **C** was reported by Gunnlaugsson as a pH sensor.¹¹⁷

An additional feature of these systems is that, upon complexation, they are known to form concave structures in solutions, of either square antiprism or twisted square antiprism geometry.⁶⁷ Consequently, we sought to take advantage of these structural features and build upon them by extending the ‘walls’ of a possible cavity through choice of pendant arms. Such pendant arms would be the platform for the incorporation of moieties, that we will refer to as ‘**co-factors**,’ that could further aid the ability of the complex to accelerate the hydrolysis of phosphodiester.

Since the ultimate aim was to successfully mimic the active site of a ribonuclease, such a compound would have many of the features required, as illustrated in **Figure 2.2**; a metal centre providing a positive charge, a concave structure that could potentially act as a hydrophobic cavity when suitable co-factors were chosen, and metal-bound water molecule(s).

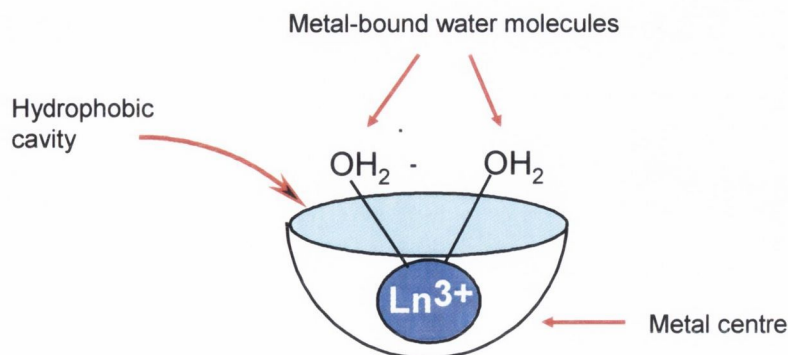


Figure 2.2 Schematic of a cyclen-based lanthanide complex, illustrating the features which may help to promote phosphodiester hydrolysis.

The co-factors that will be discussed in this chapter are pseudo ‘dipeptides’ that could extend the size of the cavity. Before describing the synthesis and characterisation of these compounds, a brief history will be provided of the use of amino acids in phosphodiester cleavage.

2.1.1 Use of amino acids to promote phosphodiester hydrolysis

As previously discussed in Section 1.3, amino acids play an important role in the activity of ribonucleases, for example, His in RNase A,²¹ and Arg is found in the X-ray crystal structure of Staphylococcal nuclease.²¹ These amino acids residues can play the dual roles of coordinating mechanistically important metal ions as well as themselves promoting hydrolysis; for example, by acting as general acids or bases, or by providing a nucleophile. Amino acids and polypeptides have been extensively investigated for many years and found to promote cleavage of oligonucleotides.^{118,119} Barbier *et al.* investigated the effect of incubating various polypeptides with ApAp.¹¹⁸ These measurements were carried out at 50 °C and pH 8.0, using 50 mM Gly-Gly buffer. The percentage of ApAp hydrolysed after seven days by each polypeptide is presented in **Table 2.1**. The reactions were followed by HPLC, and the production of cyclic AMP (the hydrolysis product) was observed, indicating the degree to which each polypeptide promoted alkaline hydrolysis. It was found that polycationic polypeptides containing arginine or lysine promoted such hydrolysis. These were preliminary results and the varying activities could not be explained. However, it was suggested that the greater activity of poly(Leu-Lys) over that of poly(Ala-Lys) could be due to activity increasing with hydrophobicity, caused by the Leu side-chain.¹¹⁸

Table 2.1 Percentage of phosphodiester bonds hydrolysed by various polypeptides¹¹⁸

Peptide	% of phosphodiester bonds hydrolysed
Poly(Leu-Lys)	85
Poly(Arg-Leu)	68
Poly(Leu-Lys-Lys-Leu)	58
Poly (Ala-Lys)	33.1
Poly Lys	27.1
Poly(Arg-Thr-Lys-Pro)	4.1
Free lysine	2.1
Control	1.6

Similar work, involving the use of combinatorial chemistry, was reported in 1999.¹¹⁹ This involved building a library of 625 solid-phase-bound undecapeptides. The combinations that were synthesised are shown in **Figure 2.3**. These were complexed with various transition metals and tested for hydrolase activity. This combinatorial approach involved the incorporation of L-Arg, L-His, L-Tyr, L-Trp and L-Ser (amino acids that were expected to be hydrolytically active) between traditionally 'inactive' GlyGly spacers.

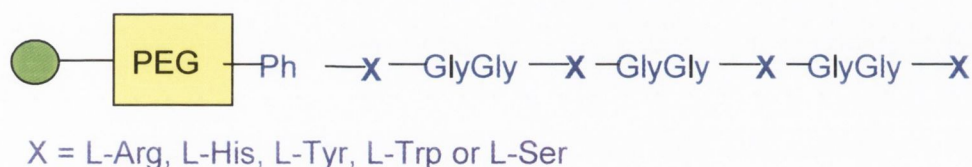
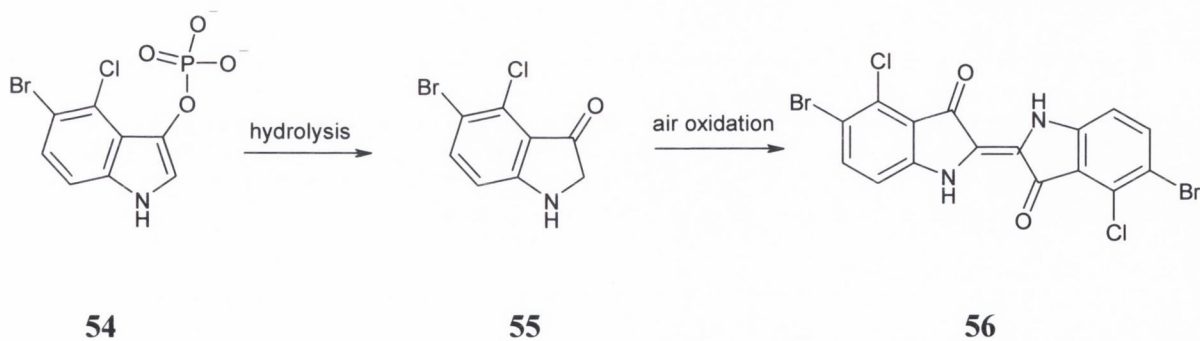


Figure 2.3 Solid-phase-bound undecapeptides¹¹⁹

A 3-hydroxyindolyl phosphate ester **54** was employed in these measurements, the structure and hydrolysis of which are shown in **Scheme 2.1**. The hydrolysis product of this substrate **55** is further oxidized in air to give **56**, an insoluble coloured dye. Therefore, when the polymer beads were added to a solution of metal ions and reacted with the ester, the most highly coloured beads were isolated and subjected to an Edman degradation. From these investigations it was found which combinations were most effective.¹¹⁹



Scheme 2.1 The structure 3-hydroxyindolyl phosphate ester and its hydrolysis products.¹²⁸

Active sequences

- H₂N-Ser-Gly-Gly-His-Gly-Gly-Arg-Gly-Gly-His-Phe-CO₂H** **A**
H₂N-Ser-Gly-Gly-Ser-Gly-Gly-Ser-Gly-Gly-His-Phe-CO₂H **B**
H₂N-Ser-Gly-Gly-Arg-Gly-Gly-His-Gly-Gly-His-Phe-CO₂H **C**

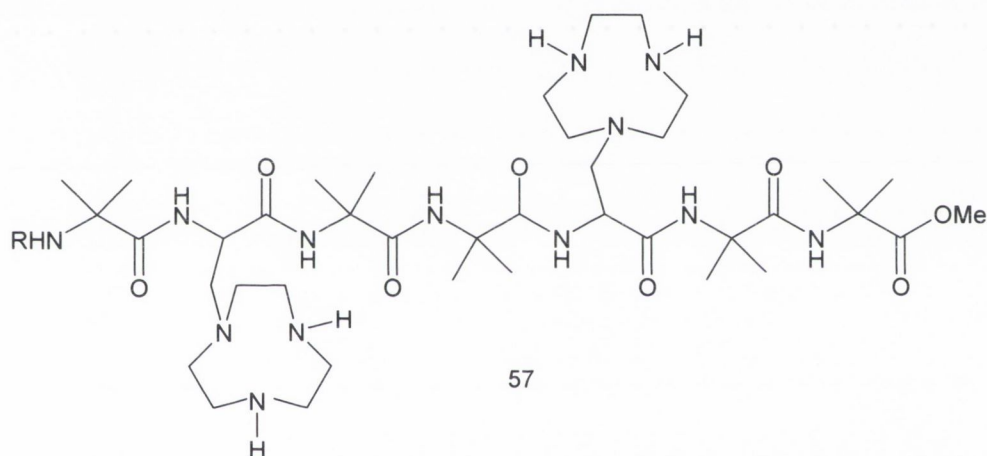
Inactive sequences

$\text{H}_2\text{N-Trp-Gly-Gly-Arg-Gly-Gly-Trp-Gly-Gly-Arg-Phe-CO}_2\text{H}$ **D**

$\text{H}_2\text{N-Arg-Gly-Gly-Ser-Gly-Gly-Arg-Gly-Gly-Trp-Phe-CO}_2\text{H}$ **E**

Figure 2.4 Undecapeptide sequences tested by Barbier *et al.*¹¹⁹

Figure 2.4 shows the various polypeptide sequences that were tested and which were found to be active. This was preliminary work and no explanation of the differing activities was presented; however, it was noted that the inactive sequences both carried two positive charges (on the Arg residues), while the active sequences carried either one or no Arg residue.



The use of a heptapeptide to support two small macrocycles, **57**, has been reported by Scrimin *et al.*^{120,121} The triaza-crowns were then complexed with Zn(II), Cu(II) and Ni(II) to provide what was essentially a ribonuclease mimic. This compound was then tested against HPNP at 40 °C, pH 7.0 in 50 mM HEPES buffer and the Zn(II) complex was found to be most effective. The results are presented in **Table 2.2**.

Table 2.2¹²¹ First order rate constants for the cleavage of HPNP by metal complexes of 57

Complex	$10^6 k_{\text{obs}} \text{ s}^{-1}$	k_{rel}
Zn ₂ [57]	21.0	54
Ni ₂ [57]	6.0	15
Cu ₂ [57]	4.0	10

The results were compared to those obtained when Zn(II)-complexed triazacyclononane was used (which cleaved HPNP with a rate of $7.0 \times 10^{-6} \text{ s}^{-1}$) and the bis-system found to be far superior, indicating a degree of co-operativity between two the metal ions. This effectiveness was explained by the helical conformation adopted by the heptapeptide, which leaves the two metal complexes facing one another on the same side of the helix, providing a cavity for the phosphodiester substrate.¹²¹

These results indicate that the incorporation of amino acid moieties, either in combination with one another, or incorporated into a macrocyclic system, can promote the hydrolysis of phosphodiester. With this in mind, it was decided to use amino acids in conjunction with the cyclen ligand to build a hydrophobic molecule that could complex lanthanide ions and be used to promote phosphodiester hydrolysis.

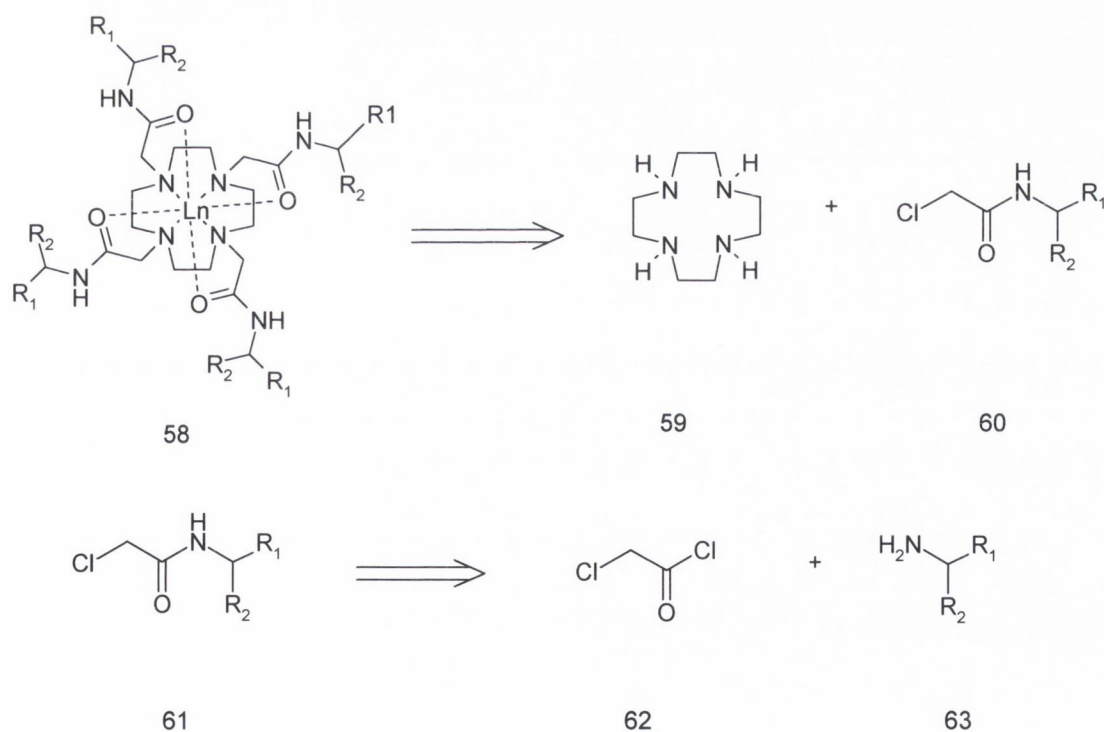
2.2 Synthesis and Characterisation of Glycine-based Macrocycles

In light of these findings, it was decided to investigate the effect of incorporating various amino acids as cofactors into the cyclen framework and examine the effect of this on the rate and specificity of RNA cleavage by the resulting complexes. While the amino acids found to be of use in literature studies were principally histidine, serine, lysine and arginine, we began by making relatively simple ‘model compounds’ which incorporated simple amino acids such as glycine, alanine, valine, leucine and phenylalanine. It was necessary to work with the esters of these substrates in order to preserve the overall positive charge on the final lanthanide complexes. These amino ester contained no functionality that would be expected to enhance the rate of phosphodiester cleavage, *ie*, possess no nucleophile and no capacity to aid acid-base catalysis. Therefore, their only contribution to the effectiveness of a cyclen-based lanthanide complex as a ribonuclease mimic is a hydrophobic contribution. It was hoped that the incorporation of these amino ester as pendant arms would extend the

'walls' of a hydrophobic cavity upon complexation with a lanthanide ion. The incorporation of glycine, the simplest amino acid, into the cyclen framework will be discussed initially, followed by work with amino acids that possess a chiral centre.

2.2.1 Synthesis of Glycine-based Ribonuclease Mimics

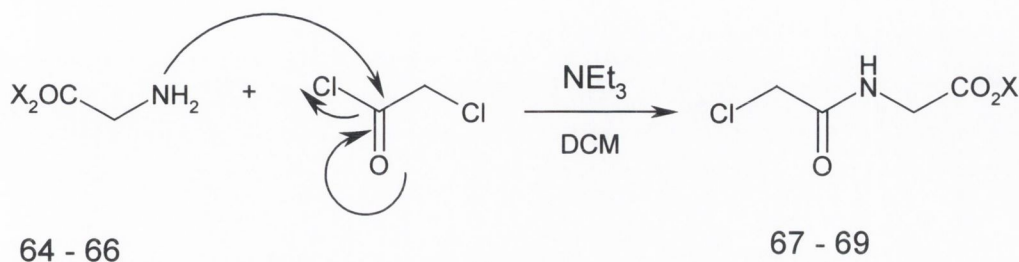
The aim of this work was to synthesise tetrasubstituted cyclen systems of the general form **58**. As was discussed in Chapter 1, lanthanide ions in such systems tend to be either nine- or ten-coordinate. Such a ligand has been shown to provide eight donor sites, leaving one to two coordination sites available for small molecule binding, depending on the size of the complexed lanthanide.^{68,69,71} The general tetrasubstituted cyclen ligand **58** can be prepared by reacting cyclen **59** with four equivalents of an appropriate α -chloroamide **60**, as shown in **Scheme 2.2**. There are various ways of preparing such a pendant arm of general form **60**, for example, by a peptide coupling method, but the procedure chosen involved reaction of the chosen amine **63** with chloroacetyl chloride **61**. The following section will discuss the synthesis and characterisation of compounds incorporating the simplest amino ester, glycine.



Scheme 2.2 Retrosynthesis of the desired cyclen-based lanthanide complex. The lanthanide complexation step is omitted for clarity. The synthetic equivalents, rather than the synthons, are shown.

2.2.2 Synthesis of glycine-based α -chloroamine pendant arms.

The pendant arms were essentially ‘dipeptides,’ formed by the addition of the required amino ester to chloroacetyl chloride. These were readily prepared by a modified literature method, shown in **Scheme 2.3**.^{122,123}



Scheme 2.3 Synthesis of α -chloroamide compounds, incorporating glycine-based dipeptide residues.

Compound	Ester Used	Yield (%)
67	X = CH ₃	71.7
68	X = CH ₂ CH ₃	81.4
69	X = CH ₂ Ph	83.8

In the case of **67**,¹²² glycine methyl ester hydrochloride was added to DCM and three molar equivalents of triethylamine and cooled to between -10 and -20 °C by means of a liquid nitrogen/acetone bath. To this, a solution of chloroacetyl chloride in DCM was added dropwise, taking care that the temperature did not rise above -10 °C. The reaction was then stirred at room temperature for 16 h, before filtering off the triethylammoniumchloride and washing the filtrate with 0.1 M HCl solution. The organic layer was dried over potassium carbonate and the solvent removed under reduced pressure to give a yellow oil in 72 % yield that solidified upon standing. It was characterised by ¹H and ¹³C NMR and Electrospray Mass Spectroscopy (ESMS). The ¹H NMR was, as expected, simple, consisting of four singlet peaks: The amide proton was found at 7.43 ppm, the acetamide methylene protons were found at 3.94 ppm, the glycine CH₂ at 3.89 ppm and the protons of the methyl ester at 3.58 ppm.¹²² A single product was also seen by ESMS and this compound was determined to be sufficiently clean to use without further purification.

Further α -chloroamide arms were prepared using the ethyl and benzyl esters of glycine. **68**¹²² and **69**¹²³ were prepared using the same method and isolated in 81 % and 84 % yields

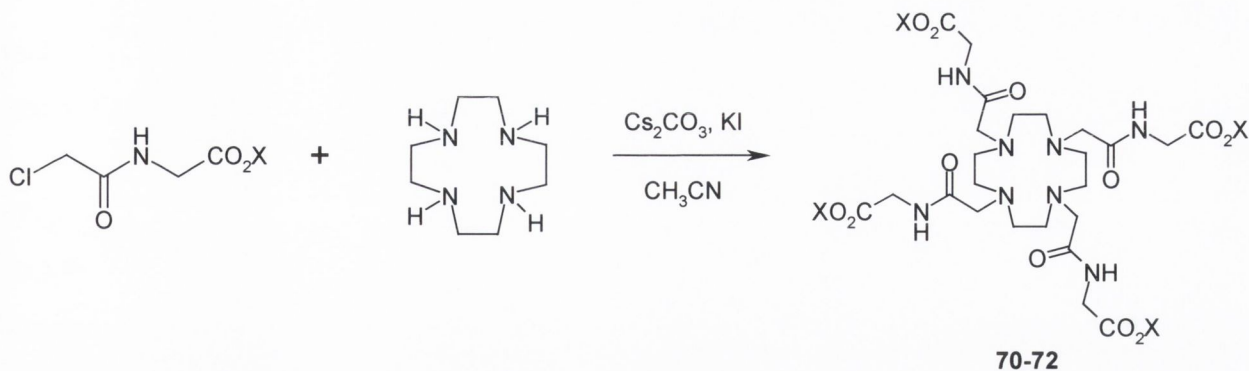
respectively. The ^1H NMRs showed similar simplicity and in each case, the product was deemed sufficiently clean to use without column chromatography. As these compounds had been previously reported, elementary analysis was not obtained.^{122,123}

2.2.3 Synthesis of Glycine-Based Cyclen Ligands.

Upon preparation of the α -chloroamide arms, the aim was to incorporate these into the cyclen system, as shown in **Scheme 2.3**. A variety of reaction conditions have been reported in the literature for the preparation of tetra-alkylated cyclen compounds, including:

- * Ethanol and triethylamine⁶⁸
- * Ethanol and potassium carbonate¹²⁴
- * DMF and cesium carbonate¹¹⁷
- * DMF and potassium carbonate¹²⁵
- * Acetonitrile and potassium carbonate¹²⁶

Initially, the aim was to investigate whether a set of reaction conditions could be found that allowed the clean and complete addition of four equivalents of **67** to cyclen, preferably without the need for subsequent column chromatography. Therefore, this reaction was attempted in a variety of solvents: DMF, ethanol and methanol. These reactions were all carried out in the presence of Cs_2CO_3 and KI. However, in each of these cases a mixture of products was formed when the reaction mixture was analysed by TLC or ESMS. When the reaction was refluxed in dry acetonitrile for 16 hours, a single, clean product was obtained in 69 % yield. The results of using various solvents at different temperatures and over different lengths of time is summarised in **Table 2.5**. From these results, it was clear that acetonitrile was the best solvent for this reaction, and it was used for all subsequent reactions involving incorporation of amino acid arms into the cyclen backbone and was found to be equally successful in every case.



Scheme 2.4 Synthesis of tetra-substituted cyclen ligands, incorporating glycine-based dipeptide residues.

Compound	Ester Used	Yield
70	X = CH ₃	69.2
71	X = CH ₂ CH ₃	36.1
72	X = CH ₂ Ph	58.9

Table 2.5 Summary of solvents and reactions conditions tested in the synthesis of 70

Solvent	Time (h)	Result of reaction
DMF (80°C)	16	Mixture of products
DMF(80°C)	48	Mixture of products
DMF(80°C)	96	Mixture of products
DMF(160°C)	48	Mixture of products
Methanol	48	Mixture of products
Ethanol	48	Mixture of products
Acetonitrile (dry)	16	Single, clean product (69 % yield)
Acetonitrile (dry)	48	single, clean product (71 % yield)
Acetonitrile (not dried)	16	Single, clean product (61 % yield)

70 was prepared by reacting 4.1 equivalents of **67** with cyclen in the presence of Cs₂CO₃ and KI in refluxing dry CH₃CN for 16 h. After cooling to room temperature, the inorganic salts were filtered off. The solvent was removed under reduced pressure to give an oily solid that was taken up into CHCl₃ and washed. Various different aqueous solutions were used to clean this product, including H₂O and various strengths of KOH solution. However, saturated KCl solution was found to be most effective and in subsequent reactions, this was used. After repeated washings with KCl solution, the organic phase was dried over K₂CO₃

and the solvent was removed under reduced pressure to give a yellow oil. This was dried under vacuum to give a white, hygroscopic solid in 64 % yield.

Characterisation of the cyclen-based ligands was principally by ^1H and ^{13}C NMR and ESMS, as well as elementary analysis. The ^1H NMR of **74** is shown in Figure 2.5 and showed a very simple pattern, due to the four-fold symmetry of the ligand. In this, the simplest of the amino-acid substituted compounds, the ring protons appeared as a singlet at 2.6 ppm, with the glycine CH_2 at 3.85 ppm, the ester CH_3 at 3.6 ppm and the CH_2 spacer that serves as the second ‘Gly’ residue at 3.0 ppm. It can be seen that the ‘Gly’ residue is coupled to the amide protons, with $J = 6.2$ Hz. CHN analysis of the compound revealed the presence of a potassium ion, which is to be expected since KCl was used during the work-up of this reaction, and ligands such as this are known to take up Na^+ and K^+ ions.^{124,127}

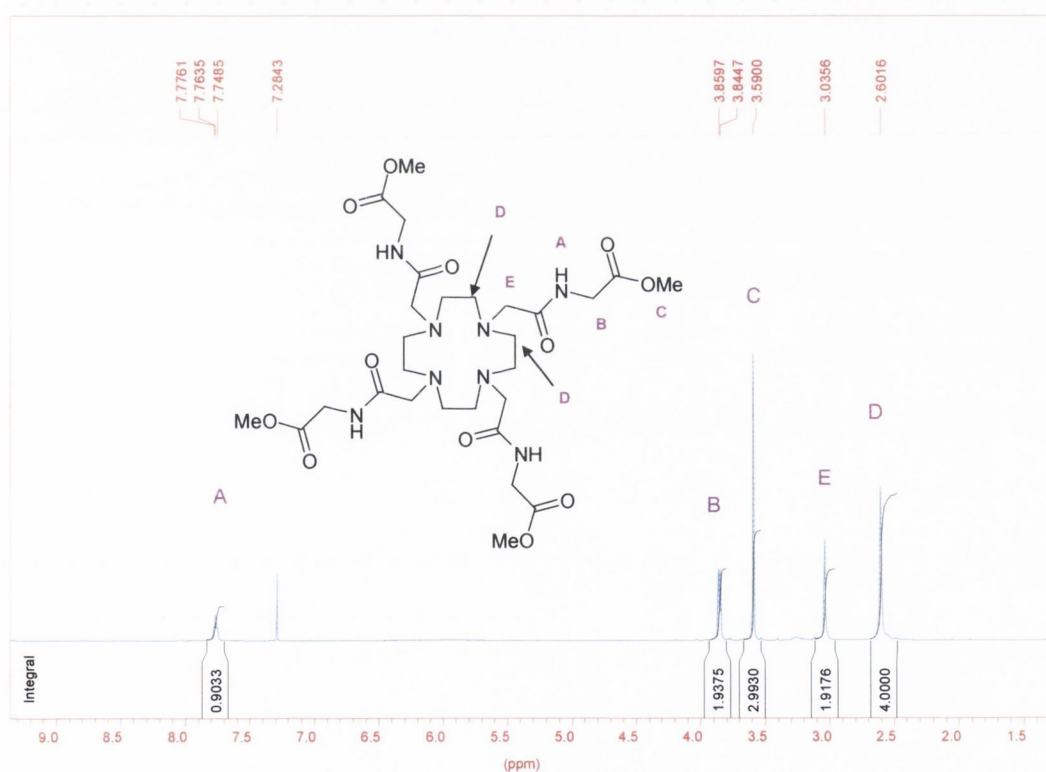


Figure 2.5 ^1H NMR of **70** in CDCl_3 , exhibiting the C_4 symmetry of the ligand.

Compounds **71** and **72** were prepared using identical procedures, and isolated in 36 and 59 % yields, respectively. In every case, the compound was found to be hygroscopic, and was stored under argon in an airtight container. **71** and **72** were characterised in the same way as

70, using ^1H and ^{13}C NMR and ESMS. Changing the ester from methyl to ethyl or benzyl made no effect on the pattern of the ^1H NMRs, and the same simple symmetry was observed in each case. The ^1H NMR of **72** can be seen in **Figure 2.6**. Once again, the ring protons were observed as a singlet, at 2.64 ppm. The methylene protons of the benzyl ester appeared at 5.09 ppm, the ‘spacer’ CH_2 appeared at 3.98 ppm and the ‘glycine’ CH_2 appeared at 3.09 ppm. Again, it was seen that the acetamide CH_2 was split, presumably by the amide protons, with $J = 6$ Hz, however in this NMR the corresponding splitting could not be observed in the amide peak, due to its broadness.

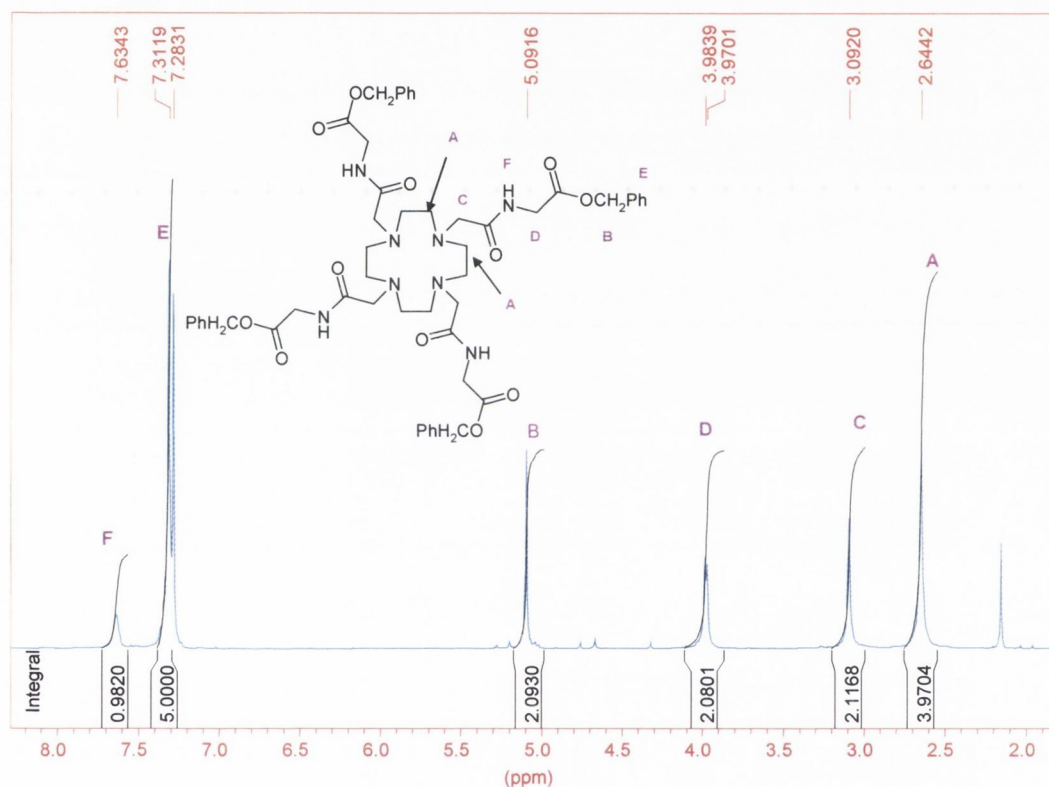
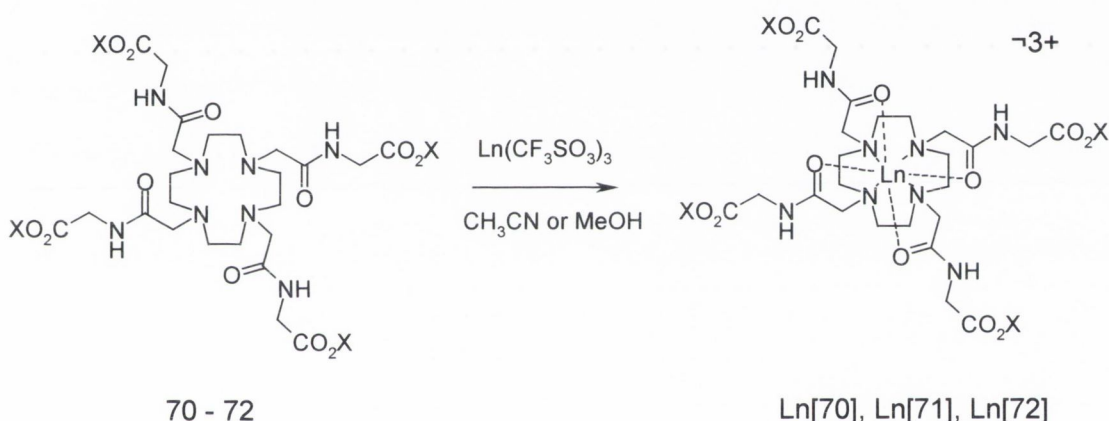


Figure 2.6 ^1H NMR of **72** in CDCl_3 , demonstrating C_4 symmetry of the ligand.

These ligands were easily examined by electrospray mass spectroscopy, with a single m/z peak found that corresponded to MH^+ in each case. The presence of a MNa^+ or MK^+ peak could also be observed in some cases, illustrating the readiness of these compounds to acquire cations.^{124,127}

2.2.4 Complexation of Glycine-Based Cyclen Ligands.

As was previously discussed, the aim of this project was to synthesise lanthanide ion based cyclen complexes. The incorporation of a lanthanide into the type of cyclen ligand prepared in Section 2.2.2 can be seen in **Scheme 2.5**. These reactions were generally straightforward, using 1.1 equivalents of the appropriate lanthanide trifluoromethane sulfonate (triflate) in a small volume of refluxing acetonitrile (~ 5 mL).^{124,127} **70** was successfully complexed with Ce(III), Pr(III), Nd(III), Eu(III), Gd(III), Tb(III), Yb(III), and Lu(III) under these conditions. The La(III) complex proved more difficult to form, perhaps because of the larger size of the ion. Under the same conditions of 1.1 molar equivalents of $\text{La}(\text{CF}_3\text{SO}_3)_3$ no complexation was observed, even after refluxing the reaction for 48 hours. However, the reaction was successful when a large volume of methanol (25 mL) was used instead of acetonitrile.⁶⁸



Scheme 2.5 Lanthanide complexation of tetrasubstituted cyclen ligand using lanthanide triflates, where $X = \text{Me}$ or CH_2Ph .

Similarly, La(III), Eu(III) and Yb(III) complexes were formed with **71**, using the same reaction conditions. On this occasion, the La(III) complex was formed in ethanol, while the Eu(III) and Yb(III) complex were formed in acetonitrile. Lanthanide complexes of **72** were also prepared; La(III), Ce(III), Nd(III) and Eu(III) complexes all were formed in refluxing acetonitrile using the appropriate lanthanide triflate.

Table 2.6 Glycine-base cyclen complexes and yields.

Complex	Yield (%)	Complex	Yield (%)	Complex	Yield (%)
La[70]	43.9	La[71]	46.7	La[72]	49.2
Ce[70]	53.8	Eu[71]	48.5	Ce[72]	46.0
Pr[70]	46.9	Yb[71]	39.1	Nd[72]	39.3
Nd[70]	41.8			Eu[72]	47.1
Eu[70]	22.0				
Gd[70]	61.9				
Tb[70]	51.1				
Lu[70]	60.4				

Characterisation of the lanthanide complexes was again by ^1H NMR and ESMS. Lanthanides are shift reagents.¹²⁸ In our case, the ring protons of cyclen and the acetamide CH_2S were shifted, according to their proximity to the lanthanide ion.^{129,130} In some cases, this was visible as six clearly shifted peaks. However, due to the strong relaxation properties of these compounds, at times the shifted peaks were so broadened as to be indistinguishable from the baseline.¹³¹ This difficulty could be minimised by low temperature NMR experiments,^{132,133} however, such a facility was not available while this work was being carried out. In light of this, it was decided to look at the Yb(III) ^1H NMRs in each case as they tend to show less line broadening.¹³⁴

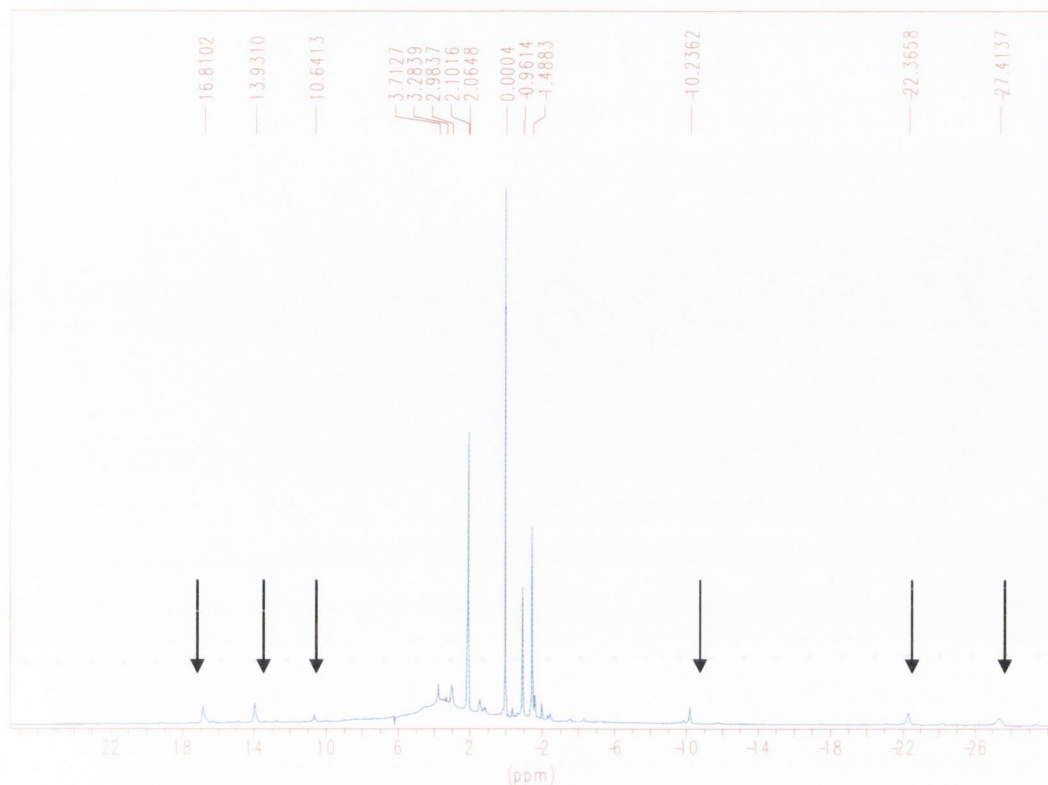


Figure 2.8 ^1H NMR of **Yb[70]** in CD_3CN , demonstrating the effect of a paramagnetic metal. The shifted cyclen protons are illustrated with arrows.

Mass spectrometry is a particularly useful tool for examining the lanthanide complexes. The spectra are considerably less simple than those of the ligands, with multiple peaks present due to the charges and counter ions. It was expected that the charged lanthanide complex would have three counter ions, in the form of triflate anions.^{83,127} Later in this chapter, evidence of this will be seen in crystal structures obtained of such complexes. However it was also of interest to us to see how these complexes behaved in the solution state, as that is the form in which biological testing is performed. In **Table 2.8**, the various species observed in the ESMS of **Eu[70]** are listed. This particular complex has been chosen for discussion because its crystal structure has been solved and therefore a comparison between solid state and solution state can be made. In the ESMS, *ie*, in the solution state, peaks were found that correspond to the complex occur both without any triflates ($m/z = 420$ and $m/z = 280$ for a +2 and +3 charge respectively) and with one triflate counterion and a charge of +2. No peaks were found to represent species with greater numbers of triflate counterions. As will be seen in the next section, a crystal structure of the same complex shows the presence of three triflate counterions in the solid state, as well as a metal bound water molecule that was not observed by ESMS. A peak that was of some

interest occurred at $m/z = 220$. It was thought that this could be due to the Eu(III) complex with an associated potassium ion and therefore a + 4 charge. This proposal was later backed up by the evidence of a crystal structure.

Table 2.8 Analysis of the ESMS peaks for Eu[70]

Species	Molecular weight	Charge	m/z
Eu[70]	840	+2	420.2
Eu[70]	840	+3	280.1
Eu[70] + Triflate	989	+2	494.5
Eu[70] + K	879	+ 4	219.9

While these numbers are taken from the analysis of one particular complex, similar patterns were observed for each lanthanide complex prepared.

Successful complexation can also be indicated by IR spectroscopy.^{83,127} In the case of **70** the carbonyl stretching frequency was seen to shift from 1672 cm^{-1} for the uncomplexed ligand to $1629\text{-}1633\text{ cm}^{-1}$ for the various lanthanide complexes prepared, with these values presented in **Table 2.9**.

Table 2.9 The carbonyl stretching frequencies of 70 and some of its Ln complexes

Complex	Carbonyl stretching freq (cm^{-1})
70	1672
La[70]	1631
Ce[70]	1629
Nd[70]	1632
Eu[70]	1632
Tb[70]	1633
Lu[70]	1638

2.2.5 Solid State Analysis of Eu[70]

Lanthanide ions tend to be nine or ten coordinate in tetrasubstituted cyclen systems,^{68,69,71} with eight of the donor atoms coming from the cyclen framework; the four cyclen nitrogens

and four carbonyl oxygens. We expect the lanthanide ions to fulfil their coordination requirement with either one or two water molecules, depending on the size of the lanthanide. The presence of these water molecules can be investigated in solution by lifetime measurements,¹³⁵ or, less commonly, by potentiometric titrations,¹³⁶ however ideally we would like to verify their presence by a crystal structure. Attempts were made to recrystallise all of the lanthanide complexes discussed in this chapter, however, in most cases this was unsuccessful.

Single crystals of **Eu[70]** were obtained upon slow precipitation from methanol by addition of chloroform and a crystal structure of this complex was obtained by Dr. M. Neuwenheuzen in the Department of Chemistry, Queen's University of Belfast. The resulting crystal structure provides a great deal of information about the solid state structure of this family of lanthanide complexes.

As expected, a crystal structure of **Eu[70]** showed the Eu(III) ion bound to the eight expected donor atoms, with the ninth coordination site being a water molecule. As illustrated in **Table 2.2**, the Eu...O bonds and the Eu...N bonds are of equal length, measuring 2.369 Å and 2.661 Å respectively. This provided further evidence that the C₄ symmetry exhibited in the ¹H NMR of the ligand was retained in the complex. The bond with the water molecule was slightly longer, at 2.445 Å. It should be noted that the expected three triflate counterions were observed to be associated with the complex, however, in **Figure 2.5** the triflate anions as well as all hydrogens have been removed for clarity. An unusual feature observed in this crystal structure was the presence of a nearby potassium ion. While this cation would not be expected in proximity to a positively charged complex, it was associated with a fourth triflate anion, and supported the findings of ESMS.

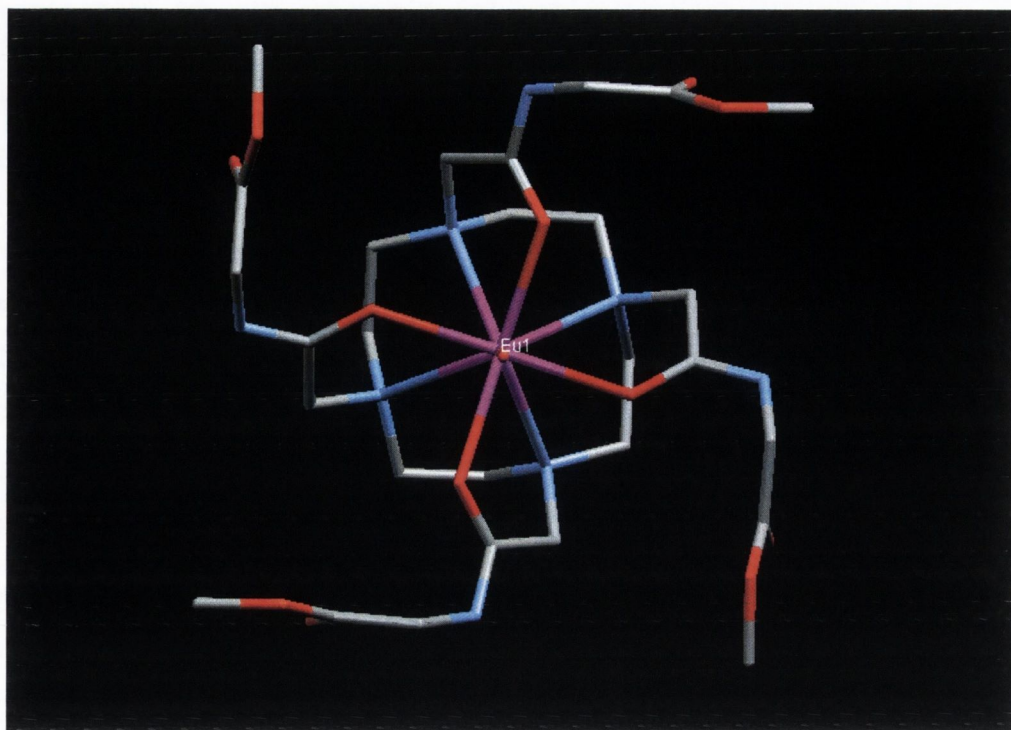


Figure 2.5 X-ray crystal structure of **Eu[70]**, showing the C_4 symmetry of the complex. Hydrogens have been omitted for clarity.

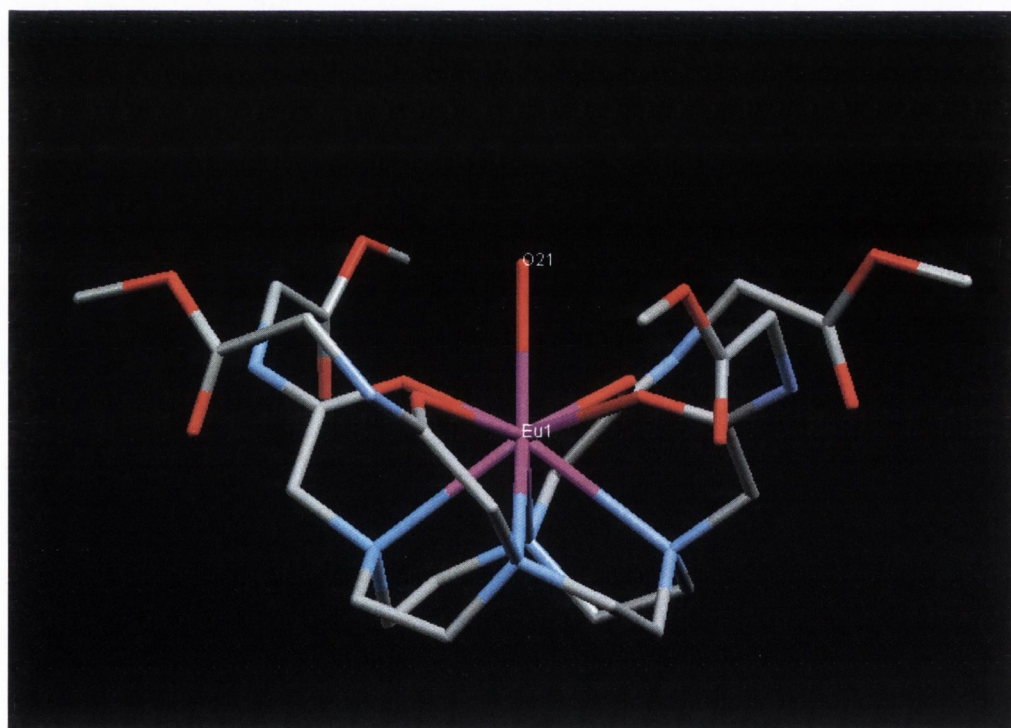


Figure 2.6. X-ray crystal structure of **Eu[70]**, showing the cavity created by the pendant arms, and the position of the metal-bound water molecule.

From a side view of the molecule, it can be observed that the Eu(III) ion is located in the centre of a cavity, the walls of which are formed by the pendant arms. This can be seen in **Figure 2.6**. From this angle, the orientation of the metal-bound water molecule is also clearly visible.

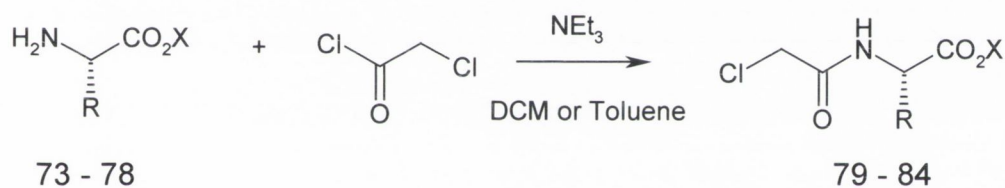
There are two elements of chirality present in such a cyclen-based lanthanide complex; these are associated with the torsion angles of five membered rings caused by the lanthanide and N-C-C-N, and the lanthanide and N-C-C-O.^{67,137,138} The torsion angle of the N-C-C-O ring defines the complex as having Δ or Λ chirality, while the torsion angle of the N-C-C-N ring defines the complex as being $\delta\delta\delta\delta$ or $\lambda\lambda\lambda\lambda$. Therefore, there are four possible isomers for any such system.¹³⁷ As can be seen from **Table 2.10**, the torsion angle of the N-C-C-O ring in **Eu[70]** has a value of -22.42° , defining the complex as being $\delta\delta\delta\delta$ while the torsion angle of the N-C-C-N ring has a value of 59.11° , defining the complex as Λ .¹³⁷

2.3 Synthesis of amino acid-based ribonuclease mimics incorporating alanine, valine, leucine or phenylalanine

The crystal structure of **Eu[70]** revealed the presence of a small cavity in the solid state (possibly distorted by the presence of an adjacent potassium ion). The formation of such a cavity had been one of the aims of incorporating amino esters into the cyclen framework as co-factors. Having seen some success with the glycine-based compounds, in terms of ease of preparation, successful formation of a cavity upon complexation and, of primary importance, their ability to cleave phosphodiester (Chapter 4, Chapter 5), it was decided to incorporate other amino acids into the cyclen framework in order to see if these properties could be improved on. It was of great interest to see if larger amino acids could further extend the concave structure of these lanthanide complexes by lengthening the ‘walls’ of the cavity. Further, it was possible that a more hydrophobic cavity could be engineered by the choice of such co-factors. Therefore a series of compounds were prepared, based upon *L*-alanine, *L*-valine, *L*-leucine and *L*-phenylalanine. This gives an array of compounds that differ in size, while still containing no ‘active’ group that could itself help to promote phosphodiester hydrolysis, either by acidic or basic catalysis or by nucleophilic action. The synthesis of these compounds is described below.

2.3.1 Synthesis of chiral aminoester-based α -chloroamine pendant arms.

The synthesis of these α -chloroamide arms was carried out using the same procedure as that described for the glycine arms in Section 2.2.1.¹²² In each case the appropriate amino ester was reacted with chloroacetyl chloride in the presence of triethylamine, keeping the temperature below $-10\text{ }^{\circ}\text{C}$. In these reactions, either toluene or DCM could be used as a solvent. The reactions were stirred at room temperature for 16 hours, the triethylammonium chloride salts were filtered off and the solvent was removed under reduced pressure. The residue was taken up in CHCl_3 and washed with 0.1 M HCl solution. The organic layer was reduced to yield the relevant product, **79-84**. **79**,¹²² using alanine methyl ester, was isolated as a brown oil in 66.5 % yield. **80**, incorporating alanine benzyl ester was isolated as a pale brown oil, that solidified upon standing, in 98.1 % yield. **81**¹²² and **82**¹²² were isolated as a pale brown solids in 76.4 % and 76.3 % yields respectively. **83**¹²² and **84** were white solids, obtained in 91.4 % and 73.4 % yield respectively.



Scheme 2.6 Synthesis of α -chloroamide compounds, incorporating alanine, valine, leucine and phenylalanine -based dipeptide residues.

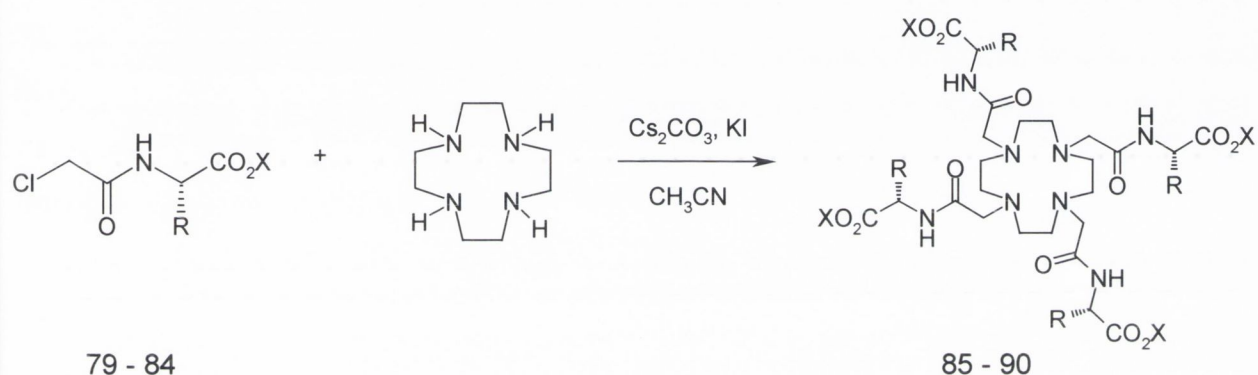
Table 2.9 α -chloroamide arms incorporating amino esters other than glycine

Compound	R	X	Cofactor	Yield (%)
79	CH_3	CH_3	Alanine methyl ester (73)	67
80	CH_3	CH_2Ph	Alanine benzyl ester (74)	98
81	$\text{CH}_2(\text{CH}_3)_3$	CH_3	Valine methyl ester (75)	76
82	$\text{CH}_2\text{CH}(\text{CH}_3)_2$	CH_3	Leucine methyl ester (76)	76
83	CH_2Ph	CH_3	Phenylalanine methyl ester (77)	91
84	CH_2Ph	CH_2Ph	Phenylalanine benzyl ester (78)	73

Characterisation of these arms was principally by ^1H NMR, and, in the case of novel products, by CHN. These compounds were sufficiently clean to use without further purification.

2.3.2 Synthesis of aminoester -based cyclen ligands.

Each of the α -chloroamide arms mentioned above (**79-84**) was in turn incorporated into a tetra-alkylated cyclen system, such as that shown in **58**. The reaction conditions were identical to those described in Section 2.2.3: four equivalents of each arm were reacted with cyclen in the presence of cesium carbonate and potassium iodide and refluxed in dry acetonitrile for 16 hours.



Scheme 2.7 Synthesis of tetra-coordinated cyclen-based compounds, incorporating alanine, valine, leucine and phenylalanine -based dipeptide residues.

Table 2.11 Cyclen-based ligands incorporating co-factors 77-82.

Compound	R	X	Cofactor	Yield
85	CH_3	CH_3	Alanine methyl ester (79)	49.3
86	CH_3	CH_2Ph	Alanine benzyl ester (80)	74.0
87	$\text{CH}_2(\text{CH}_3)_3$	CH_3	Valine methyl ester (81)	59.6
88	$\text{CH}_2\text{CH}(\text{CH}_3)_2$	CH_3	Leucine methyl ester (82)	52.7
89	CH_2Ph	CH_3	Phenylalanine methyl ester (83)	57.9
90	CH_2Ph	CH_2Ph	Phenylalanine benzyl ester (84)	50.0

The inorganic salts were then filtered off and the acetonitrile was removed under reduced pressure. The residue was taken up in CHCl_3 and washed repeatedly with saturated KCl solution. The organic layer was dried over K_2CO_3 before the solvent was removed under

reduced pressure and the resulting products were dried under vacuum to yield the relevant products, **85-90**. **85** and **86** incorporating alanine methyl and benzyl esters were isolated as pale brown hygroscopic solids in 49.3 and 74.0 % yield respectively. **87** and **88** were isolated as cream, hygroscopic solids in 59.6 and 52.7 % yields. **89** and **90** were white solids, obtained in 57.9 % and 50.0 % yield respectively.

The glycine based compounds discussed in Section 2.2.2 were all achiral, however compounds **85-90** all possess a stereogenic centre α to the carbonyl esters. The effect of this is evident in the ^1H NMR spectra of these compounds as the signature protons of the cyclen ring become magnetically inequivalent. For example, in the case of compounds **70-72**, the ring protons were found as a singlet, whereas examining the ^1H NMR of **85** it is evident that the cyclen ring protons now appear as a double doublet due to the presence of the alanine cofactors. From the coupling constants (10 Hz), this geminal splitting is due to interactions between the ring protons themselves. This is further verified by a CH COSY, which showed that the two doublets are connected to a single carbon. The methyl ester peak was observed at 3.71 ppm, the alanine CH at 4.58 ppm, coupling with $J = 7.5$ Hz to the alanine CH_3 (found at 1.42 ppm) and further split, with $J = 7.5$ Hz by the NH.

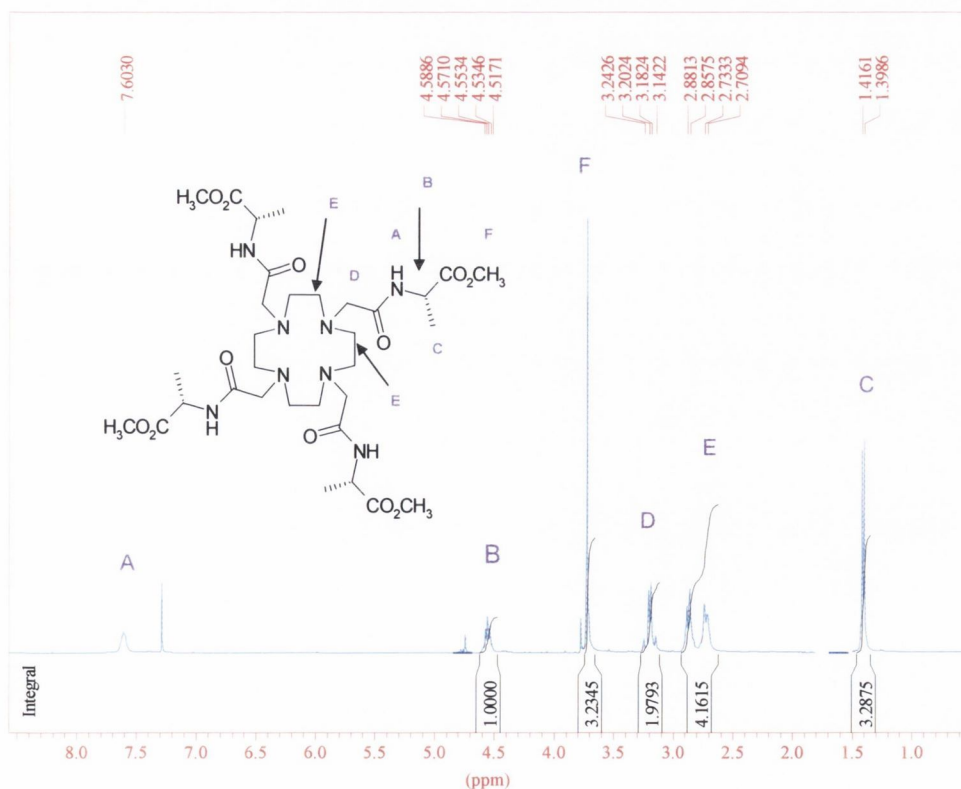
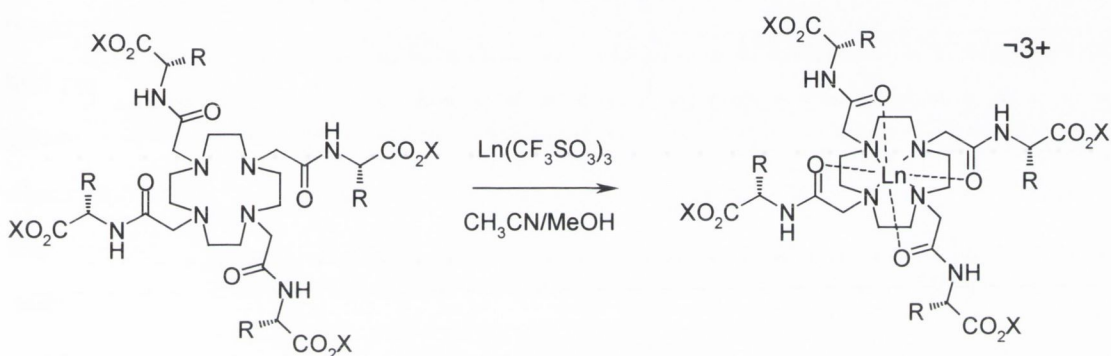


Figure 2.10 ^1H NMR of **85** in CDCl_3 , demonstrating C_4 symmetry of the ligand.

^1H NMR analysis of compounds **86-90** followed a similar pattern, specifically with regard to the splitting of the cyclen ring protons. All compounds were also analysed by IR, ESMS and elementary analysis.

2.3.3 Complexation of aminoester-based cyclen ligands

The complexation of compounds **85-90** with a variety of lanthanide ions was achieved using the general method outlined in Section 2.2.3; refluxing the relevant ligand with a 1.1 equivalents of a lanthanide salt in dry acetonitrile.



Scheme 2.8 Complexation of compounds **85-90** using lanthanide triflates

Table 2.12

Complex	Yield (%)	Complex	Yield (%)	Complex	Yield (%)	Complex	Yield (%)
La[85]	53.0	La[86]	27.7	La[87]	49.2	La[89]	58.6
Eu [85]	18.5	Nd[86]	39.2	Eu[87]	45.8	Eu[89]	52.5
Tb[85]	34.3	Eu[86]	31.1	Yb[87]	51.9		
Yb[85]	29.3	Tb[86]	36.3			La[90]	39.2
		Yb[86]	43.2	La[88]	47.0	Eu[90]	54.
				Eu[88]	51.3		
				Yb[88]	39.3		

85 was complexed with Eu(III), Tb(III) and Yb(III) in acetonitrile. Complexation with La(III) was unsuccessful in acetonitrile, but worked when the reaction was carried out in a larger volume of methanol. **86** was complexed with Nd(III), Eu(III), Tb(III) and Yb(III) in acetonitrile. Again, the corresponding La(III) complex could not be formed under these experimental conditions, but instead was synthesised by stirring at room temperature in ethanol over a period of 48 h. No evidence of transesterification was observed by either ^1H NMR or ESMS. **87** and **88** were each complexed with La(III), Eu(III) and Yb(III), all in acetonitrile. **89** and **90** were complexed with La(III) and Eu(III) under the same conditions.

Eu[85] and **Eu[86]** gave particularly clear ^1H NMR spectra with very little line broadening. In these we can clearly see the six shifted proton signals from the ring protons and the acetamide protons. The ^1H NMR spectrum of **Eu[85]** is shown in **Figure 2.11**. On closer examination of the shifted peaks of **Eu[85]**, two separate sets of peaks can be observed, caused by the two structural isomers these complexes tend to assume in solution. The predominant isomer in solution is mono capped square antiprismatic, with the minor isomer being the tricapped trigonal prism.⁶⁷ From the relative integrations, the major isomer is present in approximately a 92/8 ratio, evidenced by the several smaller resonances visible at high field as well as the single resonance at 51.3 ppm.

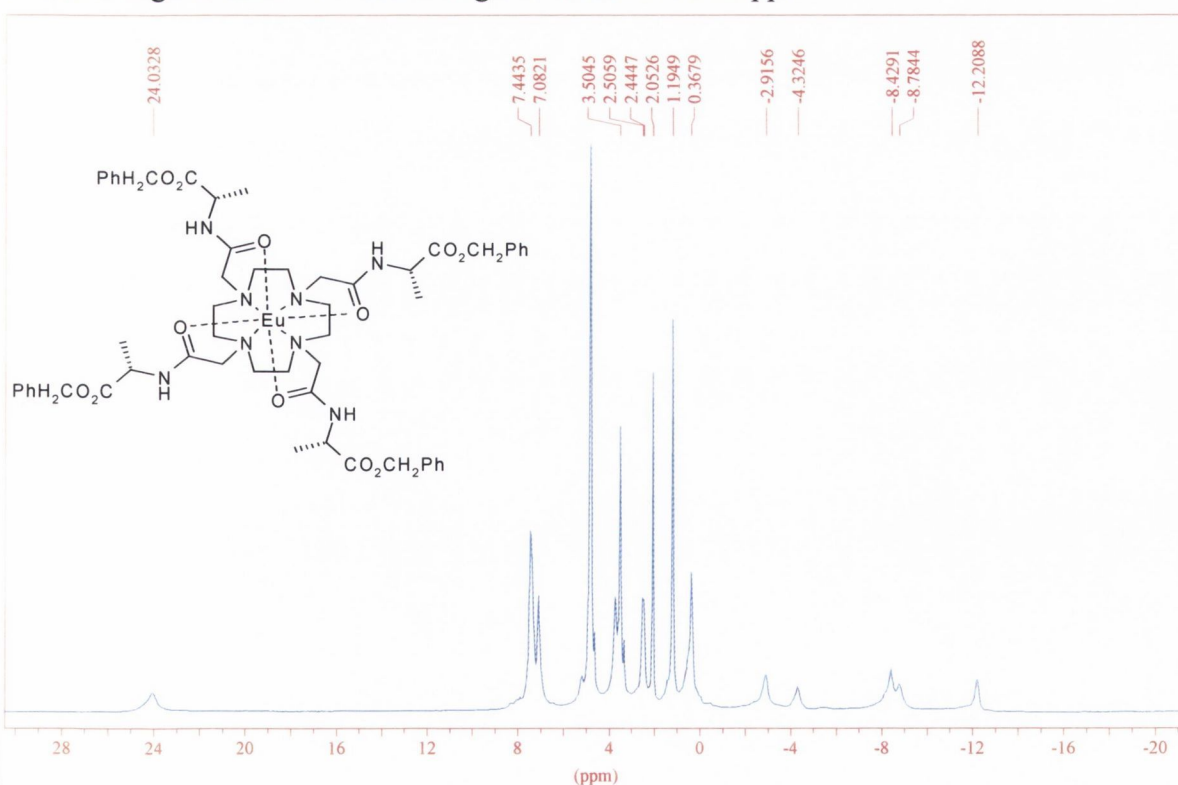


Figure 2.11 ^1H NMR of **Eu[85]** in CD_3CN , demonstrating the broad shifted proton resonances due to the presence of a paramagnetic metal centre.

2.3.4 Solid State Analysis of Tb[86]

Single crystals of **Tb[86]** were obtained upon crystallisation from methanol/diethyl ether. Solid state analysis of these crystal was carried out by Dr. M. Neuwenheyzen in the Chemistry Department, Queens College Belfast. The crystal structure obtained, shown in **Figure 2.8**, provides an insight into the nature and potential reactivity of these families of complexes.

Table 2.14 Selected bond lengths [Å] and angles [°] for Tb[86]

Tb(1)	O(24C)	2.350(6)	O(24C)-Tb(1)-O(24D)	82.25(18)
Tb(1)	O(24D)	2.358(5)	O(24C)-Tb(1)-O(24B)	87.90(18)
Tb(1)	O(24B)	2.369(5)	O(24D)-Tb(1)-O(24B)	145.17(16)
Tb(1)	O(1W)	2.383(4)	O(24C)-Tb(1)-O(1W)	73.0(2)
Tb(1)	O(24A)	2.391(6)	O(24D)-Tb(1)-O(1W)	72.37(16)
Tb(1)	N(2)	2.617(7)	O(24B)-Tb(1)-O(1W)	72.80(16)
Tb(1)	N(4)	2.614(6)	O(24C)-Tb(1)-O(24A)	144.50(16)
Tb(1)	N(1)	2.642(7)	O(24D)-Tb(1)-O(24A)	85.47(18)
Tb(1)	N(3)	2.668(7)	O(24B)-Tb(1)-O(24A)	83.47(17)
			O(1W)-Tb(1)-O(24A)	71.5(2)
			O(24C)-Tb(1)-N(2)	73.3(2)
			O(24D)-Tb(1)-N(2)	139.58(19)
			O(24B)-Tb(1)-N(2)	66.46(18)
			O(1W)-Tb(1)-N(2)	127.19(19)
			O(24A)-Tb(1)-N(2)	132.1(2)
			O(24C)-Tb(1)-N(4)	130.34(19)
			O(24D)-Tb(1)-N(4)	66.53(18)
			O(24B)-Tb(1)-N(4)	138.94(18)
			O(1W)-Tb(1)-N(4)	126.50(19)
			O(24A)-Tb(1)-N(4)	72.53(19)
			N(2)-Tb(1)-N(4)	106.3(2)
			O(24C)-Tb(1)-N(1)	141.2(2)
			O(24D)-Tb(1)-N(1)	132.62(19)
			O(24B)-Tb(1)-N(1)	71.41(19)
			O(1W)-Tb(1)-N(1)	127.1(2)
			O(24A)-Tb(1)-N(1)	66.9(2)
			N(2)-Tb(1)-N(1)	68.5(2)
			N(4)-Tb(1)-N(1)	68.7(2)
			O(24C)-Tb(1)-N(3)	65.66(19)
			O(24D)-Tb(1)-N(3)	72.80(18)
			O(24B)-Tb(1)-N(3)	132.16(19)
			O(1W)-Tb(1)-N(3)	128.5(2)
			O(24A)-Tb(1)-N(3)	140.4(2)
			N(2)-Tb(1)-N(3)	68.0(2)
			N(4)-Tb(1)-N(3)	68.6(2)
			N(1)-Tb(1)-N(3)	104.4(2)

Examination of the crystal structure of **Tb[86]** reveals a concave structure, with the GlyAla arms of the complex acting as walls to give a bowl-shaped cavity, with Tb(III) in the centre.

The Tb(III) ion is nine coordinate, with eight of these coordination sites donated by the cyclen ligand; the metal ion is coordinated to the four ring nitrogens of cyclen (with an average bond length of 3.635 Å) and the four amide carbonyl oxygens of the glycine residues on the GlyAla pendant arms (with an average Tb...O bond length of 2.423 Å). At the centre of the cavity, it can be seen that Tb(III) is coordinated to one water molecule, making this a nine coordinate complex. In **Table 2.14**, a complete list of bond angles and lengths between the Tb(III) ion and its coordinating sites is shown.

Of some interest to us was the presence of an ether molecule within the cavity, hydrogen-bonded to the metal-bound water. This indicates that a small molecule could fit inside the bowl-shaped cavity, and presents the possibility that the complex could act as a hydrophobic basket in which a reaction might take place. **Figure 2.7** shows a space-filling diagram of this cavity, complete with enclosed ether molecule. **Figure 2.8** shows an overhead view of the structure, in which the C_4 symmetry of the complex, through the central ion, can be seen. There are three elements of chirality in this complex, which can be assigned from examination of the X-ray crystal structure. Firstly, chirality is present due to the chiral *L*-alanine cofactor, and these are assigned as *SSSS*. The other elements of chirality are due to the conformations of the pendant arms, and the N-C-C-O and N-C-C-N torsion angles, as previously discussed for **Eu[70]**. In the case of this structure $\lambda\lambda\lambda\lambda$ geometry is observed with regard to the N-C-C-N five-ring chelates, with a torsion angle of -58.55° . Thirdly, the pendant arms can adopt either clockwise (Δ) or anticlockwise (Λ) enantiomeric conformations and in this case, only the Δ isomer is observed, with a torsion angle of 24.84° observed in the case of the N-C-C-O ring.

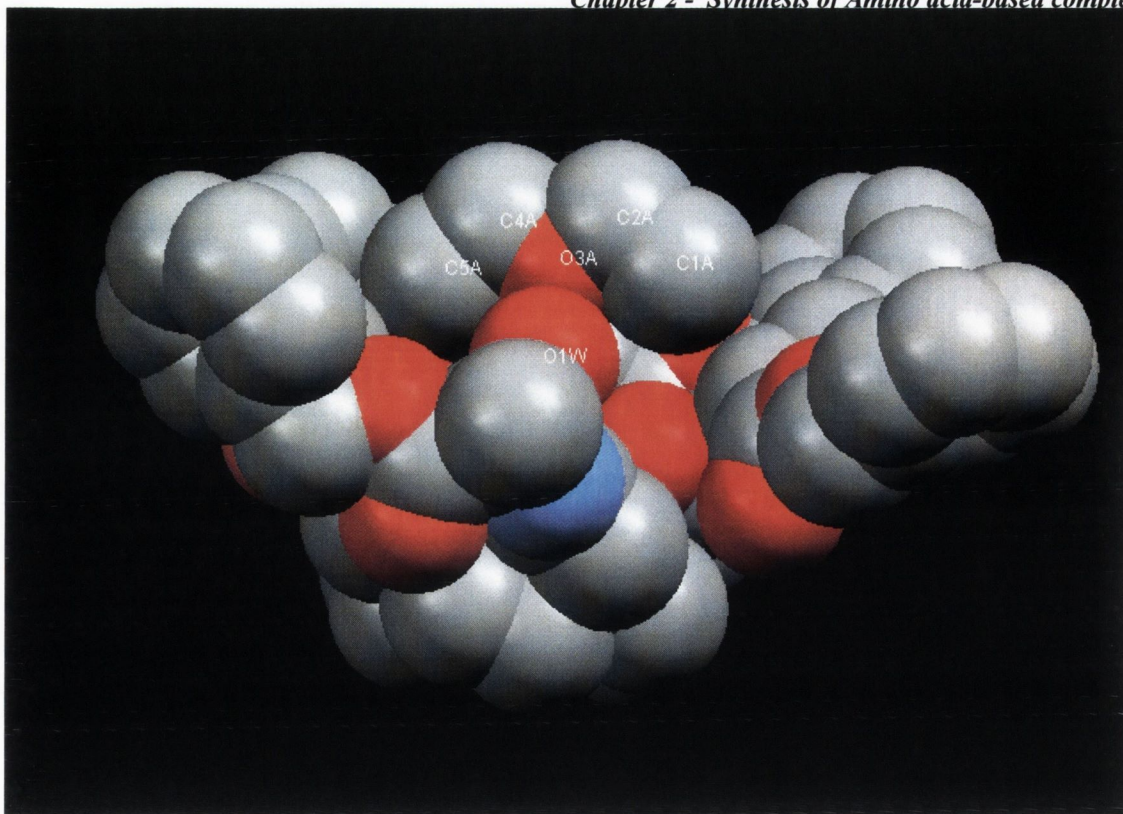


Figure 2.7 X-ray crystallographic structure of *Tb[86]*, showing the metal-bound water molecule within a bowl-shaped cavity.

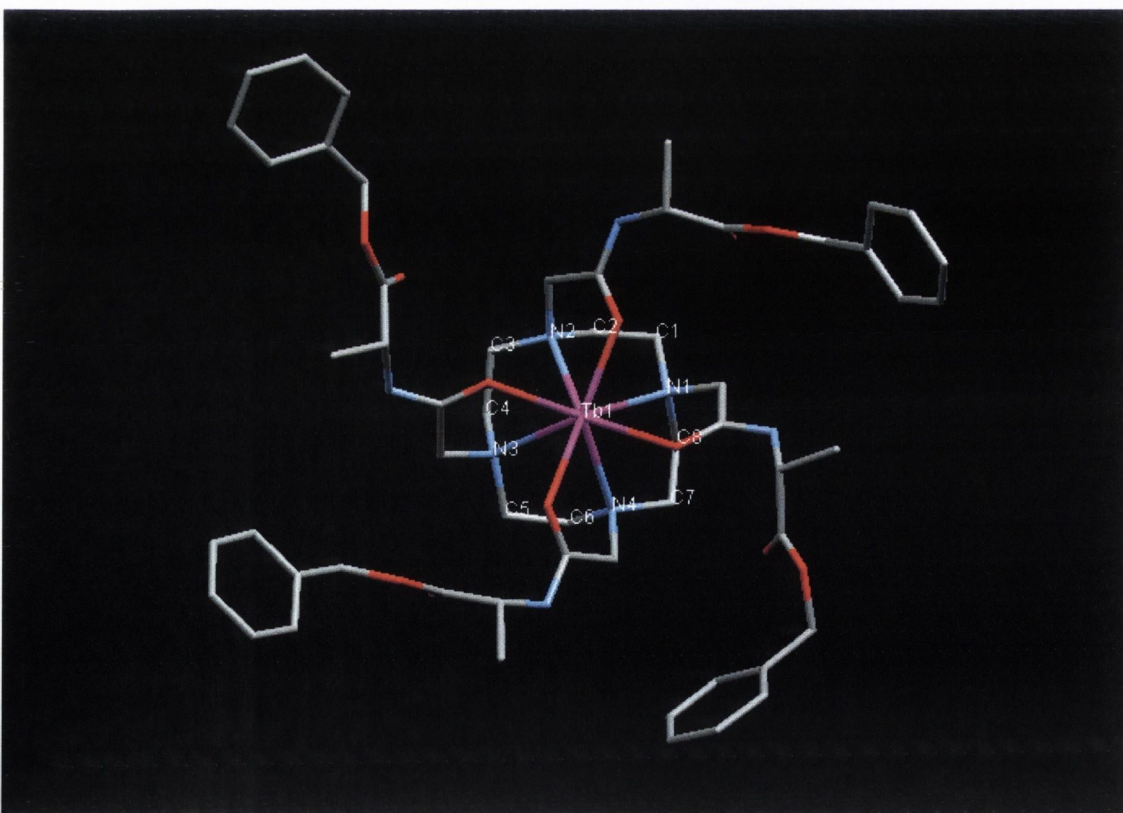


Figure 2.8 X-ray crystallographic structure of *Tb[86]*, showing the C_4 symmetry of the complex.

2.4 Lifetime Studies

As explained before, both Eu(III) and the Tb(III) complexes were expected to possess one labile metal-bound water molecules. This was verified for two of these complexes by determining their solid-state structures. The number of metal-bound water molecules can also be evaluated by estimating the hydration state or number of the complexes using a luminescent method, where the rate constant for the radiative decay (k) of the 5D_0 excited state of Eu(III) and the 5D_4 excited state of Tb(III) are measured in H₂O (k_{H_2O}) and D₂O (k_{D_2O}) respectively.¹³⁹ These values can be obtained by direct excitation of the lanthanide ion complexes at high concentrations. The hydration number (q) can then be determined from equations (i) and (ii) for the Eu and Tb complexes respectively.

$$(i) \quad q^{Eu(III)} = 1.2 [(1/\tau_{H_2O} - 1/\tau_{D_2O}) - 0.25 - 0.075x]$$

$$(ii) \quad q^{Tb(III)} = 5 [(1/\tau_{H_2O} - 1/\tau_{D_2O}) - 0.06]$$

Here the prefixes 1.2 and 5 in equations (i) and (ii) respectively, are proportionality constants that mirror the sensitivity of the corresponding ions to quenching by metal bound water molecules. The correction terms -0.25 and -0.06 represent quenching by second sphere water molecules, whereas $-0.075x$ in equation (i) represents the quenching by $N-H$ oscillators, where x is the number of such oscillators within a given complex.^{139,140,141}

Luminescent lifetime measurements described here were carried out on Varian Carey Eclipse Fluorimeter for a selection of Eu(III) and Tb(III) complexes. In each case the metal complex was dissolved in the minimum CH₃OH or CD₃OD, prior to dissolution in H₂O or D₂O. Filtration was found to be necessary in the case of the less water soluble compounds, and as a precaution, all solutions were filtered.

Figure 2.9 and **Figure 2.10** show the decay profiles found for **Eu[85]** as measured in D₂O and H₂O respectively.

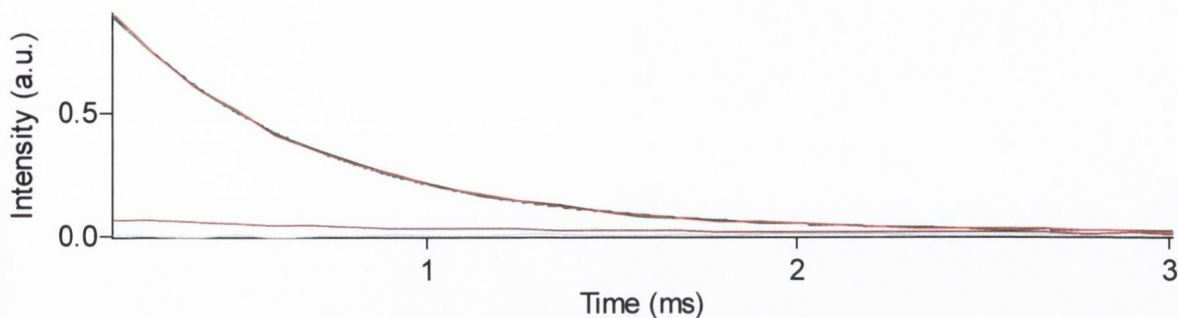


Figure 2.9 Decay profile for **Eu[71]** in D_2O

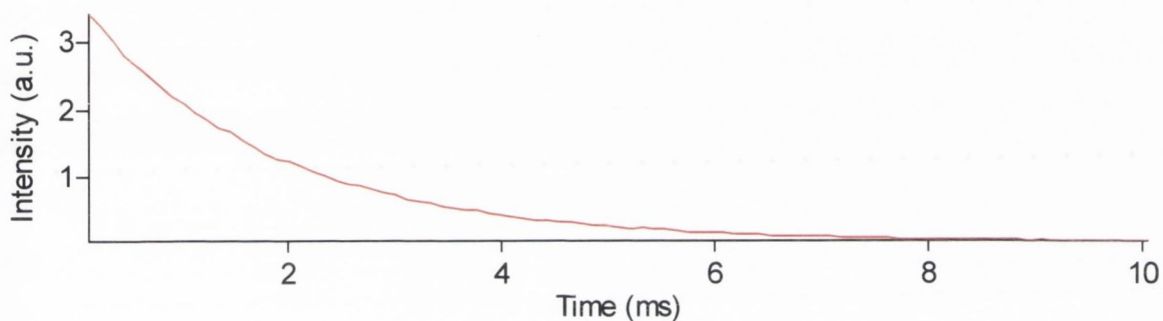


Figure 2.10 Decay profile for **Eu[71]** in H_2O

Table 2.15 summarises the observed lifetimes (τ_{Ln}), the corresponding k_{H_2O} and k_{D_2O} values and the q (± 0.5) values for the above complexes. Beginning with **Eu[70]**, a lifetime (t) of 0.523 ms was obtained in H_2O and 2.044 ms in D_2O , allowing a q value of 1.41 to be calculated from *Equation (i)*. In the case of the corresponding Tb(III) complex, lifetimes of 1.590 ms and 2.286 ms were measured in H_2O and D_2O respectively, leading to a q value of 0.79. Given the error of 0.5 involved in calculating the q value, in each case it is possible to say that that one water molecule is bound to each of the lanthanide ions. When the more hygroscopic **Eu[71]** was measured, a q value of 1.17 was calculated, indicating that the change from methyl ester to benzyl ester did not affect the hydration state of the lanthanide ion. Likewise, **Eu[85]** and **Tb[85]** gave q values of 1.33 and 1.21 respectively, while **Eu[87]** and **Eu[88]** had q values of 1.24 and 1.08. In each of these cases, it is reasonable to say that a single metal-bound water molecule is present under the experimental conditions. In the case of **Eu[85]**, the pH and pD were raised to 7.4 in order to mimic biological conditions as well as the conditions under which later experimental procedures would be

carried out. Lifetimes of 0.526 ms in H₂O and 1.478 ms in D₂O were found, leading to a *q* value of 1.17, indicating that pH did not affect the hydration state.

In all of these cases, approximately one water molecule was found to be coordinated to the metal centre, however, when **Eu[90]** was tested, a *q* value of 1.85 was measured. This value is significantly higher than any other obtained, and this may be due to the more hydrophobic nature of the environment around the water molecule.

Table 2.15 Lifetime studies for Eu(III) and Tb(III) complexes

Compound	$\tau_{\frac{1}{2}} \text{H}_2\text{O}$ [ms]	$k \text{H}_2\text{O}$ [ms^{-1}]	$\tau_{\frac{1}{2}} \text{D}_2\text{O}$ [ms]	$k \text{D}_2\text{O}$ [ms^{-1}]	<i>q</i> (± 0.5)
Eu[70]	0.523	1.913	2.044	0.489	1.41
Tb[70]	1.590	0.630	2.286	0.438	0.79
Eu[71]	0.561	1.784	1.794	0.558	1.17
Eu[71]	0.497	2.014	1.534	0.652	1.33
Tb[85]	0.517	1.934	0.613	1.632	1.21
Eu[86]	0.343	2.919	0.686	1.458	1.45
Tb[86]	0.605	1.652	0.782	1.280	1.56
Eu[871]	0.340	2.945	0.602	1.663	1.24
Eu[88]	0.354	2.833	0.595	1.683	1.08
Eu[90]	0.234	4.283	0.401	2.493	1.85

2.5 *pK_a* Evaluation

While the importance of the presence of metal-bound water molecules has been noted, and the presence of such water molecules has been verified in the case of two of the lanthanide complexes under discussion here, the *pK_a* of such a water molecule is also of crucial importance. As discussed in Chapter One, and will be emphasized in Chapter Four, it is a metal-bound hydroxide that can be of assistance in promoting the hydrolysis of phosphodiesteres. Therefore, the *pK_a* of such a water molecule will determine the pH range within which the greatest activity may be observed. Ideally, such complexes should show maximum activity in the physiological pH range.

Some preliminary *pK_a* analysis was carried out on a number of these complexes by R. Viguiet.¹⁴² The measurements were carried out at 37 °C, with all the solutions prepared

using degassed and doubly distilled water. The relevant lanthanide (III) complex (0.00049 M) was titrated with standardized 0.082 M tetramethylammonium hydroxide, using an automatic titrator system, MOLSPIN, equipped with a combined glass electrode (Metrohm, filled with KCl 3 M solution) and connected to a Gateway microcomputer. The titration data were refined by the non-linear least squares refinement program SUPERQUAD to determine the deprotonation constants. Typically, about 250 data points were collected over the pH range 4-11. The value of the pK_a was the mean value calculated from three independent titrations. The results obtained from these measurements are presented in

Table 2.16

Table 2.16 pK_a Evaluations

Complex	pK_a
La[70]	8.2, 8.5
Eu[70]	7.4
Yb[70]	7.5

The most important implication of these results is the evidence for two metal bound water molecules in the case of the La(III) complex and only one such water molecule in the case of the Eu(III) and Yb(III) complexes. Further discussion about the effects of these pK_a will be found in Chapter Four.

2.7 Conclusion

In conclusion, a family of amino ester based cyclen systems were synthesized and characterized. A variety of lanthanide complexes were subsequently prepared from these novel ligands. X-ray crystal structures of two such complexes were obtained, revealing that Eu(III) and Tb(III) are nine-coordinate in such systems with eight coordination sites provided by the ligand while the ninth is a metal bound water molecule. The crystal structures also indicated the formation of a cavity, which, in one case, was found to hold a diethyl ether molecule, suggesting that these compounds may form hydrophobic pockets. The presence of a metal bound water molecule in the solution state was verified by photophysical methods, with a q value of one found in the case of most Eu(III) and Tb(III) complexes. The exception to this rule was the more hydrophobic **Eu[90]**, which was found to have a q value of 2, indicating that the environment around this water molecule might be more hydrophobic. This was expected from the design of the molecule.

Chapter Three

Synthesis of Non Amino
Acid Based Cyclen
Complexes

3.1 Introduction

In Chapter 2, the synthesis and characterisation of a family of tetra-alkylated cyclen compounds incorporating amino ester residues as co-factors was discussed. This chapter will deal with the attempted synthesis of two other families of cyclen-based compounds; first, a set of tetrasubstituted cyclen compounds that incorporate amino pyridine co-factors and secondly, the synthesis of a tri-substituted cyclen compound incorporating methyl acetamide arms. The reasons behind the synthesis of these compounds will be discussed, followed by the methods of preparation and the characterisation of the resulting compounds.

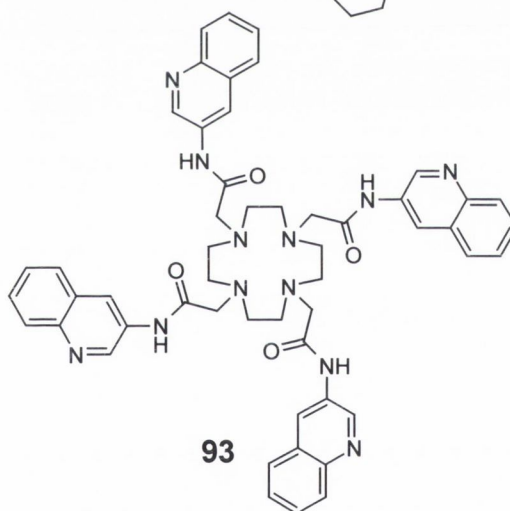
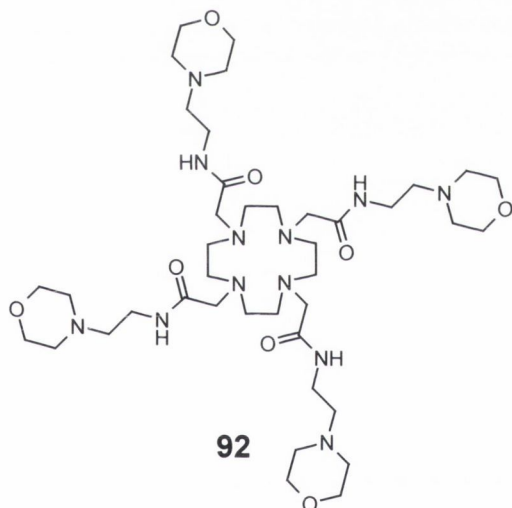
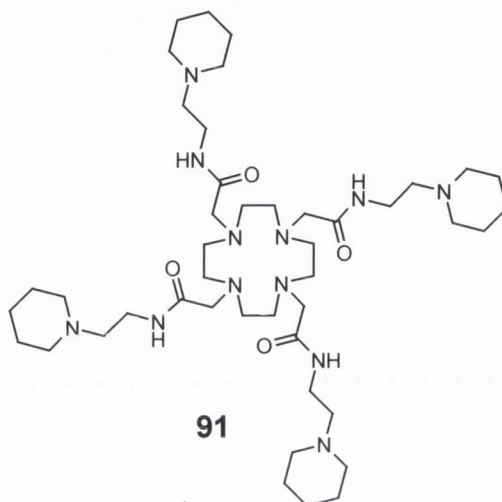
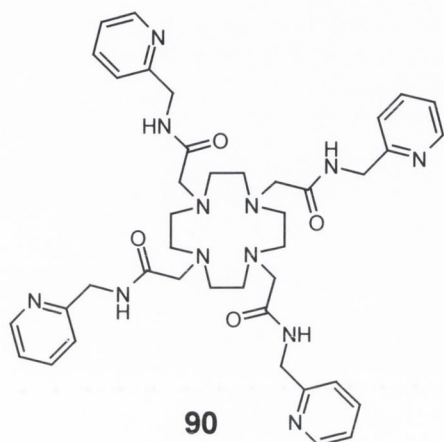
3.2 Use of Amino Pyridine Moieties as Co-factors.

Having prepared a selection of compounds that incorporated amino acid-based moieties, it was decided to synthesise analogous cyclen complexes that incorporated moieties that could potentially act as a source of acid-base catalysis. It has been postulated that acid-base catalysis plays a vital role in the hydrolysis of phosphodiester, as discussed in Section 1.4. Indeed, in Section 1.5.1, the role of acid-base catalysis in the activity of RNase A was discussed;²⁴ in this case the hydrolysis was catalysed by general-acid and general-base catalysis by two histidine residues, His-12 and His-119, as shown in **Figure 1.5**.²⁴ For this reason, it was decided to build similar co-factors, capable of such activity, into the type of cyclen-based lanthanide complexes that were discussed in Chapter 2.1. Such a complex would have the following features, useful for the promotion of phosphodiester hydrolysis:

- **A cationic metal centre**
- **Metal bound water molecule(s)**
- **A hydrophobic cavity**
- **Co-factors capable of promoting acid-base catalysis**

A number of tetra-substituted cyclen compounds with a similar type of pendant arm have been prepared within the Gunnlaugsson group in recent years. **90**, **91** and **92** were prepared by Viguié as potential MRI contrast agents.¹⁴² These compounds incorporated pyridine, piperidine and morpholine moieties respectively. **93** was reported by Gunnlaugsson as a pH

sensor.¹¹⁷ In the case of the work discussed in this chapter the moiety to be introduced into the cyclen system was a set of amino pyridine compounds. In the following section, the synthesis and characterisation of such complexes will be discussed.

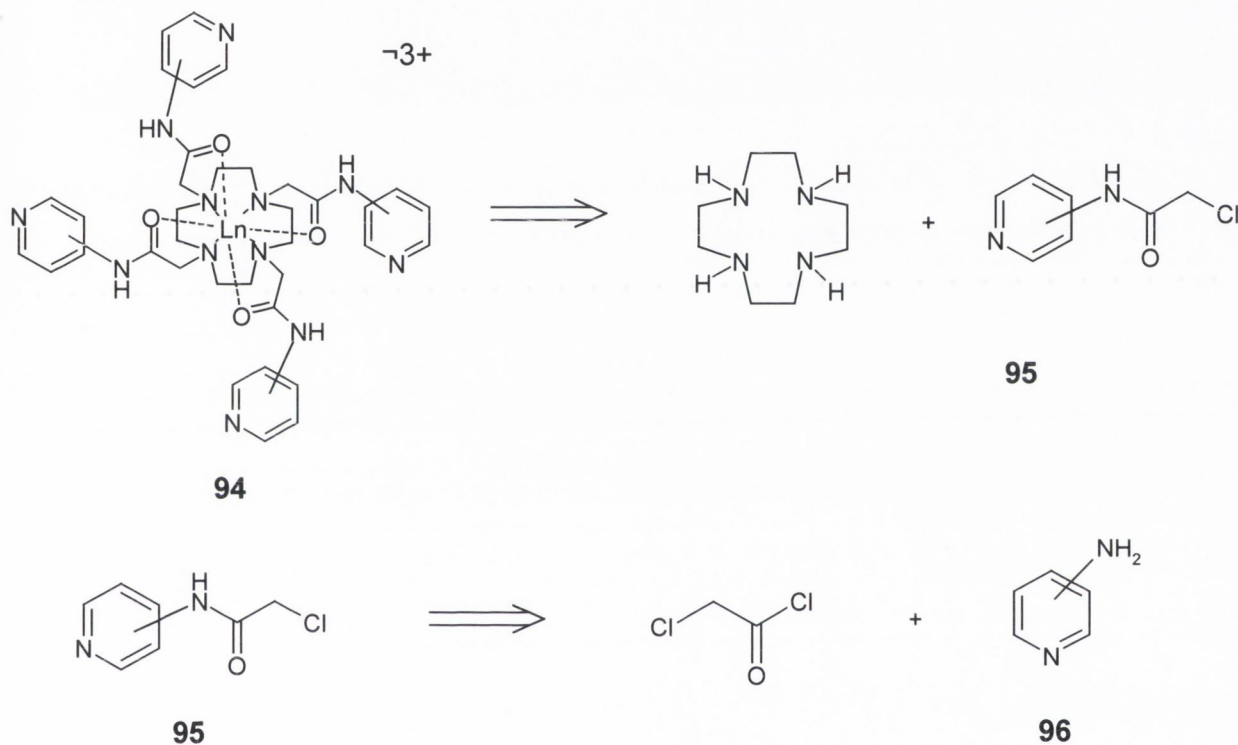


3.2 Pyridine acetamide as cofactor

In **Scheme 3.1**, the retrosynthesis of compound **94**, a tetra-substituted cyclen complex incorporating amino pyridine co-factors, is shown. The proposed procedure is similar to that described in Section 2.2.1, with the tetra-alkylated cyclen prepared by the addition of four equivalents of an α -chloroamide substituent **95** to cyclen. The α -chloroamide arms are prepared by the addition of the appropriate amino pyridine to chloroacetyl chloride, again, in the manner described in Section 2.2.1. There are three structural isomer to consider when dealing with amino pyridine; 2-aminopyridine, 3-aminopyridine and 4-aminopyridine. The

Chapter 3 – Synthesis of Non Amino Acid – based cyclen complexes

aim of this section of the project was to prepare a tetra-alkylated cyclen system with each isomer of the amino pyridine, and to subsequently investigate whether this influenced the activity of the complexes towards phosphodiester. The synthesis of the α -chloroamide arms will be discussed first, followed by the cyclen-based ligands, and finally the lanthanide complexes.



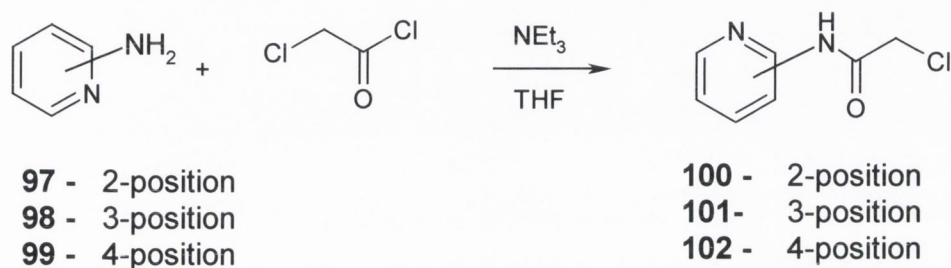
Scheme 3.1 The retrosynthesis of a family of terasubstituted cyclen complexes that incorporate amino pyridines. The lanthanide complexation step is omitted for clarity. The synthetic equivalents are shown in place of the synthons.

3.2.1 Synthesis of α -chloroamides incorporating amino pyridines

The first step, shown in **Scheme 3.2**, was to prepare the pendant arms **100**,¹⁴³ **101**,¹⁴⁴ **102**,¹⁴⁴ by means of modified literature procedure. Each amino pyridine in turn was added to THF and three molar equivalents of triethylamine and cooled to between -10 and -20 °C by means of a liquid nitrogen/acetone bath. To this, a solution of chloroacetyl chloride in THF was added dropwise, taking care that the temperature did not rise above -10 °C. The reaction was then stirred at room temperature for 16 h, before filtering off the inorganic salts and reducing the filtrate under reduced pressure. The residue was taken up in CHCl_3 and washed with 0.1 M HCl solution. The organic layer was dried over potassium carbonate and the

Chapter 3 – Synthesis of Non Amino Acid – based cyclen complexes

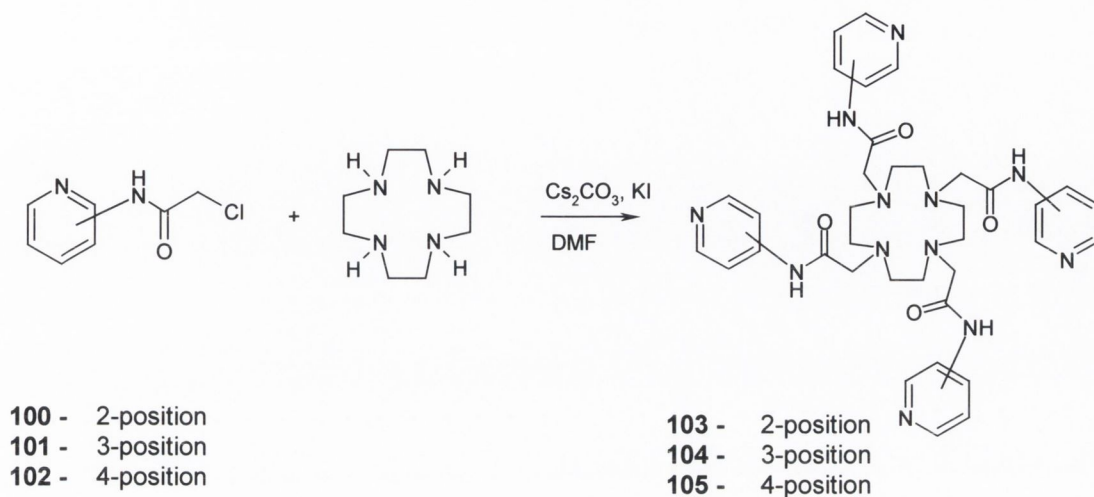
solvent was removed under reduced pressure to give a brown solid in each case. These were recrystallised from methanol to give **100**, **101** and **101** as cream/yellow solids in 50, 74 and 70 % yield respectively. As the preparation of these compounds has been previously reported, they were characterised only by ^1H NMR and ESMS.^{143,144}



Scheme 3.2 Synthesis of α -chloroamides incorporating amino pyridines, where the amino group is in the 2-, 3- and 4-position respectively.

3.2.2 Synthesis of tetrasubstituted cyclen incorporating amino pyridines

The synthesis of the macrocyclic ligands **103**, **104** and **105** was then attempted, using these α -chloroamides arms. by reacting four equivalents of the pyridine-acetamide arm with cyclen, using DMF, cesium carbonate and potassium iodide. The formation of **103** proceeded easily and the product was crystallised from methanol to yield **103** as a white powder in 30 % yield. This was characterised by ^1H NMR, ESMS, IR and elementary analysis. The ^1H NMR is shown in **Figure 3.1**, and the C_4 symmetry of the compound can be clearly seen. The cyclen ring protons appeared as a singlet at 3.01 ppm, the methylene protons of the acetamide spacers as a singlet at 3.36 ppm, and the aromatic pyridine protons between 6.91-8.15 ppm. The ESMS of this product showed a single peak at $m/z = 355$, corresponding to the M^{2+} peak.



Scheme 3.3 Synthesis of tetrasubstituted cyclen incorporating amino pyridines where the amino group is in the 2-, 3- and 4-position respectively.

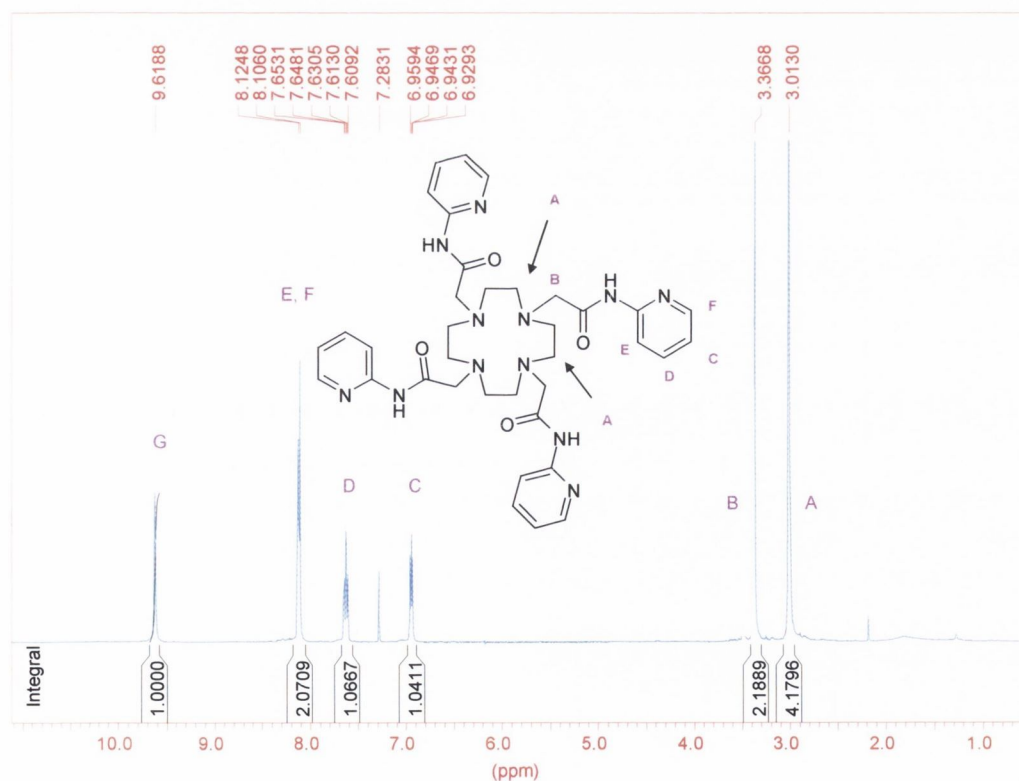
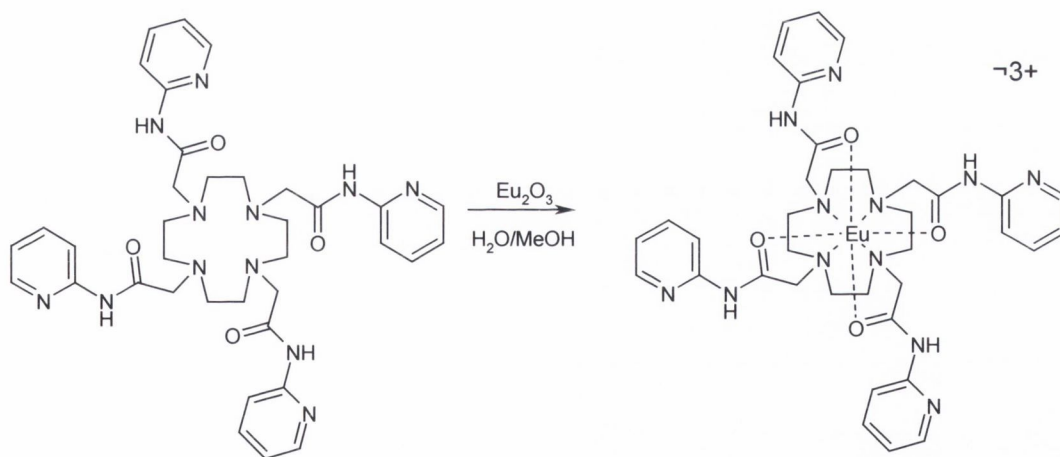


Figure 3.1 ^1H NMR of **103**, in CD_3Cl , showing the C_4 symmetry of the compound

104 and **105**, incorporating the *m*- and *p*- aminopyridine isomers, could not be successfully prepared despite the attempted use of a variety of reaction conditions. Methanol, ethanol, acetonitrile, chloroform, DCM and DMF were used as solvents, and Cs₂CO₃, K₂CO₃ and KHCO₃ were used as bases. The reaction was attempted with and without the addition of potassium iodide, and the reaction was also carried out using up to 6 equivalents of each arm. In no case was the tetra-substituted product formed, according to ESMS. Both ESMS and TCL showed the formation of the di- and tri- substituted products only, even when the reactions were carried out with an excess of α -chloroamide arm.

3.2.3 Lanthanide Complexation of 103

Complexing **103** proved more difficult than the complexes described in the previous chapter. Refluxing the ligand with a lanthanide triflate in acetonitrile, methanol or ethanol proved unsuccessful, with no evidence of complexation according to ESMS or ¹H NMR, even after refluxing for up to one week. **Eu[103]** was finally formed using europium oxide, by refluxing in H₂O/MeOH, 80/20 for 48 hours.¹⁴⁵



Scheme 3.4 Complexation of **103** with **Eu(III)**

A ¹H NMR of this complex in CD₃OD was obtained, shown in **Figure 3.2**, which clearly shows the shifted axial and equatorial protons of the cyclen ring. This compound was never

Chapter 3 – Synthesis of Non Amino Acid – based cyclen complexes

fully characterised, due to its instability. Within approximately eight weeks, it had decomposed, with ESMS showing only the uncomplexed ligand. Due to this instability, neither elementary analysis nor accurate mass were obtained, and it was not tested with HPNP. All subsequent attempts to prepare it were unsuccessful, even following the same experimental procedure.

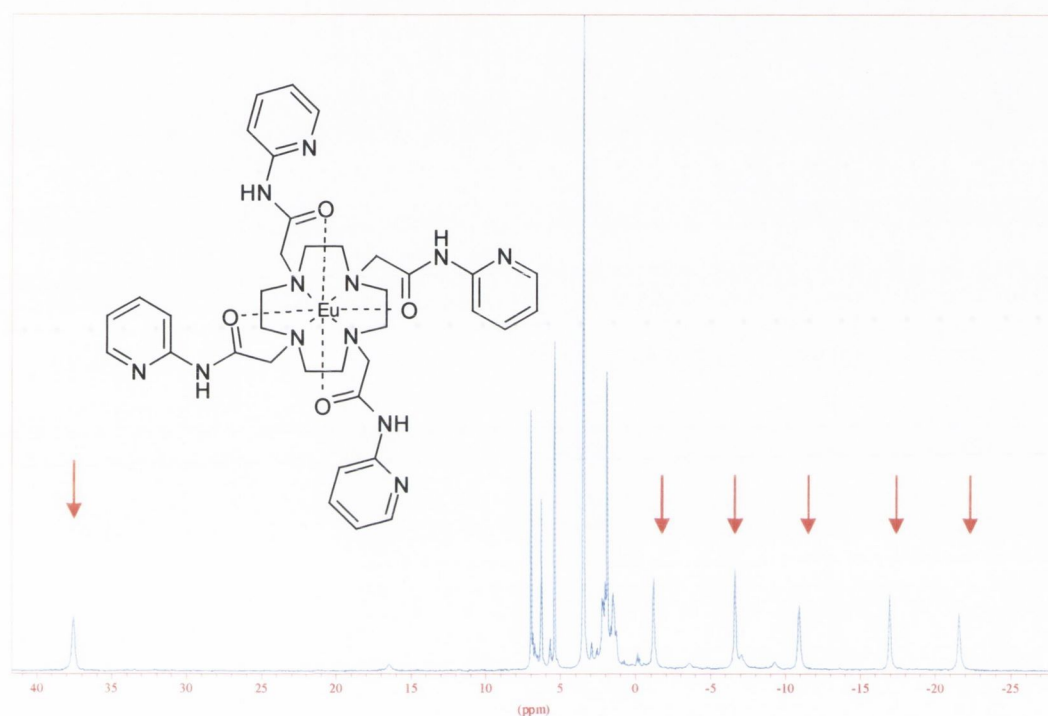


Figure 3.2 ^1H NMR of $\text{Eu}[103]$ in CD_3OD , showing the effect of the paramagnetic metal centre

3.3 Three-arm Cyclen Systems

As well as investigating tetrasubstituted cyclen systems, some preliminary work was begun upon three-armed cyclen systems. In such a tri-alkylated compound, the fourth cyclen nitrogen would remain free for later modification. This is of advantage because, in theory, such a compound could be incorporated into an oligonucleotide *via* a spacer attached to the fourth cyclen nitrogen, as shown in **Figure 3.3**. This would create, in effect a ribozyme mimic, as the attached oligonucleotide could be designed to be complementary to any RNA

sequence desired. This is the ultimate aim of the work described in this thesis, and so the synthesis of some simple tri-alkylated cyclen complexes was desirable.

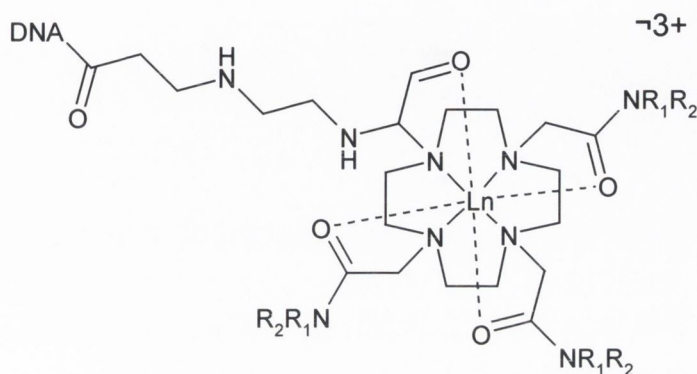


Figure 3.3 The incorporation of a tri-substituted cyclen complex into an oligonucleotide

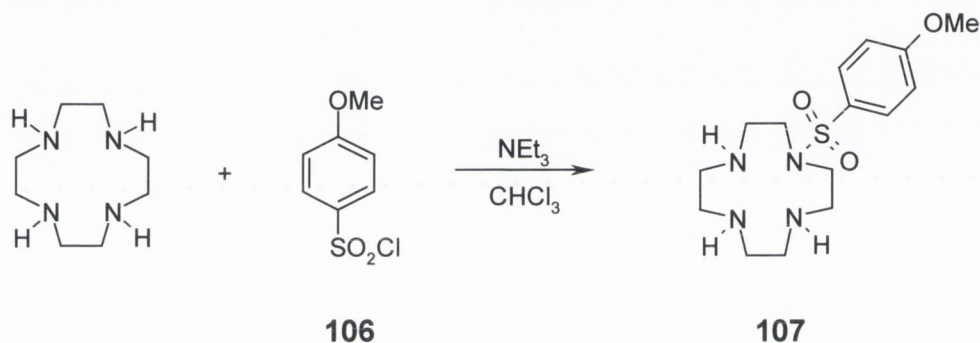
A further possible advantage of tri-substituted cyclen lies in the number of coordination sites available for lanthanide complexation. As discussed in Chapter 1, lanthanides tend to have a coordination number of 9-10 when complexed by cyclen-based ligands.^{68,69,71} While the tetra-alkylated cyclen systems described previously have eight coordination sites, leaving one vacant site to be taken by a small molecule such as water, a trisubstituted cyclen system is heptadentate. Therefore, it could be expected that a complexed lanthanide would require at least two metal-bound water molecules to be coordinatively saturated. The importance of a metal-bound water molecule to our design has been previously discussed in Chapter 2 and it might be hoped that the presence of two such metal-bound waters could aid the promotion of phosphodiester hydrolysis by means of nucleophilic attack.^{68,71}

3.2 Synthesis of tri-substituted cyclen

The synthesis of such heptadentate cyclen systems was less straightforward than that described for the tetra-alkylated cyclen systems in the previous section and in Chapter 2. This difficulty arises from the need for three of the four cyclen nitrogens to be selectively alkylated while the fourth is left free. There are two general methods available for such synthesis. The first involves direct addition of three equivalent of the appropriate α -chloroamide to cyclen, followed by purification by column chromatography. This method has been developed with great success within the Gunlaugsson group recently.^{146,147} The

3.2.1 Mono-protection of cyclen

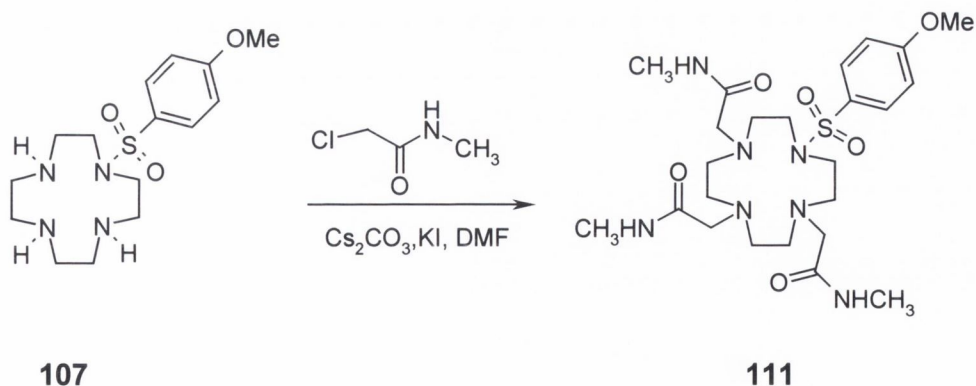
Synthesis of the protected cyclen, **107**, was achieved by reaction of **106** with cyclen, as shown in **Scheme 3.6**.¹⁴⁹ This procedure involved the dropwise addition of a solution of *p*-methoxybenzylsulphonyl chloride in CHCl_3 to a solution of cyclen in CHCl_3 at 36-39 °C, with triethylamine used as a base. As previously reported by Parker *et al.*, with sufficiently slow addition of *p*-methoxybenzylsulphonyl chloride, a clean product was obtained without need for further purification. This was evident from the presence of two doublets at 7.72 ppm and 7.01 ppm and a singlet at 3.38 ppm in the ^1H NMR spectrum in CD_3Cl .¹⁴⁹



Scheme 3.6. Reaction of cyclen with *p*-methoxybenzylsulphonyl chloride to give mono-protected cyclen.

3.2.2 Tris-alkylation of cyclen

Alkylation of the three remaining nitrogens, using **107**, was carried out in DMF at 80 °C, in the presence of Cs_2CO_3 and KI, as shown in **Scheme 3.7**. **111** was prepared according to literature procedure, from chloroacetyl chloride and methyl amine.¹⁴⁹

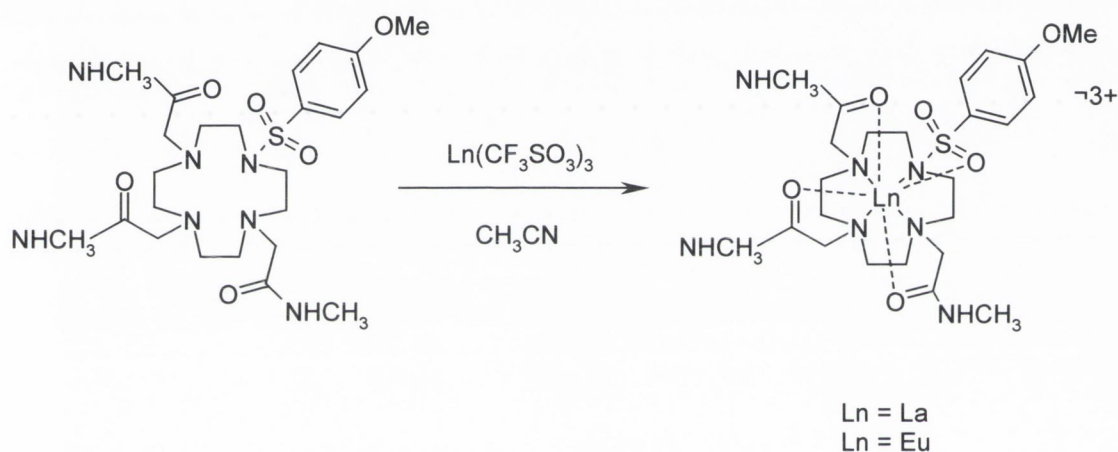


Scheme 3.7 Alkylation of three cyclen nitrogens

111 was obtained as an oil which was crystallised from CHCl_3 solution. The crystals obtained were suitable for X-ray crystallography, and the crystal structure can be seen in **Figure 3.4**. From this, the three mono methyl acetamide arms attached to cyclen are visible, as is the *p*-methoxybenzylsulphonyl protecting group.

3.2.4 Complexation of **111**

Eu(III) and La(III) complexes of **111** were prepared using the same procedure as previously described in Chapter 2 and shown in **Scheme 3.8**: refluxing in dry acetonitrile with 1.1 equivalents of the appropriate lanthanide triflate.



Scheme 3.8 Complexation of **111** with La(III) and Eu(III) triflate.

Eu[111] was characterized by ^1H NMR, mass spectroscopy and IR. Again, the characteristic broad, shifted proton resonances were found in the ^1H NMR, indicating the presence of the paramagnetic metal centre. ESMS showed peaks for the complex with one and with two triflate counterions. In the IR, the carbonyl stretching frequency shifted from 1654 cm^{-1} for the uncomplexed ligand to 1637 cm^{-1} . **La[111]** was also prepared, this time refluxing the reaction in ethanol, rather than CH_3CN . In this case, crystals suitable for X-ray crystallography were obtained when hexane was added to the reaction mixture. The X-ray crystal structure is shown in **Figure 3.5**.

Table 3.2 Selected Bond Lengths and Bond Angles for La[111]

Bond	Length (Å ^o)	Bond	Angle (Å ^o)
La1 O5	2.458(2)	O5 La1 N10	62.57(8)
La1 O4	2.512(2)	O4 La1 N7	61.33(7)
La1 O3	2.514(2)	O3 La1 N4	63.42(7)
La1 O13	2.554(2)	O2 La1 N1	50.94(7)
La1 O2	2.694(2)		
La1 N1	2.989(3)	N-C-C-O	-45.0(4)
La1N10	2.842(3)	N-C-C-O	-27.8(4)
La1 N7	2.808(3)	N-C-C-O	31.8(4)
La1 N4	2.784(3)		

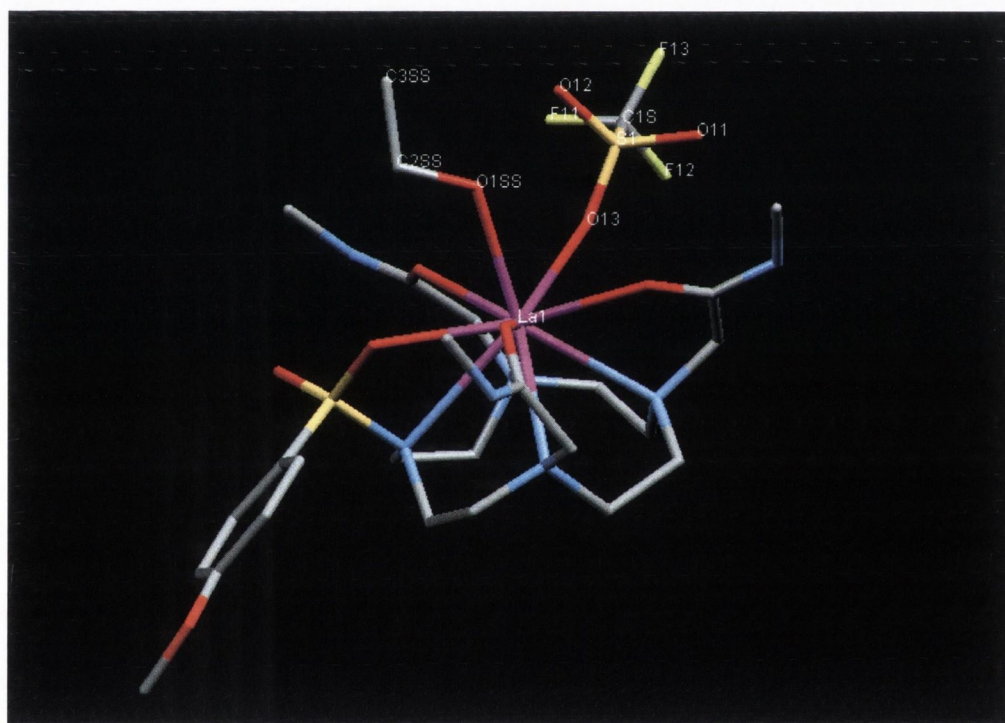


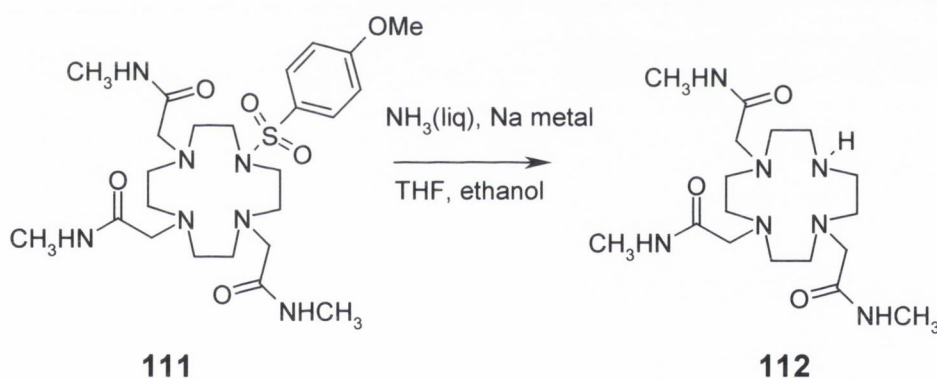
Figure 3.5 X-ray crystal structure of La[111]

From this crystal structure it can be seen that the La(III) ion is ten-coordinate, coordinating to the four cyclen nitrogens, the three carbonyl oxygens associated with the acetamide arms as well as to one carbonyl from the sulfonyl group. In addition to these eight coordination sites, there are two metal-bound molecules; an ethanol solvent molecule and a triflate which binds to the La(III) center through one of the oxygens. This helps to confirm that La(III)

tends to be ten-coordinate when complexed by these cyclen-based systems. Although the crystal structure of this compound was obtained, it could not be further characterized. When ESMS was attempted, only the parent ligand peak was observed, suggesting that the complex had completely dissociated. Further attempts to prepare it were met with the same result: the complex, once formed, seemed to dissociate in solution, or upon standing in air.

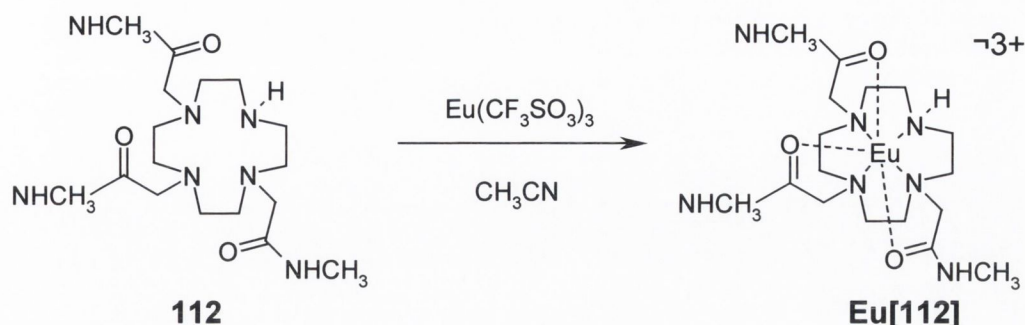
3.2.3 Removal of the protecting group

Having successfully alkylated three of the cyclen nitrogens, the *p*-methoxybenzylsulfonyl protecting group was removed under Birch conditions, as shown in **Scheme 3.9**.¹⁴⁹ **111** was stirred in anhydrous THF in the presence of sodium metal and liquid ammonia at -60 °C. The ammonia was allowed to evaporate and the product was purified by acid-base extraction. Continuous extraction was necessary to isolate **112**, however a yield of only 36 % was obtained.



Scheme 3.9 Removal of the *p*-methoxybenzylsulfonyl protecting group under Birch conditions

Both **111** and **112** were characterised by ¹H NMR and mass spectroscopy. Due to the hygroscopic nature of these compounds, elemental analysis was not possible. The ¹H NMR of **112** revealed the C₂ symmetry of this ligand, with the plane of symmetry running through the free nitrogen of the cyclen. Two N-H singlets were found at 7.60 ppm and 7.30 ppm, in a ratio of 1:2. These signals corresponded to the carboxylic amide protons. Similarly, the methylene protons from the pendant arms were found at 3.06 ppm and 2.97 ppm in a ratio of 4:2 while the protons of the methyl groups appeared at 2.75 ppm and 2.67 ppm in a ratio of 6:3. The cyclen protons were found as broad singlets between 2.4 and 2.7 ppm.



Scheme 3.5 Complexation of 112 with Eu(III) triflate

Eu[112] was formed by refluxing the ligand with one equivalent of europium triflate in acetonitrile. The reaction was cooled and added to stirring diethyl ether, and the resulting white precipitate was collected by suction filtration. The ^1H NMR of the resulting complex showed evidence of the paramagnetic metal centre, with broad proton signals found over a wide ppm range.

Table 3.3 Bond lengths and Bond Angles for Eu[112]

Bond	Length (Å ^o)	Bond	Angle (Å ^o)
Eu1 O14	2.337(6)	O22 Eu1 N7	65.98(19)
Eu1 O22	2.393(6)	O18 Eu1 N4	65.5(2)
Eu1 O18	2.399(6)	O14 Eu1 N1	66.1(2)
Eu1 O1W	2.448(6)	O1W Eu1 O2W	70.9(2)
Eu1 O2W	2.485(6)		
Eu1 N1	2.673(7)	N-C-C-O	-30.0(7)
Eu1N10	2.618(7)	N-C-C-O	-32.7(1)
Eu1 N7	2.670(7)	N-C-C-O	-36.4(5)
Eu1 N4	2.678(7)		

A crystal structure of this Eu(III) complex (**Figure 3.5**) confirmed the presence of two metal-bound water molecules in this heptadentate system. From this it can also be seen that the Eu(III) is bound to the four nitrogens of the cyclen as well as the three carbonyl oxygens of the acetamide arms.

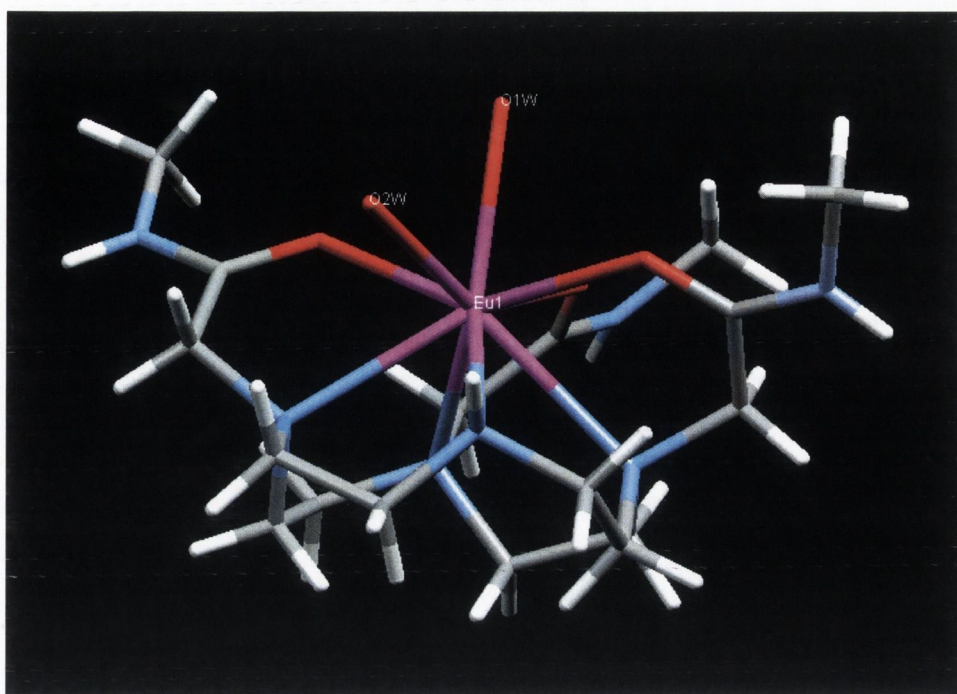


Figure 3.5 X-ray crystal structure of Eu[112], showing the two metal bound water molecules

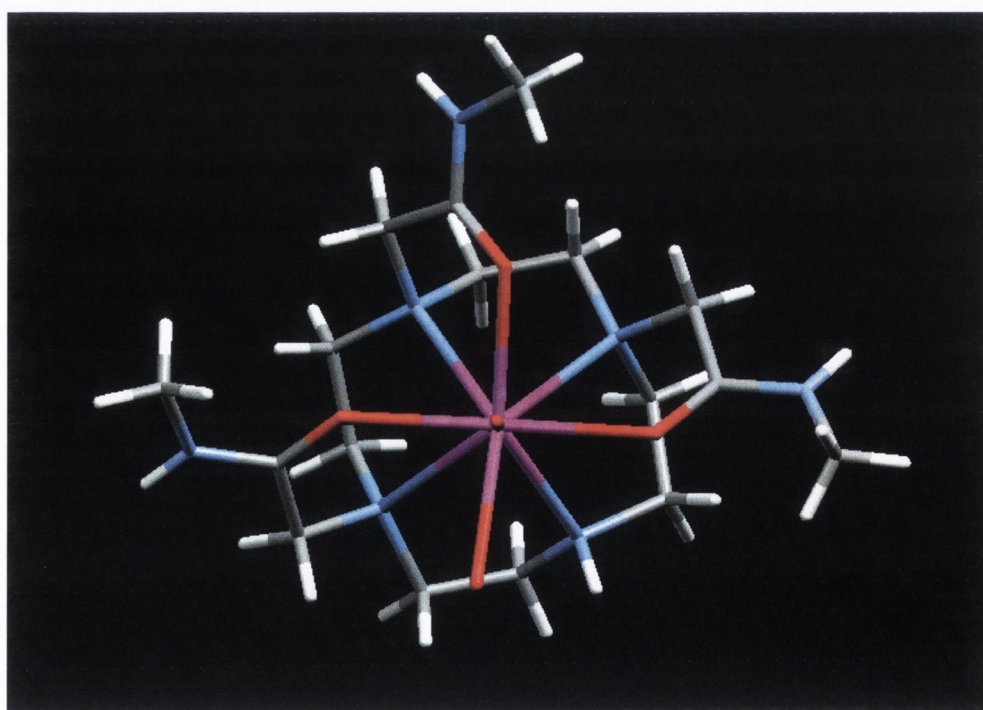


Figure 3.5 X-ray crystal structure of Eu[112], showing the C₂ symmetry of the molecule

3.4 Conclusion

This chapter has described the attempted synthesis of tetra-substituted cyclen complexes incorporating amino pyridine co-factors. Limited success was had, with only one such lanthanide complex successfully formed **Eu[103]**, and this was unstable over time and impossible to reproduce. Further work in this area is ongoing within the Gunnlaugsson group. Analysis of the ability of this complex to cleave an RNA strand will be discussed in Chapter 5.

Synthesis of a tri-substituted cyclen was achieved through regioselective mono-protection of the cyclen ring with a *p*-methoxybenzylsulphonyl group which was later removed under Birch conditions to give **112**. Crystallographic data provided evidence that **Eu[112]**, *i.e.*, a lanthanide within a heptadentate cyclen system has two metal-bound water molecules. An X-ray crystal structure of **La[111]** provided evidence that a La(III) ion within an octadentate cyclen environment can have two metal-bound moieties. Further analysis of the complexes prepared in this chapter will be discussed in Chapter 5.

Chapter Four

Interactions with Phosphodiesterases

4.1 Introduction

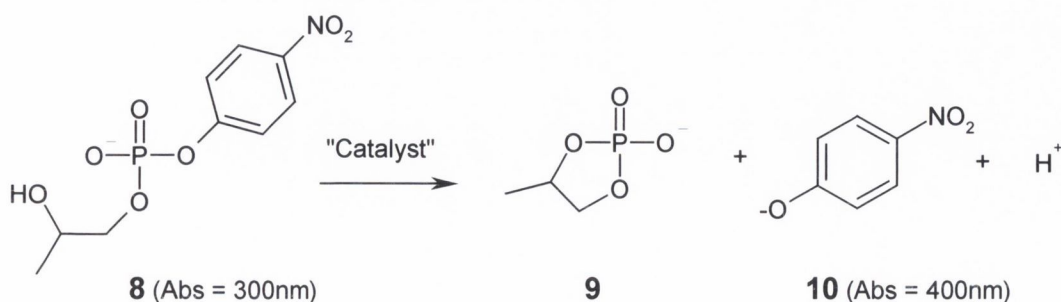
As outlined in Section 1.5, 2-hydroxypropyl *p*-nitrophenyl phosphate, or **HPNP**, is a useful model compound for evaluating the efficiency of potential RNA cleavage agents.⁴³ It is a phosphodiester with a good leaving group, *i.e.* the *p*-nitrophenolate and a hydroxyl group that can mimic the nucleophilic behaviour of the 2'-hydroxy group of RNA.⁴³ A principal advantage of using this compound to evaluate hydrolytic activity lies in the UV/*vis* activity of both **HPNP** itself and its hydrolysis product *p*-nitrophenolate. **HPNP** absorbs at 290 nm and *p*-nitrophenolate absorbs at 400 nm.⁴³ Therefore, the path of the hydrolysis is relatively straightforward to follow since the primary product is easily identified and easily monitored. The progress of such hydrolysis can be measured by the rate of change in the absorption spectrum, either at 290 nm (the decrease of the **HPNP**) or at 400 nm (the increase in *p*-nitrophenolate) as a function of time. In this chapter the results obtained from its hydrolysis by the lanthanide complexes described in Chapter 2 are discussed.

As discussed in Chapter 1, an important means of evaluating the potential of new ribozyme and ribonuclease mimics is to measure the kinetics of the hydrolysis reactions of phosphodiester. Such work has been widely reported.^{43,48,68,76,95} Due to the wide variety of phosphate models used, as well as the different mechanisms employed by each type of ribozyme or ribonuclease mimic, it can be difficult to reasonably compare the results reported by different research groups. Within the results obtained from studies using **HPNP** hydrolysis, in which we are most interested, a variety of experimental conditions are reported; different research groups evaluate hydrolysis at different pHs^{68,54} and temperatures,^{68,91} or using different buffers.^{68, 105} Indeed, not all such measurements are carried out in H₂O.^{68, 57-62} This makes direct comparison of the rates quoted often impossible. As well as these physical differences in performing the experiments, some research groups have been found to give results based on the initial slope of the absorbance *vs* time rate curve, while others quote pseudo first order rate constants for the same experiment.¹⁵² These factors were necessary to take into account when coming up with a method for evaluating and comparing the hydrolytic abilities of the lanthanide complexes discussed here.

4.1.1. Hydrolysis of HPNP.

HPNP was chosen as a model compound for RNA due to its good leaving group and because its decomposition can be monitored by observing the changes in the absorption spectrum, as shown in **Scheme 4.1**.⁴³ HPNP absorbs at 300 nm and one of its hydrolysis products, 4-nitrophenolate **58**, absorbs at 400 nm. Therefore the rate of reaction (k) can be calculated by following the increase in absorption at 400 nm. A rate of cleavage of HPNP without catalyst of $1.2 \times 10^{-4} \text{ h}^{-1}$ was determined by Breslow *et al.* in 1991, at 37 °C and pH 7.4, using 10 mM HEPES buffer.⁴³ Using this figure as the rate of background hydrolysis, the rate of acceleration of hydrolysis due to the lanthanide complexes discussed in Chapter 2, 3 can be calculated.⁴³

All of the experiments discussed in this chapter were performed using an *Agilent 8453* photodiode array spectrophotometer fitted with a circulating temperature controlled water bath, and water driven mechanical stirring. A 50 mM HEPES solution was prepared (1.19 g) in water (100 mL). The pH of this was adjusted to 7.40 using NaOH and HCl solutions. Using this buffer solution, a solution of 0.18 mM HPNP was prepared. The concentration was adjusted such that $A_{290} = 1.22$ ($\epsilon = 21374$). 2.4 ml of this HPNP solution was then incubated in a UV cell at 37 °C for 10 minutes. This gave a final concentration of 4.32×10^{-7} mol of the phosphate. A solution of the appropriate lanthanide complex was prepared in methanol such that 100 μl contained 4.32×10^{-7} mol of the complex. 100 μl of the complex solution was then added to the HPNP at 37 °C and the reaction was monitored by observing the changes in the absorption spectrum over at least 16 h. The pH of the reaction mixture was monitored again at the end of the reaction and was found to have changed by no more the 0.04 pH units. Every rate quoted is an average of 2-3 measurements, agreeing to within 10%. The observed plot of A vs time was fitted using a fitting program to give k . k can also be calculated by fitting a plot of A vs time by hand, and this was verified in the case of some of the compounds, as shown in Appendix I.



Scheme 4.1 Decomposition of HPNP (Abs = 290 nm) in the presence of a catalyst to produce *p*-nitrophenolate (Abs = 400 nm) and a cyclic phosphate

4.1.2 Effect of Agitation on the Reaction Mixture

An important feature of this design was the mechanical stirrer, which constantly agitated each hydrolysis reaction as it was monitored. Its importance can be understood by looking at **Figure 4.1**, which shows two simple UV/*vis* spectra. This picture illustrates the way in which the hydrolysis of **HPNP** can be followed by the changes in UV/*vis*, with the **HPNP** peak observed at 290 nm and the *p*-nitrophenolate hydrolysis product observed at 400 nm. In this simple experiment, a drop of 2 M NaOH was added to a 0.18 mM solution of **HPNP** in a UV cell. The UV/*vis* spectrum was followed over the next hour, without the reaction being stirred. The results can be seen in the set of spectra marked 'A'; the **HPNP** still shows an absorbance of 1.2 AU and there is no significant peak at 400 nm to indicate the formation of a hydrolysis product. A stirring bar was then added to the cell and the result of agitating the reaction can be seen from the set of spectra marked 'B'. The absorbance at 290 nm has decreased, indicating the disappearance of **HPNP** while a peak has appeared at 400 nm, showing the formation of *p*-nitrophenolate. This simple experiment illustrates the importance of keeping these reactions, which can be followed over a period of 48 h, constantly stirred.

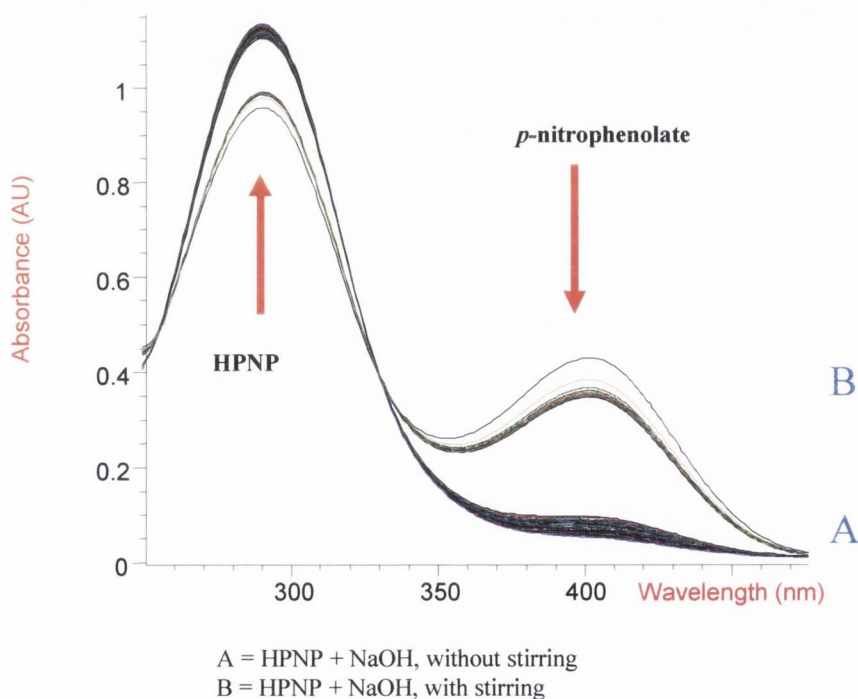
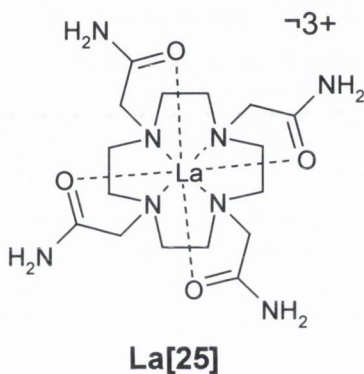


Figure 4.1 A plot of Absorbance vs wavelength showing two samples of a 0.18 mM **HPNP** solution to which NaOH has been added. Spectrum **A** shows **HPNP** when a drop of NaOH has been added and the reaction has not been agitated, and no peak is observed at 400 nm. Spectrum **B** shows the result of agitating the reaction – a peak at 400 nm indicated the production of *p*-nitrophenolate.

4.2 Hydrolysis of HPNP by La[25]

The first system to be examined was **La[25]**, which was reported by Morrow *et al.* in 1994 to cleave **HPNP** with $k = 0.056 \text{ h}^{-1}$.⁶⁸ This complex was synthesised and characterised according to literature procedure⁶⁸ and tested with **HPNP**. Using identical experimental conditions to those reported, pH 7.4, 37 °C and 10 mM HEPES solution,⁶⁸ the rate of hydrolysis was measured and a rate of 0.059 h^{-1} was obtained, reproducible when repeated on several occasions. This was within 5 % of the literature value.⁶⁸ This result gave an indication that the experimental procedure used for the rest of the experiments could provide a reasonable comparison to results quoted by other research groups.



4.3 HPNP hydrolysis by glycine derivatised complexes.

The **Ln[70]** series was the first to be tested for hydrolytic activity with **HPNP**. When examined using the conditions described (37.0 °C, pH 7.40, 10 mM HEPES buffer and equimolar amounts of **HPNP** and complex), it became apparent that 10 mM HEPES buffer, as was used by Breslow *et al.* and Morrow *et al.*, was insufficient to maintain a constant pH for the duration of the reaction (generally in the region of 24 h). A pH drift was observed from pH 7.40 at the beginning to pH 7.25 by the end of the reaction when 10 mM HEPES was used, although it should be noted that this combination of buffer and phosphate concentrations had been used previously in the literature.³⁷ Maintaining a constant pH was of great importance in these experiments, as the hydrolysis reaction can be extremely pH dependent. This will be discussed in greater detail in Section 4.3.2. Therefore, the concentration of buffer was raised to 50 mM and the pH drift was reduced to < 0.04 pH units. Using 50 mM HEPES, the pH of the reaction of **HPNP** with complex **La[70]** remained unchanged, within acceptable error; after 48 h, the pH drifted from 7.40 to 7.37. 50 mM HEPES buffer solution was used in all subsequent measurement, to minimise the possibility of pH drift.

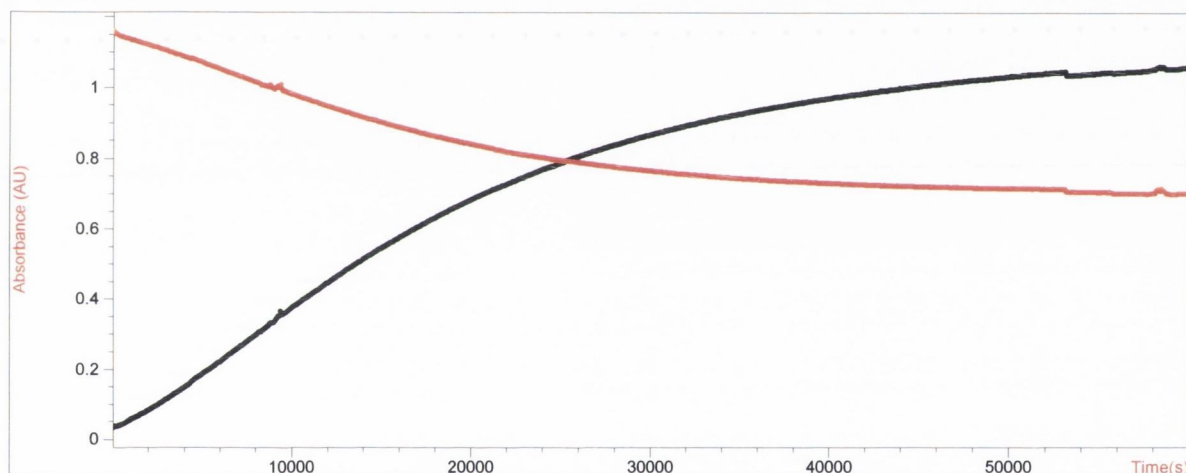
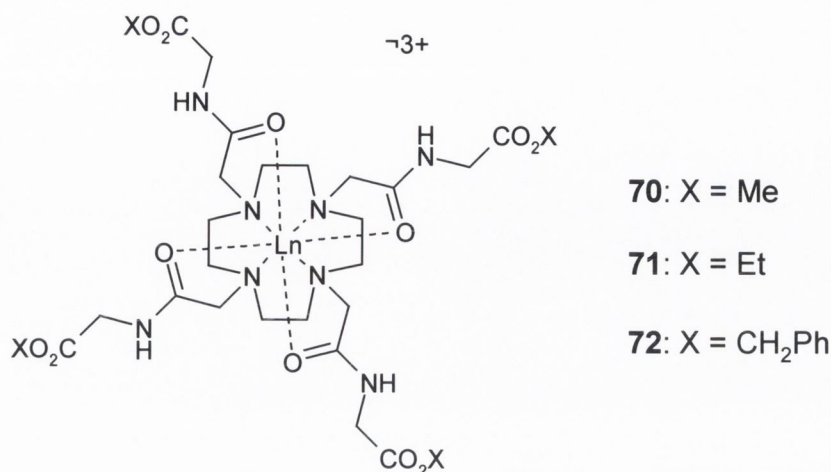


Figure 4.2. Increase of *p*-nitrophenolate (black line) and decrease of *HPNP* (red line) in the presence of *La*[70] as a function of time

4.3.1 Rate of *HPNP* hydrolysis by *Ln*[70] at pH 7.40

The results of incubating one molar equivalent of *HPNP* with each lanthanide complex of **70** at pH 7.40 and 37.0 °C are presented in **Table 4.1**. This shows the rate of hydrolysis (k) in h^{-1} , the half-life of the reaction in h, and the relative rate of the reaction, which is the increase in hydrolysis by the lanthanide complex relative to the hydrolysis of *HPNP* in the absence of such a complex.⁴³ The most obvious feature of these results is that it can be seen the rate of hydrolysis is directly dependant upon the size of the lanthanide ion in the complex, with the larger ions showing the greatest activity, and the smaller lanthanides the least. Before looking at these results, it is worth recalling some factors that may govern the relationship between the rate

of **HPNP** hydrolysis and the choice of lanthanide within a given ligand were discussed in Section 2.1 and include:

- The smaller lanthanide ions have a larger charge density, and may therefore be better able to stabilize the reaction intermediate
- The larger lanthanides have a higher coordinate requirement, and therefore, within the cyclen framework, a greater capacity for small molecule binding. It has been shown in the literature that La(III) complexes can have two metal-bound water molecules, as opposed to the single metal-bound water of a corresponding Eu(III) complex⁶⁸
- Larger lanthanides may not sit as deeply within the ligand cavity as the smaller ions, as they form stronger bonds with the amino moieties of the cyclen structure. This presents the possibility that the larger ions may be better able to interact with the substrate by virtue of special proximity. This also means that the size of the encapsulated lanthanide will affect the size of the cavity, which in turn will affect its interaction with the substrate⁷⁹
- The choice of lanthanide will affect the pK_a of the metal-bound water molecule. This in turn will determine the pH range in which a given complex will show the maximum activity¹⁵³

From the results in **Table 4.1** it can be seen that the rate of cleavage by **La[70]**, 0.410 h^{-1} which gives $t_{1/2} = 1.69 \text{ h}$. This rate represented a 3417-fold rate increase over that of the uncatalysed reaction.⁴³ This rate also represented an 8-fold increase in activity over the cyclen based La(III) complex **La[25]**, which suggests that the incorporation of glycine methyl ester co-factors had a significant effect upon hydrolytic activity. This is one of the fastest accelerations of **HPNP** hydrolysis reported in the literature to date, and to the best of our knowledge, the fastest for a trivalent ion system.

It can also be seen that all of the complexes of this ligand show surprisingly fast cleavage, with the rate of cleavage decreasing with the size of the incorporated lanthanide ion. It can be seen that even the Lu(III) complex surpassing the activity shown by **La[25]**, with a rate of 0.072 h^{-1}

and $t_{1/2} = 9.62$ h. These results are surprising, not only because they show such an increase in activity over that demonstrated by similar complexes,⁶⁸ but because they show that hydrolysis can be achieved using complexes that bear only one metal-bound water molecule. Previous cyclen based complexes, discussed in Section 1.10, were generally only found to exhibit hydrolytic activity when two metal-bound water molecules were available.^{68,70,71} The crystal structure of **Eu[70]** showed only one metal-bound water, and it can therefore be assumed that all smaller lanthanides in this series (Gd(III), Tb(III), Yb(III), Lu(III)) have a minimum of one metal-bound water, however all of these complexes hydrolysed **HPNP**.

Given the substantial increase in activity of these complexes over the type, **25**, reported by Morrow *et al.*,^{68,70,71} it was decided to investigate the effect of the uncomplexed ligand upon **HPNP**. However, hydrolysis of **HPNP** by **70** was found to be negligible, demonstrating the necessity of the lanthanide ion for promotion of phosphodiester hydrolysis. A Cu(II) complex **Cu[70]** was also synthesised and tested, and no **HPNP** cleavage was observed over 24 hours at pH 7.4 and 37 °C when this complex was present. This Cu(II) system still provides a positive charge, and therefore has the potential to stabilize the phosphodiester cleavage reaction, but it was found to be ineffective. One reason for this is that Cu(II) is coordinatively saturated in this ligand, and should therefore possess no metal-bound water molecules. This suggests that the metal-bound water molecules found in the corresponding lanthanide systems play a significant role in the activity of those compounds.

Table 4.1. **HPNP** hydrolysis for Ln[70] at pH 7.40

Ln[70]	k (h ⁻¹)	$t_{1/2}$ (h)	k_{rel}
La[70]	0.410(±0.026)	1.70	3417
Ce[70]	0.371(±0.031)	1.87	3083
Pr[70]	0.299(±0.025)	2.11	2500
Nd[70]	0.201(±0.021)	3.35	1667
Eu[70]	0.153(±0.013)	4.53	1250
Gd[70]	0.118(±0.008)	5.87	1000
Tb[70]	0.093(±0.006)	7.45	779
Yb[70]	0.076(±0.007)	9.12	633
Lu[70]	0.072(±0.007)	9.62	600

4.3.2 Dependence of the rate of HPNP hydrolysis by Ln[70] on pH

Having examined the Ln[70] series and found that the La(III) complex was by far the fastest at cleaving HPNP, further studies were carried out on this complex to investigate the effect of pH upon rate. The rate was found to be strongly dependant upon the pH at which the hydrolysis reaction was carried out, with the results of these measurements presented in **Table 4.2**. It can be seen that below pH 7.0, the rate was found to be negligible. Between pH 7.0 and 8.5, the rate increases steadily, from $k = 0.147 \text{ h}^{-1}$ ($T_{1/2} = 4.27 \text{ h}$) to $k = 0.80 \text{ h}^{-1}$ ($T_{1/2} = 0.87 \text{ h}$). At pH 8.5 a 6725-fold rate enhancement over the uncatalysed reaction is found – almost twice the rate enhancement found at pH 7.4. Between pH 8.5 and pH 9.0, the rate was found to decrease, despite the fact that more alkaline conditions are favourable to hydrolysis of HPNP (as the hydroxy-group can be deprotonated, thus promoting self-hydrolysis.) The results can be plotted as a ‘pseudo bell-shaped’ curve, with a peak at pH 8.5, as shown in **Figure 4.3**.

These results give us an insight into the possible mechanism at work in these reaction, which will be presented in more detail in Section 4.11. Initially, as the pH increases, the metal-bound water molecule becomes deprotonated, increasing the rate of reaction as the concentration of the active metal-bound hydroxide is increased. However, above a certain pH, the water molecule is completely deprotonated and may bind irreversibly to either the substrate or the product. The maximum rate is achieved at the pH where a balance is struck between the ability of the lanthanide complex to cleave the substrate and its ability to bind to it. This idea is proposed by Reinhoudt *et al.*⁵⁷⁻⁶² amongst others and will be discussed further at the end of this chapter.

Table 4.2. Hydrolysis of HPNP by La[70] at different pHs.

pH	$k \text{ (h}^{-1}\text{)}$	$t_{1/2} \text{ (h)}$	k_{rel}
7.00 ± 0.01	$0.147(\pm 0.012)$	4.27	1225
7.40 ± 0.01	$0.410(\pm 0.026)$	1.7	3417
8.00 ± 0.01	$0.57(\pm 0.045)$	1.16	4750
8.25 ± 0.01	$0.65(\pm 0.058)$	0.97	5417
8.50 ± 0.01	$0.80(\pm 0.062)$	0.866	6667
8.75 ± 0.01	$0.511(\pm 0.032)$	1.23	4259
9.00 ± 0.01	$0.433(\pm 0.034)$	1.595	3608

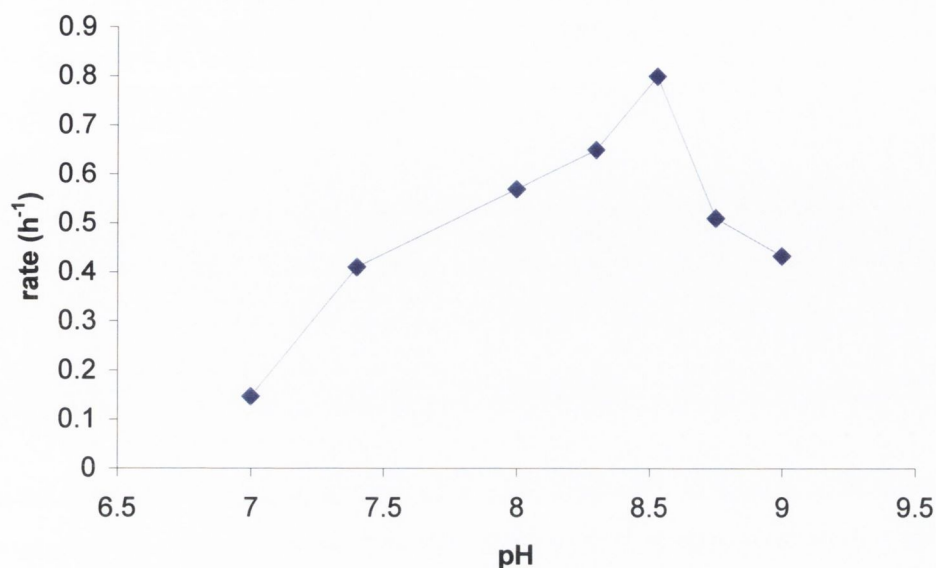


Figure 4.3. *pH-rate profile for La[70], showing a maximum rate at pH 8.5.*

Despite finding that the maximum rate of **HPNP** cleavage can occur at a higher pH, all complexes discussed in this chapter were primarily examined at the biological pH of 7.4, and all rates, unless otherwise stated, were determined at this pH. Potentiometric titrations calculated the pK_a of a single metal-bound water molecule to be 7.4.

The full pH profile of the corresponding Eu(III) complex, **Eu[70]**, was not tested, but preliminary measurements at pH 7.2 and pH 7.5 showed that negligible hydrolysis occurred over 24 hours. Thus, pH 7.4 appeared to be at least a local maximum. The differing pH-rate profiles of the La(III) and Eu(III) complexes can be attributed to the difference in the pK_a s of the metal-bound water molecules.

4.3.3 Effect of degassing the solution

As mentioned previously, an important feature of these lanthanide complexes is the number of metal-bound water molecules they possess. Such water molecules can aid the nucleophilic attack upon a phosphodiester, as illustrated in Section 1.5. Their importance in such a reaction was highlighted by the inactivity of **Cu[70]**, which was coordinatively saturated, and should therefore possess no metal-bound water molecules. However, Parker *et al.* have shown that cyclen-based lanthanide systems can bind to carbonate, with the carbonate replacing the two

metal-bound waters.¹⁵⁴ If this process occurred in the measurements described here, it could prevent or reduce binding to **HPNP** and nucleophilic activation of the hydrolysis reaction. In order to assess the possibility that this was occurring in these measurements, the effect of degassing the reactions was examined. Degassing was not found to effect the rate of cleavage by the La(III) complex; results were within 10 % of the values for the gassed reactions, as shown in **Table 4.3**

Table 4.3 Effect of degassing upon rate of HPNP hydrolysis by La[70]

La81	k (h^{-1})	$t_{1/2}$ (h)	k_{rel}
In air	0.410(\pm 0.026)	1.69	3417
Under argon	0.419(\pm 0.031)	1.65	3492

4.3.4 The effect of changing the buffer

The effect of buffer upon the hydrolysis of phosphodiesterases is a subject that has been widely discussed and debated.^{155,156} As mentioned previously, the choice of buffer for these reactions was examined primarily to establish a buffer system that allowed for the maintenance of a constant pH over the course of the hydrolysis reaction. Initially, 10mM HEPES was used but the pH drift over longer reactions was unacceptably large (> 0.2 unit) and 50 mM solution was found to be necessary. The rates of reaction for different buffer solutions are presented in **Table 4.5**.

Table 4.4. Dependence of HPNP hydrolysis by La[70] upon buffer.

Buffer	k (h^{-1})	$t_{1/2}$ (h)	k_{rel}
20mM TRIS	0.27(\pm 0.025)	2.5	2250
10mM HEPES	0.364(\pm 0.029)	1.9	3033
50mM HEPES	0.410(\pm 0.026)	1.7	3417

It can be seen that changing the HEPES buffer from 10 mM to 50 mM caused the rate to differ by less than 15 %. Changing the buffer to TRIS had a greater effect, altering the rate by 35 %. The effect of buffer on these reactions was not investigated in further detail, as 50 mM HEPES was shown to be sufficient to maintain a constant pH for the duration of the reactions, while

allowing some degree of comparison between the results obtained and the results reported for similar systems in the literature. However, it is clear that changes in the choice of buffer could have a significant effect on the rate of **HPNP** hydrolysis.

4.3.5 Investigation of Catalytic Turnover by La[70]

A point of interest in these studies was whether such systems would exhibit catalytic turnover. The kinetics of enzymes are discussed in Section 1.4.²¹ The first experiment carried out involved incremental addition of equivalents of **HPNP** to a solution of **La[81]**. From the absorbtion profile, shown in **Figure 4.4**, it can be seen that initially, a **HPNP** solution was incubated with one molar equivalent of catalyst until the reaction to slow down, at which point a second molar equivalent of **HPNP** was added to the reaction. As can be seen in **Figure 4.4**, the addition of a second and then a third aliquot of phosphate does increase the production of *p*-nitrophenolate after it had previously decreased, but ultimately, after 3 equivalents of **HPNP** have been added, less than one equivalent of *p*-nitrophenolate has been produced in total ($A = 1.31$, conc = 0.0655 mmol). This was a disappointing result, indicating that the complex was incapable of catalytic turnover.

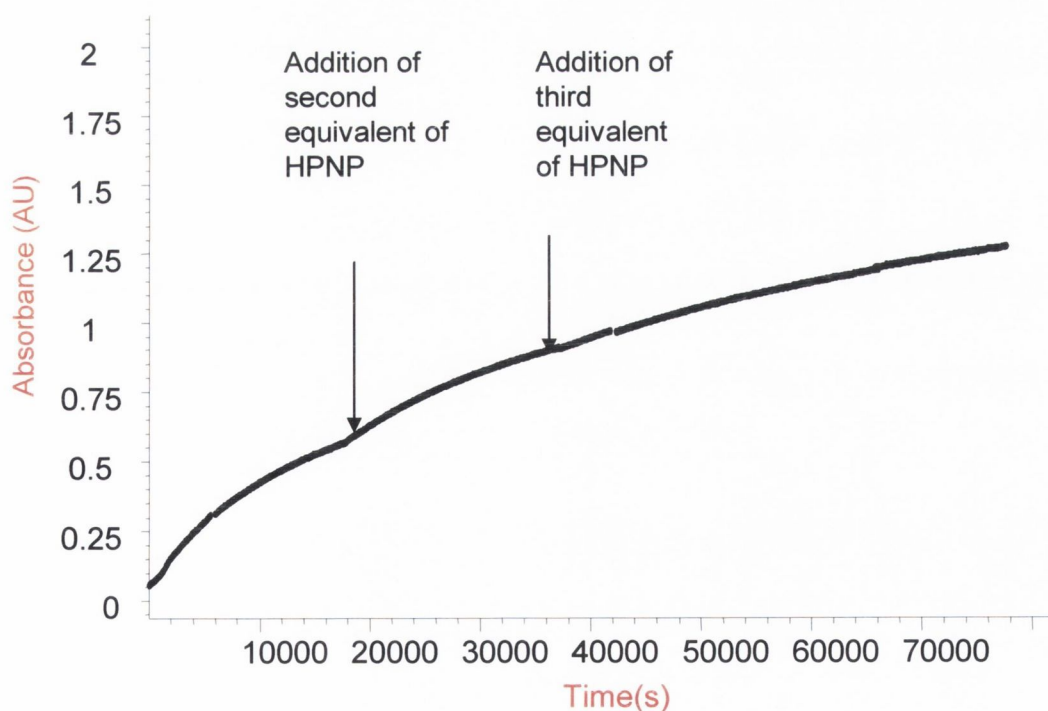


Figure 4.4 The addition of three subsequent equivalents of **HPNP** to **La[70]**

In the case of a catalytic reaction, the Michaelis-Menten kinetics should be examined. If the reaction was indeed catalytic, the rate of reaction would remain constant as additional equivalents of substrate were added, *ie*, the rate of reaction when two equivalents of **HPNP** were present would be equal to or greater than the rate when one molar equivalent of **HPNP** was present. **Table 4.6** documents the rates and half-lives obtained when **La[70]** was reacted with different concentrations of **HPNP**. It can be seen that even a relatively small increase in the concentration of **HPNP** over the concentration of **La[70]** (1.25 equivalents of **HPNP**) caused the rate to fall from 0.410 h^{-1} to 0.308 h^{-1} . When ten equivalents of **HPNP** were present, the rate decreased by a factor of five and when 100 equivalents were added, the rate decreased by a factor of 80.

Table 4.5. Dependence of Rate of cleavage of HPNP upon concentration of HPNP

Equivalents of HPNP	$k \text{ (h}^{-1}\text{) (av)}$	$t_{1/2}\text{(h) (av)}$	k_{rel}
100	$0.0052(\pm 3 \times 10^{-4})$	133	43
10	$0.084(\pm 0.005)$	8.25	700
3.33	$0.1095(\pm 0.006)$	6.4	912
1.25	$0.308(\pm 0.026)$	2.3	2567
1.0	$0.41(\pm 0.019)$	1.7	3417
0.5	$0.4533(\pm 0.031)$	1.53	3777
0.2	$0.545(\pm 0.048)$	1.27	4541

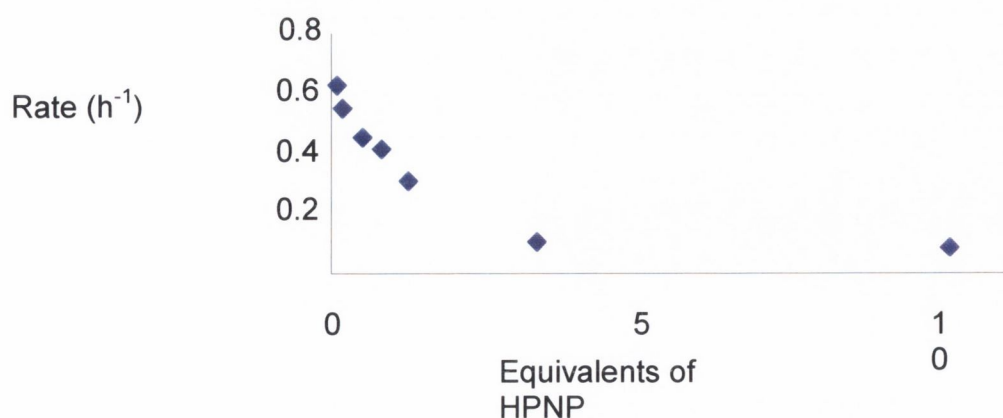


Figure 4.5. Dependence of rate of HPNP hydrolysis upon molar equivalents of La[70]

It was quickly seen that the rate decreased when there was more phosphate than complex (more substrate than ‘catalyst’.) This confirmed that this compound does not exhibit turnover.

4.4 Changing the Co-factor: Increasing the Size of the Ester

Section 4.3 has shown how the introduction of a simple co-factor into the cyclen framework can drastically alter the effect of the resulting lanthanide complexes upon **HPNP**. In light of the activity of the **Ln[70]** series, analogous glycine-based systems were prepared which used ethyl and benzyl ester in place of methyl ester. Recalling **Figure 2.1**, the principal features of these systems are the encapsulated metal ion, the metal-bound water molecules and the hydrophobic cavity that the complexes form. It was hoped that by changing the nature of the esters to more bulky groups, this would affect the micro-environment of the cavity. The two crystal structures discussed in Chapter 2 illustrate that changing the nature of the ester may have a significant effect on the size and depth of the cavity, which in turn may affect the metal-bound water molecules, or the position of the different sized lanthanides within the ligand. Thus, by altering the co-factors and measuring testing the rates of hydrolysis of **HPNP** in the presence of each complex, the effect of different co-factors on hydrolytic activity could be assessed.

4.4.1 Hydrolysis of HPNP by Ln[71]

The ethyl ester derivative **71** and **La[71]**, **Eu[71]** and **Yb[71]** complexes were prepared as described in Chapter 2. **La[71]** was tested with **HPNP** under the same conditions described previously (37.0 °C, pH 7.40 and using 50 mM HEPES buffer) and the half-life for the hydrolysis of **HPNP** was 3.11 hours; considerably longer than the corresponding **La[70]** complex, which cleaved **HPNP** with a half-life of 1.69 h. Therefore, it can be immediately seen that that changing the ester from a methyl to an ethyl group can affect the rate of hydrolysis. **Eu[71]** showed considerably slower kinetics, cleaving **HPNP** with a half-life of 7.14 h, while a half-life of 19.8 h was found in the case of **Yb[71]**. It can be seen from these results that the hydrolysis of **HPNP** was slower in each case compared to that by the corresponding **Ln[70]** complexes. However, within the system, a similar trend of activity emerged, with activity decreasing with the size of the lanthanide ion used - (La(III)> Eu(III)>Yb(III)).

Table 4.6. HPNP hydrolysis by Ln[71]

Ln(III)	k (h^{-1})	$t_{1/2}$ (h)	k_{rel}
La[71]	0.23(\pm 0.012)	3.11	1917
Eu[71]	0.097(\pm 0.008)	7.14	808
Yb[71]	0.035(\pm 0.002)	19.8	311

4.4.2 Hydrolysis of HPNP by Ln[72]

Incorporating a glycine benzyl ester co-factor into the cyclen system was expected to greatly increase both the steric bulk of the complexes, and the size and depth of the potential cavity. The X-ray crystal structure of **72**, an analogous that incorporated alanine benzyl ester co-factors, revealed that such a compound could possess a deep, bowl-like structure.

The results of HPNP hydrolysis for the Ln[72] series are presented in Table 4.7, with the measurements carried out under the conditions previously described. **La[72]** showed considerably greater activity than any of the previous compounds, with a rate of 0.473 h^{-1} and a half-life of 1.47 h for the reaction. This is significantly faster than the hydrolysis by either **La[70]** or **La[71]**, indicating that activity is strongly influenced by the choice of co-factor. However, it could not be said that any particular trend was emerging at this point; while changing from the methyl ester to the bulkier, more hydrophobic benzyl ester gave the greatest increase in rate, the rate *decreased* upon changing from the methyl ester to the bulkier ethyl ester.

Table 4.7. HPNP hydrolysis by Ln[72]

Ln(III)	k (h^{-1})	$t_{1/2}$ (h)	k_{rel}
La[72]	0.473(\pm 0.023)	1.467	3937
Ce[72]	0.0843(\pm 0.005)	8.2	702
Nd[72]	0.0372(\pm 0.003)	18.6	310
Eu[72]	0.0216(\pm 0.001)	32.1	180

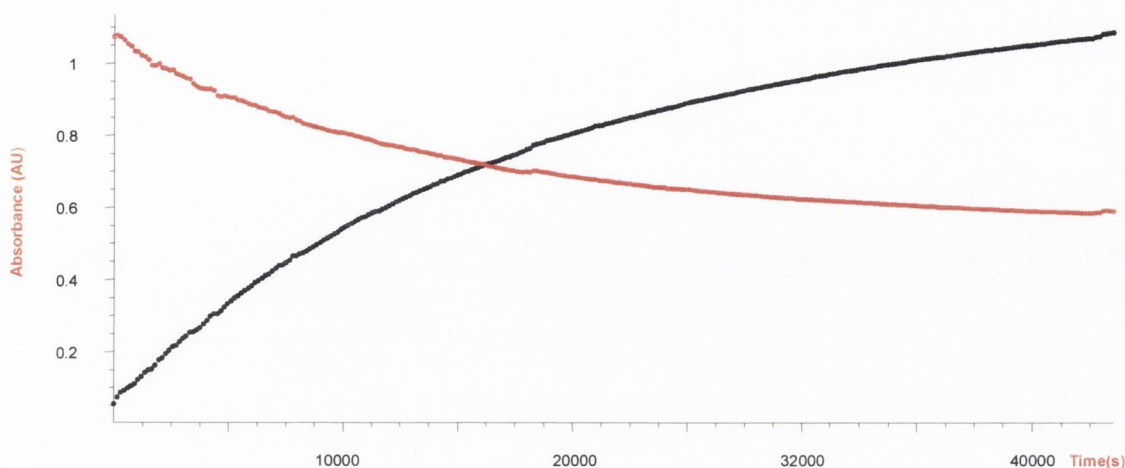


Figure 4.5 Increase of *p*-nitrophenolate (black line) and decrease of **HPNP** (red line) in the presence of **La[72]**

The impressive activity of **La[72]** was not mirrored in the activities of the rest of the family. When the encapsulated lanthanide was Ce(III), k decreased from 0.473 to 0.084 h⁻¹, a 5.6-fold decrease in the acceleration of the hydrolysis. This was unexpected as the ionic radius of Ce(III) is of similar size to that of La(III) and the Ce(III) complex would be expected to similarly possess two metal-bound water molecules. The difference in activity cannot be explained at this point, but might be due to the pK_a of the water molecules. Similarly, **Nd[72]** was found to be slower still, with $k = 0.0372$ h⁻¹, while **Eu[72]** proved to be essentially inactive. Thus the behaviour of this family of compounds differs dramatically from that of the glycine methyl ester. The activity of **La[72]** can be seen as indication that a hydrophobic cavity plays an important role in the activity of these compounds. However, there are other factors to consider, such as the pK_a of the lanthanide bound water molecule and the binding between **HPNP** and the hydrophobic cavity, in order to understand why the same ligand can change in activity so dramatically depending on the ion.

4.4.2.1 Dependence of the rate of **HPNP** hydrolysis by **Ln[72]** on pH

The hydrolysis of **HPNP** by **La[72]** was evaluated as a function of pH, the results of which are presented in **Table 4.8**. When k was plotted as a function of pH, the result was again a bell-shaped profile, with a maximum rate at pH 7.5. Minimal hydrolysis was observed below pH 7.2, with the rate beginning to increase at pH 7.3 before increasing sharply at pH 7.4. The maximum

rate was found at pH 7.5, with a gradual decrease at 7.6, before the rate decreased sharply at pH 7.7.

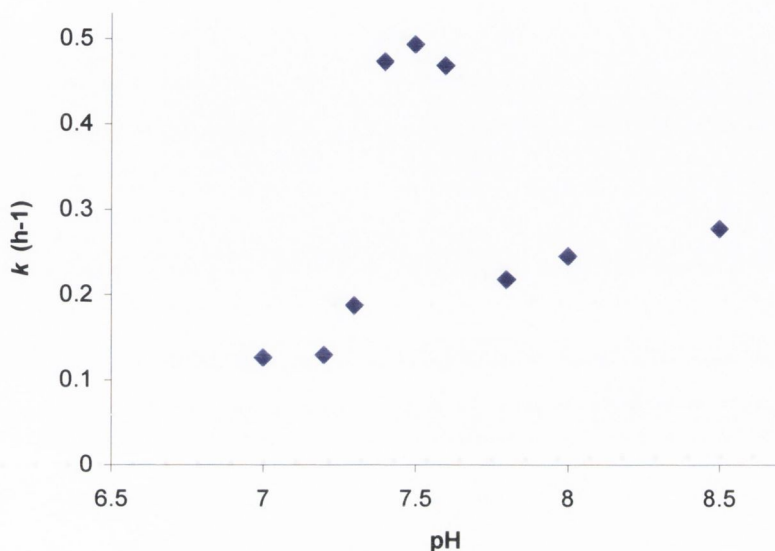


Figure 4.7 pH – rate curve for **La[72]**, showing a maximum at pH 7.5

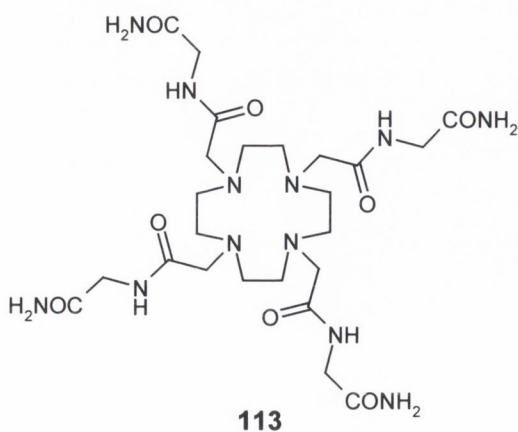
The pH-rate dependence is very different to that of **La[70]**, with glycine methyl ester as co-factor, where the maximum activity was found at pH 8.5. In the case of **La[70]** the pH-rate curve had a sharp peak at pH 8.5, with the rate decreasing significantly on either side of that pH. In the case of **La[142]**, the activity is low below pH 7.3, climbing sharply at pH 7.4, where the $k = 0.473 \text{ h}^{-1}$. The activity reaches a peak between pH 7.4 and 7.6, with $k = 0.493 \text{ h}^{-1}$ at pH 7.5. Above pH 7.6, the activity was observed to drop again, although at higher pHs there was a slight increase in the rate of hydrolysis, presumably due to background hydrolysis of the **HPNP**. When the pH rate profiles of the **La[70]** and **La[72]** are compared, it can be seen that the properties of these compounds can be drastically altered by tuning the nature of the ester moiety. By changing the co-factor from glycine methyl ester to glycine benzyl ester, the shape of the profile was changed significantly, with the two compounds showing very different behaviour. The most obvious change was the pH at which maximum activity was found to occur, which changed from pH 8.5 in the case of **La[70]** to pH 7.5 in the case of **La[72]**.

Table 4.8 Dependence of the rate of hydrolysis by La[72] on pH

pH	k (h^{-1})	$t_{1/2}$ (h)	k_{rel}
7.0	0.126(\pm 0.009)	5.49	1053
7.2	0.129(\pm 0.011)	5.355	1079
7.3	0.187(\pm 0.009)	3.71	1661
7.4	0.473(\pm 0.023)	1.47	3938
7.5	0.493(\pm 0.032)	1.41	4379
7.6	0.468(\pm 0.021)	1.48	3899
7.8	0.218(\pm 0.015)	3.18	1814
8.0	0.345(\pm 0.021)	2.01	2877
8.5	0.277(\pm 0.026)	2.5	2311
9.0	0.310(\pm 0.027)	2.24	2581

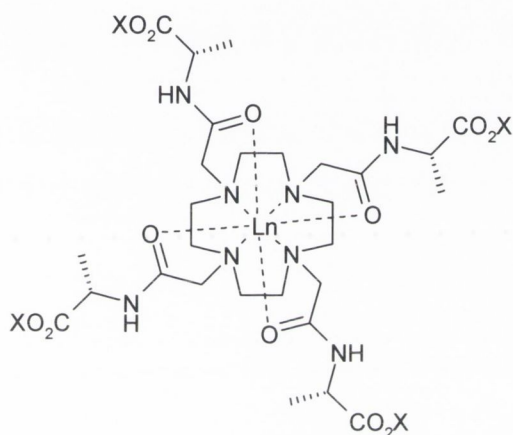
4.4.3 Removing the ester completely

Compound **113**, was also prepared within the Gunnlaugsson group, and was also tested with **HPNP**. The cofactors in this case comprise the GlyGly dipeptide that had proved so effective, but the ester was replaced with an amide. This was prepared by bubbling ammonia through a methanolic solution of **70**. Initially, it had been hoped that this structure might promote phosphodiester hydrolysis due to the presence of the amide. Only **Eu[113]** was prepared, and it was tested with **HPNP** under the usual condition. The activity was found to have decreased, relative to that of **Eu[70]**. This work is currently being continued by.

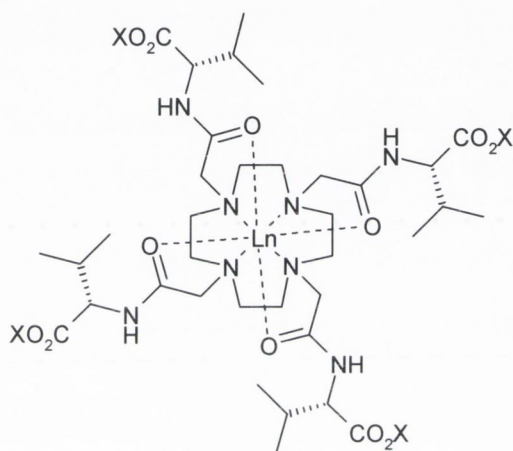


4.5 Increasing the size of the amino acid

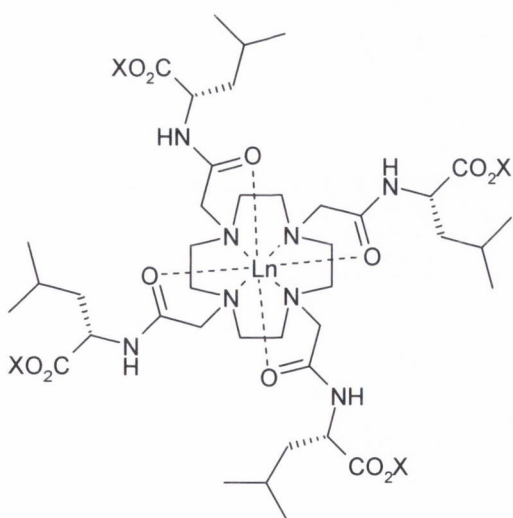
Taking **70** as a model compound, albeit a very active one, the effect of modifying the basic system by changing the cofactor was examined. There are two ways in which this can be studied; firstly, by altering the nature of the amino acid and secondly by changing the size of the ester groups. It was of interest here to see if the dimensions and properties of the hydrophobic cavity formed by these complexes could be fine-tuned by altering the size and length of these co-factors.



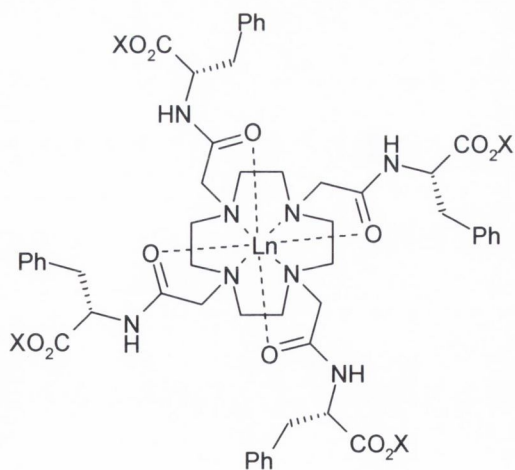
85: X = Me
85: X = CH₂Ph



87: X = Me



88: X = Me



89: X = Me
90: X = CH₂Ph

Initially, the choice of amino acid was changed, working with the methyl ester in each case. The co-factors were all simple amino acids, with no nucleophilic or basic moieties, *eg.* alanine, valine, leucine and phenylalanine were used. This gradually increases the size of this ligand, creating greater steric bulk. The effect of this change of co-factor upon the hydrolysis of **HPNP** will be discussed in this section.

4.5.1 Hydrolysis of HPNP by Ln[85]

After glycine, the simplest amino acid is alanine, possessing only an extra methyl group. However, this introduces a chiral centre, and it was of interest to see whether this affected the hydrolysis of **HPNP** (which is a chiral molecule). **La[85]**, **Eu[85]** and **Tb[85]** were prepared and tested, the results of which are presented in **Table 4.9**.

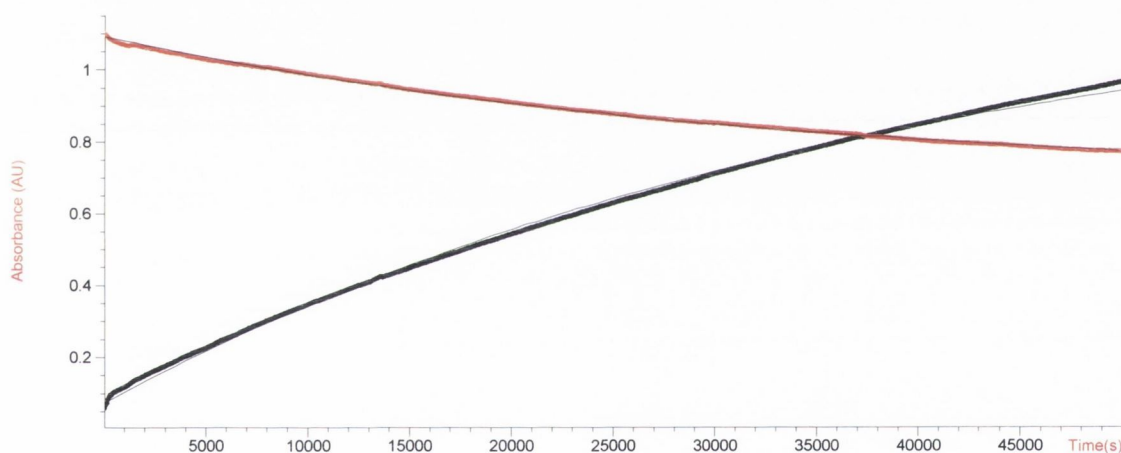


Figure 4.6. Change in Abs at 400nm with time when **HPNP** is treated with **Eu[85]**.

Table 4.9. HPNP hydrolysis by Ln[85]

Complex	k (h^{-1})	$t_{1/2}$ (h)	k_{rel}
La [85]	0.039(\pm 0.002)	17.6	325
Eu [85]	0.09026(\pm 0.004)	7.7	752
Tb [85]	0.142(\pm 0.009)	4.88	1183

In the case of the compounds discussed previously, the activity was found to increase with the size of the lanthanide ion, with the La(III) complexes found to exhibit the greatest activity. It can be seen in **Table 4.9** that this is not the case in this family of compounds. When L-alanine

methyl ester was incorporated as a co-factor, the activity of the Tb(III) complex was found to be greater than that of the Eu(III) complex. More dramatically, the rate of **HPNP** hydrolysis by **La[85]**, ($k = 0.039 \text{ h}^{-1}$) was significantly less than for **Eu[85]**, ($k = 0.09026 \text{ h}^{-1}$) and much slower than that for the corresponding **La[70]** reaction. This would seem to contradict the idea that the larger lanthanides are most active, and that in this type of ligand, hydrolytic activity decreases with ionic radius, and is surprising as the La(III) complex should possess a second metal-bound water molecule which should promote hydrolysis of **HPNP**. Therefore these results were quite surprising.

In order to further investigate these results, the rate of **HPNP** cleavage was measured as a function of pH, the results of which are presented in **Table 4.10**. The activity was found to be low below pH 6.8, rising to a peak at pH 7.0 before dropping off between pH 7.0 and 7.4. The rate shows a sharp, pseudo bell-shaped pH dependence between pH 6.8 and 7.4, with highest activity at pH 7.0, as shown in **Figure 4.7**.

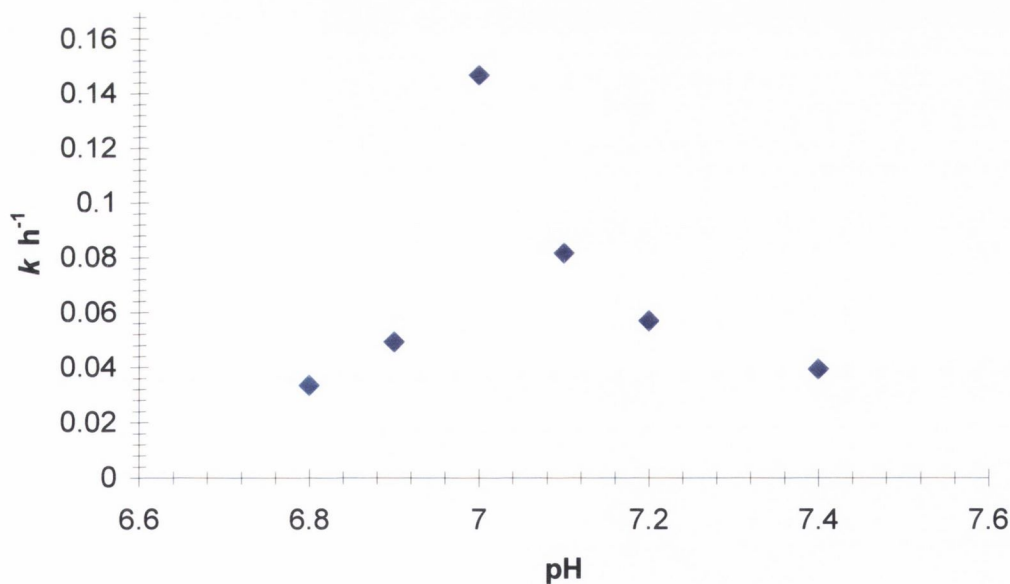


Figure 4.7 Dependence of Rate of **HPNP** by **La[85]** cleavage upon pH.

The activity then drops significantly so that what had been observed at pH 7.4, the physiological pH, was the ‘well’ of the curve. In contrast, when **Eu[85]** was examined, the relatively high activity at pH 7.4 was found to be the peak of its pH-rate dependence profile; however as the

rate becomes zero order outside of the biological pH region, a pH rate curve could not be obtained.

The benzyl ester of alanine was also incorporated into cyclen, to examine the effect of changing the ester group from the methyl to the benzyl ester La(III), Nd(III), Eu(III) and Tb(III) complexes of **86** were prepared, and tested with **HPNP** under the usual conditions. The results are presented in **Table 4.10**.

Table 4.10. HPNP hydrolysis by Ln[86]

Ln(III)	k (h ⁻¹)	$t_{1/2}$ (h)	k_{rel}
La[86]	0.1855(±0.013)	3.74	1546
Nd[86]	0.0545(±0.004)	12.71	455
Eu[86]	0.0567(±0.002)	12.22	472
Tb[86]	0.0628(±0.004)	11.04	523

This time, the La(III) complex was found to be extremely active at pH 7.40, with a half-life of 3.74 h, corresponding to a rate enhancement of 1546-fold. This is in contrast to the inactivity of **La[85]** at pH 7.40. Again, this shows how a slight alteration of the co-factor can have a dramatic affect upon the hydrolytic activity. When **Eu[86]** and **Tb[86]** were tested, they were found to be considerably less active, with $k = 0.0567$ h⁻¹ and 0.0628 h⁻¹ respectively. To check for any correlation between lanthanide ion size and activity, **Nd[86]** was prepared as the Nd(III) ion has a radius mid-way between that of La(III) and that of Eu(III). The activity of **Nd[86]** was almost identical to that of **Eu[86]**, suggesting that apart from the high activity of **La[86]**, there was little dependence upon lanthanide size in the activity of this series.

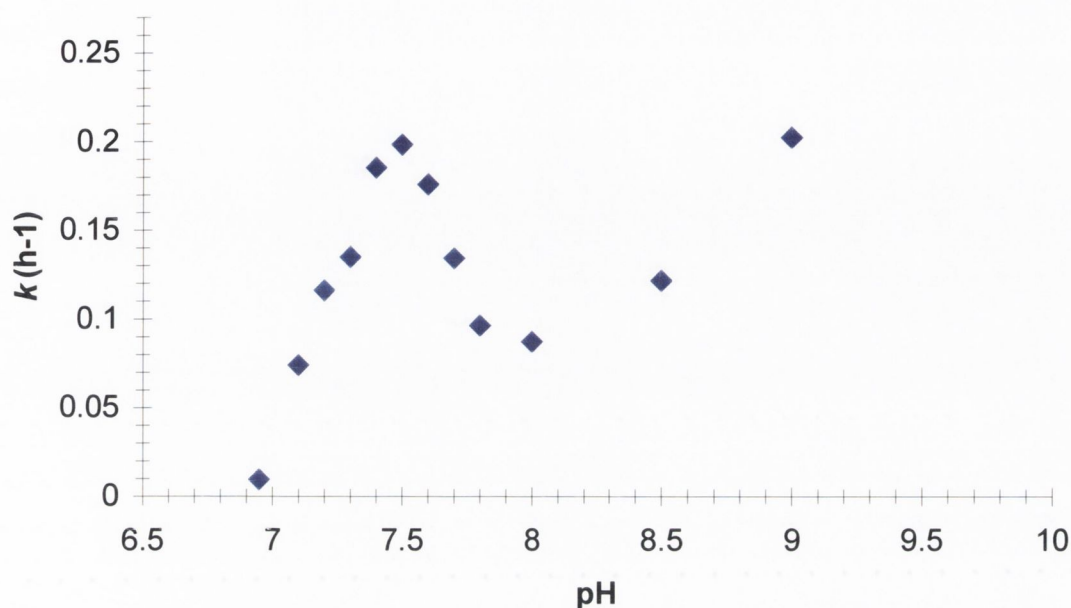


Figure 4.8 pH rate curve for La[86], showing a maximum rate at pH 7.5

4.5.1.1 Dependence of the rate of HPNP hydrolysis by La[86] on pH

The pH dependency of the La[86]-promoted hydrolysis was examined in the same way as described previously. The hydrolysis was found to be slow below pH 7.0, rising steadily between pH 7.0 and pH 7.5, and peaking at pH 7.5 with a rate of 0.1986 h^{-1} or a 1655-fold rate enhancement. Above pH 7.5, the rate dropped once more. These results are plotted in **Figure 4.8**, and give a bell-shaped curve.

Comparing the pH dependencies of La[85] and La[86] shows the effect that changing a co-factor can bring about. La[85] shows a maximum rate at pH 7.2, while La[86] has a maximum rate at pH 7.5. This suggests that it may indeed be possible to ‘fine-tune’ complexes such as these, to produce maximum activity at the desired pH. The shape of the pH-rate profiles of the two compounds is also very different, with La[85] having a very sharp maximum rate at pH 7.2, which drops dramatically on either side of that pH, while the high rates for La[86] are found between pH 7.4 and 7.6. Although the mechanisms of the two compounds are not known, it is possible that this behaviour can be explained by the presence of the two different co-factors, and their influence on the micro-environment of the cavities.

4.5.2 Hydrolysis of HPNP by Ln[87]

The next family of compounds to be tested incorporated L-valine methyl ester as a co-factor. This increased the steric bulk of the complexes, compared to those that used glycine or alanine, possibly deepening the hydrophobic cavity. **La[87]**, **Eu[87]** and **Yb[87]** were prepared and tested. The measurements with **HPNP** were carried out under the same conditions as previously described (37 °C, pH 7.40), and the results are presented in **Table 4.11**.

Table 4.11. HPNP hydrolysis by Ln[87]

Complex	k (h^{-1})	$t_{1/2}$ (h)	k_{rel}
La[87]	0.16335(\pm 0.008)	4.24	1360
Eu[87]	0.0987(\pm 0.008)	7.02	822
Yb[87]	0.07996(\pm 0.005)	8.67	666

La[87] cleaved **HPNP** with a half-life of 4.24 h, which represented a 1360-fold rate enhancement. Within this family of compounds, the activity can be seen to decrease with the size of the lanthanides, with La(III) > Eu(III) > Yb(III). The activity of the complexes was generally less than that seen for the corresponding **Ln[70]** series, suggesting that the replacement of glycine with valine decreased the hydrolytic activity of the complexes. However, it is difficult to explain why this would be the case. A number of factors must be taken into account; the pK_a of the metal bound water molecule(s) and the shape and size of the hydrophobic cavity, amongst others.

4.5.3 Hydrolysis of HPNP by Ln[88]

La[88], **Eu[88]** and **Yb[88]** complexes were prepared. This family of compounds incorporated L-leucine methyl ester as a cofactor. The complexes were tested with **HPNP**, under the usual conditions and the results are presented in **Table 4.12**.

Table 4.12. HPNP hydrolysis by Ln[Leu]

Complex	k (h^{-1})	T1/2 (h)	k_{rel}
La[88]	0.1143(\pm 0.008)	6.05	952
Eu[88]	0.07485(\pm 0.007)	9.2	624
Yb[88]	0.0483(\pm 0.003)	14.35	402

The **Ln[88]** series shows the relationship between activity and lanthanide ion size, with **La[88]** > **Eu[88]** > **Yb[88]**. It can also be seen that for each complex, the activity is slightly lower than the corresponding **Ln[87]** complex. Thus, there seems to be a rough correlation of activity with the size of the amino acid used with the rate decreasing as we go from glycine to valine to leucine. It should be noted that the promotion of **HPNP** hydrolysis by all of these compounds is still an improvement over that by **La[25]**, showing that the introduction of amino ester co-factors has a significant effect upon activity.

4.5.4 Hydrolysis of HPNP by Ln[89]

The complexes that have been described so far have incorporated increasingly larger amino acids; glycine, alanine, valine and leucine. It has been seen that the rate of hydrolysis seems to increase as larger amino acids are used, with **Ln[70]** proving faster than **Ln[87]**, which in turn was faster than **Ln[88]**. It has also been seen that when the methyl and benzyl ester of a given amino acid were used (as in the case of glycine and alanine), that the bulkier, more hydrophobic benzyl esters containing compounds proved more active.

Therefore, the last amino acid that will be discussed is phenylalanine. A cyclen system was prepared that incorporated phenylalanine methyl ester co-factors, **89**. **La[89]** and **Eu[89]** were prepared and tested with **HPNP**, the results of which are presented in **Table 4.13**

Table 4.13. HPNP hydrolysis by Ln[89]

Complex	k (h^{-1})	$t_{1/2}$ (h)	k_{rel}
La[89]	0.1239(\pm 0.010)	5.59	1032
Eu[89]	0.0659(\pm 0.005)	10.52	549

La[89] was found to produce a 1032-fold rate enhancement of the **HPNP** hydrolysis reaction, with a rate of 0.1239 h^{-1} , while **Eu[89]** cleaved **HPNP** with the considerably slower rate of 0.0659 h^{-1} . These rates are faster than those obtained by the **Ln[88]** family, indicating that the activity does not directly depend upon the size of the amino acid.

4.5.5 Increasing the hydrophobic cavity

An examination into the importance of the hydrophobic cavity on **HPNP** hydrolysis was carried out, using phenylalanine benzyl ester as a co-factor to the cyclen framework **90**. This maximises the hydrophobic potential, with a total of eight benzyl groups on each molecule. The effect was considerable; by incorporating the phenylalanine benzyl ester groups into the structure, **La[90]** The half-life of the hydrolysis reaction was decreased to less than an hour. Looking at the absorbance vs time, it was seen that one equivalent of *p*-nitrophenolate ($A = 1.8$) was produced in about four hours. This was considerably faster than any of the other compounds discussed in this chapter, giving $k = 0.8225 \text{ h}^{-1}$, and a half-life of 0.84 h. From first appearances, this compound seemed to be the most active to date.

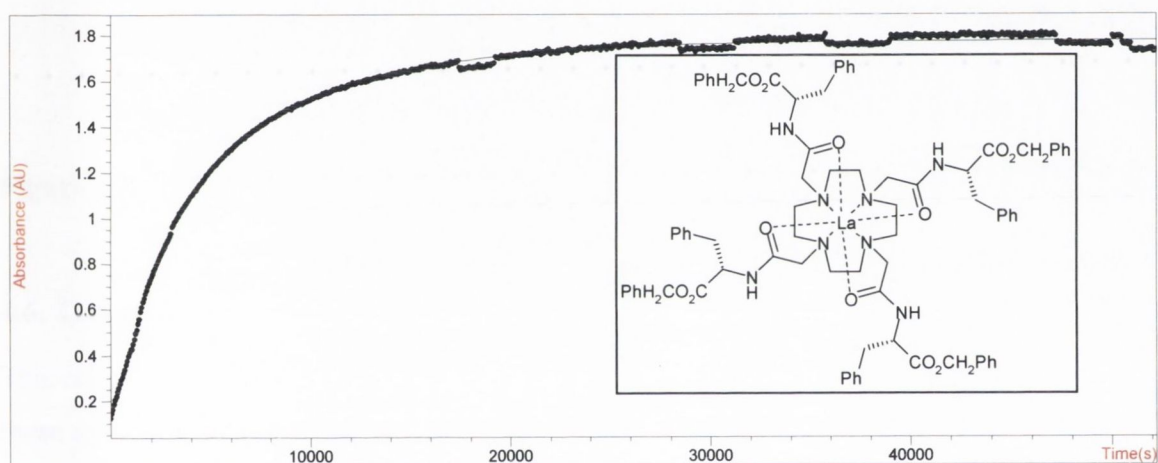


Figure 4.8 Rate of *p*-nitrophenolate production by **La[90]**.

Given the extraordinary activity of this complex relative to the others discussed in this chapter, it was a prime candidate for catalysis studies and preliminary results, **Figure 4.9**, showed that the complex could indeed cleave more than one equivalent of **HPNP**.

However, the reactivity of this compound has been called into question as it was found that a precipitate was formed during the hydrolysis reaction. This precipitate seemed to affect the UV/*vis* spectrum and was possibly the reason for the seemingly fast rate of reaction. When a sample of **La[90]** was stirred in pH 7.40 50 mM HEPES solution at 37 °C, a change in the UV/*vis* spectrum was observed over the period of an hour. This change consisted of a rise in absorbance at 330 nm, which in turn increased the net absorbance at 400 nm. The same effect was observed when the complex was stirred in water. Such decomposition was not observed with

any other complex reported in this thesis. The cause of the decomposition has not been determined and is the subject of ongoing studies. However, the activity of this compound cannot be assessed with any degree of certainty at the time being.

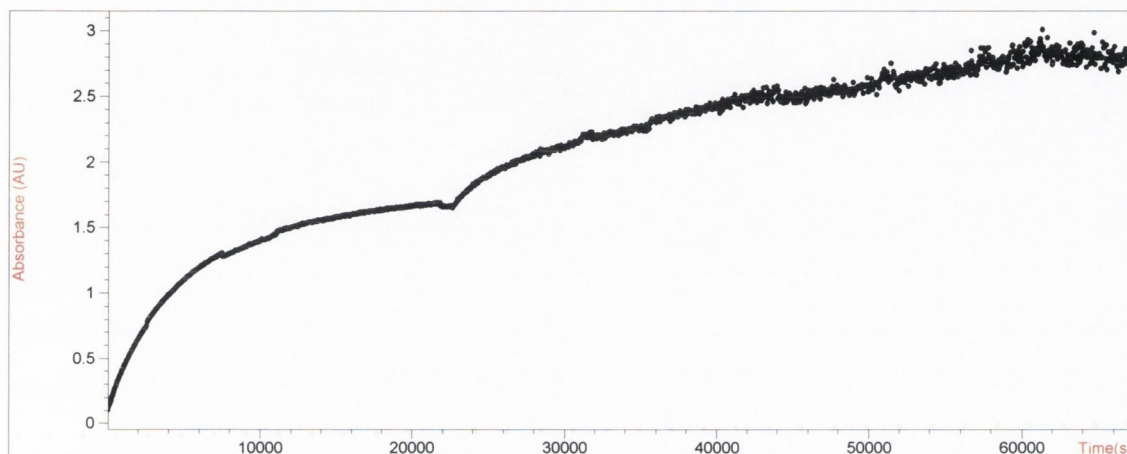


Figure 4.9 Reaction of **La[90]** with two subsequent additions of **HPNP**

4.6. Trends of Reactivity

The crystal structures discussed in Chapter 2 (**Figure 2.10** and **Figure 2.13**) confirmed that these cyclen-based complexes formed bowl-shaped cavities. The size, shape and depth of such cavities could be influenced by the choice of pendant arm (*ie*, the ‘bulkiness’ of the co-factor), the choice of lanthanide (smaller ions may sit more deeply inside the cavity),¹⁹⁶ or other, external factors, such as the presence of a K^+ ion in the crystal structure of **Eu[70]**. While the occurrence of the hydrophobic cavity may in turn influence such features as the pK_a of the metal-bound water molecules, it is also possible that the cavity may act as a basket in which the hydrolysis of **HPNP** can occur. This theory was put forward by Oh *et al.*⁶⁹ in relation to lanthanide cryptate complexes, and discussed in Section 1.7. As yet, there is no crystallographic data available in relation to the interaction between **HPNP** and cyclen-based complexes, however Parker *et al.* have recently obtained a crystal structure of the binding between a tri-substituted cyclen system and methionine. This structure is reproduced in **Figure 4.10**, with permission from Parker *et al.*¹⁹⁷

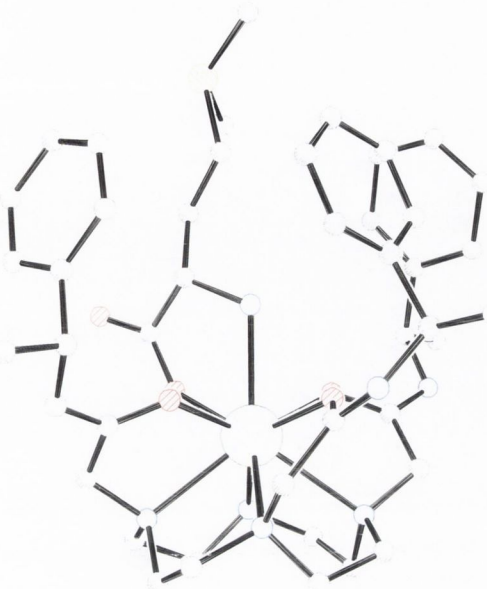


Figure 4.10 X-ray crystal structure of a tri-substituted cyclen complex binding to a methionine moiety. Upon binding, a deep, bowl-like cavity is formed around the guest.

This crystal structure illustrates what we assume may happen with the complexes discussed in this chapter and **HPNP**. It is thought that the phosphate would bind to the metal centre, probably through the displacement of a metal-bound water molecule. This binding would be promoted by the formation of a hydrophobic cavity.

It had been hoped that by evaluating the rate of **HPNP** hydrolysis by different lanthanides and different ligands, some insight into the structure/activity relationship would emerge. Initially, some trends seem to appear:

- The larger lanthanides generally show faster than the smaller ions, presumably due to their larger coordination spheres.
- For most systems, illustrated by the **Ln[70]** series, the activity is directly related to ion size, decreasing for the smaller lanthanides, *ie*, La(III) > Eu(III) > Yb(III).
- Bulkier ligands seem to promote faster hydrolysis (*ie*, benzyl esters rather than methyl esters.)

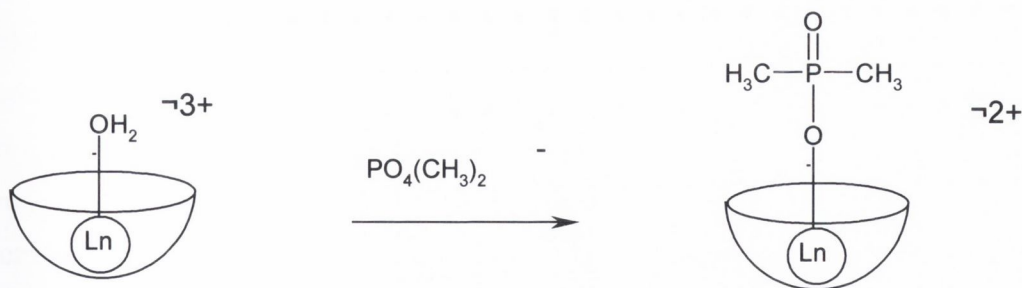
However these rules do not apply in all cases. For the alanine methyl ester series, the Eu(III) complex proved faster than the La(III) complex, due to the different pK_a s of the metal-bound water molecules. Within the alanine benzyl ester series, the La(III) complex shows the fastest kinetics of the series, but rate was not found to directly vary with the size of the lanthanide for the rest of the series.

As well as this disparity regarding the dependence of rate on lanthanide size, no clear relationship between changing the ligand and changing the hydrolytic activity emerged. Generally, it could be summarised that those ligands containing benzyl esters are more active than those with methyl esters. This reinforces the theory that an important feature of all of these systems is the presence of a hydrophobic cavity.

4.7 Binding of lanthanide complexes to phosphates

4.7.1. Evaluating binding to diethyl phosphate by ^{31}P NMR

Of great interest to us was the binding potential of the lanthanide compounds described in this chapter, in particular, their ability to bind to phosphates by replacement of the metal bound water molecule, as shown in scheme 4.1. It has been indicated by Morrow *et al.*⁹⁶ that the ability of a lanthanide complex to bind to diethyl ether was a useful measure of its ability to cleave **HPNP**. The results of Morrow *et al.* showed that **Eu[25]**, which was inactive when incubated with **HPNP**, did not bind to diethyl ether, while **La[25]**, which cleaved **HPNP** with a half-life of 12 h, did bind to diethyl ether, with a binding constant of $5 \pm 0.5 \text{ M}^{-1}$.⁹⁶



Scheme 4.1. Binding of lanthanide complex to dimethyl phosphate by replacement of the metal bound water molecule

Dimethyl phosphate was used these tests because it can bind in the same way as other phosphodiester (such as **HPNP**) but it will not be cleaved by the type of complex examined

here because it lacks the hydroxyl group of **HPNP** that can act as an internal nucleophile.⁸⁰ The binding can be followed easily as it can be measured as a function of the change in the ^{31}P NMR signal.

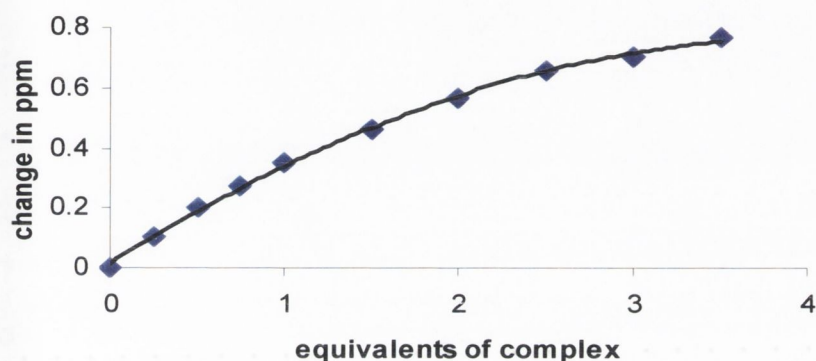


Figure 4.11 Change in ^{31}P NMR as a function of molar equivalents of **La[25]** added.

Once again, we began by testing Morrow's **La[25]** complex for the purposes of comparison. In this case, a sample of diethyl phosphate was prepared and the change in ^{31}P signal observed as **La[25]** was added. Plotting the change in the ^{31}P NMR (in ppm) against the molar equivalents of complex added to the diethyl phosphate, it can be seen from **Figure 4.11** that the plot began to plateau after three equivalents of complex, indicating that binding was complete.

When the same experiment was carried out using **La[70]**, it was found that even after 13 equivalents of complex had been added to the diethyl phosphate, a plateau had not been reached, as seen in **Figure 4.12**. After thirteen equivalents of complex solubility became a problem, and therefore the experiment was repeated, this time adding diethyl phosphate to a solution of the complex. This was more successful, and as can be seen in **Figure 4.13**, the change in the NMR spectrum plateaued after approximately 25 equivalents of diethyl phosphate had been added. This indicates that binding is rather poor. However it has been previously recorded that this complex successfully cleaved **HPNP** with a rate of 0.41 h^{-1} . Therefore, the theory put forward by Morrow *et al.* that ability of a complex to bind a phosphate ester does not seem to hold true in this case. This complex, **La[70]** exhibits relatively weak binding to a phosphate ester and yet has been found to cleave **HPNP** extremely quickly. One possible factor that could be considered

here is that as well as binding to the phosphate ester in question, a good cleavage agent must also bind the substrate reversibly, releasing the product fragments after hydrolysis has occurred. Although this compound was not found to act catalytically, it is possible that the weak phosphate binding shown here can aid the rate of hydrolysis.

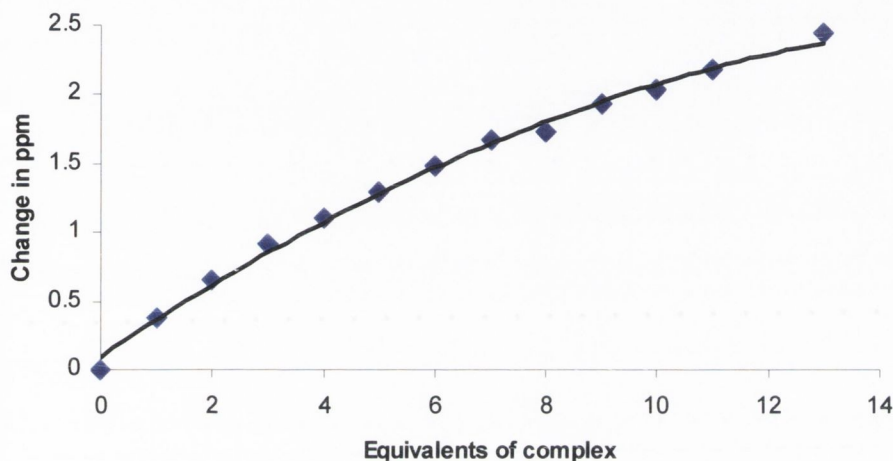


Figure 4.12 Change in ^{31}P NMR as a function of molar equivalents of $\text{La}[70]$ added to a solution of diethyl phosphate.

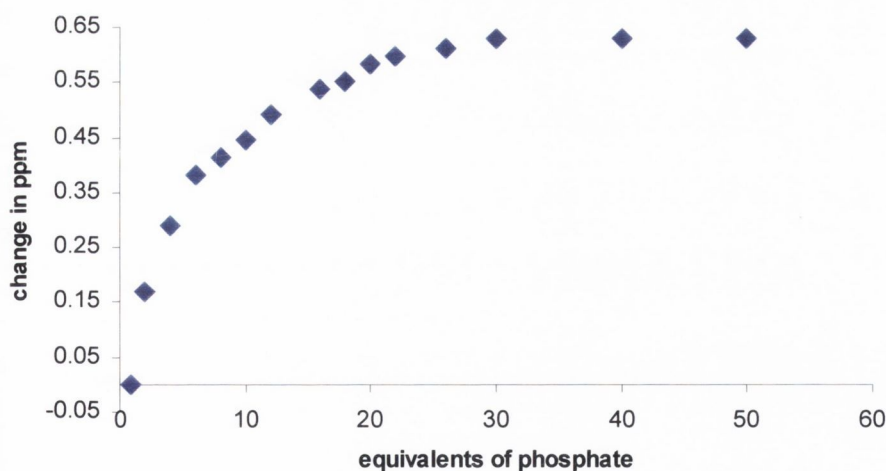


Figure 4.13 Change in ^{31}P NMR as a function of molar equivalents of diethyl phosphate added to $\text{La}[70]$

When $\text{Eu}[70]$ was examined, adding one equivalent of dimethyl phosphate at a time, it initially seemed to exhibit strong binding, with a plateau observed after only three equivalents of phosphate had been added, as shown in **Figure 4.14**. When this was repeated, adding 0.1 molar

equivalents of phosphate in each titre, the graph was seen to plateau even more quickly, at about 0.6 equivalents, as shown in **Figure 4.15**. This did not make sense, unless two molecules of complex bound to one of the phosphate. A further experiment was carried out in which 0.05 equivalents of phosphate were added in each titre and in this case, the graph shown in **Figure 4.16** was produced. Here, it can be seen that the plateau occurs even sooner, after about 0.3 equivalents of phosphate. This result gave an indication that there was a problem with the procedure, and visual inspection of the NMR tube revealed an extremely fine dispersion coming out of solution as further phosphate was added. Thus the change in the ^{31}P NMR was perhaps not due to a lanthanide shift as **Eu[70]** bound to the phosphate, but due to the disappearance of the phosphate as it precipitated out of solution. However, it was established clearly that both **Eu[70]** and diethyl phosphate were completely soluble in the solvent system used in this procedure ($\text{H}_2\text{O}/\text{MeOH}$, 90/10), so the precipitate seems likely to be the ternary complex formed when the two compounds bind to one another. Therefore, from the experimental evidence, it is likely that the Eu(III) complex binds the diethyl phosphate more strongly than the corresponding La(III) complex, although this could not be confirmed. The precipitate could not be redissolved for further analysis and attempts to crystallise a sample of the adduct were not successful.

The results obtained here would seem to disagree with the work of Morrow *et al.*, who found that the more hydrolytically active **La[25]** was a better binder of diethyl phosphate than **Eu[25]**. The proposed explanation of this was that the extra coordination sites of the La(III) complex enhanced its ability to bind a phosphate and thus promoted the rate of hydrolysis. In the case of **La[70]** and **Eu[70]**, it has been found that the La(III) complex may be a poorer binder of an inert phosphate ester, while cleaving an activated phosphate ester more easily.

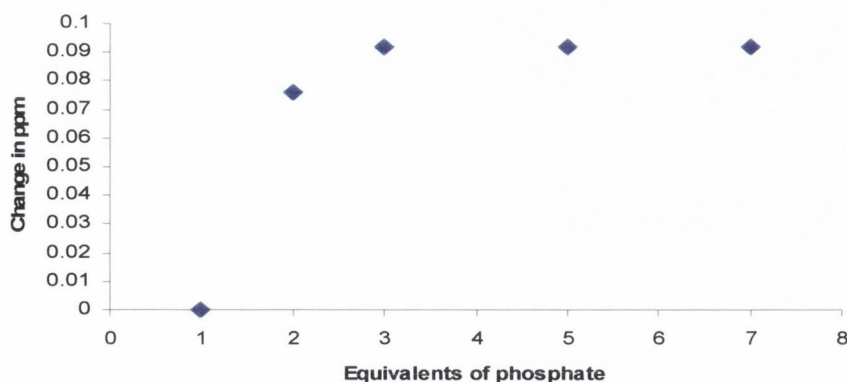


Figure 4.14 Change in ^{31}P NMR as a function of molar equivalents of diethyl phosphate added to **Eu[70]** (one molar equivalent added per titre.)

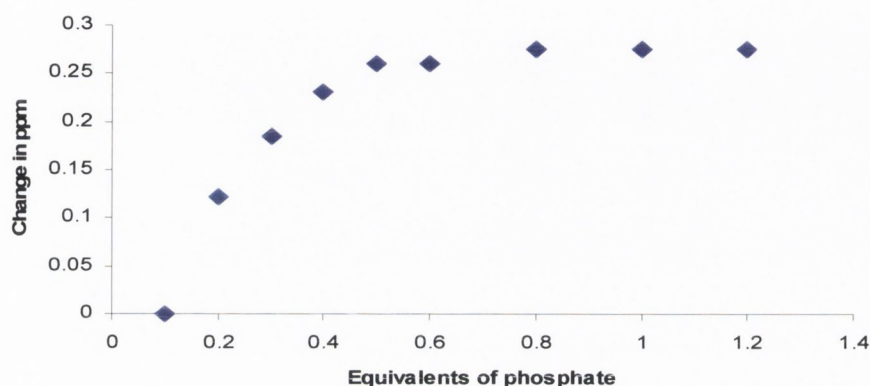


Figure 4.15 Change in ^{31}P NMR as a function of molar equivalents of diethyl phosphate added to **Eu[70]** (0.1 molar equivalent added per titre.)

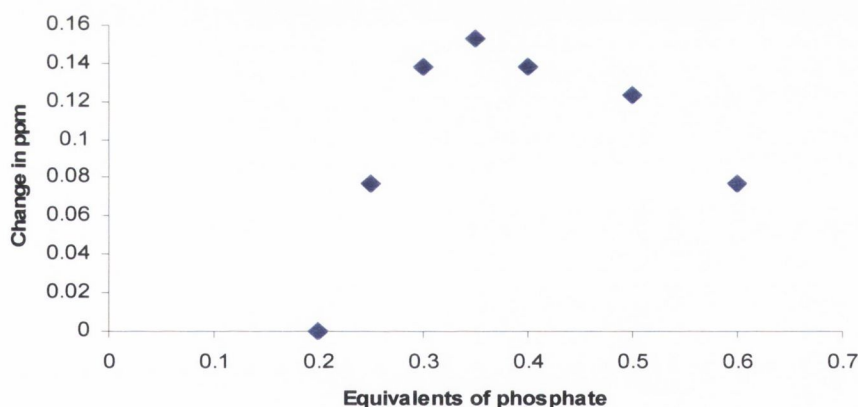


Figure 4.16 Change in ^{31}P NMR as a function of molar equivalents of diethyl phosphate added to **Eu[70]** (0.05 molar equivalent added per titre.)

4.7.2. Evaluating binding to various groups by luminescence methods

Another method of evaluating the ability of a molecule to bind to these lanthanide complexes is to see if, in the presence of such of group, the metal bound water molecule is replaced.¹⁹⁸ Having previously determined the q value (or number of metal bound water molecules) as described in section 2.10, the same procedure was carried out in the presence of possible binding groups. In these experiments, it was necessary to know the exact concentration of both complex and binding group, so the more hydrophobic, less water soluble complexes could not

be examined. Under the conditions described in section 2.10, some of these compounds had not been fully soluble, even with the addition of up to 5 % methanol, and had required filtering before fluorometric measurements could be carried out. For this reason, **Eu[85]** was chosen as the lanthanide complex to be tested for binding properties with EDTA, sodium acetate, diethyl phosphate and **HPNP**.

Table 4.14 Lifetime measurements for Eu[85] in the presence of possible binding groups

Compound	$\tau_{1/2} \text{H}_2\text{O}$ [ms]	$k \text{H}_2\text{O}$ [ms^{-1}]	$\tau_{1/2} \text{D}_2\text{O}$ [ms]	Rate in D_2O [ms^{-1}]	q
1 eq diethyl phosphate	0.574	1.746	1.925	0.520	1.17
5 eq diethyl phosphate	0.495	2.019	1.594	0.628	1.37
1 eq HPNP	0.410	2.440	1.045	0.957	1.48

1.2×10^{-3} M stock solutions of **Eu[85]** were prepared, in both H_2O and D_2O . Addition of one molar equivalent of diethyl ether produced a q value of 1.17. While this is slightly smaller than the value given without the presence of diethyl ether ($q = 1.33$), it is well within the statistical error of ± 0.5 .¹³⁰ In order to further test this, the experiment was repeated with five molar equivalents of diethyl ether present, and a q value of 1.37 was found. This suggested that the diethyl ether did not replace the metal bound water molecule, even when present in excess. This result would seem to back up what was observed for the ^{31}P NMR titrations with **Eu[85]** and diethyl ether; that a great excess of the phosphate would be required (in the region of a 20-fold excess) before significant binding will occur. A similar experiment was carried out using **HPNP**, and again the q value was not found to be significantly altered, at 1.48.

Moving away from phosphates, binding tests were carried out using EDTA. EDTA can act as a trap for free lanthanide ions, and is a method of determining the stability of a complex. In this case, a change in the q value could provide information about both the binding ability of the complex and its stability in a competitive environment. When one molar equivalent of EDTA was used, the q value was found to be 1.33, which was identical to the value given when no EDTA was present. When five equivalents of EDTA were added, the q value was 1.08, which is a reduction from the previous figure, but not statistically significant in the light of the ± 0.5 error

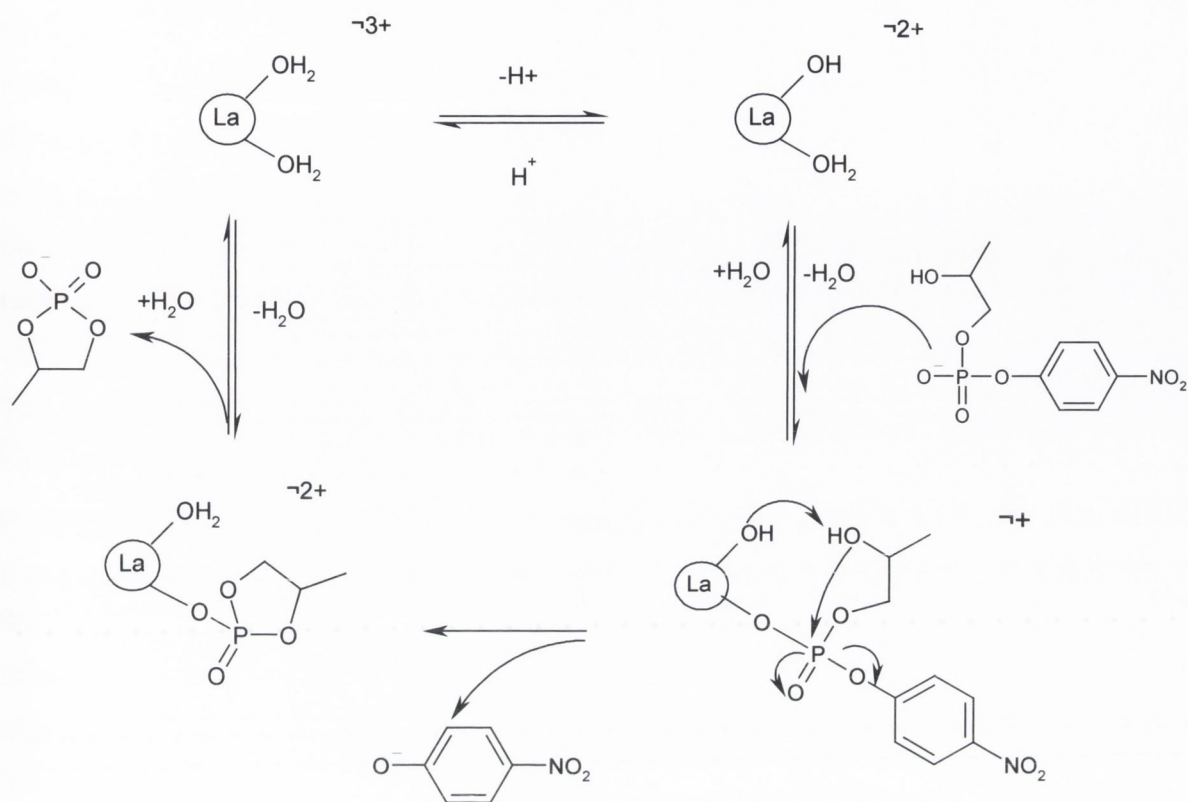
in these calculations. To see whether this reduction was due to the increase in EDTA or merely statistical error, a further experiment was carried out, using ten equivalents of EDTA. In this case, the q value was found to be 1.10. Therefore, given the error involved in these calculations, it can be said that one metal-bound water molecule was present in each case, and that up to ten equivalents of EDTA could be added without affecting this. A final binding test was carried out by adding five equivalents of sodium acetate to **Eu[85]**, using the same conditions and concentrations as in the previous experiments. Again, a q value of 1.36 was found, indicating that binding did not occur between the NaOAc and **Eu[85]**.

Table 4.15 Lifetime measurements for Eu[85] in the presence of EDTA

Compound	$\tau_{1/2} \text{H}_2\text{O}$ [ms]	$k \text{H}_2\text{O}$ [ms^{-1}]	$\tau_{1/2} \text{D}_2\text{O}$ [ms]	Rate in D_2O [ms^{-1}]	q
1 eq EDTA	0.487	2.057	1.667	0.601	1.33
5 eq EDTA	0.571	1.750	1.654	0.605	1.08
10 eq EDTA	0.554	1.805	1.820	0.549	1.21
5 eq NaAc	0.500	2.000	1.627	0.615	1.36

4.8 Towards a reaction mechanism

In light of the results presented in this chapter it becomes possible to comment on the potential mechanism of the hydrolysis of **HPNP** by the lanthanide complexes. Firstly, it should be noted that the mechanism must be dependant upon the number of metal-bound water molecules present in the lanthanide complex. From the evidence of crystal structures shown in Chapters 1 and 2 and discussed in literature,^{94,139,199} it seem reasonable to assume that La(III) and Ce(III) complexes have two metal-bound water molecules when embedded in such cyclen systems, while smaller lanthanides (Eu(III), Tb(III), Yb(III) *etc.*) possess one metal-bound water molecule. The possible mechanism that will be discussed here will concentrate on the more effective La(III) complexes, as a greater amount of research has been carried out on these.



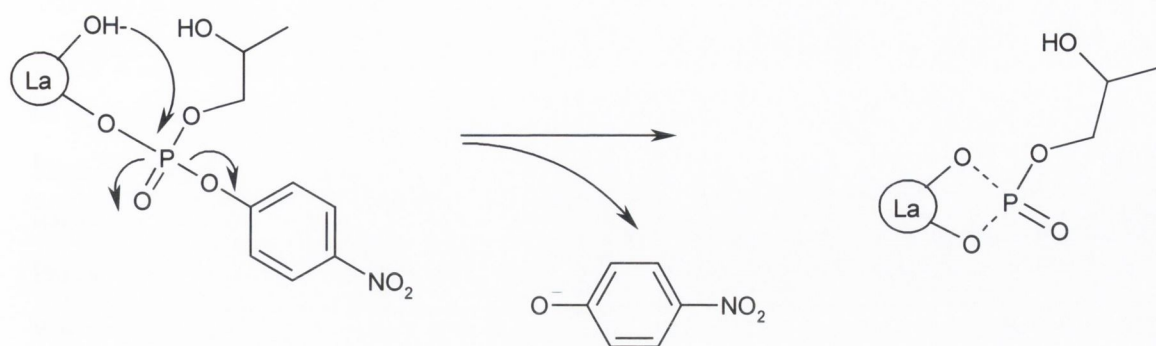
Scheme 4.2 A proposed mechanism for the hydrolysis of **HPNP** by cyclen-based **La(III)** complexes.

A possible, catalytic pathway for the hydrolysis of **HPNP** by a **La(III)** complex is shown in **Scheme 4.2**. The first step involves the deprotonation of one metal-bound water molecule. As these reactions have all been carried out under physiological conditions (pH 7.4 and 37 °C), the pK_a of the metal bound water is of crucial importance in this step. It has been proposed that the optimal rate of hydrolysis will occur at a pH where one water molecule is deprotonated and one remains protonated.²⁰⁰ If neither water molecule is deprotonated, hydrolysis cannot be promoted by a metal-bound hydroxide, while if both water molecules are deprotonated, the complex may bind too strongly to the phosphate, preventing release of the products and inhibiting catalysis. The pH-rate profiles obtained for four **La(III)** complexes show the bell-shaped curve that is associated with the behaviour of ribonucleases. (Section 1.4.3). In the case of **La[70]**, the maximum rate is found at pH 8.5; for **La[72]** it is at pH 7.5. This is a significant difference, caused only by exchanging methyl ester groups for benzyl ester. It may be assumed that the change in the cavity ‘walls’ affects the local environment of the metal bound water molecule, and in turn the pK_a . Similarly, the pH-rate profile for **La[21]** shows the maximum rate at pH 7.2,

while for **La[86]** it is at pH 7.5. Again, the only difference is the exchange of a methyl ester for a benzyl ester, with an apparent effect upon the pK_a of the metal-bound waters. In the case of the alanine-based compounds (**La[86]** and **La[85]**), the shape of the pH-rate curves also differs, with the **La[85]** curve showing a very sharp peak at pH 7.2, with the rate dropping significantly on either side of pH 7.2. The pH-rate curve for **La[86]** has a broader curve, with similarly high rates of hydrolysis found between pH 7.4 and pH 7.6. This again illustrates the significant effects of altering the pendant arms, and, in turn, the micro-environment of the complex.

The second step of the proposed reaction mechanism shown in **Scheme 4.2** involves **HPNP** binding to the complex by replacing the metal-bound water. It is important that this step is reversible, or catalysis will not be possible. Binding studies have been carried out with diethyl phosphate, as described in Section 4.10. ^{31}P NMR studies suggested that in the case of **70** and **86**, La(III) complexes do not bind strongly to the phosphate; significantly stronger binding was found between the phosphate and the Eu(III) complexes in each case. It was proposed by Morrow *et al.* that strong binding is necessary for the promotion of phosphodiester hydrolysis,⁹⁴ however other research groups have suggested that if such binding is too strong, hydrolysis will be inhibited.²⁰¹

The third step of the proposed mechanism involves the hydrolysis of the bound **HPNP** and the release of *p*-nitrophenolate. There are two possible mechanistic routes for this reaction. Scheme 4.1 shows the activation of the 2'-hydroxy group by the metal bound hydroxide, and the subsequent nucleophilic attack on the phosphate by the 2'-hydroxy group. Alternatively, the metal-bound hydroxide may provide direct nucleophilic attack upon the phosphate, going through a four-membered intermediate, as shown in **Scheme 4.3**. The choice of mechanism at this step is probably determined by steric factors; principally, whether or not the metal bound water molecule is in sufficiently close proximity to the phosphate to attack it nucleophilically. At this point, it cannot be said with any degree of certainty which of these mechanisms is occurring.



Scheme 4.3 The metal-bound hydroxy directly attacks the phosphate, displacing *p*-nitrophenolate and producing a 4-membered ring chelate

The release of the *p*-nitrophenolate is of importance at this point; if the negatively charged product binds to the Ln(III) complex, it may result in the inhibition of further reaction. All hydrolysis reactions were followed by UV/*vis*, and the formation of the *p*-nitrophenolate was observed by following the rise in the absorption band at 400 nm. As no secondary bands were seen to form in that region of the spectrum, it seems unlikely that *p*-nitrophenolate was binding to any other species in solutions.

The final step of the reaction involves the release of the phosphate, presumably in the form of the five-membered ring shown in **Scheme 4.2**. However, since it has been shown that the complexes described in this thesis do *not* exhibit turnover, it is possible that this step can explain why. What may happen is that the complexes bind too strongly to the negatively charged phosphate, preventing its release. It is also possible that the hydrophobic cavity formed by the cyclen-based complexes enhances the binding of the lanthanide to the phosphate, again preventing its release. If the phosphate is not released, the complex is prevented from binding to and cleaving a second equivalent of **HPNP**, and the catalytic cycle is interrupted.

4.9 Conclusion

This chapter has described the results of **HPNP** hydrolysis by an extended family of cyclen-based lanthanide complexes that incorporated amino ester residues as co-factors. These complexes included the important features of a metal ion, metal-bound water molecule(s) and the occurrence of a hydrophobic cavity, three features that are known to play important roles in the active sites of ribonucleases.²¹ The hydrolysis of **HPNP** by these compounds was found to be surprisingly fast, relative to similar cyclen-base complexes investigated previously.^{94,95,96,97}

Chapter 4 – Interactions with Phosphodiester

This was surprising given the simple nature of the amino ester moieties that were used in these complexes, which did not include the capacity for acid-base catalysis or nucleophilic promotion of phosphodiester hydrolysis.

Investigation of these complexes established that the presence of a metal centre was necessary for activity (**HPNP** was not hydrolysed in the presence of free ligands), that generally the larger lanthanide ions are more effective than the smaller ions, and that the pK_a of the metal-bound water may play a role in the activity of the complexes. From the X-ray crystal structure presented in Chapter 2, it can be postulated that the conformation adopted by these lanthanide complexes, *ie*, a deep, bowl-shaped cavity, may play a role in their activity. It seems possible that this may act as a hydrophobic cavity, similar to that employed in many ribonucleases.

While an attempt has been made here to present a basic reaction mechanism for the promotion of **HPNP** hydrolysis by this type of complex, it must be emphasised that this is preliminary work and part of ongoing studies within the Gunnlaugsson group to investigate the nature and behaviour of these complexes.

Ultimately, the goal of this work is to create compounds that can selectively cleave the phosphodiester bonds of RNA, *ie*, true ribozyme and ribonuclease mimics. Having looked at the activity of these complexes in the presence of RNA model compounds, the final chapter will examine the effect of a selection of these complexes on a strand of RNA.

Chapter Five

Cleavage of an RNA Oligonucleotide

with model compounds, it was highly desirable to test at least a selection of our complexes with an actual RNA strand. The behaviour of RNA and RNA model compounds can differ quite significantly.⁷ It has been previously mentioned that RNA model compounds generally possess good leaving groups; this is true in the case of **HPNP** which was the principal phosphodiester used in Chapter 4. Apart from that, model compounds cannot mimic the complex, polymeric, polyanionic nature of the longer mRNA strands.⁷ A lesson can be learned from investigations into the activity of copper(II) terpyridine as a promoter of phosphodiester hydrolysis; having failed to promote the cleavage of **BNPP**, it was surmised that this compound was generally inactive.¹⁶⁰ However, subsequent studies by Bashkin *et al.* discovered that it successfully catalyses the hydrolysis of RNA dimers and oligomers and in fact inhibits the cleavage of **BNPP**, by forming a stable complex with this compound.¹⁶¹ Therefore, alongside studies using model compounds, it was deemed necessary to examine the effects of a selection of these novel cyclen complexes upon polymeric RNA. The strand that was chosen for this purpose was a 23-mer sequence from the gag RNA gene of the HIV virus, which has previously been used by Bashkin *et al.* in their investigations of Zn(II) compounds.¹⁰² The sequence used by Bashkin *et al.* is shown in **Figure 5.2** in its entirety, with the 23-mer sequence that was chosen for our work underlined.

5'-¹(775)GGAGAAAUUUAUAAAGAUGGAUAAUCCUGGGAUUAAAUAAA
 AUAGUAAGAAUGUAUAGCCCUACCCAGCAUUCUAGACAUAAGACAAGGACC
 AAAGAACCCUUUAGAGACUAUGUAGACCGGUUCUAUAAAACUCUAAGAGCC
 GAGCAAGUUCAGAG (933)-3'

Figure 5.2 A 218-mer RNA sequence from the GAG RNA of the HIV gene, with an underlined 23-mer sequence which was used in this chapter

5.2 Preparation of mRNA and Reaction Conditions and Procedures

The 23-mer RNA strand, purchased from Dharmacon Research, was provided protected in the 2' position as seen in **Figure 5.3**. This protection prevents degradation of the RNA prior to experimental work, as well as minimizing secondary structure.¹⁶²

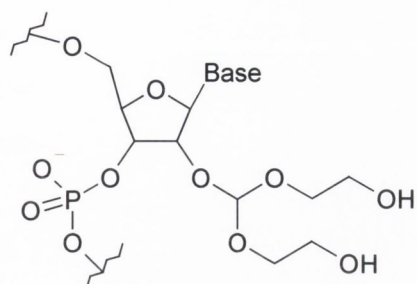
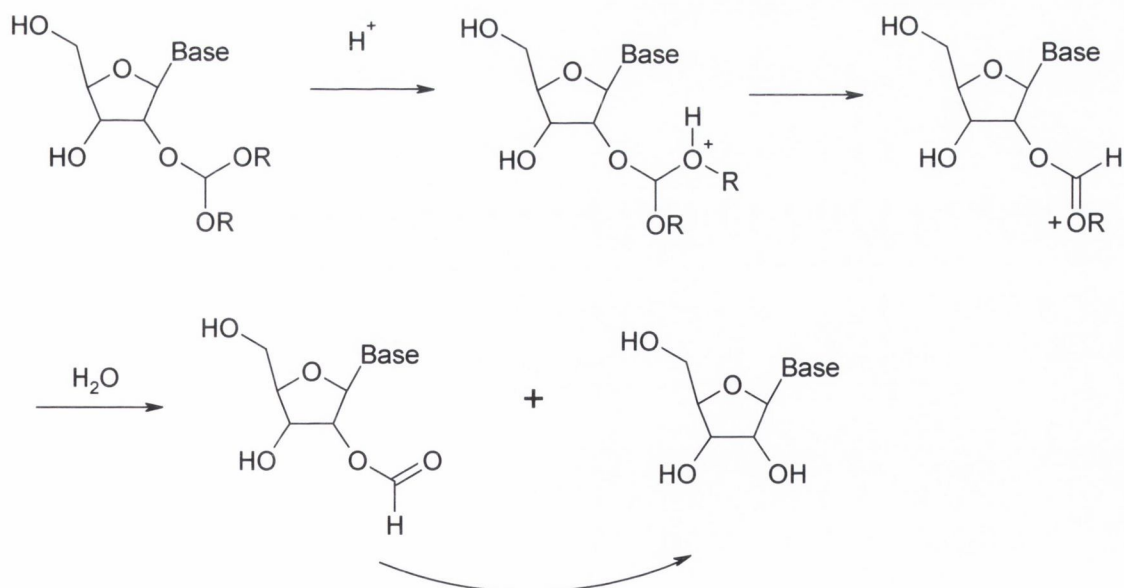


Figure 5.3 A protected RNA base

Prior to conducting any hydrolysis experiments, the synthetic RNA segment had to be purified, deprotected and radiolabelled.¹⁶³ A sample was first purified by polyacrylamide gel electrophoresis, a method of purification based on the premise that a molecule with a net charge will move in an electric field. The polyacrylamide gel on which the separation is carried out acts as a molecular sieve, enhancing separation.¹⁶³ Thus, molecules that are small relative to the pore size of the gel move faster than larger molecules. When the electrophoresis was complete, the bands were observed by UV shadowing. The main band was excised from the gel and passed through a biotrap to separate the RNA from the polyacrylamide. The RNA solution was then extracted with *n*-butanol and dried under vacuum.



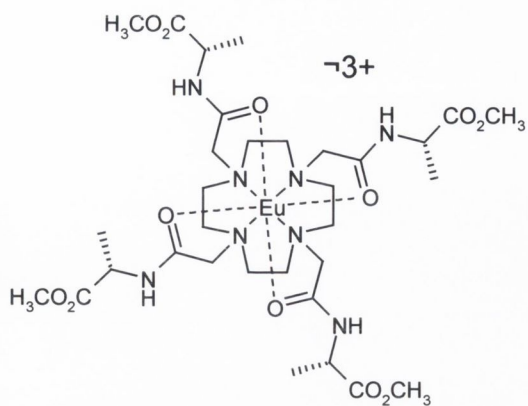
Scheme 5.1 Deprotection of the RNA bases using acid.

The protecting group was then removed using 0.1 M acetic acid, adjusted to pH 3.8 with TEMED. The mechanism of this reaction is shown in **Scheme 5.1**. The reaction mixture was lyophilized to remove water and the volatile side products of the deprotection reaction.

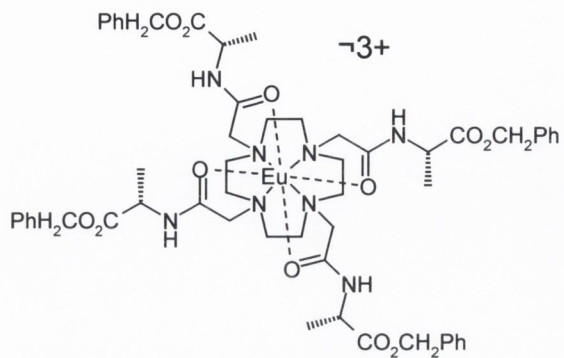
The 23-mer was then radio labelled at the 5'-position using ^{32}P ATP and T4 polynucleotide kinase, which catalyses the transfer and exchange of the ^{32}P from the γ position of the ATP to the 5' hydroxyl terminus of the RNA strand. The reaction was carried out in 70 mM Tris-HCl buffer at pH 7.6, 10 mM MgCl_2 and 5 mM dithiothreitol. The radio-labelled material was purified by means of a Sephadex G-25 column (eluted with ammonium formate) and the evaporated to dryness. Portions of the radio-labelled RNA, containing in the order of 400,000 Cerenkov counts per minute, were incubated with each catalyst at 37 °C for four hours, using 50 mM HEPES buffer at pH 7.4. The reaction products were analysed by polyacrylamide gel electrophoresis (PAGE).

5.3 Results of RNA cleavage experiments carried out with Eu(III) complexes

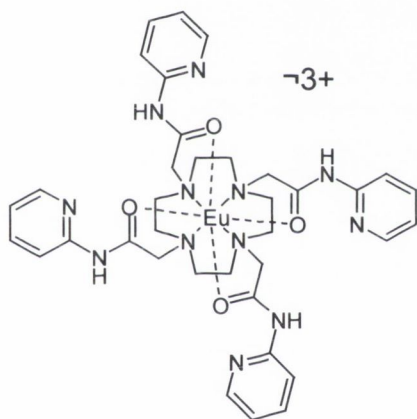
In the first set of experiments, a selection of Eu(III) complexes were tested, in order to ascertain the effects of changing the ligand when the lanthanide remained a constant. The results of these experiments are shown in the gel in **Figure 5.4**. The gel is divided into 6 'lanes', with each lane consisting of two experiments. For each europium complex tested, two experiments were carried out, with the second experiment in each lane using twice the concentration of Eu(III) complex as the first.



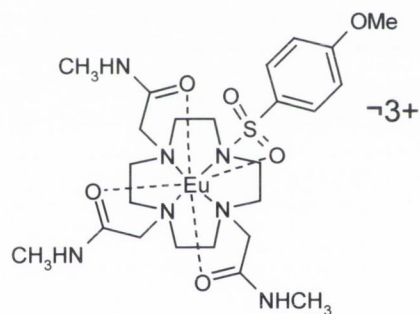
Eu[85]



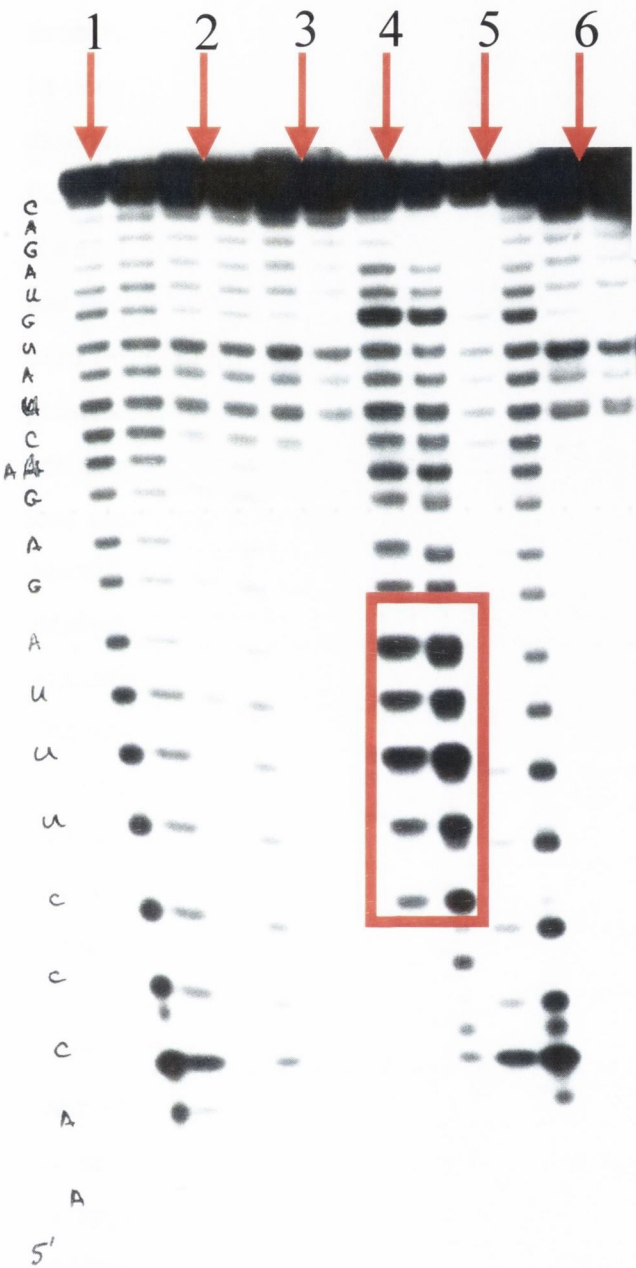
Eu[86]



Eu[103]



Eu[111]



Lane 1: Eu[85]
Lane 2: Eu[86]
Lane 3: 86
Lane 4: Eu[103]
Lane 5: Eu[111]
Lane 6: RNA without complex

Figure 5.4. PAGE gel, showing results of incubating a set of Eu(III) complexes with a 23-mer RNA sequence.

Due to the sensitivity of RNA towards hydrolytic cleavage, a control experiment was very important, in order to establish that any mRNA degradation observed in the experiments is

due only to the presence of the lanthanide complex and not to any background hydrolysis. In **Figure 5.4, Lane 6** shows the result of incubating sample of RNA incubated for the same time and under the same conditions as the other experiments but without any catalyst. It can be seen that very little cleavage has occurred in the absence of a catalyst. This allows us to assume that all other hydrolysis that may occur in these experiments is due to the presence of the relevant complex and not to any background hydrolysis.

Lane 1 shows the result of incubating the 23-mer with **Eu[85]**. It can be seen that cleavage has occurred at every base pair, as would be expected. The lane contains two experiments, with the second experiment having been carried out with twice the concentration of complex present. **Lane 2** shows the result of using **Eu[86]**, and it can be seen that again, cleavage occurred at each base pair. From visual inspection of the gel, it would appear that significantly less cleavage occurred compared to the experiment using **Eu[85]**, however this was not quantified. **Lane 3** shows the result of using an uncomplexed ligand, in this case **86**, and no cleavage was observed in these experiments, suggesting, once again, that the presence of a lanthanide ion is necessary for cleavage to occur. **Lane 5** shows the result of using **Eu[111]**; cleavage occurred at every base pair. **Lane 6**, as mentioned before, is a sample of RNA incubated for the same time and under the same conditions as the other experiments but without any compound that could enhance hydrolysis. It can be seen that very little cleavage has occurred without the presence of a lanthanide complex, beyond the first few bases at the 3'-end.

Lane 4 shows the result of incubating **Eu[103]** with RNA, and again, cleavage was seen to occur at every base pair. However, by visual inspection of the gel, it was thought that some degree of specificity might have occurred, with some of the cleavage spots in the centre of the gel appearing darker than others. This could be seen more clearly when a more lightly developed gel was prepared, and a densitometry study of this gel was carried out which can be seen in **Figure 5.5**. The densitometry trace shows that an elevated amount of cleavage occurred within a cluster of five adjacent nucleotides. When the position of the elevated cleavage was compared to the position of the various bases in the 23-mer, there was a suggestion of preferential attack at the 3'-AUUUC-5' tract. This was an unexpected result, as none of these catalysts had been designed with selectivity in mind. It was anticipated that in

order for any of them to cleave a sequence selectively, they would need to be attached to a complementary oligonucleotide, which would provide the means for targeting cleavage to a specific base residue. Untethered, these compounds were expected to attack any and every phosphodiester linkage, as was found to occur with the other catalysts and as can be seen quite clearly in the densitometry study of **Eu[85]**, which can be seen in **Figure 5.6**. In this densitometry study, there is no pattern of elevated cleavage at particular base pairs. The densitometry studies carried out on the gel show the difference in cleavage patterns obtained from use of different catalysts. **Eu[85]** shows a similar amount of cleavage between each base pair but it seems that when **Eu[103]** is used that there is preferential attack at a uracil rich segment of five bases.

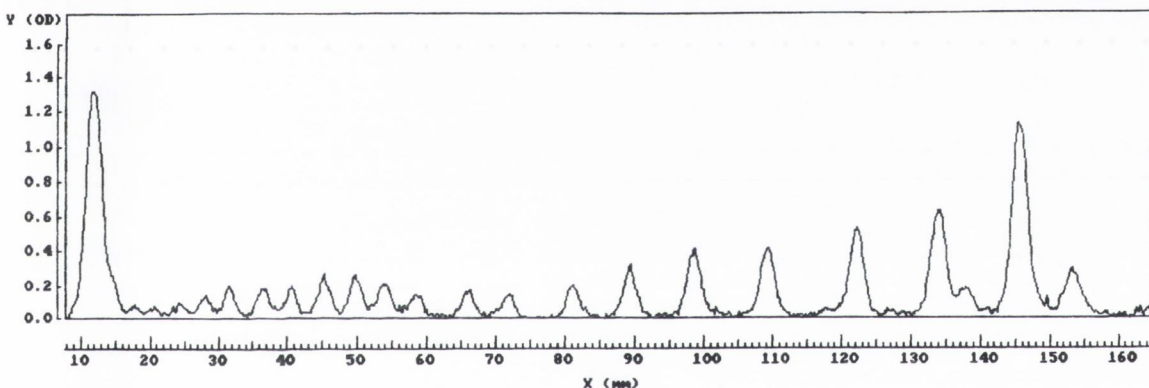


Figure 5.6 Densitometry study of cleavage by **Eu[85]**

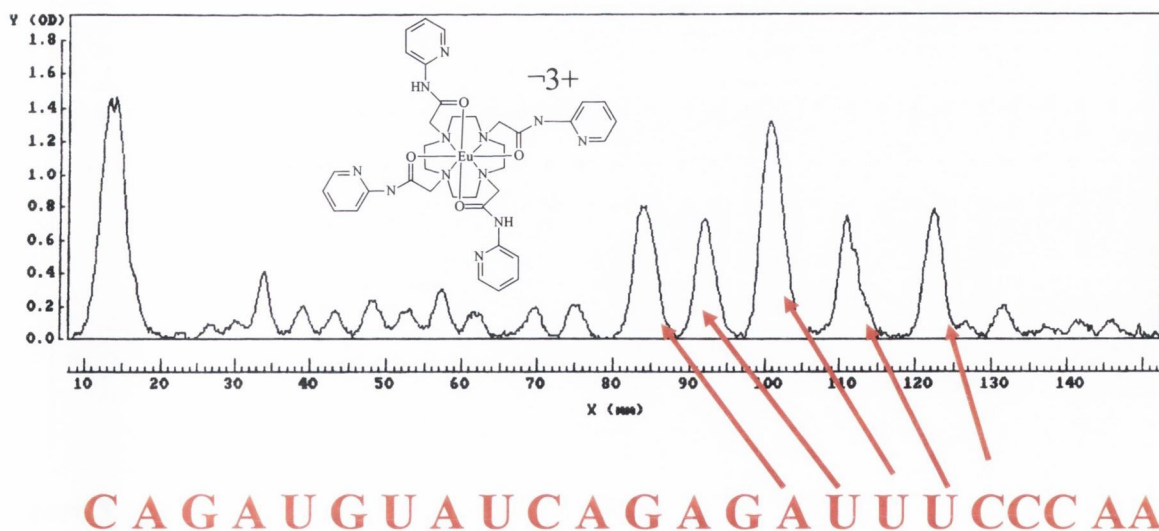


Figure 5.5 Densitometry study of strand cleavage by **Eu[103]**

5.4 Results of mRNA experiments carried out with Ln[70] complexes

A further set of experiments investigated the effect of changing the lanthanide ion within a given macrocyclic system. The ligand chosen was **70**, as these compounds had demonstrated impressive hydrolysis of HPNP. In this set of experiments, La(III), Eu(III) and Lu(III) complexes were tested, providing an early, middle and late lanthanide respectively. Each experiment was incubated at 37 °C and pH 7.4 for a period of 5 hours, alongside a control experiment of RNA without a catalyst. The products were again analysed by PAGE, and the results are shown in **Figure 5.7**.

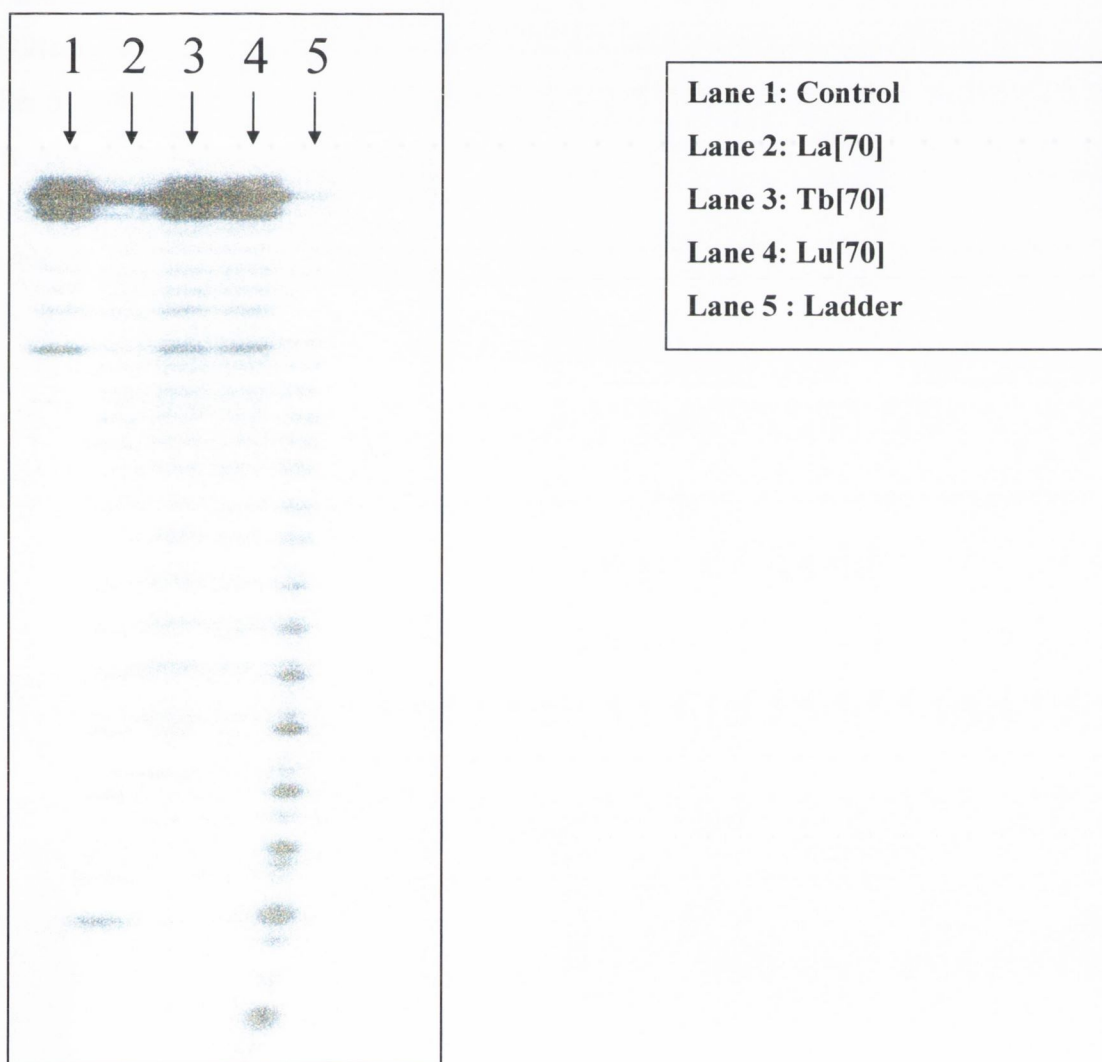
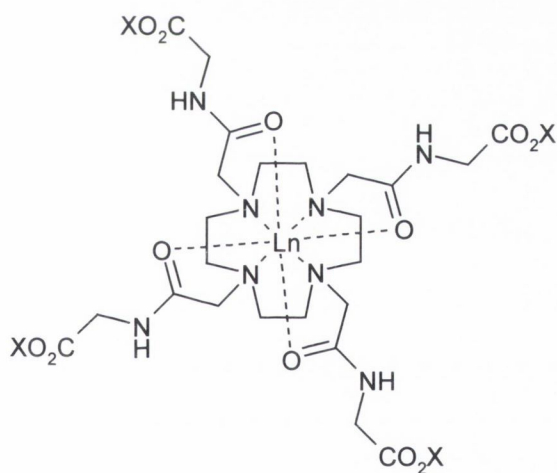


Figure 5.7. PAGE gel, showing results of incubating various complexes of **70** with a 23-mer RNA sequence.

It is difficult to quantify the degree of hydrolysis that occurred in these mRNA experiments, however, it can be discussed qualitatively by visual inspection of the PAGE gels and the subsequent densitometry. In a very general sense, the degree of hydrolysis can be measured by the reduction in size of the parent band (the top band in each PAGE gel). This provides a measure of the quantity of 23-mer remaining at the end of each experiment and can be compared to the parent band of the control experiment. From this gel it can be seen that the effect of **La[70]** is far greater than that of **Tb[70]** or **Lu[70]** when these compounds are tested with the same mRNA strand under the same conditions. The control experiment shows minimal cleavage of the strand occurred without the presence of a catalyst. When **La[70]** complex was used, the parent band at the top of the gel was considerably reduced within 5 hours, indicating that the concentration of the 23-mer had been reduced, whereas the same effect was not seen with either of the other metals. In the case of each complex, hydrolysis was found to occur at each base, indicating that the complex cleaved each phosphodiester linkage, without any specificity.



Ln = La(III), Eu(III), Lu(III)

70

5.5 Conclusion

The research described in Chapter 4, involving the use of **HPNP** as an mRNA model compound, established the ability of these cyclen-based lanthanide complexes to hydrolyse activated phosphodiester. We have hypothesized that this activity is due to a number of factors, including charge stabilization of the reaction intermediate, the presence of a metal-bound water molecule which can provide additional nucleophilic action, and the fact that these compounds have been found to form bowl-shaped structures, which may act as hydrophobic cavities. However, it has been established that the behaviour of such complexes can differ significantly between dealing with model compounds and mRNA.⁷ Therefore, it was imperative that the ability of these compounds to cleave the phosphodiester linkages of an RNA strand was established. This was accomplished, as can be seen from both **Figure 5.4** and **Figure 5.7**. In every experiment, incubation of a lanthanide complex with the mRNA 23-mer resulted in some degree of cleavage at every base pair. The cleavage was not site-specific, and it was not intended to be; the ultimate aim of this project is the modification of these complexes for incorporation into an oligonucleotide, which would provide specificity.

An important feature of these mRNA experiments was the indication they gave of whether the activity of the lanthanide complexes might indeed differ when dealing with RNA, compared to the activity they exhibited in relation to **HPNP**. In the case of the ligand **70**, the three complexes that were tested, (La(III), Tb(III) and Lu(III)), showed the same trend of activity when tested with either **HPNP** or mRNA. In each case, activity seemed to increase with the size of the lanthanide.

In the first set of experiments, involving Eu(III) complexes of various ligands, it was found that they promoted hydrolysis of mRNA over a period of four hours. In each case, cleavage was found to occur at every base pair. It is possible to say that **Eu[85]** showed greater cleavage than **Eu[86]** under these conditions (37 °C, pH 7.4, 50 mM HEPES buffer), and this corresponds with the results obtained when the same compounds were tested with **HPNP**. In one case, when **Eu[103]** was tested, a degree of selectivity was found to occur in the cleavage, with preferential attack at a uracil-rich quintet of bases. This result cannot yet be explained, and further work is being carried out in conjunction with these compounds by the Gunnlaugsson group to further understand the mechanism at work.

Chapter Six

Experimental

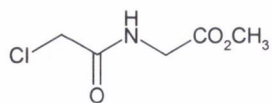
6.1 General Experimental Details

Melting points were determined using a Gallenkamp melting point apparatus. Infrared spectra were recorded on a Mattson Genesis II FTIR spectrophotometer equipped with a Gateway 2000 4DX2-66 workstation. Oils were analysed using NaCl plates, solid samples were dispersed in KBr and recorded as clear pressed discs. ^1H NMR spectra were recorded at 400 MHz on a Bruker Spectrospin DPX-400 instrument. Tetramethylsilane (TMS) was used as an internal reference standard, with chemical shifts expressed in parts per million (ppm or δ) downfield from the standard and coupling constants (J) expressed in Hz. ^{13}C NMR spectra were recorded at 100 MHz on a Bruker Spectrospin DPX-400 instrument. Mass spectra were determined by detection using Electrospray on a Micromass LCT spectrometer, using a Shimadzu HPLC or Waters 9360 to pump solvent, controlled by MassLynx 3.5 on a Compaq Deskpro workstation. Accurate Mass was determined relative to a standard of leucine Enkephaline (Tyr-Gly-Gly-Phe-Leu). Elementary Analysis was performed in the Microanalytical Laboratory, University College Dublin.

The preparation and characterisation of the compounds in this chapter will be discussed in terms of ‘families’ of compounds. First, the relevant α -chloroamide arm will be discussed, followed by the preparation of the cyclen-based ligand, followed in turn by the various lanthanide complexes formed from said ligand. It should be noted at this point that many of the compounds described herein were found to be hygroscopic, thus prohibiting the acquisition of melting points.

6.2 Synthesis for Chapter 2

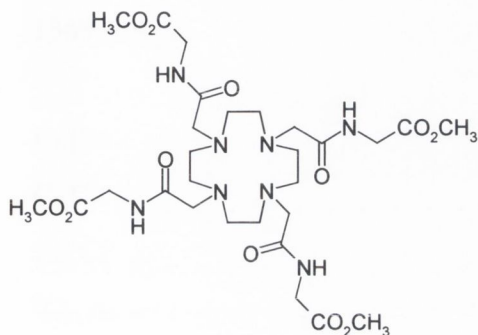
(2-Chloro-acetylamino)-acetic acid methyl ester¹²² [67]



Glycine methyl ester hydrochloride (2.005 g, 15.9 mmol) and triethylamine (2.5 mL, 17.5 mmol) were added to DCM (120 mL) and cooled below $-10\text{ }^\circ\text{C}$ in a liquid nitrogen/acetone bath. To this a solution of chloroacetyl chloride (1.2 mL, 15.9 mmol) in DCM (30 mL) was added dropwise over an hour. The reaction was stirred at room temperature for a further 16 hours. It was filtered through celite and the filtrate was washed with 0.1 M HCl (50 mL x 3). The organic layer was dried over K_2CO_3 and the solvent was removed under reduced pressure to yield a white solid, (1.895 g, 11.4 mmol, 71.7 %). **mp** $42\text{--}45\text{ }^\circ\text{C}$, (lit¹²² $41\text{--}43\text{ }^\circ\text{C}$); δ_{H} (CDCl_3 ,

400Hz): 7.43 (1 H, br s, N-H), 3.94 (2 H, s, Cl-CH₂), 3.89 (2 H, s, NH-CH₂-), 3.58 (3 H, s, CO₂CH₃); δ_C (CDCl₃, 100MHz): 168.6, 165.7, 67.0, 41.9, 41.1.

(2-{4,7,10-Tris-[(ethoxycarbonylmethyl-carbamoyl)-methyl]-1,4,7,10 tetraaza-cyclododec-1-yl}-acetyl-amino)-acetic acid methyl ester [70]



A solution of **67** (1.603 g, 9.67 mmol) in dry acetonitrile (10 mL) was added to cyclen (0.405 g, 2.36 mmol), cesium carbonate (3.154 g, 9.67 mmol) and potassium iodide (1.607 g, 9.67 mmol) in dry acetonitrile (30 mL). This was then refluxed under argon for 48 hours. The mixture was filtered through celite and the solvent removed under reduced pressure.

The residue was taken up in chloroform and washed with water. The organic layer was dried over K₂CO₃ and the solvent was removed under reduced pressure to yield a white hygroscopic powder, (1.124 g, 1.63 mmol, 69.2 %). **mp** 161-163 °C; Anal. Calcd for C₂₈H₄₈N₈O₁₂K: C, 46.21; H, 6.65; N, 15.37. Found: C, 46.64; H, 6.88; N, 14.95; δ_H (CDCl₃, 400Hz): 7.77 (1 H, t, *J* = 6, NH), 3.86 (2 H, d, *J* = 6 CH₂), 3.59 (3 H, s, CH₃), 3.03 (2 H, s, CH₂), 2.60 (4 H, s, cyc-CH₂); δ_C (CDCl₃, 100Hz): 171.1, 170.1, 58.8, 52.8, 51.8, 40.2; **M/Z**: 689 (M⁺), 711 (M+Na)⁺; **IR**_{vmax} (cm⁻¹): 3435, 3071, 2956, 2824, 1749, 1672, 1543, 1439, 1439, 1369, 1310, 1214, 1096, 1003, 883, 806, 700.

Procedure 1

Synthesis of lanthanide complexes

Lanthanide complexes were prepared by refluxing the ligand with 1.1 molar equivalents of the appropriate lanthanide triflate in dry acetonitrile (10mL) for 16 hours except in the case of the La(III) complex, where dry methanol was used. The complexes were isolated by precipitation in dry ether (100 mL) and subsequent suction filtration. ¹H NMR spectra of lanthanide complexes consisted of very broad signals and therefore are not fully characterised. The same properties prevent ¹³C spectra from being obtained. For ¹H NMR spectra, spectral width was set at 100 ppm. Additional spectral widths were obtained by adjusting the central offset (ie, -150 ppm to -50 ppm, 0 ppm to 150 ppm etc).

La[70]

La[70] was prepared according to Procedure 1, using **70** (0.203 g, 0.330 mmol) and La(CF₃SO₃) (0.215 g, 0.370 mmol) and yielded 0.185 g, 0.145 mmol (43.9 %); **mp** 263-266 °C; **Accurate Mass**: Expected for C₂₈H₄₈N₈O₁₂La(CF₃SO₃): 976.1976 (M+Trif)⁺, Found: 976.1954; δ_{H} (CD₃OD, 400Hz): 8.3, 4.1, 3.7, 3.4, 2.7, 1.9, 1.1; **M/Z**: 275 (M⁺³), 289 (M+K)⁺³, 487 (M+Trif)⁺²; **IR**_{vmax} (cm⁻¹): 3444, 3132, 2961, 2359, 2341, 1758, 1631, 1443, 1369, 1251, 1169, 1030, 968, 888, 761.

Ce[70]

Ce[70] was prepared according to Procedure 1, using **70** (0.109 g, 0.158 mmol) and Ce(CF₃SO₃) (0.102 g, 0.174 mmol) and yielded 0.110 g, 0.085 mmol (53.8 %); **mp** 260-263 °C; **Accurate Mass**: Expected for C₂₈H₄₈N₈O₁₂Ce: 828.2446 (M⁺), Found: 828.2421; δ_{H} (CD₃CN, 400Hz): 12.1, 9.9, 0.07, -9.8; **M/Z**: 276 (M⁺³), 289 (M+H₂O)⁺², 488 (M+Trif)⁺²; **IR**_{vmax} (cm⁻¹): 3454, 3132, 2924, 1738, 1629, 1416, 1273, 1229, 1168, 1030.

Pr[70]

Pr[70] was prepared according to Procedure 1, using **70** (0.123 g, 0.179 mmol) and Pr(CF₃SO₃) (0.115 g, 0.197 mmol) and yielded 0.107 g, 0.084 mmol (46.9 %); **mp** 238-241 °C; **Accurate Mass**: Expected for C₂₈H₄₈N₈O₁₂Pr: 829.2468 (M⁺), Found: 829.2482; δ_{H} (CD₃CN, 400Hz): 20.1, 17.2, 15.0, 12.4, -0.17, -26.53; **M/Z**: 276 (M⁺³), 414 (M⁺²); **IR**_{vmax} (cm⁻¹): 3436, 3272, 3128, 2960, 1758, 1631, 1368, 1248, 1165, 1028, 714.

Nd[70]

Nd[70] was prepared according to Procedure 1, using **70** (0.135 g, 0.196 mmol) and Nd(CF₃SO₃) (0.128 g, 0.216 mmol) and yielded 0.105 g, 0.082 mmol (41.8 %); **mp** 240-242 °C; **Accurate Mass**: Expected for C₂₈H₄₈N₈O₁₂Nd: 830.2469 (M⁺), Found: 830.2456; δ_{H} (CD₃CN, 400Hz): 14.6, 13.2, 11.8, 8.5, -13.1; **M/Z**: 216 (M+K)⁺⁴, 277 (M⁺³), 416 (M⁺²), 490 (M+Trif)⁺²; **IR**_{vmax} (cm⁻¹): 3456, 3121, 2959, 1748, 1632, 1372, 1263, 1165, 1079, 1030, 831, 708.

Eu[70]

Eu[70] was prepared according to Procedure 1, using **70** (0.169 g, 0.245 mmol) and Eu(CF₃SO₃) (0.162 g, 0.270 mmol) and yielded 0.069 g, 0.054 mmol (22.0 %); **mp** 249-252 °C; **Accurate Mass**: Expected for C₂₈H₄₈N₈O₁₂Eu: 841.2604 (M⁺), Found: 841.2566; δ_{H} (CD₃OD, 400Hz): 31.8, 24.7, 13.3, 9.0; **M/Z**: 280 (M⁺³), 420 (M⁺²), 494(M+Trif)⁺²; **IR** ν_{max} (cm⁻¹): 3434, 3122, 2926, 1749, 1632, 1369, 1250, 1165, 1030, 971, 832.

Gd[70]

Gd[70] was prepared according to Procedure 1, using **70** (0.112 g, 0.163 mmol) and Gd(CF₃SO₃) (0.108 g, 0.179 mmol) and yielded 0.131 g, 0.101 mmol (61.9 %); **mp** 241-245 °C; **Accurate Mass**: Expected for C₂₈H₄₈N₈O₁₂Gd(CF₃SO₃): 995.2153 (M+Trif)⁺, Found: 995.2134; **M/Z**: 282 (M⁺³), 391 (M+2Trif+2H₂O)⁺³; **IR** ν_{max} (cm⁻¹): 3420, 3131, 2961, 1736, 1633, 1578, 1415, 1269, 1137, 1079, 1030, 971.

Tb[70]

Tb[70] was prepared according to Procedure 1, using **70** (0.189 g, 0.275 mmol) and Tb(CF₃SO₃) (0.183 g, 0.302 mmol) and yielded 0.182 g, 0.140 mmol (51.1 %); **mp** 244-247 °C; **Accurate Mass**: Expected for C₂₈H₄₈N₈O₁₂Tb: 847.2645 (M⁺), Found: 487.2651; δ_{H} (CD₃OD, 400Hz): 30.7, 24.3, 12.6; **M/Z**: 423 (M⁺²), 498 (M+Trif)⁺², 1145.5 (M+2Trif)⁺; **IR** ν_{max} (cm⁻¹): 3433, 3130, 2925, 2854, 1738, 1633, 1415, 1375, 1267, 1167, 1079, 1030, 972.

Lu[70]

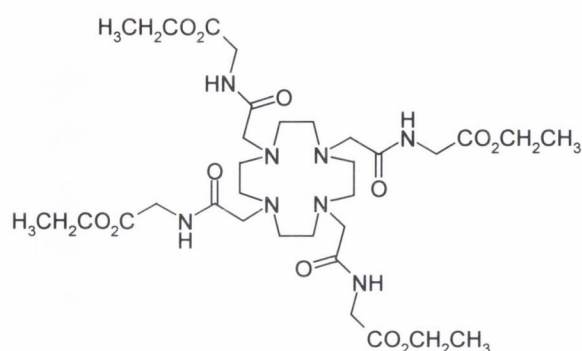
Lu[70] was prepared according to Procedure 1, using **70** (0.212 g, 0.308 mmol) and Lu(CF₃SO₃) (0.211 g, 0.338 mmol) and yielded 0.244 g, 0.186 mmol (60.4 %); **mp** 246-249 °C; **Accurate Mass**: Expected for C₂₈H₄₈N₈O₁₂Lu: 863.2800 (M⁺), Found: 863.2770; δ_{H} (CD₃OD, 400Hz): 8.6 (1 H), 4.2 (1 H), 4.0 (1 H), 3.7 (4 H), 3.4 (1 H), 2.8 (2 H), 1.9 (1 H); **M/Z**: 288 (M⁺³), 431 (M⁺²), 506 (M+Trif)⁺²; **IR** ν_{max} (cm⁻¹): 3440, 3134, 2962, 2361, 1736, 1638, 1581, 1415, 1415, 1267, 1169, 1080, 1030, 972, 892, 798.

Cu[70]

Cu[70] was prepared according to Procedure 1, using **70** (0.146 g, 0.212 mmol) and Cu(CF₃SO₃) (0.119 g, 0.233 mmol) and yielded 0.099 g, 0.083 mmol (39.2 %); **mp** 140-143 °C; **Accurate Mass**: Expected for C₂₈H₄₈N₈O₁₂Cu: 752.2766 (M⁺), Found: 752.2779; δ_{H} (CD₃OD, 400Hz): 8.7 (1 H, s, NH), 4.3 (1 H), 3.9 (1 H), 3.5 (4 H), 3.1 (1 H), 2.7 (2 H), 2.0 (1 H); **M/Z**: 303 (M+Trif)⁺³, 376 (M⁺²), 454 (M+Trif)⁺², 750 (M⁺), 900 (M+Trif)⁺; **IR**_{vmax} (cm⁻¹): 3576, 3371, 3314, 3111, 2963, 2360, 1740, 1657, 1562, 1443, 1369, 1289, 1224, 1027.

(2-Chloro-acetylamino)-acetic acid ethyl ester¹²² [**68**]

Glycine ethyl ester hydrochloride (2.001 g, 14.0 mmol) and triethylamine (6.0 mL, 43 mmol) were added to DCM (80 mL) and cooled to below -10 °C in a liquid nitrogen/acetone bath. To this a solution of chloroacetyl chloride (1.1 mL, 9.9 mmol) in DCM (30 mL) was added dropwise over an hour. The reaction was stirred at room temperature for a further 16 hours. The mixture was filtered through celite and the filtrate was washed with water (3 x 50 mL) and with 0.1 M HCl (3 x 50 mL). The organic layer was dried over K₂CO₃ and the solvent was removed under reduced pressure to yield a light brown solid, 2.035 g, 11.39 mmol (81.4 %). **mp** 64-66 °C, (lit²⁸⁰ 62-65 °C); δ_{H} (CDCl₃, 400Hz): 7.10 (1 H, bs, N-H), 4.29 (2 H, q, *J* = 8, CO₂CH₂CH₃), 4.11 (2 H, s, Cl-CH₂), 3.82 (2 H, d, *J* = 5, NH-CH₂), 1.33 (3 H, t, *J* = 8, CO₂CH₂CH₃); δ_{C} (CDCl₃, 100MHz): 168.7, 165.7, 61.3, 41.9, 41.1, 13.7; **IR**_{vmax} (cm⁻¹): 3268, 3090, 2990, 2947, 1739, 1650, 1569, 1474, 1419, 1376, 1207, 1160, 1036, 934, 873, 719.

(2-{4,7,10-Tris-[(ethoxycarbonylmethyl-carbamoyl)-methyl]-1,4,7,10 tetraazacyclododec-1-yl}-acetylamino)-acetic acid ethyl ester [**71**]

Cyclen (0.207 g, 1.2 mmol), **68** (0.886 g, 4.9 mmol), cesium carbonate (1.601g, 4.9 mmol) and potassium iodide (0.824 g, 4.9 mol) were added to dry acetonitrile (30 mL) and heated to 80 °C for 48 hours. The mixture was filtered through celite and reduced under

vacuum, before the residue was taken up in chloroform and washed with water. The organic layer was dried over K_2CO_3 and the solvent was removed under reduced pressure to yield a white hygroscopic powder, 0.324 g, 4.349 mmol (36 %). Anal. Calcd. for $C_{32}H_{56}N_8O_{12}$: C, 51.60; H, 7.58; N, 15.04. Found: C, 51.43; H, 7.77; N, 15.31. **mp** 127-130 °C; δ_H ($CDCl_3$, 400MHz): 7.56 (1 H, t, $J = 6$ N-H), 4.20 (2 H, q, $J = 7$, $CO_2CH_2CH_3$), 3.95 (2 H, d, $J = 6$, NH-CO- $\underline{CH_2}$), 3.17 (2 H, s, NH- $\underline{CH_2}$ -), 2.72 (4 H, s, cyc- $\underline{CH_2}$), 1.27 (3 H, t, $J = 7$, $CO_2CH_2CH_3$); δ_C ($CDCl_3$, 100MHz): 170.9, 169.6, 60.9, 58.6, 52.7, 40.5, 13.6; **M/Z**: 745 (M^+); **IR** v_{max} (cm^{-1}): 3382, 3069, 2981, 2826, 1751, 1672, 1561, 1459, 1375, 1205, 1118, 1023, 972.

La[71]

La[71] was prepared according to Procedure 1, using **71** (0.165 g, 0.221 mmol) and $La(CF_3SO_3)$ (0.143 g, 0.243 mmol) and yielded a yellow hygroscopic powder, 0.135 g, 0.102 mmol (46 %); **mp** 102-104 °C; **Accurate Mass**: Expected for $C_{32}H_{56}N_8O_{12}La$: 883.3081 (M^+), Found: 883.3069; δ_H (d_6 Acetone, 400MHz): 9.27 (1 H), 4.21 (3 H), 2.96 (2 H), 2.06 (1 H), 1.27 (2 H), 0.00 (2 H); **M/Z**: 440.7 (M^+); 515.6 ($M + Trif$) $^+$; **IR** v_{max} (cm^{-1}): 3457, 2924, 1739, 1630, 1451, 1418, 1259, 1166, 1106, 1030, 972, 809.

Eu[71]

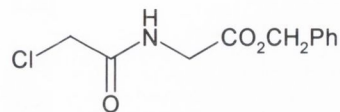
Eu[71] was prepared according to Procedure 1, using **71** (0.126 g, 0.169 mmol) and $Eu(CF_3SO_3)$ (0.111 g, 0.186 mmol) and yielded a yellow hygroscopic powder, 0.109 g, 0.081 mmol (48 %); **mp** 104-107 °C; **Accurate Mass**: Expected for $C_{32}H_{56}N_8O_{12}Eu$: 897.3230 (M^+), Found: 897.3215; δ_H (d_6 Acetone₃, 400MHz): 24.4, -2.5, -4.67, -8.3, -9.2, -12.4; **M/Z**: 299 (M^{+3}), 313 ($M+K$) $^{+3}$, 327 ($M+2K$) $^{+3}$, 448 (M^{+2}), 523 ($M+Trif$) $^{+2}$; **IR** v_{max} (cm^{-1}): 3425, 3131, 2998, 1736, 1634, 1466, 1418, 1281, 1227, 1166, 1079, 1030, 973, 891, 831, 762.

Yb[71]

Yb[71] was prepared according to Procedure 1, using **71** (0.141 g, 0.189 mmol) and $Yb(CF_3SO_3)$ (0.129 g, 0.208 mmol) and yielded a yellow hygroscopic powder, 0.101 g, 0.074 mmol (39 %); **mp** 110-113 °C; **Accurate Mass**: Expected for $C_{32}H_{56}N_8O_{12}Yb(CF_3SO_3)$: 1067.2927 (M^+), Found: 1067.2959; δ_H (d_6 Acetone₃, 400MHz): 26.1, -

3.5, -6.84, -9.2, -11.3, -14.6; **M/Z**: 306 (M^{+3}), 458 (M^{+2}), 533 ($M+\text{Trif}$) $^{+2}$, 1216 ($M+2\text{Trif}$) $^{+}$; **IR** v_{max} (cm^{-1}): 3406, 1732, 1638, 1416, 1249, 1172, 1031.

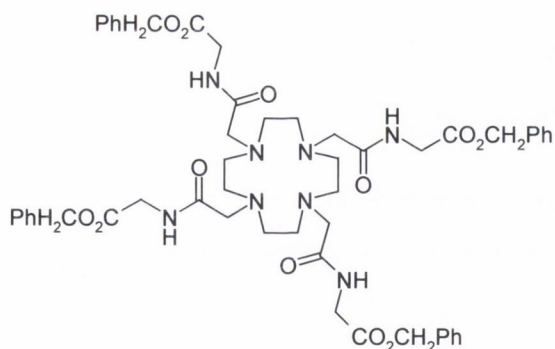
(2-Chloro-acetylamino)-acetic acid benzyl ester^{122,123} [69]



Glycine benzyl ester hydrochloride (2.002 g, 9.9 mmol) and triethylamine (1.52 mL, 10.8 mmol) were added to DCM (80 mL) and cooled below $-10\text{ }^{\circ}\text{C}$ in a liquid nitrogen/acetone bath.

To this a solution of chloroacetyl chloride (0.8 mL, 9.9 mmol) in DCM (30 mL) was added dropwise over an hour. The reaction was stirred at room temperature for a further 16 hours. It was filtered through celite and the filtrate was washed with water (3 x 50 mL) and with 0.1 M HCl (3 x 50 mL). The organic layer was dried over K_2CO_3 and reduced to yield a colourless liquid, 2.007 g, 8.29 mmol (83.8 %). δ_{H} (CDCl_3 , 400Hz): 8.21 (1 H, t, $J = 6$, N-H), 7.36 (5 H, m, Ar-H), 7.22 (1 H, br s, N-H), 5.19 (2 H, s, $\text{CH}_2\text{-CO}$), 4.11 (2 H, d, $J = 6$, NH- CH_2), 4.07 (2 H, s, Cl- CH_2); δ_{C} (CDCl_3 , 100Hz): 168.7, 166.0, 134.6, 128.20, 128.18, 127.9, 66.9, 41.9, 41.1; **M/Z**: 242 (M^{+}), 264 ($M+\text{Na}$) $^{+}$; **IR** v_{max} (cm^{-1}): 3389, 1729, 1677, 1527, 1407, 1357, 1261, 1210, 1210, 1111, 1029, 942, 762, 699.

(2-{4,7,10-Tris-[(benzyloxycarbonylmethyl-carbamoyl)-methyl]-1,4,7,10 tetraazacyclododec-1-yl}-acetylamino)-acetic acid benyl ester [72]



A solution of **69** (0.540 g, 2.24 mmol) in dry acetonitrile (10 mL) was added to cyclen (0.094 g, 0.54 mmol), cesium carbonate (0.730 g, 2.24 mmol) and potassium iodide (0.370 g, 2.24 mmol) in dry acetonitrile (20 mL). This was refluxed under argon for 48 hours. The mixture was filtered through celite and reduced before the residue was taken up in chloroform and washed with water. The organic layer was dried over K_2CO_3 and reduced to yield a hygroscopic powder, 1.314 g, 1.323 mmol (58.9 %). Anal. Calcd for $\text{C}_{52}\text{H}_{64}\text{N}_8\text{O}_{12}\cdot\text{H}_2\text{O}$: C, 61.77; H, 6.58; N, 11.08. Found: C, 62.03; H, 6.79; N, 10.81. δ_{H} (CDCl_3 , 400Hz): 7.63 (1 H, t, $J = 6$, N-H), 7.32-7.28 (5H, m, Ar-H), 5.09 (2 H, s, -CH_2), 3.98 (2 H, d, $J = 6$, CH_2CONH), 3.09 (2 H, s, CH_2), 2.64 (4 H, s, cyc- CH_2); δ_{C} (CDCl_3 , 100Hz): 171.3, 169.1, 134.3, 128.2, 128.1, 128.0, 127.9, 127.8, 127.7, 126.4 67.4,

57.2, 53.1, 40.3, 29.9; **M/Z**: 993.5 (M^+), 1015.5 ($M+Na$)⁺; **IR**_{vmax} (**cm**⁻¹): 3324, 3064, 2938, 2820, 1748, 1663, 1529, 1455, 1386, 1357, 1260, 1191, 1101, 1032, 804, 740.

La[72]

La[72] was prepared according to Procedure 1, using **72** (0.165 g, 0.166 mmol) and La(CF₃SO₃) (0.107 g, 0.183 mmol) and yielded 0.128 g, 0.081 mmol (49.2 %); **mp** 123-126 °C; **Accurate Mass**: Expected for C₅₂H₆₄N₈O₁₂La: 1131.3707 (M^+), Found: 1131.3723; **δ_H** (**d₆ acetone, 400Hz**): 9.2 (1-H, s, N-H), 7.4 (5 H, Ar-H), 5.2 (2 H, s), 4.2 (2 H, s), **δ_C** (**acetone, 400Hz**): 176, 168, 135, 128, 127.8, 127, 66.5, 60.5, 41; **M/Z**: 497 (M^{+3}), 565 (M^{+2}), 640 ($M+Trif$)⁺²; **IR**_{vmax} (**cm**⁻¹): 3452, 3284, 3123, 2957, 1746, 1631, 1246, 1081, 1030, 744.

Ce[72]

Ce[72] was prepared according to Procedure 1, using **72** (0.119 g, 0.120 mmol) and Ce(CF₃SO₃) (0.077 g, 0.132 mmol) and yielded 0.087 g, 0.055 mmol (46.0 %); **mp** 124-126 °C; **Accurate Mass**: Expected C₅₂H₆₄N₈O₁₂Ce(CF₃SO₃): 1281.3218 ($M+Trif$)⁺, Found: 1281.3206; **δ_H** (**d₆ acetone, 400Hz**): 17.2, 13.6, -1.8, -3.5, -7.3, -16.8; **M/Z**: 377.5 (M^{+3}), 566.5 (M^{+2}), 641.1 ($M+Trif$)⁺; **IR**_{vmax} (**cm**⁻¹): 3466, 3121, 2959, 1747, 1631, 1459, 1415, 1360, 1253, 1167, 1080, 1030, 758, 700.

Nd[72]

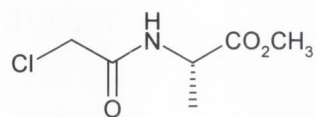
Nd[72] was prepared according to Procedure 1, using **72** (0.172 g, 0.173 mmol) and Nd(CF₃SO₃) (0.113 g, 0.190 mmol) and yielded 0.106 g, 0.067 mmol (39.3 %); **mp** 90-93 °C; **Accurate Mass**: Expected C₅₂H₆₄N₈O₁₂Nd: 1134.3721 (M), Found: 1134.3676; **δ_H** (**d₆ acetone, 400Hz**): 15.5, 12.0, -1.3, -4.8, -7.9, -11.5; **M/Z**: 567 (M^{+2}), 642 ($M+Trif$)⁺²; **IR**_{vmax} (**cm**⁻¹): 3438, 3291, 3124, 2957, 1744.5, 1631, 1250, 1080, 1030, 758.

Eu[72]

Eu[72] was prepared according to Procedure 1, using **72** (0.103 g, 0.104 mmol) and Eu(CF₃SO₃) (0.068 g, 0.114 mmol) and yielded 0.078 g, 0.049 mmol (47.1 %); **mp** 70-73

$^{\circ}\text{C}$; **Accurate Mass:** Expected $\text{C}_{52}\text{H}_{64}\text{N}_8\text{O}_{12}\text{Eu}$: 1145.3856 (M), Found: 1145.3867; δ_{H} (d_6 acetone, 400Hz): 22.3, -2.8, -3.6, -7.3, -8.4, -11.3; **M/Z:** 572 (M^{+2}), 647 ($\text{M}+\text{Trif}$) $^{+2}$; **IR** ν_{max} (cm^{-1}): 3285, 3126, 2925, 1746, 1633, 1248, 1080, 1029, 743, 699.

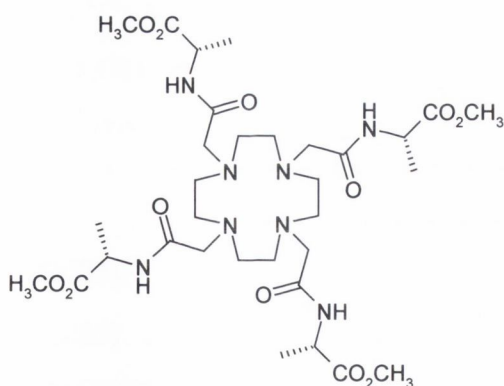
2-(2-Chloro-acetylamino)-propionic acid methyl ester¹²² [79]



Alanine methyl ester hydrochloride (3.002 g, 21.5 mmol) and triethylamine (8.94 mL, 64.5 mmol) were added to DCM (140 mL) and cooled below -10°C in a liquid nitrogen/acetone bath.

To this, a solution of chloroacetyl chloride (1.7 mL, 21.5 mmol) in DCM (30 mL) was added dropwise over an hour. The reaction was stirred at room temperature for a further 16 hours. It was filtered through celite and the filtrate was washed with water (3 x 50 mL) and with 0.1 M HCl (3 x 50 mL). The organic layer was dried over K_2CO_3 and reduced to yield a light brown solid, 2.573 g, 14.3 mmol (66.5 %). δ_{H} (CDCl_3 , 400Hz): 7.15 (1 H, bs, N-H), 4.57 (1 H, m, $\text{CHCH}_3\text{CO}_2\text{CH}_3$), 4.01 (2 H, s, ClCH_2), 3.71 (3 H, s, CO_2CH_3), 1.40 (3 H, d, $J = 7$, $\text{CHCH}_3\text{CO}_2\text{CH}_3$); δ_{C} (CDCl_3 , 100MHz): 172.2, 165.2, 52.0, 47.9, 41.8, 17.5; **IR** ν_{max} (cm^{-1}): 3300, 2956, 1744, 1666, 1536, 1454, 1271, 1164, 854.

2-(2-{4,7,10-Tris-[(methoxycarbonyl-ethylcarbamoyl)-methyl]-1,4,7,10 tetraazacyclododec-1-yl}-acetylamino)-propionic acid methyl ester [85]



Cyclen (0.213 g, 1.24 mmol), **79** (1.000 g, 5.57 mmol), cesium carbonate (1.816 g, 5.57 mmol) and potassium iodide (0.920 g, 5.57 mmol) were added to dry acetonitrile (30 mL) and freeze-thawed three times before being heated to 80°C for 48 hours. The reaction mixture was then filtered, the solvent was removed under reduced pressure and the remaining solid was dissolved in chloroform. This was washed

three times with a saturated KCl solution. The organic extract was dried over potassium carbonate and the solvent was removed under reduced pressure to yield a brown oil which was dried under vacuum to give a pale brown hygroscopic solid, 0.456 g, 6.120 mmol (49.3 %). Anal. Calcd. for $\text{C}_{32}\text{H}_{56}\text{N}_8\text{O}_{12}$: C, 51.60; H, 7.58; N, 15.04. Found: C, 51.52; H, 7.28; N, 14.74. **Accurate Mass:** Expected for $\text{C}_{32}\text{H}_{56}\text{N}_8\text{O}_{12}$: 745.4096 (MH^+), Found: 745.4058;

δ_{H} (CDCl_3 , 400MHz): 7.9 (1 H, d, $J = 7$, N-H), 4.6 (1 H, m, $J = 7$ and 7.5, $\text{CHCH}_3\text{CO}_2\text{CH}_3$), 3.7 (3 H, s, CO_2CH_3), 3.2 (2 H, dd, $J = 14$ and 17, $\text{CH}_2\text{CO}-$), 2.88 (4 H, dd, $J = 10$, cyc- CH_2), 1.4 (3 H, d, $J = 7$, $\text{CHCH}_3\text{CO}_2\text{CH}_3$); δ_{C} (CDCl_3 , 100MHz): 173.5, 170.6, 58.4, 52.5, 51.9, 47.4, 17.0; **M/Z**: 745 (M^+), 768 ($\text{M}+\text{Na}$) $^+$; **IR** ν_{max} (cm^{-1}): 3384, 3048, 2954, 2825, 1745, 1667, 1539, 1455, 1291, 1212, 1163, 1102, 1055, 1012, 951, 898, 850, 757.

La[85]

La[85] was prepared according to Procedure 1, using **85** (0.165 g, 0.166 mmol) and $\text{La}(\text{CF}_3\text{SO}_3)$ (0.107 g, 0.183 mmol) and yielded 0.128 g, 0.081 mmol (53.0 %); **mp** 262-265 °C; **Accurate Mass**: Expected for $\text{C}_{32}\text{H}_{56}\text{N}_8\text{O}_{12}\text{La}$: 883.3081 (M^+), Found: 883.3099; δ_{H} (d_6 acetone, 400 MHz): 9.2 (1 H), 4.6 (1 H), 4.0 (1 H), 3.7 (3 H), 2.9 (5H), 1.5 (4 H), 0.01 (2 H); **M/Z**: 294 (M^{+3}), 308 ($\text{M}+\text{K}$) $^{+3}$, 321 ($\text{M}+2\text{K}$) $^{+3}$, 515 ($\text{M}+\text{Trif}$) $^{+2}$, 1180 ($\text{M}+2\text{Trif}$) $^+$; **IR** ν_{max} (cm^{-1}): 3448, 2926, 2856, 1750, 1625, 1579, 1459, 1259, 1162, 1029, 956.

Eu[85]

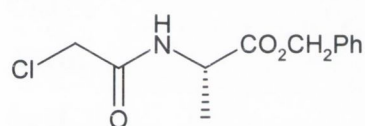
Eu[85] was prepared according to Procedure 1, using **85** (0.136 g, 0.183 mmol) and $\text{Eu}(\text{CF}_3\text{SO}_3)$ (0.120 g, 0.200 mmol) and yielded 0.046 g, 0.0338 mmol (18.5 %); **mp** 270-273 °C; **Accurate Mass**: Expected for $\text{C}_{32}\text{H}_{56}\text{N}_8\text{O}_{12}\text{Eu}$: 897.3230 (M), Found: 897.3273; δ_{H} (CD_3OD , 400 MHz): 24.4, -2.7, -4.3, -8.1, -8.9, -12.2; **M/Z**: 299 (M^{+3}), 448 (M^{+2}), 523 ($\text{M}+\text{Trif}$) $^{+2}$; **IR** ν_{max} (cm^{-1}): 3466, 2926, 2360, 1736, 1626, 1473, 1260, 1168, 1084, 1031, 958.

Tb[85]

Tb[85] was prepared according to Procedure 1, using **85** (0.199 g, 0.267 mmol) and $\text{Tb}(\text{CF}_3\text{SO}_3)$ (0.178 g, 0.294 mmol) and yielded 0.123 g, 0.091 mmol (34.3 %); **mp** 267-269 °C; **Accurate Mass**: Expected for $\text{C}_{32}\text{H}_{56}\text{N}_8\text{O}_{12}\text{Tb}$: 903.3271 (M^+), Found: 903.3276; δ_{H} (d_6 acetone, 400 MHz): 24.2, 16.9, 13.9, 1.3; **M/Z**: 301 (M^{+3}), 452 (M^{+2}), 526 ($\text{M}+\text{Trif}$) $^{+2}$, 1202 ($\text{M}+2\text{Trif}$) $^+$; **IR** ν_{max} (cm^{-1}): 3436, 3119, 2961, 2360, 1743, 1629, 1460, 1249, 1164, 1083, 1030, 959.

Yb[85]

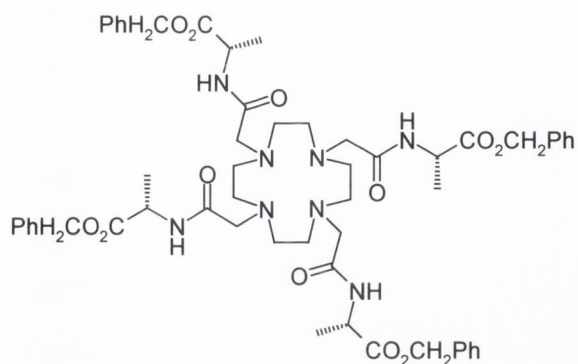
Yb[85] was prepared according to Procedure 1, using **85** (0.153 g, 0.205 mmol) and Yb(CF₃SO₃) (0.140 g, 0.226 mmol) and yielded 0.081 g, 0.059 mmol (29.3 %); **mp** 272-275 °C; **Accurate Mass**: Expected for C₃₂H₅₆N₈O₁₂Yb: 918.3406 (M⁺), Found: 918.3374; **δ_H** (**d₆ acetone, 400 MHz**): 16.8, 13.9, -1.5, -10.2, -22.3, -27.4; **M/Z**: 306 (M⁺³), 459 (M⁺²), 533 (M+Trif)⁺²; **IR_{vmax}** (**cm⁻¹**): 3446, 2925, 2360, 1743, 1637, 1459, 1260, 1163, 1084, 1031, 960, 913, 761.

2-(2-Chloro-acetylamino)-propionic acid benzyl ester [80]

L-alanine methyl benzyl hydrochloride (0.504 g, 2.32 mmol) was added to triethylamine (0.96 mL, 6.96 mmol) and toluene (20 mL) and was cooled in an acetone/liquid nitrogen bath to below -10 °C. A solution of chloroacetyl chloride (0.26 g, 2.32 mmol) in toluene (10 mL) was added dropwise over an hour, keeping the temperature below 0 °C. The reaction was stirred at room temperature for a further 16 hours. The reaction was filtered and the toluene removed from the filtrate. The remaining brown liquid was extracted with chloroform and water and then washed with 0.1M HCl. The organic layer was dried over potassium carbonate and the solvent removed under reduced pressure to yield a brown oil that solidified to an oily solid upon standing, 0.581 g, 2.27 mmol (98.1 %). Anal. Calcd for C₁₂H₁₄ClNO₃: C, 56.37; H, 5.52; N, 5.48. Found: C, 55.90; H, 5.47; N, 5.37; **δ_H** (**CDCl₃, 400MHz**): 7.36 (4.5H, m, Ar-H), 7.19 (1 H, s, N-H), 5.23 (2 H, dd, *J*₁ = 12, *J*₂ = 8, CH₂Ph), 4.68 (1 H, *J* = 8, NH-CH-CH₃), 4.03 (2 H, s, Cl-CH₂-CO-), 1.47 (3 H, d, *J* = 8, NH-CH-CH₃); **δ_C** (**CDCl₃, 100MHz**): 171.6, 165.7, 134.8, 128.2, 66.8, 48.1, 41.9, 17.6; **M/Z**: 278 (M+H₂O)⁺, 279 (M+Na)⁺; **IR_{vmax}** (**cm⁻¹**): 3278, 3073, 2966, 2362, 2343, 1731, 1656, 1556, 1452, 1353, 1313, 1224, 1141, 948, 752.

2-(2-{4,7,10-Tris-[(1-benzyloxycarbonyl-ethylcarbamoyl)-methyl]-1,4,7,10 tetraazacyclododec-1-yl}-acetylamino)-propionic acid benzyl ester [86]

Cyclen (0.098 g, 0.57 mmol), **[80]** (0.602 g, 2.3 mmol), cesium carbonate (0.75 g, 2.3 mmol) and potassium iodide (0.38 g, 5.96 mmol) were added to dry acetonitrile (30 mL) and freeze-thawed three times before being heated to 80 °C for 48 hours. The reaction mixture



was then filtered, the acetonitrile was removed under reduced pressure and the remaining solid was dissolved in chloroform. This was washed three times with KCl solution and twice with saturated 1M KOH solution. The organic extract was dried over potassium carbonate and the solvent removed

under reduced pressure to yield a brown oil which was dried under vacuum to give a light brown hygroscopic solid, 0.445 g, 4.24 mmol (74.0 %). Anal. Calcd for C₅₆H₇₂N₈O₁₂K(2H₂O): C, 59.82; H, 6.81; N, 9.97; Found: C, 60.13; H, 6.69; N, 9.98; **Accurate Mass**: Expected for C₅₆H₇₂N₈O₁₂Na: 1072.5246 (M+H+Na)⁺, Found: 1072.5205; δ_{H} (CDCl₃, 400MHz): 7.68 (1 H, s N-H), 7.36 (5H, m, Ar-H), 5.19 (2 H, dd, $J_1 = 12$, $J_2 = 8$, Ar-CH₂-), 4.71 (1 H, t, $J = 7$, NH-CH-CH₃), 3.16 (2 H, d, $J = 12$, cyc-CH₂-CO-), 2.82 (2 H, dd, $J = 10$, cyc-CH₂), 2.65 (2 H, d, $J = 10$, cyc-CH₂), 1.42 (3 H, d, $J = 7$, NH-CH-CH₃); δ_{C} (CDCl₃, 100MHz): 172.3, 170.4, 162.0, 134.9, 128.1, 66.6, 58.9, 52.4, 47.4, 17.3; **M/Z**: 524 (M²⁺) 1049 (M⁺), 1072 (M+Na)⁺; **IR** ν_{max} (cm⁻¹): 3421, 2925, 2854, 2364, 2345, 1735, 1654, 1542, 1508, 1457, 1261, 1155, 1099, 1027, 802, 736.

La[86]

La[86] was prepared according to Procedure 1, using **86** (0.129 g, 0.123 mmol) and La(CF₃SO₃) (0.079 g, 0.135 mmol) and yielded 0.056 g, 0.034 mmol (27.7 %); **mp** 120-123 °C; **Accurate Mass**: Expected for C₅₆H₇₂N₈O₁₂La(CF₃SO₃): 1336.3854 (M+Trif)⁺, Found: 1336.3857; δ_{H} (d₆ acetone, 400 MHz): 9.32 (1H, br s, N-H), 7.42 (5 H, s, Ar-H), 5.23, 4.64, 4.09, 3.79, 3.45, 1.40; **IR** ν_{max} (cm⁻¹): 3449, 2929, 1736, 1627, 1469, 1258, 1164, 1083, 1031, 957, 759.

Nd[86]

Nd[86] was prepared according to Procedure 1, using **86** (0.168 g, 0.160 mmol) and Nd(CF₃SO₃) (0.104 g, 0.176 mmol) and yielded 0.102 g, 0.062 mmol (39.2 %); **mp** 118-121 °C; **Accurate Mass**: Expected for C₅₆H₇₂N₈O₁₂Nd(CF₃SO₃): 1339.3867 (M+Trif)⁺, Found: 1339.3887; δ_{H} (d₆ acetone, 400 MHz): 15.9, 14.9, 13.3, 9.3, -15.3; **M/Z**: 447.4 (M+Trif)⁺³,

596.5 (M^{+2}), 671.1 ($M + \text{Trif}$)⁺, **IR**_{v_{max}} (**cm**⁻¹): 3448, 3281, 3118, 2958, 1742, 1626, 1579, 1459, 1248, 1162, 1082, 1029, 958, 757.

Eu[86]

Eu[86] was prepared according to Procedure 1, using **86** (0.147 g, 0.140 mmol) and Eu(CF₃SO₃) (0.092 g, 0.154 mmol) and yielded 0.072 g, 0.043 mmol (31.1 %); **mp** 96-99 °C; **Accurate Mass**: Expected for C₅₆H₇₂N₈O₁₂Eu: 1201.4482 (M^+), Found: 1201.4486; **δ_H** (**CD**₃**OD**, **400MHz**): 24.03, -2.91, -4.32, -8.42, -12.20; **M/Z**: 600 (M^{+2}), 675 ($M + \text{Trif}$)⁺², 1200 (M^+), 1350 ($M + \text{Trif}$)⁺, 1499 ($M + 2\text{Trif}$)⁺; **IR**_{v_{max}} (**cm**⁻¹): 3421, 3289, 3122, 2923, 2854, 2362, 1743, 1632, 1457, 1259, 1162, 1029, 958, 802, 759.

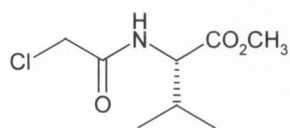
Tb[86]

A brown solid was obtained and was crystallised from methanol/ether to give brown crystals.

Tb[86] was prepared according to Procedure 1, using **86** (0.182 g, 0.173 mmol) and Tb(CF₃SO₃) (0.115 g, 0.191 mmol) and yielded 0.103 g, 0.062 mmol (36.3 %); **mp** 210-212 °C; **Accurate Mass**: Expected for C₅₆H₇₂N₈O₁₂Tb: 1207.4523 (M^+), Found: 1207.4496; **δ** (**CD**₃**CN**, **400MHz**): 24.76, 25.06, 13.6, 10.45 -1.9, -1.4; **M/Z**: 603 (M^{+2}), 1206 (M^+), 1355 ($M + \text{Trif}$)⁺, 1505 ($M + 2\text{Trif}$)⁺, 1676 ($M + 3\text{Trif}$)⁺; **IR**_{v_{max}} (**cm**⁻¹): 3448, 3270, 3120, 2960, 2923, 2360, 2343, 1741, 1629, 1457, 1257, 1160, 1029, 960, 802;

Yb[86]

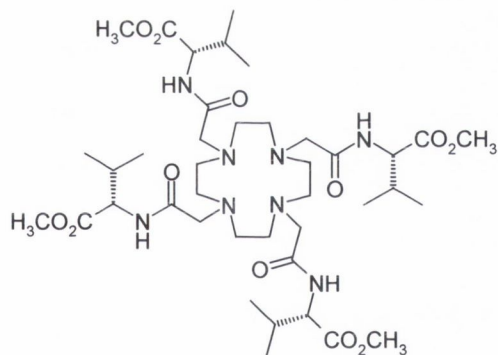
Yb[86] was prepared according to Procedure 1, using **86** (0.159 g, 0.151 mmol) and Yb(CF₃SO₃) (0.103 g, 0.167 mmol) and yielded 0.108 g, 0.065 mmol (43.2 %); **mp** 112-115 °C; **Accurate Mass**: Expected for C₅₆H₇₂N₈O₁₂Yb(CF₃SO₃): 1371.4179 ($M + \text{Trif}$)⁺, Found: 1371.4121; **δ_H** (**d**₆ **acetone**, **400 MHz**): 16.9, 13.9, -1.0, -10.3, -22.5, -27.6; **M/Z**: 407 ($M^+/3$); 611 ($M^+/2$); 685 ($M\text{trif}^+/2$); **IR**_{v_{max}} (**cm**⁻¹): 3449, 2925, 2360, 2342, 1737, 1631, 1459, 1256, 1164, 1084, 1030.

2-(2-Chloro-acetylamino)-3-methyl-butyric acid methyl ester¹²² [81]

L-Valine methyl ester hydrochloride (2.000 g, 12.0 mmol) and triethylamine (5.0 mL, 36.0 mmol) were added to DCM (80 mL) and cooled below -10°C in a liquid nitrogen/acetone bath. To this a

solution of chloroacetyl chloride (0.95 mL, 12.0 mmol) in DCM (30 mL) was added dropwise over an hour. The reaction was stirred at room temperature for a further 16 hours.

It was filtered through celite and the filtrate was washed with water (3 x 100 mL) and 0.1 M HCl (3 x 100 mL). The organic layer was dried over K_2CO_3 and reduced to yield a brown oil, 1.895 g, 9.17 mmol (76.4 %). δ_{H} (CDCl_3 , 400Hz): 7.07 (1 H, d, N-H), 4.46 (1 H, CH), 4.02 (2 H, s, Cl- CH_2 -), 3.70 (3 H, t $J = 7.1$, CO_2CH_3), 2.17 (1 H, CH), 0.91 (6H, m, $\text{CH}(\text{CH}_3)_2$); δ_{C} (CDCl_3 , 100Hz): 171.2, 165.5, 56.9, 51.7, 42.0, 30.7, 18.3, 17.1; IR_{vmax} (cm^{-1}): 3300, 2967, 1739, 1665, 1536, 1438, 1359, 1212, 1003, 758.

3-Methyl-2-(2-{4,7,10-tris-[(1-methoxycarbonyl-2-methylpropylcarbamoyl)-methyl]-1,4,7,10 tetraaza-cyclododec-1-yl}-acetylamino)-butyric acid methyl ester [87]

A solution of **81** (0.581 g, 4.18 mmol) in dry acetonitrile (10 mL) was added to cyclen (0.175 g, 1.02 mmol), cesium carbonate (1.36 g, 4.18 mmol) and potassium iodide (0.694 g, 4.18 mmol) in dry acetonitrile (30 mL). The mixture was then refluxed under argon for 48 hours. This was filtered through celite and reduced before the residue was taken up in chloroform and washed with saturated KCl solution (3 x 100 mL). The organic layer was dried over K_2CO_3 and reduced to yield a brown oil which was dried under vacuum to give a brown powder, 2.135 g, 2.49 mmol (59.6 %). **mp** 131-134 $^{\circ}\text{C}$; Anal. Calcd for $\text{C}_{40}\text{H}_{72}\text{N}_8\text{O}_{12}$: C, 56.06; H, 8.47; N, 13.07. Found: C, 56.22; H, 8.31; N, 13.38. δ_{H} (CDCl_3 , 400Hz): 7.63 (1 H, bs, N-H), 4.5 (1 H, q, -CH), 3.7 (3 H, s, $\text{CO}_2\text{-CH}_3$), 3.29 (2 H, s, Cl- CH_2), 2.21 (4 H, dd, cyc- CH_2), 0.97 (6 H, t, $\text{CH}(\text{CH}_3)_2$); δ_{C} (CDCl_3 , 400Hz): 172.4, 170.6, 58.5, 56.6, 51.7, 30.3, 18.7, 17.9; **M/Z**: 428 (M^{+2}), 857.5 ($\text{M}+\text{H}$)⁺, Expected, 857.5348; IR_{vmax} (cm^{-1}): 3368, 2965, 1743, 1670, 1534, 1436, 1263, 1209, 1153, 1112, 1005, 753.

La[87]

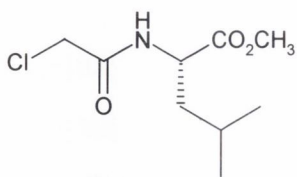
La[87] was prepared according to Procedure 1, using **87** (0.138 g, 0.161 mmol) and $\text{La}(\text{CF}_3\text{SO}_3)$ (0.104 g, 0.177 mmol) and yielded 0.114 g, 0.079 mmol (49.2 %); **mp** 65-67 °C; **Accurate Mass**: Expected for $\text{C}_{40}\text{H}_{72}\text{N}_8\text{O}_{12}\text{La}(\text{CF}_3\text{SO}_3)$: 1144.3854 (M^+), Found: 1144.3822; δ_{H} (d_6 acetone, 400 MHz): 8.33, 4.9, 3.7, 3.4, 1.9, 1.1, 0.9; **M/Z**: 331 (M^{+3}), 467 ($\text{M}+2\text{Trif}+6\text{H}_2\text{O}$) $^{+3}$, 480 ($\text{M}+3\text{Trif}$) $^{+3}$, 497 (M^{+2}), 572 ($\text{M}+2\text{Trif}$) $^{+2}$; **IR** ν_{max} (cm^{-1}): 3454, 3283, 3122, 2968, 1744, 1623, 1455, 1241, 1169, 1084, 1031.

Eu[87]

Eu[87] was prepared according to Procedure 1, using **87** (0.173 g, 0.202 mmol) and $\text{Eu}(\text{CF}_3\text{SO}_3)$ (0.133 g, 0.222 mmol) and yielded 0.135 g, 0.093 mmol (45.8 %); **mp** 68-70 °C; **Accurate Mass**: Expected for $\text{C}_{40}\text{H}_{72}\text{N}_8\text{O}_{12}\text{Eu}(\text{CF}_3\text{SO}_3)$: 1158.4002 (M^+), Found: 1158.3923; δ_{H} (d_6 acetone, 400 MHz): 13.4, -1.3, -4.6, -8.9, -14.0, -20.5; **M/Z**: 336 (M^{+3}), 504 (M^{+2}), 578 ($\text{M}+\text{Trif}$) $^{+2}$, 1306 ($\text{M}+\text{Trif}$) $^{+}$; **IR** ν_{max} (cm^{-1}): 3453, 3282, 3120, 1742, 1627, 1459, 1244, 1166, 1084 1031.

Yb[87]

Yb[87] was prepared according to Procedure 1, using **87** (0.165 g, 0.192 mmol) and $\text{Yb}(\text{CF}_3\text{SO}_3)$ (0.131 g, 0.212 mmol) and yielded 0.147 g, 0.099 mmol (51.9 %); **mp** 75-78 °C; **Accurate Mass**: Expected for $\text{C}_{40}\text{H}_{72}\text{N}_8\text{O}_{12}\text{Yb}(\text{CF}_3\text{SO}_3)$: 1179.4179 (M^+), Found: 1179.4167; δ_{H} (d_6 acetone, 400 MHz): 19.5, -3.3, -4.9, -7.7, -9.8, -17.2; **M/Z**: 303 ($\text{M}+\text{Trif}+\text{K}$) $^{+4}$, 343 (M^{+3}), 357 ($\text{M}+\text{K}$) $^{+2}$, 515 (M^{+2}), 590 ($\text{M}+\text{Trif}$) $^{+2}$; **IR** ν_{max} (cm^{-1}): 3463, 3283, 3119, 2963, 2926, 1740, 1631, 1579, 1572, 1466, 1251, 1165, 1084, 1031.

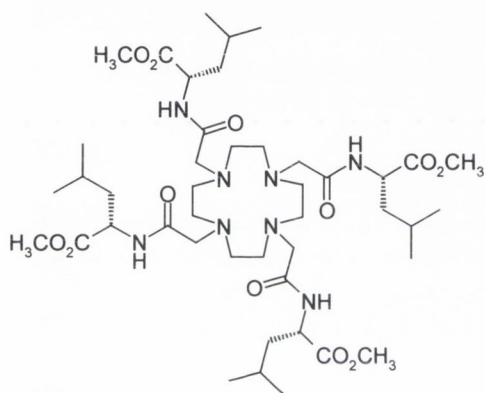
2-(2-Chloro-acetylamino)-3-methyl-pentanoic acid methyl ester¹²² [82]

L-Leucine methyl ester hydrochloride (4.003 g, 22.0 mmol) and triethylamine (9.0 mL, 66.0 mmol) were added to DCM (100 mL) and cooled below -10 °C in a liquid nitrogen/acetone bath. To this a solution of chloroacetyl chloride (1.75 mL, 22.0 mmol) in DCM (40

mL) was added dropwise over an hour. The reaction was stirred at room temperature for a further 16 hours. It was filtered through celite and the filtrate was washed with water (2 x

100 mL) and with 0.1 M HCl (3 x 50 mL). The organic layer was dried over K_2CO_3 and reduced to give a brown oil, 3.726, 16.8 mmol (76.3 %). δ_H ($CDCl_3$, 400Hz): 6.91 (1 H, d, N-H), 4.49 (1 H, dt, CH), 4.08 (2 H, s, Cl-CH₂-), 3.77 (3 H, t, CO₂CH₃), 1.70 (3 H, m, CH₂CH(CH₃)₂), 0.98 (6H, d, CH(CH₃)₂); δ_C ($CDCl_3$, 100Hz): 172.2, 165.2, 51.9, 50.6, 41.9, 40.9, 24.4, 22.2, 21.5; $IR_{v_{max}}$ (cm^{-1}): 3296, 3071, 2957, 1738, 1658, 1547, 1439, 1370, 1230, 1160, 1025, 982, 757.

4-Methyl-2-(2-{4,7,10-tris-[(1-methoxycarbonyl-3-methylbutylcarbamoyl)-methyl]-1,4,7,10 tetraaza-cyclododec-1-yl}-acetylamino)-pentanoic acid methyl ester [88]



A solution of **82** (2.011 g, 9.64 mmol) in dry acetonitrile (10 mL) was added to cyclen (0.405 g, 2.35 mmol), cesium carbonate (3.142 g, 9.64 mmol) and potassium iodide (1.602 g, 9.64 mmol) in dry acetonitrile (40 mL). This was then refluxed under argon for 48 hours. The mixture was filtered through celite and reduced before the residue was taken up in chloroform and washed with a saturated KCl solution (3 x 100 mL). The organic layer was dried over K_2CO_3 and reduced to give a brown oil which was dried under vacuum to yield a brown powder, 4.642 g, 5.08 mmol (52.7 %). Anal. Calcd for $C_{44}H_{80}N_8O_{12} \cdot H_2O$: C, 56.75; H, 8.88; N, 12.03. Found: C, 57.03; H, 8.55; N, 11.77. **mp** 83-85 °C; δ_H ($CDCl_3$, 400Hz): 7.48 (1 H, bs, N-H), 4.63 (1 H, q, -CH), 3.70 (3 H, d, CO₂-CH₃), 3.21 (2 H, d, CO-CH₂), 2.88 (4 H, dd, cyc-CH₂), 1.66 (3 H, m, CH₂CH(CH₃)₂), 0.94 (6H, t, CH(CH₃)₂); δ_C ($CDCl_3$, 100Hz): 173.3, 170.1, 58.7, 52.3, 51.7, 49.9, 40.6, 24.5, 22.3, 21.3; **M/Z**: 912.4 (M^+); $IR_{v_{max}}$ (cm^{-1}): 3437, 2957, 1743, 1655, 1543, 1449, 1376, 1261, 1157, 1101, 809.

La[88]

La[88] was prepared according to Procedure 1, using **88** (0.119 g, 0.130 mmol) and $La(CF_3SO_3)_3$ (0.084 g, 0.143 mmol) and yielded 0.092 g, 0.061 mmol (47.0 %); **mp** 105-107 °C; **Accurate Mass**: Expected for $C_{44}H_{80}N_8O_{12}La$: 1051.4959 (M^+), Found: 1051.5028; δ_H (d_6 acetone, 400 MHz): 9.1, 5.2, 4.1, 2.9, 1.7, 1.1, 0.2; **M/Z**: 350 (M^{+3}), 364 ($M+K+H$)⁺³,

525 (M^{+2}), 600 ($M+\text{Trif}^{+2}$); $\text{IR}_{\text{vmax}} (\text{cm}^{-1})$: 3471, 3115, 2961, 2925, 1743, 1626, 1579, 1459, 1280, 1239, 1167, 1083, 1030, 963.

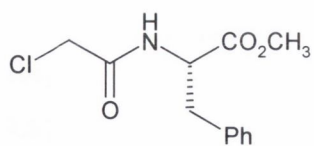
Eu[88]

Eu[88] was prepared according to Procedure 1, using **88** (0.156 g, 0.171 mmol) and $\text{Eu}(\text{CF}_3\text{SO}_3)$ (0.113 g, 0.188 mmol) and yielded 0.133 g, 0.088 mmol (51.3 %); **mp** 103-105 °C; **Accurate Mass**: Expected for $\text{C}_{44}\text{H}_{80}\text{N}_8\text{O}_{12}\text{Eu}$: 1065.5108 (M^+), Found: 1065.5161; δ_{H} (**d_6 acetone, 400 MHz**): 24.2, 19.1, -2.1, -3.7, -22.7, -24.8; **M/Z**: 355 (M^{+3}), 367.9 ($M+\text{K}^{+3}$), 532 (M^{+2}), 606 ($M+\text{Trif}^{+2}$); $\text{IR}_{\text{vmax}} (\text{cm}^{-1})$: 3476, 3281, 3113, 2961, 1743, 1629, 1582, 1469, 1248, 1164, 1082, 1031.

Yb[88]

Yb[88] was prepared according to Procedure 1, using **[88]** (0.160 g, 0.175 mmol) and $\text{Yb}(\text{CF}_3\text{SO}_3)$ (0.119 g, 0.193 mmol) and yielded 0.106 g, 0.069 mmol (39.3 %); **mp** 105-107 °C; **Accurate Mass**: Expected for $\text{C}_{44}\text{H}_{80}\text{N}_8\text{O}_{12}\text{Yb}$: 1086.5284 (M^+), Found: 1086.5338; δ_{H} (**d_6 acetone, 400 MHz**): 28.4, 13.3, -4.2, -8.7, -15.5, -19.6; **M/Z**: 362 (M^{+3}), 375 ($M+\text{Trif}+\text{K}^{+3}$), 450 ($M+\text{Trif}+3\text{K}^{+3}$), 542 (M^{+2}), 618 ($M+\text{Trif}^{+2}$); $\text{IR}_{\text{vmax}} (\text{cm}^{-1})$: 3456, 3275, 3117, 2962, 2876, 1743, 1632, 1471, 1249, 1164, 1083, 1031.

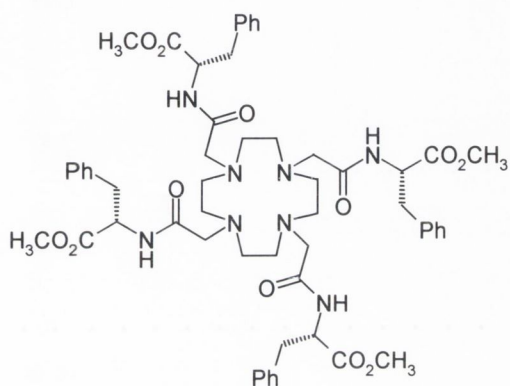
2-(2-Chloro-acetylamino)-3-phenyl-propionic acid methyl ester¹²² [83]



Phenylalanine methyl ester hydrochloride (3.002 g, 13.9 mmol) and triethylamine (3.9 mL, 27.8 mmol) were added to DCM (150 mL) and cooled below -10 °C in a liquid nitrogen/acetone bath. To this a solution of chloroacetyl chloride (1.1 mL, 13.9 mmol) in DCM (30 mL) was added dropwise over an hour. The reaction was stirred at room temperature for a further 16 hours. It was filtered through celite and the filtrate was washed with water (3 x 50 mL) and with 0.1 M HCl (3 x 50 mL). The organic layer was dried over K_2CO_3 and reduced to yield a pale brown solid, 3.268 g, 12.7 mmol (91.4 %). **mp** 68-72 °C, (lit²⁸⁰ 68-71 °C); $\delta_{\text{H}}(\text{CDCl}_3, 400 \text{ MHz})$: 7.3 (3 H, t, Ar-H), 7.1 (2 H, d, Ar-H), 7.01 (1 H, bs, N-H), 4.9 (1 H, d, $J=6$, CH), 4.0 (2 H, s, CH_2Cl), 3.7 (3 H, s, CO_2CH_3) 3.17 (2 H, t, $J=6$,

CH-CH₂-Ph); IR_{vmax} (cm⁻¹): 3327, 3030, 2955, 2854, 1730, 1647, 1536, 1446, 1369, 1307, 1226, 1205, 1154, 1116, 1075, 988.

3-Phenyl-2-(2-{4,7,10-tris-[(1-methoxycarbonyl-2-phenyl-ethylcarbamoyl)-methyl]-1,4,7,10 tetraaza-cyclododec-1-yl}-acetylamino)-propionic acid methyl ester [89]



A solution of **83** (1.456 g, 5.69 mmol) in dry acetonitrile (10 mL) was added to cyclen (0.234 g, 1.39 mmol), potassium carbonate (0.786 g, 5.69 mmol) and potassium iodide (0.945 g, 5.69 mmol) in dry acetonitrile (40 mL). This was then refluxed under argon for 48 hours. The mixture was filtered through celite and reduced before the residue was taken up in chloroform and washed with a saturated

KCl solution (3 x 100 mL). The organic layer was dried over K₂CO₃ and reduced to yield a brown oil which was dried under vacuum to give a white powder, 0.846 g, 0.806 mmol (57.9 %). Anal. Calcd for C₅₆H₇₂N₈O₁₂·2H₂O: C, 61.98; H, 7.06; N, 10.32. Found: C, 62.39; H, 7.26; N, 9.99. **mp** 160 °C; δ_H (CDCl₃, 400 MHz): 7.5 (1 H, br s, N-H), 7.3 (3 H, m, Ar-H), 7.1 (2 H, d, Ar-H), 4.9 (1 H, q, CH), 3.6 (3 H, s, CO₂CH₃), 3.1 (2 H, m, CH₂), 2.9 (4 H, dd, cyc-CH₂); δ_C (CDCl₃, 100 MHz): 172.7, 170.5, 136.2, 128.9, 128.6, 128.0, 126.1, 58.3, 52.3, 51.9, 51.8, 37.3; **M/Z** : 525 (M⁺²), 1049 (M⁺); IR_{vmax} (cm⁻¹): 3371, 3061, 2952, 2821, 1744, 1664, 1525, 1436, 1353, 1215, 1353, 1215, 1123, 1031.

La[89]

La[89] was prepared according to Procedure 1, using **89** (0.171 g, 0.163 mmol) and La(CF₃SO₃) (0.105 g, 0.179 mmol) and yielded 0.156 g, 0.096 mmol (58.6 %); **Accurate Mass**: Expected for C₅₆H₇₂N₈O₁₂La: 1187.4333 (M⁺), Found: 1187.4372; δ_H (d₆ acetone, 400 MHz): 9.5, 7.4, 5.0, 3.8, 3.4, 2.8, 1.1, 0.0; **M/Z**: 396 (M⁺³), 409 (M+K)⁺³, 616 (M+Na+H₂O)⁺², 668 (M+Trif)⁺², IR_{vmax} (cm⁻¹): 3461, 3280, 3119, 2957, 1745, 1625, 1456, 1279, 1252, 1168, 1031, 956, 760, 704.

through celite and reduced before the residue was taken up in chloroform and washed with KCl solution (3 x 100). The organic layer was dried over K_2CO_3 and reduced to give a yellow oil which was dried under vacuum to yield a yellow, hygroscopic solid, 0.234 g, 0.173 mmol (50.0 %). Anal. Calcd for $C_{80}H_{88}N_8O_{12} \cdot 2H_2O$: C, 69.15; H, 6.67; N, 8.06. Found: C, 68.89; H, 6.29; N, 8.42. δ_H ($CDCl_3$, 400Hz): 7.52 (1 H, br s, N-H), 7.29 (3 H, Ar-H), 7.27 (2 H, Ar-H), 7.21 (3 H, d, Ar-H), 7.04 (2 H, d, Ar-H), 5.16 (2 H, dd, CH_2), 4.9 (1 H, t, $NH-CH-CH_3$), 3.1 (2 H, m, CH_2), 2.9 (2 H, t, CH_2), 2.5 (4 H, dd, cyc- CH_2); δ_C ($CDCl_3$, 100Hz): 172.1, 170.3, 139.2, 128.9, 128.3, 127.8, 127.6, 125.4, 72.8, 58.0, 57.3, 52.2, 38.3; **M/Z**: 677 (M^{+2}), 1353.6549 ($M+H$)⁺, Expected: 1353.6600; **IR**_{vmax} (cm^{-1}): 3399, 2925, 2359, 2359, 1740, 1667, 1517, 1454, 1384, 1260, 1211, 1106, 1020, 801, 752.

La[90]

La[90] was prepared according to Procedure 1, using **90** (0.186 g, 0.137 mmol) and $La(CF_3SO_3)$ (0.088 g, 0.151 mmol) and yielded 0.104 g, 0.053 mmol (39.2 %); **Accurate Mass**: Expected for $C_{80}H_{88}N_8O_{12}La(CF_3SO_3)$: 1640.5106 (M^+), Found: 1640.5020; δ_H (acetone, 400Hz): 7.4 (10 H, m, Ar-H), 5.3 (2 H, br s), 5.0 (1 H, $CH-CH_2-Ph$), 3.3 (4 H, d), 1.3 (3 H, d, CO_2CH_3), 0.7 (2 H); δ_C ($CDCl_3$, 100Hz): 204, 170, 137, 136, 130.2, 129.3, 129.2, 129.0, 128.9, 67, 65, 55.4, 55.3, 53.5, 37, 15; **M/Z**: 497 ($M^+/3$), 511 ($M+K$)⁺³, 523 ($M+2K$)⁺³, 768 ($M+K$)⁺², 820 ($M+Trif$)⁺²; **IR**_{vmax} (cm^{-1}): 3465, 3268, 3115, 2924, 1745, 1625, 1455, 1277, 1249, 1170, 1108, 1030, 952, 758, 700.

Eu[90]

La[90] was prepared according to Procedure 1, using **90** (0.122 g, 0.090 mmol) and $La(CF_3SO_3)$ (0.059 g, 0.099 mmol) and yielded 0.096 g, 0.049 mmol (54.6 %); **mp** 183-186 °C; **Accurate Mass**: Expected for $C_{80}H_{88}N_8O_{12}Eu$: 1505.5734 (M^+), Found: 1505.5660; δ_H (d_6 acetone, 400Hz): 14.5, -2.3, -8.4, -9.7, -12.4, -22.3; **M/Z**: 502 (M^{+3}), 827 ($M+Trif$)⁺²; **IR**_{vmax} (cm^{-1}): 3466, 3267, 3121, 2924, 2360, 1744, 1628, 1456, 1250, 1168, 1030, 758, 700.

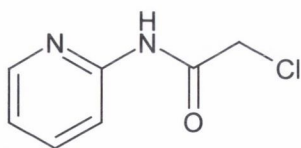
6.2 Synthesis for Chapter 2

Potentiometric Titrations

The measurements have been made at 37 °C and all the solutions were prepared with degassed and doubly distilled water. The ionic strength was fixed at $I = 0.1$ M with tetramethylammonium chloride (ALDRICH). The potentiometric titrations were performed using an automatic titrator system, MOLSPIN, equipped with a combined glass electrode (Metrohm, filled with KCl 3 M solution) and connected to a Gateway microcomputer. The electrodes were calibrated to read pH according to the classical method. (A.E.Martell, R.J.Motekaitis, *Determination and use of Stability Constants*, 2nd ed., VCH Publishers, New York, 1992.) The lanthanum (III) complex of 0.00049 M were titrated with standardized 0.082 M tetramethylammonium hydroxide. Argon was bubbled through the solutions to exclude CO₂ and O₂. Tetramethylammonium hydroxide solution was standardized against potassium hydrogenphthalate. Carbonate content was checked by Gran's method. The titration data were refined by the non-linear least squares refinement program SUPERQUAD (P.Gans, A.Sabatini, A.Vacca, *J.Chem.Soc., Dalton Trans.* 1985, 1195-2000.) to determine the deprotonation constants. Typically, about 250 data points were collected over the pH range 4-11. The value of the pK_a is the mean value calculated from three independent titrations.

6.3 Synthesis for Chapter 3

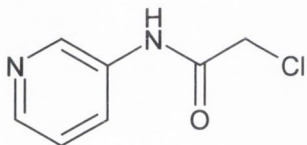
2-Chloro-N-pyridin-2-yl acetamide [100]



4-chloropyridine (18.8 g, 0.20 mol) and triethylamine (27.5 mL, 0.20 mol) were added to THF (150 mL) and cooled to below 0 °C in an acetone/liquid nitrogen bath. To this, a solution of chloroacetyl chloride (17.6 mL, 0.22 mol) in DCM (20 mL) was added dropwise over an hour, maintaining the temperature below 0 °C. A brown precipitate was observed. The reaction mixture was left to stir at room temperature for four hours. The mixture was filtered through celite and the solvent removed under reduced pressure. The residue was taken up in DCM and washed repeatedly with water. The organic layer was dried over K₂CO₃ and the solvent was removed under reduced pressure to yield a brown solid. This was recrystallised from methanol to give a yellow powder, 27.9 g, 0.16 mol (81.8 %). δ_{H} (DMSO, 400MHz):

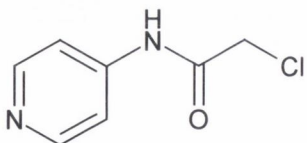
8.38 (1 H, s, N-H), 8.46 (2 H, d, $J = 6$ Ar-H), 7.57 (2 H, dd, $J_1 = 1.5, J_2 = 3.5$ Ar-H), 4.21 (2 H, s, NH-CH₂-COCl); **M/Z**: 171 (MH⁺).

2-Chloro-N-pyridin-3-yl acetamide [101]



4-chloropyridine (4.712 g, 0.05 mol) and triethylamine (5.554 g, 0.055 mol) were added to DCM and cooled to below 0 °C in a acetone/liquid nitrogen bath. To this, a solution of chloroacetyl chloride (6.187 g, 0.055 mol) in DCM (20 mL) was added dropwise over an hour, maintaining the temperature below 0 °C. A bright yellow precipitate was observed. The reaction mixture was left to stir at room temperature for four hours. The precipitate was filtered and the filtrate was washed with 1 M HCl. The organic layer was discarded and the pH of the aqueous layer was adjusted using KOH solution until a precipitate was observed (pH ~ 5). This was extracted with chloroform and the organic extract was dried over potassium carbonate and the solvent removed under reduced pressure. The brown solid was recrystallised from methanol to give a yellow powder, 6.363 g, 0.037 mol (74.6 %). δ_{H} (DMSO, 400MHz): 10.67 (1 H, s, N-H), 8.46 (2 H, d, $J = 6$ Ar-H), 7.57 (2 H, dd, $J_1 = 1.5, J_2 = 3.5$ Ar-H), 4.31 (2 H, s, NH-CH₂-COCl); δ_{C} (DMSO, 100MHz): 162, 141, 139.5, 58.4; **M/Z**: 171 (MH⁺), 210 (M+K)⁺

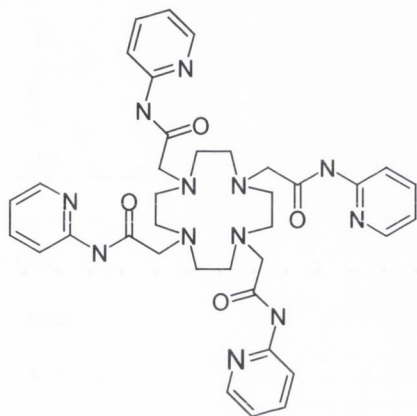
2-Chloro-N-pyridin-4-yl acetamide [102]



4-chloropyridine (4.712 g, 0.05 mol) and triethylamine (5.554 g, 0.055 mol) were added to DCM and cooled to below 0 °C in a acetone/liquid nitrogen bath. To this, a solution of chloroacetyl chloride (6.187 g, 0.055 mol) in DCM (20 mL) was added dropwise over an hour, maintaining the temperature below 0 °C. A bright yellow precipitate was observed. The reaction mixture was left to stir at room temperature for four hours. The precipitate was filtered and the filtrate was washed with 1 M HCl. The organic layer was discarded and the pH of the aqueous layer was adjusted using KOH solution until a precipitate was observed (pH ~ 5). This was extracted with chloroform and the organic extract was dried over potassium carbonate and the solvent removed under reduced pressure.

The brown solid was recrystallised from methanol to give a yellow powder, 6.363 g, 0.037 mol (74.6 %). δ_{H} (DMSO, 400MHz): 10.67 (1 H, s, N-H), 8.46 (2 H, d, $J = 6$ Ar-H), 7.57 (2 H, dd, $J_1 = 1.5$, $J_2 = 3.5$ Ar-H), 4.31 (2 H, s, NH-CH₂-COCl); δ_{C} (DMSO, 100MHz): 162, 141, 139.5, 58.4; M/Z: 171 (MH⁺), 193 (M+Na)⁺.

1,4,7,10-Tetrakis(2-aminopyridine-acetamide)-1,4,7,10-tetraazacyclododecane [103]



Cyclen (1.5.2 g, 8.72 mmol), **100** (6.091 g, 35.7 mmol), potassium carbonate (4.903 g, 35.7 mmol) and potassium iodide (5.929 g, 35.7 mmol) were added to dry DMF and freeze-thawed three times before being heated to 80 °C for 48 hours. The reaction mixture was then filtered, the DMF was removed under reduced pressure and the remaining solid was dissolved in chloroform. This was washed three times with water and twice with saturated potassium chloride solution. The organic extract was

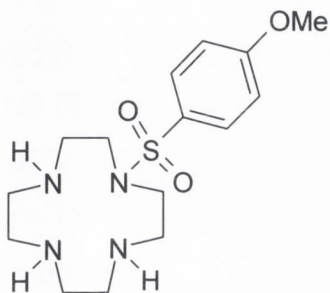
dried over potassium carbonate and the solvent removed under reduced pressure, to give a brown solid. This was crystallised from methanol to yield a white powder, 1.877 g, 2.65 mmol (30.4 %). Anal. Calcd for C₃₆H₄₄N₁₂O₄: C, 61.00; H, 6.26; N, 23.71. Found: C, 59.34; H, 6.02; N, 23.21. mp 104-106 °C; δ_{H} (CDCl₃, 400MHz): 9.62 (1 H, s, N-H), 8.12 (2 H, d, $J = 7$, Ar-H), 7.65 (1 H, t, $J = 7$ Ar-H), 6.91 (1 H, t, $J = 6$ Ar-H), 3.38 (2 H, s, -CH₂-CO-NH-), 2.9 (4 H, s, cyc-CH₂); δ_{C} (CDCl₃, 100MHz): 150.6, 147.5, 137.4, 119., 118.7, 113.6, 113.1, 76.6, 60.7, 59.5, 54.2, 46.4; M/Z: 355 (M²⁺); IR_{vmax} (cm⁻¹): 3430, 2962, 2923, 28.50, 2375, 2323, 1685, 1560, 1508, 1432, 1299, 1097, 779.

Eu[103]

103 (0.253 g, 0.36 mmol) was dissolved in methanol (5 mL) and this was added to water (30 mL) To this was added europium oxide (0.134 g, 0.4 mmol). This was refluxed for 48 hours. The reaction mixture was filtered and the filtrate reduced and dried. The product was purified by column chromatography, using neutral alumina (eluting from 100 % DCM to 90 % DCM, 10 % methanol). This gave a cream hydrophobic solid, in 20 % yield. δ_{H} (CD₃OD,

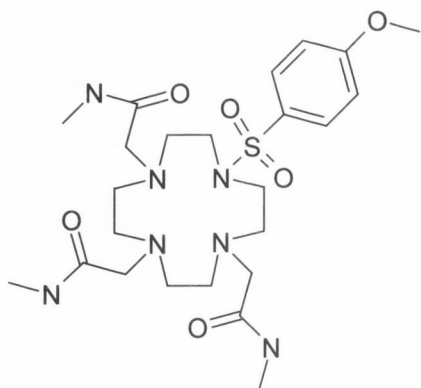
400 MHz): 38.87 (cyc), 8.38 (1 H, s, Ar-H), 7.62 (1 H, s, Ar-H), 6.75 (2 H, s, Ar-H), -5.39 (cyc), -9.495 (cyc), -15.55 (cyc), -20.00 (cyc); **IR**_{vmax} (cm⁻¹): 3401, 2923, 2852, 2377, 1617, 1398, 1261, 1085, 1020, 937, 800, 715.

1-(4-Methoxy-benzenesulphonyl)-1,4,7,20-tetraazacyclododecane [107]



Cyclen (1.00 g, 5.8 mmol) was added to CHCl₃ (50 mL) and heated to 36-37 °C. To this was added a solution of 4-methoxy phenyl sulphonyl chloride (1.20 g, 5.8 mmol) in CHCl₃ (100 mL) over a period of 8 hours. The solution was stirred overnight before being reduced to approximately 50 mL. A white solid precipitated out of this solution and was filtered off. The remaining organic solution was reduced to yield the product as a white solid, 1.6 g, 80 %. This was purified by silica column chromatography using 90:10, MeCN: MeOH (53 % recovery), to yield 0.565 g, 1.64 mmol (28.3 %) of **107** as a white solid. Expected for C₁₅H₂₇N₄O₃S: 343.1804 (MH⁺), Found: 343.1806; δ_{H} (acetone, 400Hz): 7.72 (2 H, d, *J* = 9, Ar-H), 7.01 (2 H, d, *J* = 8.5, Ar-H), 3.88 (3 H, s), 3.40 (4 H, d, *J* = 4.5, CH₂), 3.18 (4 H, d, *J* = 5, CH₂), 3.00 (4 H, d, *J* = 4, CH₂), 2.87 (4 H, d, *J* = 5, CH₂); δ_{C} (CDCl₃, 100Hz): 162.9, 128.8, 114.1, 55.2, 49.3, 48.5, 48.2, 45.5; **M/Z**: 342.2 (M⁺), 365.1 (M+Na)⁺; **IR**_{vmax} (cm⁻¹): 3432, 3095, 3008, 2842, 1712, 1594, 1492, 1438, 1363, 1261, 1222, 1155, 1091, 1052, 1024, 927, 890, 842, 804, 761.

1,4,7-Tris (N-methyl acetamide) 10, - (4- methoxy phenyl sulphonyl) - 1,4,7,10 - tetraazacyclododecane [111]



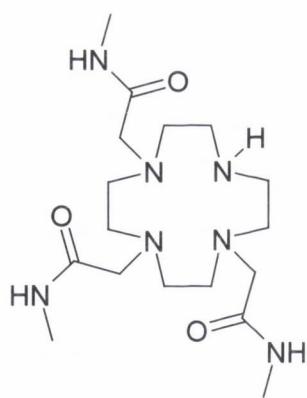
107 (1.31 g, 3.8 mmol) was dissolved in DMF (12 mL) and cesium carbonate (3.86 g, 11.8 mmol), potassium iodide (1.97 g, 11.8 mmol) and chloro-N-methyl acetamide (1.27 g, 11.8 mmol) was added. The solution was freeze-thawed twice and heated to 80 °C under argon for 16 hours. It was filtered and the filtrate added to a vigorously stirring 50/50 mixture of water and DCM. The organic layer was washed with brine, dried over K₂CO₃ and reduced, yielding 1.413 g, 2.54 mmol (91.8 %) of a yellow liquid. 600 mg were purified on an alumina column using 97:3, Ethyl acetate: Methanol, to yield 320 mg of

a yellow resin. Expected for $C_{24}H_{42}N_7O_6S$: 556.2917, Found: 556.2906; δ_H ($CDCl_3$, 400 MHz): 7.72 (2 H d, $J = 5.0$ Hz), 7.03 (2 H d, $J = 6.52$ Hz), 3.90 (3 H, s), 3.16 (s, 9H), 3.05 (3 H, s), 2.85 (8H,s), 2.67 (4 H, s); δ_C ($CDCl_3$, 100 MHz): 162.9, 129.2, 114.5, 77.2, 76.7, 75.9, 55.2, 52.9, 52.6, 48.8; M/Z : 556.6 (M^+), 578.6 ($M+Na$)⁺; $IR_{v_{max}}$ (cm^{-1}): 3421, 3077, 2925, 2854, 1654, 1596, 1542, 1457, 1409, 1338, 1261, 1155, 1093, 1022, 841, 840, 728.

Eu[111]

[111] (0.042 g, 0.075 mmol) was dissolved in dry acetonitrile (4ml) and europium triflate (0.05 g, 0.083 mmol) was added. This was freeze thawed twice and then refluxed under argon for 14 hours. It was added dropwise to stirring ether and a solid precipitated out which was filtered off. Yield: 47.6 %; Anal. Calcd for $C_{24}H_{41}N_7O_6.SEu(CF_3SO_3)$: C, 35.05; H, 4.82; N, 11.44. Found: C, 35.33; H, 4.64; N, 10.99. δ_H ($CDCl_3$, 400MHz): 30.1, 19.5, 15.8, 12.6, 9.5, 7.9, 7.2, 7.1, 1.96, -3.5, 6.8; M/Z : 857($M+Trif$)⁺, 1007($M+2Trif$)⁺; $IR_{v_{max}}$ (cm^{-1}) 3399, 2958, 2921, 2852, 2370, 2345, 1637, 1457, 1261, 1157.93, 1089.59, 1027.87, 802.24.

1,4,7-tris(N-methyl acetamide),1,4,7,10-tetraazacyclododecane [112]



111 (0.393 g, 0.707 mmol) was dissolved in THF (30 mL) and ethanol (2 mL) and cooled in isopropanol/dry ice to $-78^{\circ}C$. To this was added 100 mL of liquid ammonia. Sodium (0.73 g) was added and the reaction turned dark blue. It was left to stir at room temperature for 16 hours. 1 M HCl was added with care until the pH was 2. This was extracted with DCM. The pH of the water layer was raised to 14 using KOH pellets. This was extracted with chloroform and the organic layer was dried over K_2CO_3 and the

chloroform removed under reduced pressure to yield a yellow viscous oil. This was purified by alumina column chromatography using CH_2Cl_2 : MeOH (1-5%) to give a white powder, 0.186 g, 0.482 mmol (68.1%); δ_H ($CDCl_3$, 400 MHz): 7.6 (s, 1 H), 7.3 (s, 2 H), 3.07 (s, 4 H), 2.97 (s, 4 H), 2.76 (s, 3 H), 2.75 (s, 3 H), 2.68 (s, 4 H), 2.60 (s, 4 H), 2.54 (s, 4 H), 2.46 (s, 4 H); δ_C ($CDCl_3$, 100 MHz): 171.4, 76.9, 59.2, 57.2, 52.9, 52.3, 50.8, 45.8, 25.6; M/Z : 408.4 ($M+Na$)⁺, 424.4 ($M+K$)⁺; $IR_{v_{max}}$ (cm^{-1}): 3430, 2846, 2103, 1643, 1567, 1456, 1415, 1367, 1311, 1257, 1164, 1110, 989.

Eu[112]

112 (0.074 g, 0.19 mmol) was dissolved in dry acetonitrile (3 mL) and europium triflate (0.126 g, 0.21 mmol) was added. This was freeze thawed twice and then refluxed under argon for 12 hours. It was then added dropwise to dry ether and the precipitate was collected. Yield: 45 %; δ_{H} (CDCl_3 , 400 MHz): 12.88 (cyc), 3.3, 1.8, -0.63, -6.67, -13.04; **M/Z**: 285.4 ($\text{M}+\text{H}_2\text{O}$)⁺, 686.7 ($\text{M}+\text{Trif}$)⁺; **IR**_{v_{max}} (cm^{-1}): 3428, 2964, 2086, 1641, 1461, 1380, 1272, 1122, 1072, 1024.

6.3 Experimental Data for Chapter 4

All kinetic evaluations were carried out by using an *Agilent 8453* spectrophotometer fitted with a circulating temperature controlled water bath, and water driven mechanical stirring. The rate of hydrolysis (*k*) of the phosphodiester by above complexes were determined by fitting the data to first order rate kinetics using *Biochemical Analysis Software for Agilent ChemStation*. All reactions gave ‘pseudo’ first order kinetics. We estimate that the errors in these measurements are within $\pm 10\%$.

A 50mM HEPES solution was prepared (1.19 g) in water (100 mL). The pH of this was adjusted to 7.40 using NaOH and HCl solutions. Using this buffer, a solution of 0.18 mM HPNP was prepared. The concentration was adjusted such that $A_{290} = 1.22$. 2.4ml of this HPNP solution was then incubated in a UV cell at 37 °C for 10 minutes. This gave 4.32×10^{-7} mol of the phosphate. A solution of the appropriate lanthanide complex was prepared in methanol such that 100 μl contained 4.32×10^{-7} mol of the complex. 100 μl was then added to the HPNP at 37 °C and the reaction was monitored by UV over at least 16 h. The pH was checked again at the end of the reaction and was found to have changed by no more the 0.04.

6.4 Experimental Data for Chapter 5

All glassware was autoclaved prior to use. Gloves were worn at all times to prevent possible degradation of the RNA. All water used had been previously treated with diethyl pyrocarbonate and autoclaved for 20 minutes.

The protected RNA was first purified by polyacrylamide gel electrophoresis. The main band was observed by UV shadowing, isolated and passed through a biotrap. After 1.5 h, the sample was divided into two portions and n-butanol (800 μL) was added to each before they were vortexed and centrifuged. The butanol layer was then removed by pipette and the remaining aqueous layers were added together and washed again with butanol. When the aqueous volume was 150 μL , 19 μL of 3 M sodium acetate, pH 6, was added and the RNA precipitated by adding 600 μL ethanol and mixing. The resulting RNA pellet was taken up in water and quantified by UV spectrometry.

Radio-labelling of RNA

Two portions, of 0.3 ODU apiece, were radio-labelled. The stock (unlabelled) RNA was dissolved in H_2O (120 μL) and two 5 μL samples were taken, to give 0.3 ODU in each sample. To each was added buffer (5 μL), kinase (2 μL), [^{32}P] ATP (5 μL), and H_2O (23 μL). This was heated to 37 $^\circ\text{C}$ for 1.5 h. Labelled RNA was separated from ATP on a Sephadex G-25 column, eluted with ammonium formate. The void volume eluate was reduced to dryness and the RNA was redissolved in 100 μL H_2O and 12 μL 3 M sodium acetate. It was then precipitated by adding 400 μL ethanol and chilling at -20 $^\circ\text{C}$ overnight. The sample was then centrifuged for 8 minutes to yield a pellet and the supernatant liquid was removed.

At this point, one sample was dissolved in H_2O (100 μL) to make a stock solution, and 4 μL was counted. This gave a value of 295,368 cpm and as $\sim 400,000$ cpm were required per experiment, 6 μL of the radio-labelled RNA stock solution was used in each reaction.

Preparation of polyacrylamide Gel mix (16 %)

10 x TBE (100 mL), water (420 mL), acrylamide (152 g), bisacrylamide (8 g) and urea (420 g) were added together and stirred before being stored in the fridge. When required, the solution was de-aerated, ammonium persulfate (1.6 % w/v, 1.950 mL) was added and *N,N,N,N*-tetramethyl ethylenediamine was added immediately before the gel was poured.

Preparation of RNA ladder

A sample of radio-labelled RNA was incubated at 90 °C for 15 minutes in 10 µL of 50 mM sodium bicarbonate solution containing 1 mM EDTA at pH 9. The sample was cooled in ice for 10 minutes before H₂O (40 µL) and *n*-butanol (550 µL) were added to precipitate the RNA. The supernatant liquid was removed from the pellet by pipette. A further 90 µL of H₂O was added, along with 3 M sodium acetate (12.5 µL) and ethanol (350 µL) in order to desalt and precipitate the RNA. The sample was chilled at -20 °C and centrifuged before the supernatant liquid was removed and the RNA was dried under vacuum.

Chapter Seven

Future Work

7.1 Introduction

The results discussed in the previous six chapters give an indication of how very simple molecules can be used to promote the cleavage of the phosphodiester bonds of RNA and RNA model compounds. While the results obtained to date have been impressive, they represent only the beginning of such work within the Gunnlaugsson group. Some areas into which this work will expand are briefly discussed below

7.2 Amino Esters

The work described in Chapter Two of this thesis involved the incorporation of pseudo 'dipeptides' into the cyclen framework. However, the amino acids chosen for this work, glycine, alanine, valine, leucine and phenylalanine, were all simple molecules, containing no functional groups. Further work in this area will involve the incorporation of more complex amino acids into cyclen, in particular, serine, lysine and histidine.

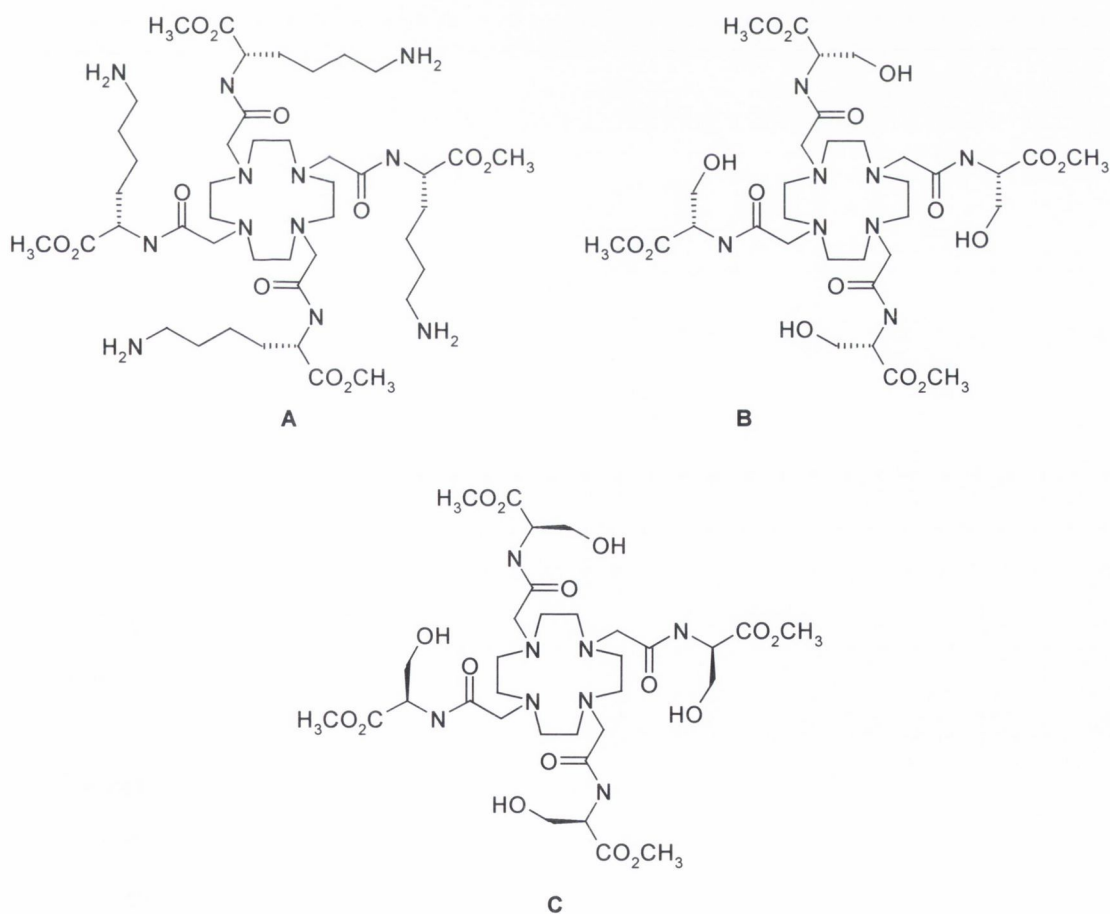


Figure 7.1 Three tetra-substituted cyclen systems. **A** incorporates *L*-Lysine methyl ester, **B** incorporates *L*-Serine methyl ester and **C** incorporates *D*-Serine methyl ester.

These compounds possess structural features which may help to promote phosphodiester hydrolysis, namely nucleophilic characteristics or the capacity to promote acid-base catalysis. A further feature of interest is the use of both the D- and L- isomers of such amino acids.

7.3 Tri-substituted Cyclen

While the synthesis of one tri-substituted cyclen system is described in Chapter Three, this is part of on-going work within the Gunnlaugsson group. The verification of the presence of two metal-bound water molecules by X-ray crystallography suggested that these compounds might prove effective promoters of phosphodiester hydrolysis. To that effect, a series of tri-substituted systems are to be prepared, incorporating the type of pseudo 'dipeptides', that have proved so active.

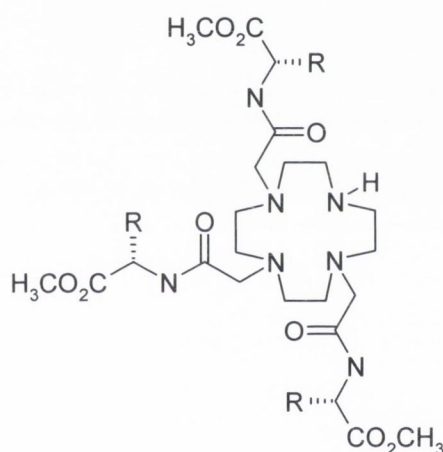


Figure 7.2 A tri-substituted cyclen system incorporating pseudo dipeptide arms. The fourth cyclen nitrogen is free for further modification.

It is hoped that a compound of this general structure could be incorporated into an oligonucleotide in the future, and its ability to selectively cleave RNA evaluated.

7.3 Evaluation of Activity

While early results have indicated that the compounds discussed in this thesis are active promoters of phosphodiester hydrolysis, there is a great deal of on-going research in this area. This includes the use of differing phosphodiester compounds, such as **BNPP** or **EPNP** as well as further investigations with **HPNP** to further

evaluate the effect of buffer, temperature and pH on the activity of various lanthanide systems.

References

References

1. Biochemistry, Cambell, N.A., Menlo Park, Wokingham :Benjamin/Cummings,1996 6th Ed
2. Biochemistry, Stryer, L., Berg, J.M., Tymoczko, J.L., *W.H. Freeman*, 2002, 5th Ed
3. Green, W.D., Roh, H., Pippin, J., Drebin, J.A., *J. Am. Coll. Surg.*, 2000, 93
4. Williams, N.H., Takasaki, B., Wall, M., Chin, J., *Acc. Chem. Res.*, 1999, **32**, 485
5. Wilcox, D.E., *Chem. Rev.*, 1996, **96**, 2435
6. Sigman, D.S., Mazumder, A., Perrin, D.M., *Chem. Rev.*, 1993, **93**, 2295
7. Trawick, Bashkin, J.K. *Chem. Rev.* 1998, **98**, 5
8. Oivanen, M., Kuusela, S., Lonnberg, H., *Chem. Rev.*, 1998, **98**, 961
9. Perreault, D.M., Anslyn, E.V., *Angew. Chem. Int. Ed. Engl.* 1997, **36**, 432
10. Cacciapaglia, R., di Stefano, S., Mandolini, L., *J. Org. Chem.*, 2001, **66**, 5926
11. Bashkin, J.K., Frolova, E.I., Sampath, U., *J. Am. Chem. Soc.*, 1994, **116**, 5981
12. Husken, D., Goodall, G., Blommers, M.J.J., Jahnke, W., Hall, J., Haner, R., Moser, H.E., *Biochemistry*, 1996, **35**, 16591
13. Chin, J., Zou, X., *J. Am. Chem. Soc.*, 1988, **110**, 223
14. Chapman Jr., W.H., Breslow, R., *J. Am. Chem. Soc.*, 1995, **117**, 5462
15. Deal, K.A., Park, G., Sgao, J., Chasteem, N.D., Brechbiel, M.W., Planalp, R.P., *Inorg. Chem.*, 2001, **40**, 4176
16. Komiyama, M., Kamitani, J., Sumaoka, J., Asanuma, H., *Chem. Lett.*, 1996, 869
17. Manseki, K., Nakamura, O., Horikawa, K., Sakamoto, M., Sakiyama, H., Nishida, Y., Sadaoka, Y., Okawa, H., *Inorg. Chem. Commun.*, 2002, **5**, 56
18. Moss, R.A., Park, B.D., Scrimin, P., Ghirlanda, G., *J. Chem. Soc., Chem. Commun.*, 1995, 1627
19. Yeh, G.C., Beatty, A.M., Bashkin, J.K., *Inorg Chem.*, 1996, **35**, 3828
20. Sawata, S., Komiyama, M., Taira, K., *J. Am. Chem. Soc.*, 1995, **117**, 2357
21. Enzyme Kinetics, Cornish-Bowden, A., Wharton, C.W., IRL Press 1990

22. Enzyme Structure and Mechanism, Fersht, A., Second Edition, W.H Freeman and Co. New York, 1985
23. Han, H., Rifkind, J.M., Mildvan, A.S., *Biochemistry*, 1991, **30**, 11104
24. Beese, L.S., Steitz, T.A., *EMBO J.*, 1991, **10**, 17
25. Steitz, T.A., Steitz, J.A., *Proc. Natl. Acad. Sci. USA*, 1993, **90**, 6498
26. Kazakov, S., Altman, S., *Proc. Natl. Acad. Sci. USA*, 1992, **89**, 7939
27. Sigman, D.S., Mazumder, A., Perrin, D.M., *Chem. Rev.*, 1993, **93**, 229
28. Markley, J.L., *Biochemistry*, 1975, **14**, 3546
29. Ribonucleases: Structures and Functions, D'Allesio G., Riordan, J.F., Academic Press.
30. Wilcox, D.E., *Chem. Rev.*, 1996, **96**, 2435
31. Altman, S., *Angew. Chem. Int. Ed. Engl.* 1990, **29**, 749
32. Hughes, M.D., Hussain, M., Nawaz, Q., Sayyed, P., Aktar, S., *DDT*, 2001, **6**, 303
33. <http://www.isip.com/antisens.htm>
34. Santoro, S.W., Joyce, G.F., *Proc. Natl. Acad. Sci.*, 1997, **94**, 4262
35. a) <http://www.isispharm.com/vitravene.html>. b)
36. Magda, D., Wright, M., Crofts, S., Lin, A., Sessler, J.L., *J. Am. Chem. Soc.*, 1997, **119**, 6947
37. Daniher, A.T., Bashkin, J.K., *Chem. Commun.*, 1998, 1077
38. Hall, J., Husken, D., Haner, R., *Nuc. Acids Res.*, 1996, **24**, 3522
39. Chin, J., *Curr. Opin. Chem. Bio.* 1997, **1**, 514
40. Kramer, R., *Coord. Chem. Rev.*, 1999, **182**, 243
41. Hegg, E.L., Burstyn, J.N., *Coord. Chem. Rev.*, 1998, **173**, 133
42. Brown, D.M., Usher, D.A., *J. Chem. Soc.*, 1965, 6558
43. Breslow, R., Huang, D.L., *Proc. Natl. Acad. Sci.*, 1991, **88**, 4080
44. Liu, S., Luo, Z., Hamilton, A.D., *Angew. Chem. Int. Ed. Engl.*, 1997, **36**, 23
45. Liu, S., Hamilton, A.D., *Chem. Commun.*, 1999, 587
46. Fernandez-Saiz, M., Schneider, H.J., Sartorius, J., Wilson W.D., *J. Am. Chem. Soc.*, 1996, **118**, 4739
47. Molenveld, P., Engbergesen, J.F.J., Reinhoudt, D.N., *Chem. Soc. Rev.*, 2000, **29**, 75
48. Morrow, J.R., Buttrey, L.A., Berback, K.A., *Inorg. Chem.*, 1992, **31**, 16
49. Moss, R.A., Zhang, J., Ragunathan, K.G., *Tet. Lett.*, 1998, **39**, 1529

50. Irisawa, M., Takeda, N., Komiyama, M., *J. Chem. Soc., Chem. Commun.*, 1995, 1221
51. Takeda, N., Irisawa, M., Komiyama, M., *J. Chem. Soc., Chem. Commun.*, 1995, 2773
52. Takeda, N., Imai, T., Irisawa, M., Sumaoka, J., Yashiro, M., Shigewa, H., Komiyama, M., *Chem. Lett.*, 1996, 599
53. Irisawa, M., Takeda, N., Komiyama, M., *J. Chem. Soc., Chem. Commun.*, 1995, 1221
54. Kamitani, J., Kawahara, R., Yashiro, M., Komiyama, M., *Chem. Lett.*, 1998, 1047
55. Yashiro, M., Ishikubu, A., Takarada, T., Komiyama, M., *Chem. Lett.*, 1995, 665
56. Yashiro, M., Ishikubo, A., Komiyama M., *Chem. Commun.*, 1997, 83
57. Molenveld, P., Engbergsen, J.F.J., Reinhoudt, D.N., *J. Org. Chem.*, 1999, **64**, 6337
58. Molenveld, P., Engbergsen, J.F.J., Kooijmaan, H., Spek, A.L., Reinhoudt, D.N., *J. Am. Chem. Soc.*, 1998, **120**, 6726
59. Molenveld, P., Engbergsen, J.F.J., Reinhoudt, D.N., *Angew. Chem. Int. Ed. Engl.*, 1999, **38**, 3189
60. Molenveld, P., Kapsabelis, S., Engbergsen, J.F.J., Reinhoudt, D.N., *J. Am. Chem. Soc.*, 1997, **119**, 2948
61. Molenveld, P., Engbergsen, J.F.J., Reinhoudt, D.N., *Eur. J. Org. Chem.*, 1999, 3269
62. Molenveld, P., Stikvoort, W.M.G., Kooijmaan, H., Spek, A.L., Engbergsen, J.F.J., Reinhoudt, D.N., *J. Org. Chem.*, 1999, **64**, 3896
63. Komiyama, M., Takeda, N., Shigekawa, H., *Chem. Commun.*, 1999, 1443
64. Roigk, A., Hettich, R., Schneider, H.J., *Inorg. Chem.*, 1998, **37**, 751
65. Sumaoka, J., Yashiro, M., Komiyama, M., *J. Chem. Soc., Chem. Commun.*, 1992, 1707
66. Hurst, P., Takasaki, B.K., Chin, J., *J. Am. Chem. Soc.*, 1996, **118**, 9982
67. Caravan, P., Ellison, J.J., Murray, T.J., Lauffer, R.B., *Chem. Rev.*, 1999, **99**, 2293

68. Morrow, J.R., Amin, S., Lake, C.H., Churchill, M.R., *Angew. Chem. Int. Ed. Engl.* 1994, **33**, 773
69. Amin, S., Voss, D.A., Horrocks, W., Lake, C.H., Churchill, M.R., Morrow, J.R., *Inorg. Chem.*, 1995, **34**, 3294
70. Chin, K.O.A., Morrow, J.R., *Inorg. Chem.* 1994, **33**, 5036
71. Kolasa, K.A., Morrow, J.R., Sharma, A.P., *Inorg Chem.* 1993, **32**, 3983
72. Voss Jr, D.A., Buttrey-Thomas, L.A., Janik, T.S., Churchill, M.R., Morrow, J.R., *Inorg. Chim. Acta*, 2001, **317**, 149
73. Oh, S.J., Park, J.W., *J. Chem. Soc., Dalton Trans.*, 1997, 753
74. Oh, S.J., Song, K.W., Park, J.W., *J. Chem. Soc., Chem. Commun.*, 1995, 575
75. Oh, S.J., Yoon, C.H., Park, J.W., *J. Chem. Soc., Perkin Trans. 2*, 1996, 329
76. Amin, S., Marks, C., Toomey, L.M., Churchill, M.R., Morrow, J.R., *Inorg. Chim. Acta*, 1996, **246**, 99
77. Baykal, U., Akkaya, M.S., Akkaya, E.U., *J. Mol. Cat. A: Chem.*, 1999, **145**, 309
78. Desreux, J.F., *Inorg. Chem.*, 1980, **19**, 1319
79. Lauffer, R.B., *Chem. Rev.*, 1987, **87**, 901
80. Comblin, V., Gilsoul, D., Hermann, M., Humblet, V., Jacques, V., Mesbahi, M., Sauvage, C., Desreux, J.F., *Coord. Chem. Rev.*, 1999, **185**, 451
81. Aime, S., Barge, A., Botta, M., Parker, D., De Sousa, A.S., *J. Am. Chem. Soc.*, 1997, 119, 4767
82. Broan, C.J., Cox, J.P.L., Craig, A.S., Katakya, R., Parker, D., Randall, A.M., Feguson, G., *J. Chem. Soc. Perkin 2.*, 1991, 87
83. Parker, D., Senanayake, P.K., Williams, J.A.G., *J. Chem. Soc. Perkin 2.*, 1998, 2129
84. Beeby, A., Clarkson, I.M., Dickens, R.S., Faulkner, S., Parker, D., Royle, L., De Sousa, A.S., Williams, J.A.G., *J. Chem. Soc. Perkin 2.*, 1999, 493
85. Dickens, R.S., Gunnlaugsson, T., Parker, D., Peacock, R.D., *Chem. Commun.*, 1998, 1643
86. Wang, C., Choudhary, S., Vink, C.B., Secord, E.A., Morrow, J.R., *Chem. Commun.*, 2000, 2509
87. Baykal, U., Akkaya, E.U., *Tet. Lett.*, 1998, **39**, 5861

88. Morrow, J.R., Aures, K., Epstein, D., *J. Chem. Soc., Chem. Commun.*, 1995, 2431
89. Chin, K.O.A., Morrow, J.R., *Inorg. Chem.* 1994, **33**, 5036
90. Chappell, L.L., Voss, D.A. Jr., DeW. Horrocks, D., Jr., Morrow, J.R., *Inorg. Chem.* 1998, **37**, 3989.
91. Michealis, K., Kalesse, M., *Chem. BioChem.*, 2001, **2**, 79
92. Kong, D.Y., Xie, Y.Y., *Polyhedron*, 2001, **19**, 1527
93. Aoiki, S., Shiro, M., Koike, T., Kimura, E., *J. Am. Chem. Soc.*, 2000, **122**, 576
94. Kimura, E., Aoiki, S., Koike, T., Shiro, M., *J. Am. Chem. Soc.*, 1997, **119**, 3068
95. Chung, Y., Akkaya, E.U., Venkatachalam, T.K., Czarnik, A.W., *Tet. Lett.*, 1990, **31**, 5413
96. Hayashi, N., Takeda, N., Shiiba, T., Yashiro, M., Watanabe, K., Komiyama, M., *Inorg. Chem.*, 1993, **32**, 5899
97. Kuzuya, A., Akai M., Komiyama M., *Chem., Lett.*, 1035, 1999
98. Michaelis, K., Kalesse, M., *Angew. Chem. Int. Ed.*, 1999, **38**, 2243
99. Michealis, K., Kalesse, M., *Chem. BioChem.*, 2001, **1**, 79
100. Kuzuya A., Komiyama M., *Chem. Commun.*, 2000, 2019
101. Matsuda, S., Ishikubo, A., Kuzuya., Yashiro, M., Komiyama, M., *Angew. Chem. Int. Ed. Engl.*, 1998, **37**, 3284
102. Bashkin, J.K., Frolova, E.I., Sampath, U., *J. Am. Chem. Soc.*, 1994, **116**, 5981
103. Stern, M.K., Bashkin, J.K., Sall, E.D., *J. Am. Chem. Soc.*, 1990, **112**, 5357
104. Modak, A.S., Gard, J.K., Merriman, M.C., Winkeler, K.A., Bashkin, J.K., Stern, M.K., *J. Am. Chem. Soc.*, 1991, **113**, 283
105. Magda, D., Miller, R.A., Sessler, J.L., Iverson, B.L., *J. Am. Chem. Soc.*, 1994, **116**, 7439
106. Magda, D., Crofts, S., Lin, A., Miles, D., Wright, M., Sessler, J.L., *J. Am. Chem. Soc.*, 1997, **119**, 2293
107. Magda, D., Wright, M., Crofts, S., Lin, A., Sessler, J.L., *J. Am. Chem. Soc.*, 1997, **119**, 6947
108. Haner, R., Hall, J., Pfutzer, A., Husken, D., *Pure & Appl. Chem.*, 1998, **70**, 111

109. Haner, R., Hall, J., *Helvetica Chimica Acta*, 1997, **80**, 487
110. Hall, J., Husken, D., Haner, R., *Nucleic Acids Research*, 1996, **24**, 3522
111. Baker, B.F., Lot, S.S., Kriegel, J., Cheng-Flournoy, S., Villiet, P., Sasmor, H.M., Chappell, L.L., Morrow, J.R., *Nucleic Acids Research* 1999, 1547
112. Dickins, R.S., Love, C.S., Puschmann, H., *Chem. Commun.*, 2001, 2308
113. Mani, F., Morassi, R., Stoppioni, P., Vacca, A., *J. Chem. Soc., Dalton Trans.*, 2001, 2116
114. Aime, S., Barge, A., Botta, M., Howard, J.A.K., Katakya, R., Lowe, M.P., Moloney, J.M., Parker, D., De Sousa, A.S, *Chem. Commun.*, 1999, 1047
115. Konig, B., Gallmeier, H.C., Reichenbach-Klinke, R., *Chem. Commun.*, 2001, 2390
116. Aime, S., Batsanov, A.S., Botta, M., Dickens, R.S., Faulkner, S., Foster, C.E., Harrison, A., Moloney, J.M., Norman, T.J., Parker, D., Royle, L., Williams, J.A.G., *J. Chem.Soc., Dalton Trans.*, 1997, 3623
117. Gunnlaugsson, T., *Tet. Lett.*, 2001, **42**, 8901
118. Barbier, B., Brack, A., *J. Am. Chem. Soc.* 1988, **110**, 6880
119. Barbier, B., Brack, A., *J. Am. Chem. Soc.*, 1992, **114**, 3511
120. Sissi, C., Rossi, P., Felluga, F., Formaggio, F., Palumbo, M., Tecilla, P., Toniolo, C., Scrimin, P., *J. Am. Chem. Soc.*, 2001, **123**, 3169
121. Rossi, P., Felluga, F., Tecilla, P., Formaggio, F., Crisma, M., Toniolo, C., Scrimin, P., *Biopolymers*, 2000, **55**, 496
122. Zlatoidsky, P., Malier, T., *Eur. J. Med. Chem.*, 1999, **34**, 1023
123. White, B.D., Mallen, J., Arnold, K.A., Fronkzek, F.R., Gandour, R.D., Gehrig, L.M.B., Gokel, G.W., *J. Org. Chem.*, 1989, **54**, 937
124. Aime, S., Barge, A., Bruce, J.I., Botta, M., Howard, J.K., Moloney, J.M., Parker, D., de Sousa, A.S., Woods, M., *J. Am. Chem. Soc.*, 1999, **121**, 5762
125. Dickens, R.S., Howard, J.A.K., Maupin, C.L., Moloney, J.M., Parker, D., Peacock, R.D., Riehl, J.P., Siligardi, G., *New J. Chem.*, 1998, 891

126. Woods, M., Aime, S., Botta, M., Howard, J.A.K., Moloney, J.M., Navet, M., Parker, D., Port, M., Rousseaux, O., *J. Am. Chem. Soc.*, 2000, **122**, 9781
127. Beeby, A., Parker, D., Williams, J.A.G., *J. Chem. Soc., Perkin Trans. 2*, 1996, 1565
128. Lanthanides and Actinides, MTP international review of science. Inorganic chemistry. Series two. Vol.7, Emeleus, H.J., Bagnall, K.W., London, Butterfield, 1975
129. The Chemistry of Contrast Agents in Medical Magnetic Resonance Imaging, Merbach, A.E., Toth, E., Wiley: New York, 2001
130. Parker, D., Dickins, R.S., Puschmann, H., Crossland, C., Howard, J.A.K., *Chem. Rev.*, 2002., **102**
131. Epstein, D. M., PhD Thesis, 2000.
132. Amin, S., PhD. Thesis, University of New York at Buffalo, 1995
133. Aime, S., Botta, M., Ermondi, G., *Inorg. Chem.*, 1992, **31**, 4291
134. Quici, S., Marzanni, G., Cavazzini, M., Anelli, P.L., Botta, M., Gianolio, E., Accirsi, G., Armaroli, N., Barigelletti, F., *Inorg. Chem.*, 2002, **41**, 2777
135. Amin, S., Voss, D.A., Horrocks, W., Lake, C.H., Churchill, M.R., Morrow, J.R., *Inorg. Chem.*, 1995, **34**, 3294
136. Gans, P., Sabatini, A., Vacca, A., *J. Chem.Soc., Dalton Trans.* 1985, 1195-2000
137. Dickens, R.S., Howard, J.A.K., Maupin, C.L., Moloney, J.M., Parker, D., Peacock, R.D., Riehl, J.P., Siligardi, G., *New J. Chem.*, 1998, 891
138. Dickens, R.S., Kenwright, A.M., Moloney, J.M., Parker, Port, M., Navet, M., Rousseau, O., Woods, M., *Chem. Commun.*, 1998, 1381
139. Beeby, A., Clarkson, I. M., Dickins, R. S., Faulkner, S., Parker, D., Royle, L., de Sousa, A. S., Williams, J. A. G., Woods, M., *J. Chem. Soc. Perkin Trans. 2*, 1999, 493.
140. Beeby, A., Dickins, R. S., Faulkner, S., Parker, D., Williams, J. A. G., *Chem. Commun.*, 1997,
141. 1401; Dickins, R. S.; Parker, D, de Sausa, A. S.; Williams, J. A. G., *Chem. Commun.* **1996**, 697.
142. Viguier, R., Gunnlaugsson, T., Unpublished results.
143. Zhuang, Z., Kung, M., Kung, H.F., *J. Med.Chem.*, 1994; **37**, 1406

144. Abdel Rahman, A. E.; El-Sherief, H. A.; Mahmoud, A. M., *J. Indian Chem. Soc.*, 1981, **58**, 171
145. a) Spirlet, M.R., Rebizant, J., Loncin, M.F., Desreux, J.F., *Inorg. Chem.*, 1984, 23, 4278. b) Parker, D., Pulukkody, K., Smith, F.C., Batsanov, A.S., Howard, J.A.K., *J. Chem. Soc., Dalton Trans.*, 1994, 689
146. Gunnlaugsson, T., Harte, A.J., Leonard, J.P., Nieuwenheyzen, M., *Chem. Commun.*, 2000, 2134
147. Leonard, J., PhD. Thesis, University of Dublin, Trinity College, 2003
148. a) Dickens, R.S., Gunnlaugsson, T., Parker, D., Peacock, R.D., *Chem. Commun.*, 1998, 1643. b) Bruce, J.I., Dickens, R.S., Govenlock, L.J., Gunnlaugsson, T., Lopinski, S., Lowe, M.P., Parker, D., Peacock, R.D., Perry, J.J.B., Aime, S., Botta, M., *J. Am. Chem. Soc.*, 2000, **122**, 9674
149. Gunnlaugsson, T., Leonard, J.P., Mulready, S., Nieuwenhuyzen, M., *Tetrahedron*, In Press.
150. Gunnlaugsson, T., Davies, R.J.H., Nieuwenhuyzen, M., Stevenson, C.S., Viguier, R., Mulready, S., *Chem. Commun.*, 2002, 2136
151. Dickens, R.S., Gunnlaugsson, T., Parker, D., Peacock, R.D., *Chem. Commun.*, 1998, 1643
152. Bruce, J.I., Dickens, R.S., Govenlock, L.J., Gunnlaugsson, T., Lopinski, S., Lowe, M.P., Parker, D., Peacock, R.P., Perry, J.J.B., Aime, S., Botta, M., *J. Am. Chem. Soc.*, 2000, **122**, 9674
153. a) Kirby, A.J., Marriott., R.E., *J. Am. Chem. Soc.*, 1995, **117**, 833. b) Beckmann, C., Kirby, A.J., Kuusela, S., Tickle, D.C., *J. Chem. Soc., Perk. Trans. 2*, 1998, 573. c) Kirby, A.J., Marriott., R.E., *J. Chem. Soc., Perk. Trans. 2*, 2002, 422
154. a) Breslow, R., Berger, D., Huang, D.L., *J. Am. Chem. Soc.*, 1990, **112**, 3686. b) Breslow, R., Huang, D.L., *J. Am. Chem. Soc.*, 1990, **112**, 9621. c) Breslow, R., Anslyn, E., Huang, D.L., *Tetrahedron*, 1991, **47**, 2365. d) Breslow, R., *Acc. Chem. Res.*, 1991, **24**, 317. Breslow, R., Dong, S.D., Webb, Y., Xu, R., *J. Am. Chem. Soc.*, 1996, 118, 6588
155. Fanning, A.M., Gunnlaugsson, T., Unpublished results
156. Parker, D., Unpublished results
157. Kim, J.H., Chin, J., *J. Am. Chem. Soc.*, 1992, **114**, 9792

158. Gunnlaugsson, T., Leonard, J.P., Harte, A., *J. Am. Chem. Soc.*, 2002, In Press.
159. Hendry, P., Sargeson, A.M., *J. Am. Chem. Soc.*, 1989, **111**, 2521
160. a) Morrow, J.R., Trogler, W.C., *Inorg. Chem.*, 1988, **27**, 3387. b) Morrow, J.R., Trogler, W.C., *Inorg. Chem.*, 1992, **31**, 1544
161. a) Bashkin, J.K., Jenkins, L.A., *J. Chem. Soc., Dalton Trans.*, 1993, 3631. b) Jenkins, L.A., Bashkin, J.K., Autry, M.E., *J. Am. Chem. Soc.*, 1996, **118**, 6822. c) Jenkins, L.A., Bashkin, J.K., *Inorg. Chim. Acta.*, 1997, **263**, 49
162. Scaringe, S.A., Winscott, F.E., Caruthers, M.H., *J. Am. Chem. Soc.*, 1998, 120, 11820
163. Principles and Techniques of Practical Biochemistry, Wilson K., Walker, J., Cambridge University Press, 2000.